frontiers | Research Topics

July 2022: sarcoma awareness month

Edited by
Liam Chen

Published in
Frontiers in Endocrinology
Frontiers in Oncology

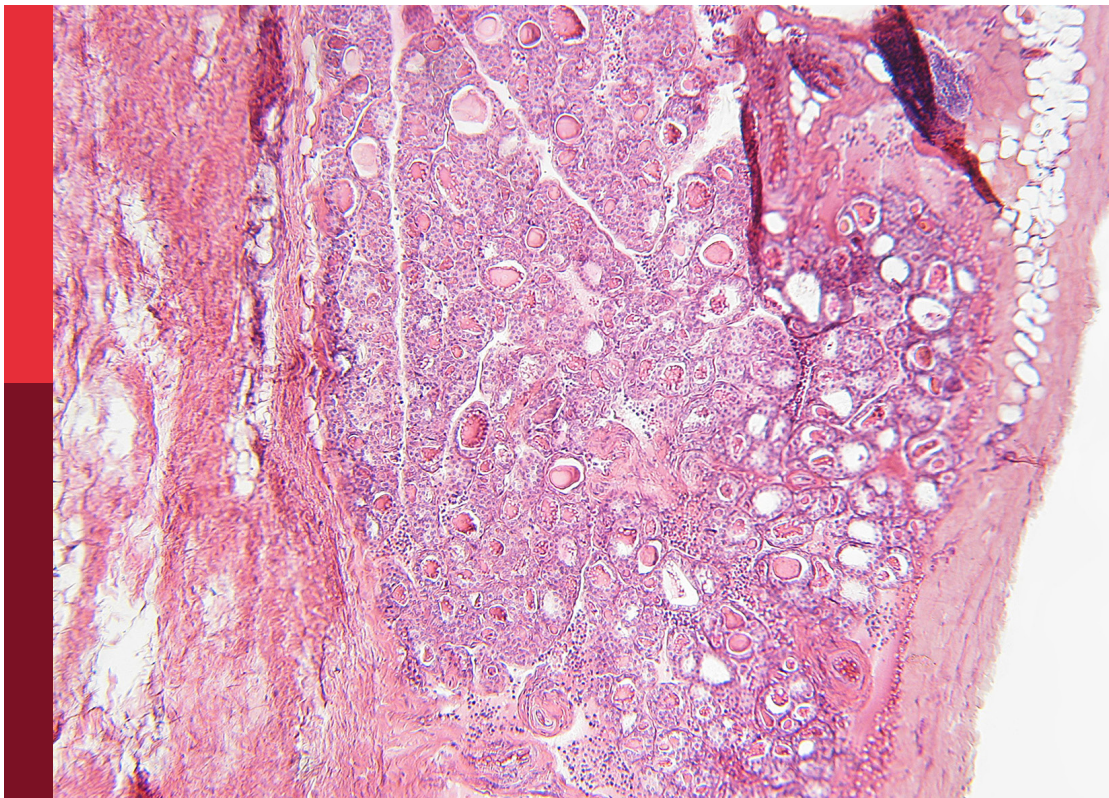

FRONTIERS EBOOK COPYRIGHT STATEMENT

The copyright in the text of individual articles in this ebook is the property of their respective authors or their respective institutions or funders. The copyright in graphics and images within each article may be subject to copyright of other parties. In both cases this is subject to a license granted to Frontiers.

The compilation of articles constituting this ebook is the property of Frontiers.

Each article within this ebook, and the ebook itself, are published under the most recent version of the Creative Commons CC-BY licence. The version current at the date of publication of this ebook is CC-BY 4.0. If the CC-BY licence is updated, the licence granted by Frontiers is automatically updated to the new version.

When exercising any right under the CC-BY licence, Frontiers must be attributed as the original publisher of the article or ebook, as applicable.

Authors have the responsibility of ensuring that any graphics or other materials which are the property of others may be included in the CC-BY licence, but this should be checked before relying on the CC-BY licence to reproduce those materials. Any copyright notices relating to those materials must be complied with.

Copyright and source acknowledgement notices may not be removed and must be displayed in any copy, derivative work or partial copy which includes the elements in question.

All copyright, and all rights therein, are protected by national and international copyright laws. The above represents a summary only. For further information please read Frontiers' Conditions for Website Use and Copyright Statement, and the applicable CC-BY licence.

ISSN 1664-8714
ISBN 978-2-8325-5527-9
DOI 10.3389/978-2-8325-5527-9

About Frontiers

Frontiers is more than just an open access publisher of scholarly articles: it is a pioneering approach to the world of academia, radically improving the way scholarly research is managed. The grand vision of Frontiers is a world where all people have an equal opportunity to seek, share and generate knowledge. Frontiers provides immediate and permanent online open access to all its publications, but this alone is not enough to realize our grand goals.

Frontiers journal series

The Frontiers journal series is a multi-tier and interdisciplinary set of open-access, online journals, promising a paradigm shift from the current review, selection and dissemination processes in academic publishing. All Frontiers journals are driven by researchers for researchers; therefore, they constitute a service to the scholarly community. At the same time, the *Frontiers journal series* operates on a revolutionary invention, the tiered publishing system, initially addressing specific communities of scholars, and gradually climbing up to broader public understanding, thus serving the interests of the lay society, too.

Dedication to quality

Each Frontiers article is a landmark of the highest quality, thanks to genuinely collaborative interactions between authors and review editors, who include some of the world's best academicians. Research must be certified by peers before entering a stream of knowledge that may eventually reach the public - and shape society; therefore, Frontiers only applies the most rigorous and unbiased reviews. Frontiers revolutionizes research publishing by freely delivering the most outstanding research, evaluated with no bias from both the academic and social point of view. By applying the most advanced information technologies, Frontiers is catapulting scholarly publishing into a new generation.

What are Frontiers Research Topics?

Frontiers Research Topics are very popular trademarks of the *Frontiers journals series*: they are collections of at least ten articles, all centered on a particular subject. With their unique mix of varied contributions from Original Research to Review Articles, Frontiers Research Topics unify the most influential researchers, the latest key findings and historical advances in a hot research area.

Find out more on how to host your own Frontiers Research Topic or contribute to one as an author by contacting the Frontiers editorial office: frontiersin.org/about/contact

July 2022: sarcoma awareness month

Topic editor
Liam Chen — University of Minnesota, United States

Citation
Chen, L., ed. (2024). *July 2022: sarcoma awareness month*.
Lausanne: Frontiers Media SA. doi: 10.3389/978-2-8325-5527-9

Table of contents

frontiers | Frontiers in Endocrinology

TYPE Editorial
PUBLISHED 30 August 2024
DOI 10.3389/fendo.2024.1480176

Check for updates

OPEN ACCESS

EDITED AND REVIEWED BY
Antonino Belfiore,
University of Catania, Italy

*CORRESPONDENCE
Liam Chen
llchen@umn.edu

RECEIVED 13 August 2024
ACCEPTED 19 August 2024
PUBLISHED 30 August 2024

CITATION
Chen L (2024) Editorial: July 2022: sarcoma awareness month.
Front. Endocrinol. 15:1480176.
doi: 10.3389/fendo.2024.1480176

COPYRIGHT
© 2024 Chen. This is an open-access article distributed under the terms of the Creative Commons Attribution License (CC BY). The use, distribution or reproduction in other forums is permitted, provided the original author(s) and the copyright owner(s) are credited and that the original publication in this journal is cited, in accordance with accepted academic practice. No use, distribution or reproduction is permitted which does not comply with these terms.

Editorial: July 2022: sarcoma awareness month

Liam Chen*

Department of Laboratory Medicine and Pathology, University of Minnesota Medical School, Minneapolis, MN, United States

KEYWORDS

sarcoma, soft tissue, bone, muscle, endocrine, diagnostics

Editorial on the Research Topic
July 2022: Sarcoma Awareness Month

Sarcomas is the general term for rare kinds of cancer growing in the bone and connective tissues. These tumors can be divided into two main groups, soft tissue sarcomas, and bone sarcomas. Interestingly, a new kind of sarcoma has been recently described, called pseudoendocrine sarcoma (1). The most common tissues affected by this kinds of sarcoma are bones, muscles, tendons, cartilage, nerves, fat, and blood vessels as well as many endocrine organs. It affects mainly children, adolescents, and adults under the age of 30, and represents 1% to 2% of all cancers. Symptoms vary depending on the part of the body that is affected, and prompt therapies are primary for increasing the survival rate of the patients. Most of the treatments for this kinds of cancers may include chemotherapy, radiation therapy and surgery. Recently, hormonal therapy has revealed to be a great strategy for the treatment of some of these tumors, especially for uterine and endometrial stromal sarcomas.

It is in this spirit that Frontiers has launched a new article collection to coincide with the Sarcoma Awareness Month. This Frontiers in Endocrinology Research Topic entitled "July 2022: Sarcoma Awareness Month" aims to address the endocrinology-specific dimensions of this devastating disease, highlighting the importance of sarcoma research and considering how to improve treatment options and prognostic predictions.

Liu et al. explored the role of copper dysregulation in osteosarcoma (OS) by identifying cuproptosis-related long non-coding RNAs (CRLs) and their potential in prognostication and treatment response. Using differential expression and correlation analyses, a CRL signature comprising four key CRLs was developed. This signature was validated through Kaplan-Meier survival analysis, ROC curves, and independent prognostic assessments, demonstrating its ability to stratify patients into low- and high-risk groups with significant differences in prognosis. The signature also correlated with immune status, responses to immunotherapy, and chemotherapy sensitivity. The findings, confirmed by RT-qPCR, suggest that this CRL signature could enhance prognostic evaluations and guide personalized treatment strategies in OS.

Study done by Zhuang et al. aimed to develop a nomogram for predicting overall survival (OS) in patients with retroperitoneal leiomyosarcoma (RLMS) following surgical resection, as no such model existed. Analyzing 118 patients who underwent surgery between September 2010 and December 2020, the researchers constructed the nomogram using Cox regression, incorporating factors such as the number of resected organs, tumor

diameter, FNCLCC grade, and multifocality of lesions. The median OS was 47.8 months, with a majority of tumors fully resected. The nomogram demonstrated good predictive performance, with a concordance index of 0.779 and strong agreement between predicted and actual OS in calibration curves. This model offers valuable guidance for postoperative consultation and patient selection for clinical trials.

Another study performed by Eichler et al. investigated the Health-Related Quality of Life (HRQoL) of adult sarcoma patients and survivors through longitudinal assessment over one year across 39 centers in Germany. Utilizing the EORTC QLQ-C30 questionnaire, researchers followed 1111 patients at baseline, with 915 continuing at 6 months and 847 at 12 months. Analysis revealed that HRQoL varied based on tumor location, with lower extremity sarcoma patients reporting poorer outcomes compared to those with upper extremity sarcomas. Additionally, treatment involving radiotherapy or systemic therapy was linked to decreased HRQoL. Among patients in complete remission, smoking negatively impacted HRQoL. Bone sarcomas consistently showed the worst HRQoL scores, and factors such as being female, aged 55-64, lower socioeconomic status, and comorbidities were associated with poorer HRQoL across both groups. Despite some improvement in HRQoL over time and with physical activity, the study highlights the need for targeted strategies to enhance HRQoL in sarcoma patients, particularly for those with bone sarcomas and other identified risk factors.

The six case reports covers interesting, yet rare sarcoma cases including hepatic inflammatory pseudotumor-like follicular dendritic cell sarcoma (Ding et al.), primary synovial sarcoma of the thyroid gland (Ren et al.), primary mediastinal Ewing's sarcoma (Su et al.), low-grade fibromyxoid sarcoma (Zhang et al.), and two primary pulmonary sarcomas (Wen et al.; Zhang et al.). Through analyzing the distinctive clinicopathologic features of these rare cases combined with literature review, valuable insights and lessons have been learned which will help better understand and manage these diseases.

With over 70 different subtypes, sarcomas can be difficult to diagnose and treat. The month-long sarcoma awareness observance seeks to educate the public about the symptoms, risks, and the need for early detection, while also supporting research and funding for improved treatments. While highlight the challenges faced by those affected, articles collected in this topic undoubtedly would drive progress in the fight against this challenging disease.

Author contributions

LC: Writing – original draft, Writing – review & editing.

Conflict of interest

The author declares that the research was conducted in the absence of any commercial or financial relationships that could be construed as a potential conflict of interest.

Publisher's note

All claims expressed in this article are solely those of the authors and do not necessarily represent those of their affiliated organizations, or those of the publisher, the editors and the reviewers. Any product that may be evaluated in this article, or claim that may be made by its manufacturer, is not guaranteed or endorsed by the publisher.

Reference

1. Papke DJ Jr., Dickson BC, Sholl L, Fletcher CDM. Pseudoendocrine sarcoma: clinicopathologic analysis of 23 cases of a distinctive soft tissue neoplasm with metastatic potential, recurrent CTNNB1 mutations, and a predilection for truncal locations. *Am J Surg Pathol.* (2022) 46:33–43. doi: 10.1097/PAS.0000000000001751

frontiers | Frontiers in Endocrinology

TYPE Original Research
PUBLISHED 13 October 2022
DOI 10.3389/fendo.2022.987942

Check for updates

OPEN ACCESS

EDITED BY
Xuyu Gu,
Southeast University, China

REVIEWED BY
Yi Zhigao,
National University of Singapore, Singapore
Xiaomeng Pei,
Hong Kong Polytechnic University, Hong Kong SAR, China

*CORRESPONDENCE
Chao Tu
tuchao@csu.edu.cn
Shasha He
heshasha611@csu.edu.cn

†These authors have contributed equally to this work and share first authorship

SPECIALTY SECTION
This article was submitted to Cancer Endocrinology, a section of the journal Frontiers in Endocrinology

RECEIVED 06 July 2022
ACCEPTED 12 August 2022
PUBLISHED 13 October 2022

CITATION
Liu B, Liu Z, Feng C, Li C, Zhang H, Li Z, Tu C and He S (2022) Identification of cuproptosis-related lncRNA prognostic signature for osteosarcoma.
Front. Endocrinol. 13:987942.
doi: 10.3389/fendo.2022.987942

COPYRIGHT
© 2022 Liu, Liu, Feng, Li, Zhang, Li, Tu and He. This is an open-access article distributed under the terms of the Creative Commons Attribution License (CC BY). The use, distribution or reproduction in other forums is permitted, provided the original author(s) and the copyright owner(s) are credited and that the original publication in this journal is cited, in accordance with accepted academic practice. No use, distribution or reproduction is permitted which does not comply with these terms.

Identification of cuproptosis-related lncRNA prognostic signature for osteosarcoma

Binfeng Liu[1,2†], Zhongyue Liu[1,2†], Chengyao Feng[1,2], Chenbei Li[1,2], Haixia Zhang[3], Zhihong Li[1,2], Chao Tu[1,2*] and Shasha He[3*]

[1]Department of Orthopaedics, The Second Xiangya Hospital, Central South University, Changsha, China, [2]Hunan Key Laboratory of Tumor Models and Individualized Medicine, The Second Xiangya Hospital of Central South University, Changsha, China, [3]Department of Oncology, The Second Xiangya Hospital, Central South University, Changsha, China

Background: Copper is an indispensably mineral element involved in various metabolic processes and functions in the active sites of many metalloproteins. Copper dysregulation is associated with cancers such as osteosarcoma (OS), the most common primary bone malignancy with invasiveness and metastasis. However, the causality between cuproptosis and OS remains elusive. We aim to identify cuproptosis-related long non-coding RNAs (lncRNAs) for osteosarcomatous prognosis, immune microenvironment response, and immunotherapy.

Methods: The Person correlation and differential expression analysis were used to identify differentially expressed cuproptosis-related lncRNAs (CRLs). The univariate, least absolute shrinkage and selection operator (LASSO), and multivariate Cox regression analysis were performed to construct the CRL signature. The Kaplan–Meier (K-M) survival analysis, receiver operating characteristic (ROC) curve, internal validation, independent prognostic analysis, and nomograph were used to evaluate the prognostic value. The functional enrichment, tumor microenvironment, immunotherapy and chemotherapy response between the two distinct groups were further explored using a series of algorithms. The expression of signature CRLs was verified by real-time quantitative polymerase chain reaction (RT-qPCR) in OS cell lines.

Results: A novel CRL signature consisting of four CRLs were successfully identified. The K-M survival analysis indicated that the OS patients in the low-risk groups had a better prognosis than that in the high-risk group. Then, the ROC curve and subgroup survival analysis confirmed the prognostic evaluation performance of the signature. Equally, the independent prognostic analysis demonstrated that the CRL signature was an independently predicted factor for OS. Friends analysis determined the hub genes that played a critical role in differentially expressed genes between two distinct risk groups. In addition, the risk score was related to immunity status, immunotherapy response, and chemotherapeutic drug sensitivity. Finally, the expression of these signature

CRLs detected by RT-qPCR was consistent with the bioinformatic analysis results.

Conclusion: In summary, our study confirmed that the novel CRL signature could effectively evaluate prognosis, tumor immune microenvironment, and immunotherapy response in OS. It may benefit for clinical decision-making and provide new insights for personalized therapeutics.

KEYWORDS

osteosarcoma, cuproptosis, metabolism, lncRNA, immunotherapy, tumor microenvironment

Introduction

Osteosarcoma (OS) is a malignant tumor derived from mesenchymal cells, which most commonly occurs in children and adolescents (1). As there is no apparent clinical manifestation in early OS, the most diagnosed patients are already in advanced stages, accompanied by distant metastasis (2). Currently, the long-term survival rate for the localized OS is approximately 68%, while it is still less than 30% in patients with recurrence or metastasis (3, 4). Meanwhile, the treatment for OS has been limited improved over the last three decades, especially in patients with multidrug resistance, recurrence or lung metastasis (5, 6). This is mainly attributed to the lack of knowledge of the pathogenic mechanisms (7). To this end, it is urgent to disclose effective prognostic biomarkers and promising signatures.

Long non-coding RNA (lncRNA) refers to non-coding RNAs longer than 200 nucleotides, a large class of gene transcripts encoded by the genome, but most do not encode proteins (8). Accumulating evidence shows that lncRNAs play critical roles in regulating cancer proliferation, metastasis, cycling, and programmed death (9–11). LncRNA HIF2PUT was demonstrated to inhibit the proliferation, migration, and invasion of osteosarcoma cells by regulating HIF2 expression (12). Iron metabolism-related lncRNA signature has also been proved to predict survival outcomes for OS (13). For instance, Zhijie Xu et al. demonstrated that the ferroptosis-related lncRNA signature could precisely predict prognosis and immune response for hepatocellular cancer (14). Therefore, metal ions regulated lncRNA signature would be prognostic candidates for OS.

Copper is an intracellular trace metal that plays an integral role in various metabolic processes. Cuprotosis is a new form of precisely regulated programmed cell death, wherein excess intracellular copper induces proteotoxicity and dysfunction of the mitochondrial tricarboxylic acid (TCA) cycle *via* lipoylated dihydrolipoamide S-acetyltransferase (DLAT) aggregation (15) LncRNAs were implied as a crucial role in copper-induced toxicity (16). Therefore, we reasoned that cuproptosis-related lncRNAs (CRLs) might be a promising biomarker for OS. Here we report the identification of prognostic CRL signature, the underlying mechanism, and *in vitro* experimental validation. This could be used for individualized survival prediction and to develop more effective strategies for systemic treatment.

Abbreviations: OS, osteosarcoma; CRL, cuproptosis-related lncRNA; LASSO, least absolute shrinkage and selection operator; K-M, Kaplan–Meier; DLAT, dihydrolipoamide S-acetyltransferase; TCA, tricarboxylic acid; lncRNA, long non-coding RNA; GSEA, gene set enrichment analysis; GSVA, gene set variation analysis; GEO, Gene Expression Omnibus; TARGET, Therapeutically Applicable Research To Generate Effective Treatments; PCA, principal component analysis; ROC, receiver operating characteristic; GO, Gene Ontology; KEGG, Kyoto Encyclopedia of Genes and Genomes; BP, Biological Process; CC, Cellular Component; MF, Molecular Function; PPI, protein-protein interaction; ESTIMATE, Estimation of Stromal and Immune Cells in Malignant Tumors using the Expression Data; ssGSEA, single sample gene set enrichment analysis; Submap, subclass mapping; IC50, half maximal inhibitory concentration; ATCC, American Type Culture Collection; DMEM/F12, Dulbecco's Modified Eagle Medium/Nutrient Mixture F12; MEM, minimum essential medium; DMEM, Dulbecco's Modified Eagle's medium; RT-qPCR, Real Time Quantitative Polymerase Chain Reaction; AUC, areas under the curve.

Materials and methods

Data sources

To explore differentially expressed CRLs in OS, we downloaded the GSE126209 dataset from the Gene Expression Omnibus (GEO, https://www.ncbi.nlm.nih.gov/geo/) database. The mRNA and lncRNA data of six normal and OS tissues were extracted from GSE126209 for further study. Meanwhile, the gene profile and corresponding clinical information of OS patients were downloaded from the Therapeutically Applicable Research To Generate Effective Treatments (TARGET, https://

ocg.cancer.gov/programs/target) database for the subsequent CRLs signature construction and related bioinformatics analysis. These expression data were further normalized by log2 (expression + 1) transformation. The detailed clinical information of the OS cohort from the TARGET database is shown in Table S1. The above expression profile was normalized to remove nonbiological impact and correct for systematic data. The cuproptosis-related genes in this study were extracted from a previous paper (15) and contained ten cuproptosis-related genes. The detailed information of these genes is displayed in Table S2.

Differential expressed lncRNA in OS

The principal component analysis (PCA) was utilized for OS tissue and normal tissue to visualize the differences in expression patterns. To identify differentially expressed lncRNAs between OS and normal tissue, we performed the differential analysis utilizing package "limma" in R software (17). The screening thresholds were $|\log2FC| \geq 1$ and adjusted P-value < 0.05.

Identification of CRLs in OS

We conducted the Pearson co-expression analysis to obtain differentially expressed CRLs in OS. Initially, Spearman correlation coefficients were calculated based on the expression value of cuproptosis-related genes and each lncRNA to identify CRLs ($|R^2| > 0.3$ and $p<0.05$) (18). Subsequently, the CRLs were intersected with those mentioned above differentially expressed lncRNAs to select differentially expressed CRLs for further investigation.

Screen CRLs are associated with the prognosis of OS

After selecting the differential expressed CRLs, the univariate COX analysis was performed to identify the CRLs associated with the prognosis of OS. The prognostic CRLs with p-value < 0.05 were screened as candidate lncRNAs for the cuproptosis-related lncRNAs prognostic signature and following analysis.

Construction and validation of the CRL signature

The OS cohort was randomly separated into a training cohort and a testing cohort in a 1:1 ratio using the "caret" package. The training cohort was used for signature building, while the testing cohort and the entire cohort were employed for validation. Primarily, the prognosis-related CRLs are subject to the least absolute shrinkage and selection operator (LASSO) Cox regression analysis to narrow down the candidate CRLs. Subsequently, the Multivariate Cox regression analysis was performed to further screen genes to optimize the CRL prognostic signature. The cuproptosis-related prognostic risk scores of each OS patient were calculated using the following formula: risk score = Σ ($Coef_i$ * Exp_i), where $Coef_i$ and Exp_i represent the corresponding coefficient and expression level of each lncRNA, respectively. Next, the OS patients in the training cohort were assigned to low-risk and high-risk groups according to the median risk score in the training cohort. The Kaplan–Meier (K-M) survival analysis compared the overall survival between the two distinct risk groups. The receiver operating characteristic (ROC) curve was further drawn to assess the predictive accuracy of the CRL prognostic signature. The risk score of each OS patient in the testing cohort and the entire cohort was calculated according to the same formula. Then, the same methodology described above was conducted to evaluate the potential and applicability of the novel signature. For each CRLs included in the novel prognostic signature, their expression levels, their relationship with cuproptosis-related genes, and their respective correlations were further explored.

Prognostic and independent analysis

The risk scores are combined with clinical information for subsequent investigation, including survival time, survival status, gender, age, metastatic status, and tumor location. To exclude the possible confounding effects from other clinical factors, we performed a subgroup survival analysis according to the age, gender, and metastasis status of the OS. Subsequently, the univariate and multivariate Cox analyses were used to determine whether the novel CRLs signature had an independent prognostic ability for OS.

Differential expression analyses between distinct risk groups

To assess differences in expression profiles between high-risk and low-risk subgroups, the differentially expressed genes between the two distinct risk groups were identified by using the limma package ($|\log2FC|>0.585$ and $FDR<0.05$). The volcano plot and clustered heat plot were used further to display the result of the differentially expressed analysis. In addition, the distribution of patients with different risk scores was displayed by utilizing PCA.

Function enrichment analysis

To further explore the functional differences between the differential genes in the distinct risk groups, we used the

"clusterProfiler" package to carry out Gene Ontology (GO) and the Kyoto Encyclopedia of Genes and Genomes (KEGG) enrichment analysis (19). The GO analysis included the Biological Process (BP), Cellular Component (CC), and Molecular Function (MF). Further, the bubble diagrams were used to visualize the enrichment results. The adjusted nominal P-values < 0.05 was selected as thresholds of significance.

Protein-protein interaction network and friends analysis

Next, a PPI network was constructed to identify hub genes among the differentially expressed genes using the String database (https://cn.string-db.org/cgi/input) with default parameters. Meanwhile, the PPI network was visualized using Cytoscape software (version 3.9.0). In addition, the Friends analysis was further performed using the "GOSemSim" package to screen out hub genes (20). Ultimately, the top ten genes screened by Friends analysis were visualized and presented as hub genes for subsequent analysis.

The expression and prognosis value of top ten hub genes

After obtaining the cuproptosis-related hub genes based on the above analysis, we further analyzed their function in OS. The co-expression analysis was used to explore the association between hub genes and cuproptosis. Additionally, the K-M survival and ROC curves were further used to evaluate the prognostic performance of the top 10 hub genes in OS.

Gene set enrichment analysis and gene set variation analysis

To further explore the molecular and biological differences between high and low-risk groups, we performed GSEA analysis by package "clusterProfiler". The KEGG dataset was extracted from the molecular signature database (https://www.gsea-msigdb.org/gsea/msigdb), and the $p < 0.05$ were selected as thresholds of significance. The GSVA was further performed to analyze the enrichment of biological processes and pathways due to CRLs risk level through package "GSVA " in R (21). Subsequently, the "limma" package was used to perform the differential analysis to screen the significantly different pathways (|log2FC|>0.1 and P-value<0.05). The screened significantly different pathways were visualized as a clustered heatmap.

Assessment of immune microenvironment and immune cell infiltration

Currently, several reliable approaches have been established for quantifying immune infiltration and the immune microenvironment in tumors based on transcriptome data, such as Estimation of Stromal and Immune Cells in Malignant Tumors using the Expression Data (ESTIMATE) (22) and single sample gene set enrichment analysis (ssGSEA) algorithm (23). In our study, we calculated and compared the immune microenvironment and immune-infiltrating cell content between high-risk and low-risk groups. The ESTIMATE is an algorithm that can detect the tumor purity and activity of immune and stromal cells in the immune microenvironment by transforming gene expression. Briefly, the ESTIMATE algorithm was used to calculate the immune score of each OS patient and then compare the difference in ESTIMATE score between the high- and low-risk groups. Also, infiltration levels of 28 immune cells were inferred by the ssGSEA algorithm and compared in the different risk groups.

Immunotherapy response and drug sensitivity analysis

The immunotherapy response difference was compared using subclass mapping (submap), with lower P-values indicating a higher similarity. Additionally, the "pRRophetic" package was utilized to predict the half maximal inhibitory concentration (IC50) of the chemotherapeutic drug, which indicates the effectiveness of a substance in inhibiting a specific biological or biochemical process (24).

Nomogram and calibration

To provide a scoring system that predicts the individual probability of patients' prognosis, we established a prognostic nomogram, which can assess the probable 1-year, 3-year and 5-year survival of OS. Meanwhile, we also drew a calibration curve to validate the predictive value of the constructed nomogram, which visualizes the consistency between the actual result and the probability predicted by the nomogram. The "rms" package was used to plot the nomogram and calibration curve. In addition, the ROC curve was applied to investigate the prognostic value of the nomogram.

Cell culture

The normal osteoblast cell line (hFOB1.19) was purchased from American Type Culture Collection (ATCC) and cultured in Dulbecco's Modified Eagle Medium/Nutrient Mixture F12 (DMEM/F12) medium (Gibco, United States). Human osteosarcoma cell lines 143B, HOS, and MG-63 were purchased from ATCC and cultured in a minimum essential medium (MEM) (Gibco, United States). Human osteosarcoma cell line ZOS was gifted by Prof. Kang Tiebang (Sun Yat-Sen University, China) and cultured in Dulbecco's Modified Eagle's medium (DMEM) (Gibco, United States). Human osteosarcoma cell line SJSA-1 was purchased from ATCC and cultured in RPMI-1640 medium (Gibco, United States). All the cell lines were cultured with 10% fetal bovine serum (Gibco, United States) and 1% penicillin-streptomycin solution (NCM Biotech, China) besides SAOS-2, which was cultured with 15% fetal bovine serum (Gibco, United States) and 1% penicillin-streptomycin solution (NCM Biotech, China). All the cell lines were cultured in a humidified atmosphere with 5% CO2 at 37°C.

Real-time quantitative polymerase chain reaction

Total cellular RNA was drawn from cell lines utilizing RNA Express Total RNA Kit (M050, NCM Biotech, China). Next, total RNAs were used for cDNA synthesis with Revert Aid First Strand cDNA Synthesis Kit (K1622, Thermo Scientific, United States). Subsequently, the expression level of each gene was quantified by Hieff qPCR SYBR Green Master Mix (High Rox Plus) (11203ES, YEASEN Biotech Co., Ltd, China) and calculated with the $2^{-\Delta\Delta CT}$ method. GAPDH was used as the internal reference for normalization. The primer sequences are listed in Table S3.

Statistical analysis

All statistical analyses and plots in the present study were performed in R version 4.0.5. The differences in the expression of signature CRLs between OS and normal cells were assessed using independent t-tests. Spearman correlation analysis was used to determine correlation. The Chi-square test was used to analyze the differences in clinical characteristics between the distinct risk groups. $P < 0.05$ was defined as statistical significance.

Results

Identification of cuproptosis-related differentially expressed lncRNAs

The flowchart of the study is illustrated in Figure S1. After batch effect correction and normalization, the mRNA and lncRNA expression profiles were extracted (Figure S2). Based on the enrolled criteria, a total of 326 differentially expressed lncRNAs between the OS tissue and normal tissue were identified, of which 278 were upregulated, and 48 were downregulated (Figures 1A, B). Then, Spearman correlation

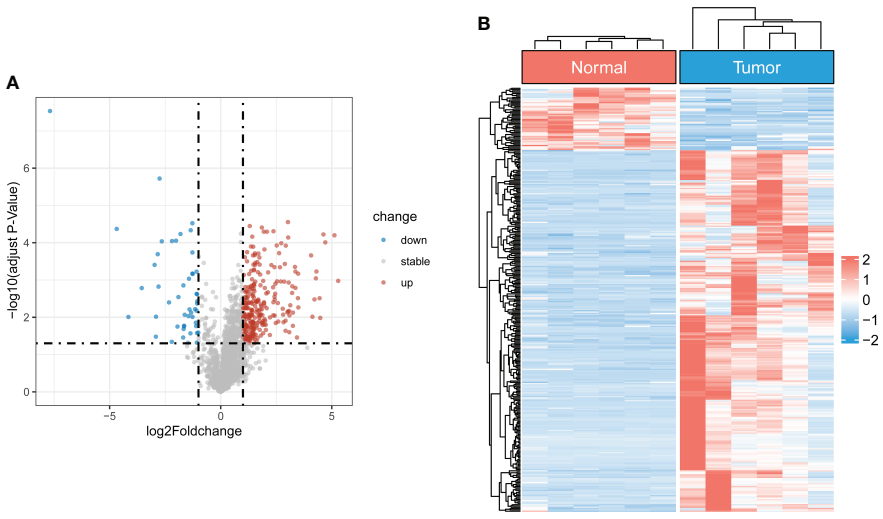

FIGURE 1
Identification of differentially expressed CRLs in OS **(A)** The volcano plot of differentially expressed lncRNAs. Blue represent down-regulated CRLs, and red represents upregulated CRLs. **(B)** Hierarchically clustered heat maps of differentially expressed lncRNAs. Red and blue represent normal and tumor tissues, respectively.

analysis was conducted between lncRNAs and cuproptosis-related genes in the OS According to the inclusion parameters of correlation coefficient ($|R^2|$) > 0.3 and p-value <0.05, there were 307 CRLs identified in OS (Table S4). Taken together, all CRLs were differentially expressed in OS (Table S5).

Derivation and validation of a CRLs prognostic signature

To screen the prognostic value of differentially expressed CRLs, we performed the univariate Cox regression analysis to explore the association between the CRLs and the overall survival of OS. As a result, 31 prognostic CRLs were identified for signature construction (Table S6). Then, these prognostic CRLs were subject to the LASSO method in the training group to determine candidate signature CRLs (Figure S3). Next, the multivariate Cox regression analysis identified the optimal CRLs prognostic risk signature composed of UNC5B-AS1, TIPARP-AS1, RUSC1-AS1 and LINC02315 (Figure 2A). In the novel CRLs signature, the corresponding cuproptosis risk score of each OS patient was calculated as the following formula: Risk Score = UNC5B-AS1*1.60588 + TIPARP-AS1*1.343192 + RUSC1-AS1*1.585861 - LINC02315*2.66553 (Table S7). According to this cutoff value of risk score, the OS patients were classified into low- and high-risk groups. The risk score distribution and survival status plot demonstrated that the death cases were mainly distributed in the high-risk group (Figure 2B). The K-M survival analysis indicated that the OS patients in the low-risk group showed a significantly better overall survival than those in the high-risk group (Figure 2C). The areas under the curve (AUC) of the ROC curve remained above 0.75 at 1, 3 and 5 years, which means the novel CRLs signature had predictive performance in predicting survival risk (Figure 2D). Notably, we further performed a validation analysis in the testing cohort and the entire cohort to determine the predictive value of the novel CRLs signature. As expected, the validation results on the test cohort and the entire cohort are similar to those of the training

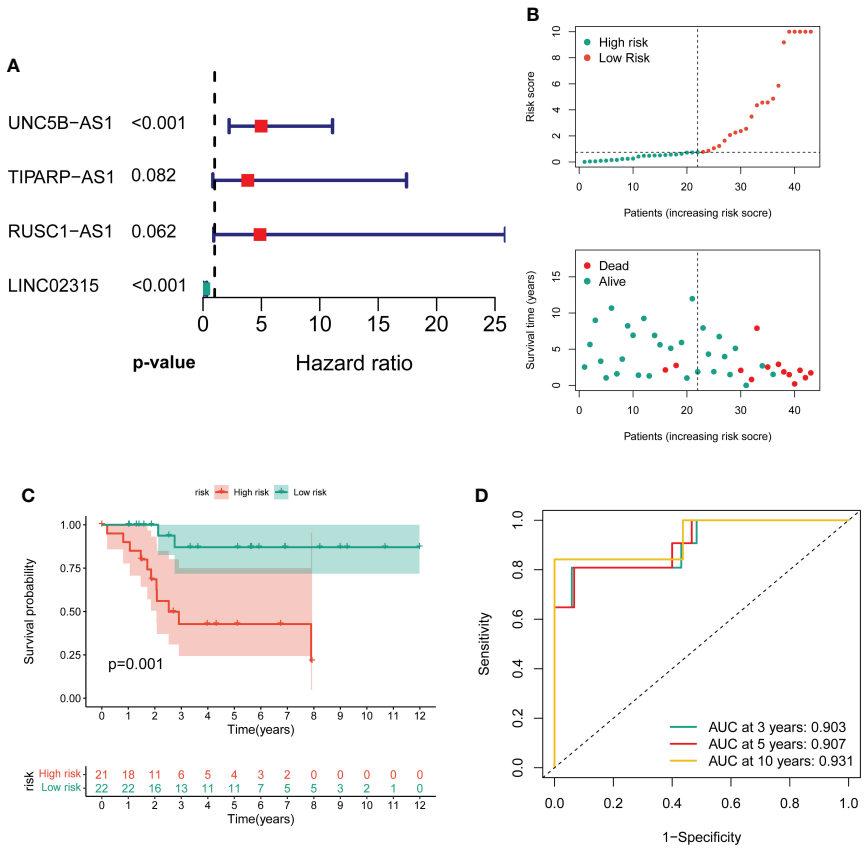

FIGURE 2
Construction of the novel CRL signature. **(A)** Forest plot of multivariate cox regression analysis for prognostic genes. **(B)** The distribution of the risk scores and the distributions of overall survival status and risk score in the training groups. **(C)** Kaplan–Meier analysis of the overall survival between the two distinct risk groups. **(D)** ROC curves to predict the sensitivity and specificity of 3-, 5-, and 10-year survival according to the novel cuproptosis-related signature.

set (Figures S4, S5). Together, these findings implied that the novel CRLs signature had a great prognostic prediction value for OS.

The independent prognostic value of signature

To further exclude the impacts of other clinical characteristics on the prognostic values of the novel signature, we performed a subgroup survival analysis according to the baseline characteristics. As shown in Figures 3A–F, the OS cohort in the high-risk group had a worse prognosis than that in the low-risk group, regardless of the clinical subgroup. Further, the univariate Cox analysis demonstrated that the novel CRLs signature was associated with the prognosis of OS patients (HR: 6.233, 95%CI: 2.371-16.388) (Figure 3G). Besides, the multivariate Cox analysis further revealed that the signature was an independent factor for the prognosis of patients with OS (HR: 8.386, 95%CI: 3.098-22.701) (Figure 3H). Collectively, these results indicated that this novel CRLs lncRNA signature could reliably serve as an independent prognostic factor for OS.

The association between signature genes with cuproptosis in OS

By performing correlation analysis, we have seen that the four signature CRLs were closely related to cuproptosis-related genes (Figure S6). Also, there was a significant positive association between the four risk CRLs (Figure S6). Subsequently, to further explore the relationship between these four CRLs and the novel signature, we analyzed the expression levels of these four CRLs between different risk groups. We observed an upregulated expression level of UNC5B-AS1, TIPARP-AS1, and RUSC1-AS1 in the high-risk group compared to the low-risk group (Figures 4A–C). On the contrary, LINC02315 was downregulated in the high-risk group, albeit not statistically significantly (Figure 4D). Meanwhile, to assess the prognostic effects of each signature CRLs on OS, we performed KM survival analysis to investigate the relevance of these four CRLs to the prognosis of OS. We found that all four signature CRLs had pronounced prognostic effects in OS (Figures 4E–H). Among them, UNC5B-AS1, TIPARP-AS1, and RUSC1-AS1 were risk factors for OS, while LINC02315 was a protective gene for OS. In sum, it is confirmed that there was an independent relevance between each signature CRLs and the cuproptosis and prognosis of OS.

Differentially expressed and functional enrichment analysis between distinct risk groups

A total of 296 differential expressed genes between high-risk and low-risk groups were identified by differential analysis (Table S8). The results demonstrated a marked difference in mRNA expression profiles between high- and low-risk groups (Figure S7). Also, we observed that most differential genes were upregulated in the high-risk group from the cluster heatmap and volcano plot (Figures 5A, B). Meanwhile, we performed a PPI network analysis of differentially expressed genes using the STRING database for subsequent hub genes identification (Figure S7). In addition, the GO and KEGG analyses were utilized to explore potential differences in biological functions and signaling pathways between different risk groups classified by the novel CRLs signature. The GO analysis showed that the CRLs signature was associated with bone metabolism-related functions (Figure 5C). The KEGG results indicated that the OS patients in the high-risk group were significantly enriched in some cancer-related pathways, such as the Wnt signaling pathway, TGF-beta signaling pathway, and Cell adhesion molecules (Figure 5D). Hence, these results implied a significant molecular functional difference between the two distinct risk groups and the novel CRLs signature was mainly associated with the tumorigenesis pathway in OS.

Identification of cuproptosis-related hub genes

To further identified potential hub genes associated with cuproptosis, we screened the top ten hub genes using Friends analysis. These ten hub genes may play potential roles in the molecular functional processes relevant to cuproptosis (Figure 5E). Meanwhile, there was a pronounced co-expression relationship between these ten hub genes and the signature CRLs (Figure 5F). Additionally, to further investigate the survival impact of these hub genes in OS, we used K-M survival analysis to detect the correlation between the expression of each gene and the prognosis of OS. Also, the AUC of the ROC curve was calculated to evaluate the predictive performance of each hub gene. From the survival analysis and ROC curve, it can be seen that the overexpression of DIRAS1, CDCA7, FGFBP2, PMAIP1, TBRG1, and FAM162A predicted poor prognosis and had good predictive performance (Figures S8, S9). However, the predictive role of DDIT4L, SRGN, VAMP5, and MAB21L2 for OS needs to be further confirmed in the future (Figures S8, S9).

10.3389/fendo.2022.987942

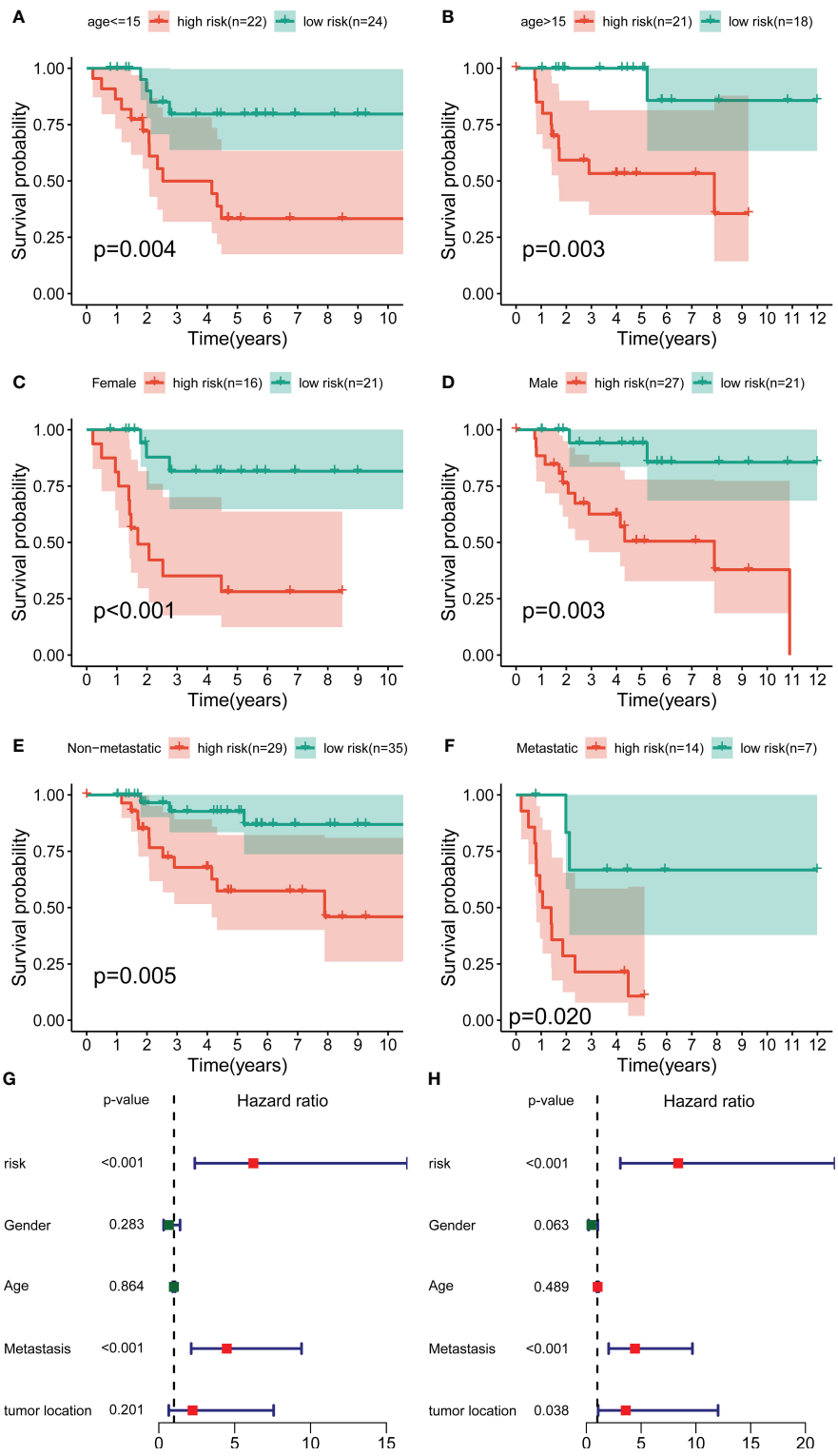

FIGURE 3
Independent prognostic value of the novel CRL signature. **(A–F)** K–M survival curves of overall survival stratified by age, gender, and metastasis status between low- and high-risk groups. **(G, H)** Univariate and multivariate Cox regression analyses demonstrated the novel CRL signature as an independent prognostic factor for OS.

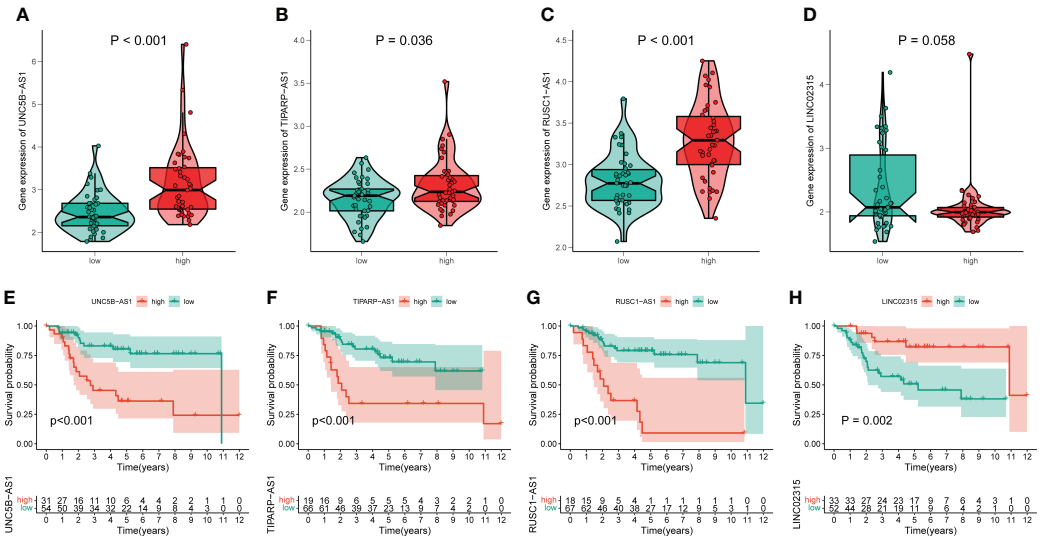

FIGURE 4
The association of these signature lncRNAs with OS. **(A–D)** The expression level of each signature lncRNAs in the low- and high-risk groups. Green and red represent the low-risk group and high-risk group, respectively. **(E–H)** The K-M survival curves for these four signature lncRNAs in OS.

The immune features between distinct risk groups

To further determine the molecular functional differences between high- and low-risk groups, we implemented GSEA and GSVA. The GSEA result showed that the high-risk groups also enriched several tumor-related pathways, which further confirmed that the novel CRLs signature was relevant to the development of OS (Figure 6A). Also, the GSVA demonstrated the OS patients with lower CRL risk scores were significantly enriched in immune-activated pathways, such as antigen process and presentation, cytokine-cytokine receptor interaction, Nod-like receptor interaction, and TOLL-like receptor signaling pathway, implying there was a significant difference in the tumor immune microenvironment between the two distinct groups (Figure 6B). Therefore, we investigated the role of the CRLs signature in the immune microenvironment of OS. Initially, the ESTIMATE analysis displayed that the low-risk group had a higher TME score (stromal score, immune score, and estimate score) than the high-risk group (Figure 6C). For the TME score, higher stromal scores or immune scores represented larger amounts of immune or stromal cellular components in the TME, while estimate scores indicated the sum of stromal or immune scores. Similarly, the ssGSEA revealed significant differences in the infiltration of most immune cells between the two risk groups (Figure 6D). The activated B cell, activated CD8 T cell, activated dendritic cell, CD56bright natural killer cell, central memory CD8 T cell, effector memory CD8 T cell, gamma delta T cell, immature B cell, immature dendritic cell, macrophage, MDSC, monocyte, natural killer cell, natural killer T cell, neutrophil, regulatory T cell, type 1 T helper cell, and type 2 T helper cell showed a more significant infiltration in the CRLs low-risk groups (Figure S10). In addition, the four signature CRLs and most cuproptosis-related hub genes were negatively relevant to the infiltration of immune cells (Figure S11). Ultimately, the heatmap revealed no significant differences between the two distinct risk groups in terms of clinical characteristics (Figure S11). Altogether, these findings suggested that the activated immune status may account for the better prognosis of OS in the low-risk group.

Immunotherapy and chemotherapy drugs response

Given the clinical role of immunotherapy and chemotherapy in OS, we then explored the relationship between the CRL risk score and immunotherapy response and drug sensitivity. Briefly, the submap demonstrated that the OS patients with low CRL risk scores were more likely to respond to anti-PD1 therapy, which may provide new insight into the immunotherapy for OS (Figure 7A). Next, we compared the difference in sensitivity to anti-tumor agents between the two distinct risk groups. As shown in Figures 7B–F, the patients in the low-risk group had lower IC50 values for Bexarotene, Bortezomib, Dasatinib, DMOG, and Lapatinib, which means these low-risk patients have a better response to these drugs. In contrast, the patients with high-risk scores were more likely to respond to ABT.263, ATRA, BIRB.0796, PD.173074, and QS11(Figures 7G–K). Overview, these findings demonstrate that the novel CRLs signature may help to predict the efficacy of immunotherapy and chemotherapy.

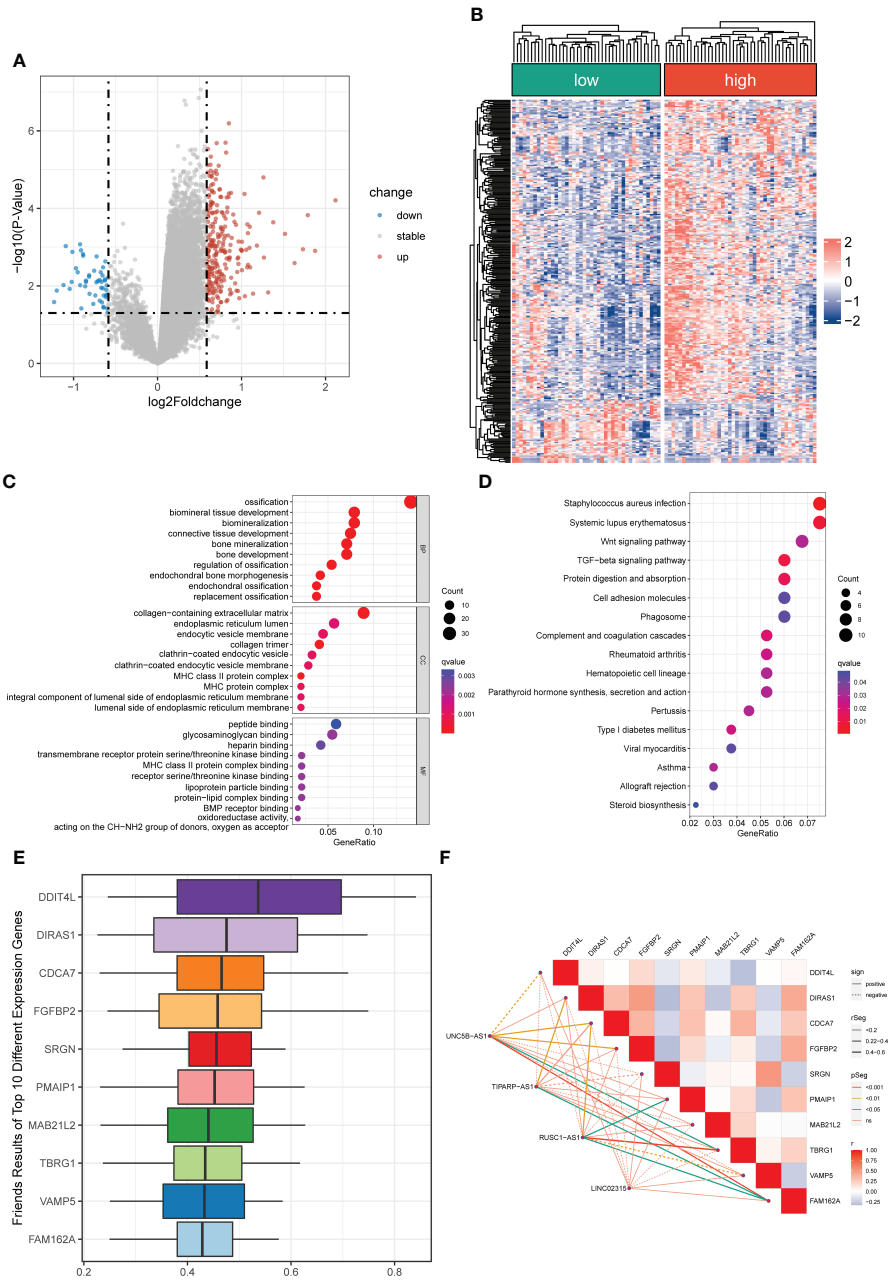

FIGURE 5
Differentially expressed and functional enrichment analysis between distinct risk groups. **(A, B)** The volcano plot and heatmap of differentially expressed genes between the low- and high-risk groups. **(C, D)** The GO analysis and KEGG enrichment pathway analysis between different risk groups. **(E)** The Friends analysis of GO-related genes. **(F)** The association between these ten hub genes and four signature lncRNAs.

Construction of the nomogram

To better utilize the novel CRLs signature for clinical application, we constructed a predictive cuproptosis-related prognostic nomogram based on the clinical characteristics, including age, gender, metastasis, and the CRL risk score. As presented in Figure 8A, the nomogram could predict the 1-, 3-, and 5-year probably overall survival rate. Notably, the prognosis predictive performance for OS is shown by the calibration curves. The calibration curve for the predictive probability showed that the nomogram-predicted overall survival was in accordant agreement with the actually observed overall survival of OS (Figure 8B). Additionally, the 1-, 3-, and 5-year AUC values of the nomogram were 0.949, 0.836, and 0.858,

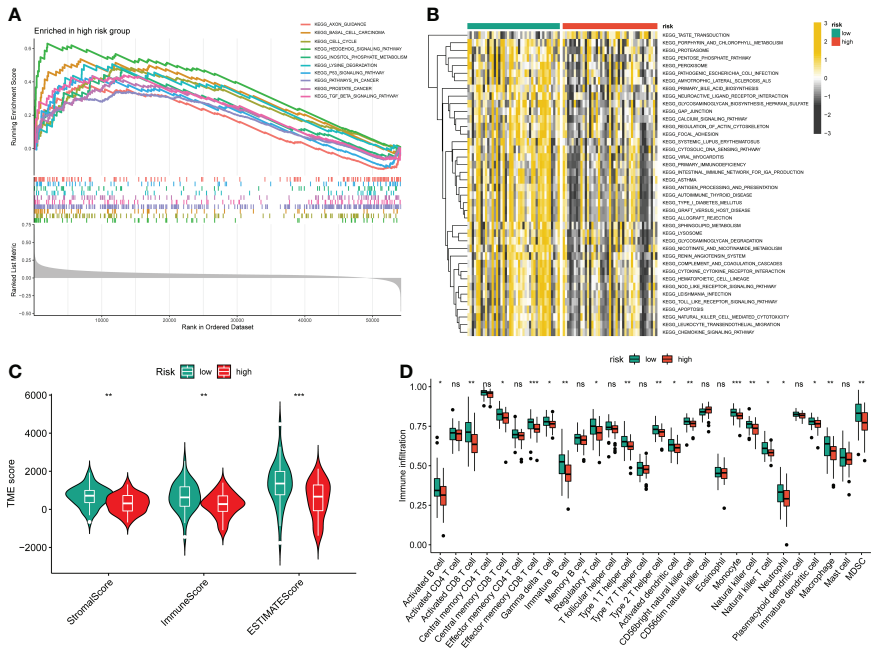

FIGURE 6
The relationship between the novel CRLs signature and tumor immune microenvironment in OS. **(A)** The GSEA between the two distinct risk groups. **(B)** The heatmaps of GSVA displayed signaling pathways between the high-risk and low-risk groups. **(C)** The TME score between distinct groups. **(D)** Box plot indicating the relative abundance of immune cells based on ssGSEA in the distinct risk groups. *p < 0.05, **p < 0.01, ***p < 0.001.

respectively (Figure 8C). Hence, these results imply that the CRLs prognostic signature was stable and accurate, which may be used in the clinical management of OS patients.

Validation of the expression of signature lncRNAs

To further evaluate the expression level of these four signature CRLs, we utilized their expression in the cell lines using RT-qPCR. As presented in Figures 9A, B, compared with those in the normal cell line (hFOB1.19), LINC02315 was downregulated in the OS cell line (including 143B, HOS, and MG63), while TIPARP-AS1 exhibited the opposite trend in 143B, HOS, and MG63 cell line. In addition, the UNC5B-AS1 and RUSC1-AS1 had a higher expression level in the OS cell line than in the normal cell line (Figures 9C, D). In sum, these results further validated the previous accuracy of our previous bioinformatics analysis.

Discussion

In the present study, we identified 120 differentially expressed CRLs in OS *via* Pearson correlation and differential expression analysis. Then, we obtained 31 CRLs associated with the prognosis using univariate regression analysis and constructed a CRL prognostic signature consisting of four prognostic CRLs by LASSO and multivariate regression analysis. Next, the novel CRL signature was evaluated utilizing survival analysis, ROC curve, internal validation, independent prognostic analysis, and *in vitro* experiments. As far as we are aware, our research first analyzed the CRLs in OS systematically and comprehensively, revealing that the novel CRL signature could be used as a promising prognostic indicator for OS. Subsequently, we found that DIRAS1, CDCA7, FGFBP2, PMAIP1, TBRG1, FAM162A, DDIT4L, SRGN, VAMP5, and MAB21L2 are hub genes in the altered process between the two distinct risk groups. Interestingly, these genes are known to play a crucial role in tumorigenesis and development. In particular, Huan Liu et al. reported that DIRAS1 regulated by METTL3 and METTL14 could control the malignant progress of OS *via* regulating the ERK pathway (25). While the effects of CDCA7, FGFBP2, and FAM162A on OS remain unclear, their role in tumors has been documented during the last few years (26–28). For instance, CDCA7 regulate the expression of CCNA2 to facilitate the tumor progression of Esophageal Squamous Cell Carcinoma (28). Given the above analyses and previous investigations, these hub genes may be a potential molecular target for the modulation of cuproptosis in OS.

Next, the KEGG and GSEA demonstrated that the OS patients in the CRL high-risk group were primarily enriched

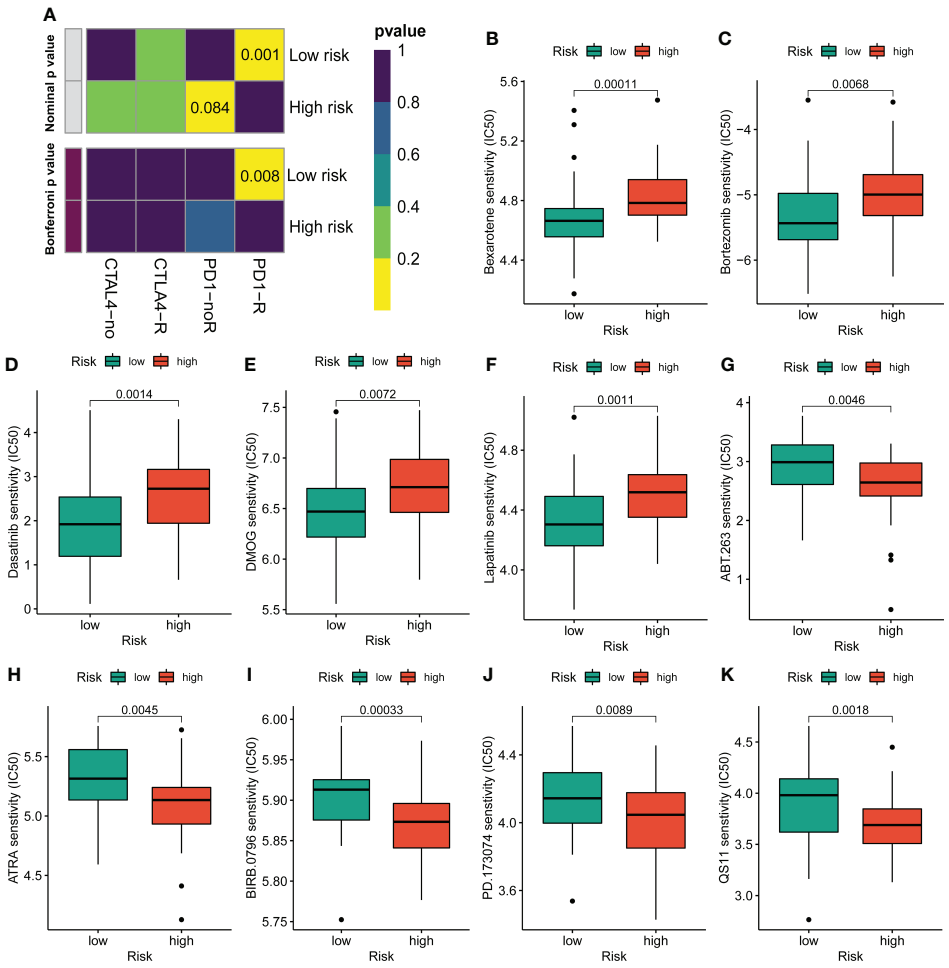

FIGURE 7
Assessment of immunotherapy and chemotherapy response efficacy in patients from different risk groups. **(A)** Sensitivity prediction of distinct groups to the two immune checkpoint inhibitors in the OS cohort. No response, noR; response, R. **(B–K)** The sensitivity to chemotherapeutic drugs was represented by the half-maximal inhibitory concentration (IC50) of chemotherapeutic drugs.

in tumor-associated biological processes, such as the Wnt signaling pathway, TGF-beta signaling pathway, and Cell adhesion molecules. These pathways have been documented to be associated with OS aggressive phenotypes. For example, NGX6 could inhibit the viability, invasion, and migration, while promoting the apoptosis of OS cell lines by suppressing the Wnt/β-catenin signaling pathway (29). This result suggests that the novel CRL signature in OS may be involved in these tumor-related signaling pathways. To further evaluate the tumor immune microenvironment in OS, we calculated the tumor microenvironment score and the degree of infiltration of different types of immune cells. Previous studies revealed that cancer patients with higher immune and stromal scores have an improved prognosis (30, 31). Consistently, our results exhibited that the low-risk OS patients had higher immune, stroma, and ESTIMATE scores than those in the high-risk group. Similarly, the ssGSEA results indicated that the infiltration rate of most immune cells in the high-risk group was lower than in the low-risk group. Some of them were reported to be tumor antagonistic immune cells (32, 33). In a previous study, the infiltration of activated CD8 T cells was proven to correlate to improved prognosis and survival of primary ovarian cancer (34). Furthermore, we also found that the four CRLs were positively relevant to the abundance of immune cells, implying the novel CRL signature could be used to assess the tumor immune microenvironment in OS. Therefore, it is reasonable to believe that a better tumor immune microenvironment may partly account for a better prognosis of OS patients in the low-risk group. Blocking the immune checkpoint therapy (such as PD-1 and CTLA-4) is a promising approach for various cancer (35). In

10.3389/fendo.2022.987942

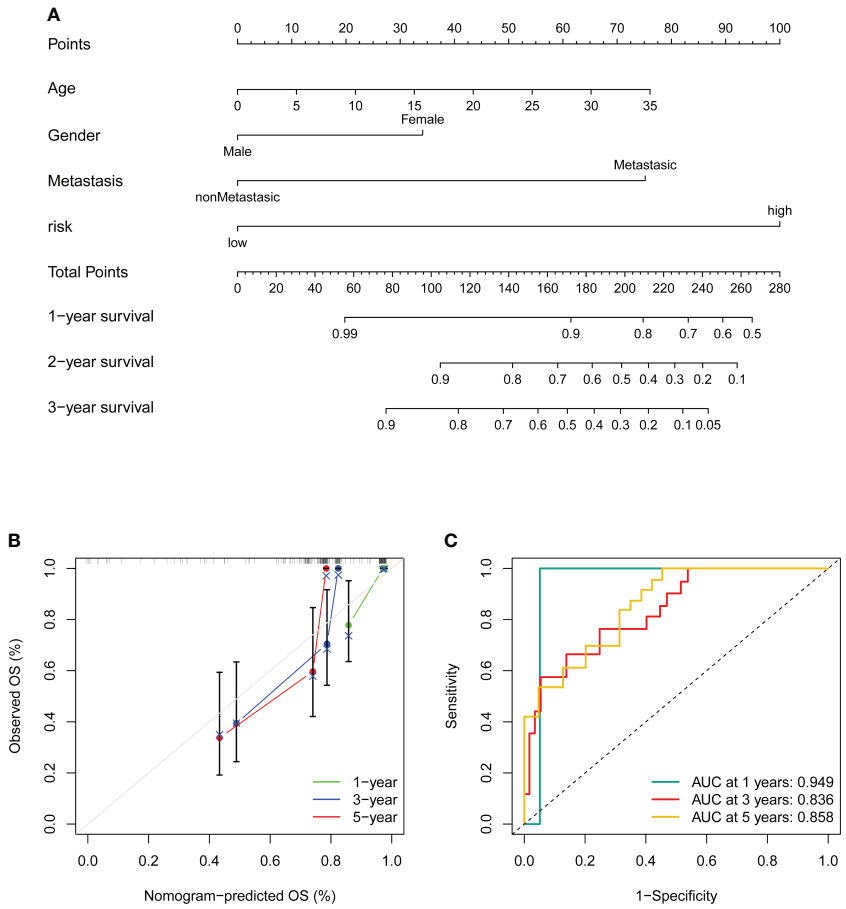

FIGURE 8
Construction and validation of a nomogram. **(A)** Nomogram for predicting the 1-, 3-, and 5- overall survival of OS patients. **(B)** Calibration curves of the nomogram for predicting the 1-, 3-, and 5- overall survival of OS patients. The dashed diagonal line in grey colour represents the ideal nomogram. **(C)** The ROC curves of the nomogram estimate the prognostic value of the nomogram.

the present study, we surprisingly found that the OS patients with lower risk scores are promising in response to anti-PD-1, suggesting that the novel CRL signature might be an underlying index for evaluating immunotherapy response in OS. In addition, we assessed the susceptibility to chemotherapeutics between the two distinct groups. We observed that the OS patients with different risk scores are different in sensitivity to chemotherapeutic drugs, which is beneficial in providing appropriate treatment options for OS. Importantly, we verified these four signature CRLs expressions in the OS cell. The expression trend was consistent with the previous bioinformatic analysis, which further proves the validity of the novel CRL signature. It is worth mentioning that some of these signature CRLs had been confirmed to play different functional roles in tumor progression. For instance, UNC5B-AS1 promotes the malignant progression of hepatocellular carcinoma, ovarian cancer, prostate cancer, lung cancer, and thyroid cancer (36–40). Notably, the tumor promotion role of RUSC1-AS1 has been well-characterized in OS (41, 42). Rui Jiang et al. reported that RUSC1-AS1 facilitate the malignancy of OS *via* the miR-101-3p-regulating Notch1 signaling pathway (41). As a candidate protective factor for lung squamous cell carcinoma, LINC02315 was diminished in lung squamous cell carcinoma tissue and had great predictive efficiency (43). Still, studies regarding the significance of TIPARP-AS1 in tumor development are not fully known. In our study, we observed that TIPARP-AS1 was elevated in OS cells and correlated with a poor prognosis of OS, but the specific roles of TIPARP-AS1 in OS need further exploration. Based on the above results and previous research, it is reasonable to believe the reliability of the novel CRLs signature.

Despite these promising findings, it is worth noting that some limitations do exist. First, the prognostic value of the novel CRLs signature needs to be further validated in prospective studies and clinical cohorts. In addition, the specific mechanisms of these signature CRLs in OS should be further confirmed using

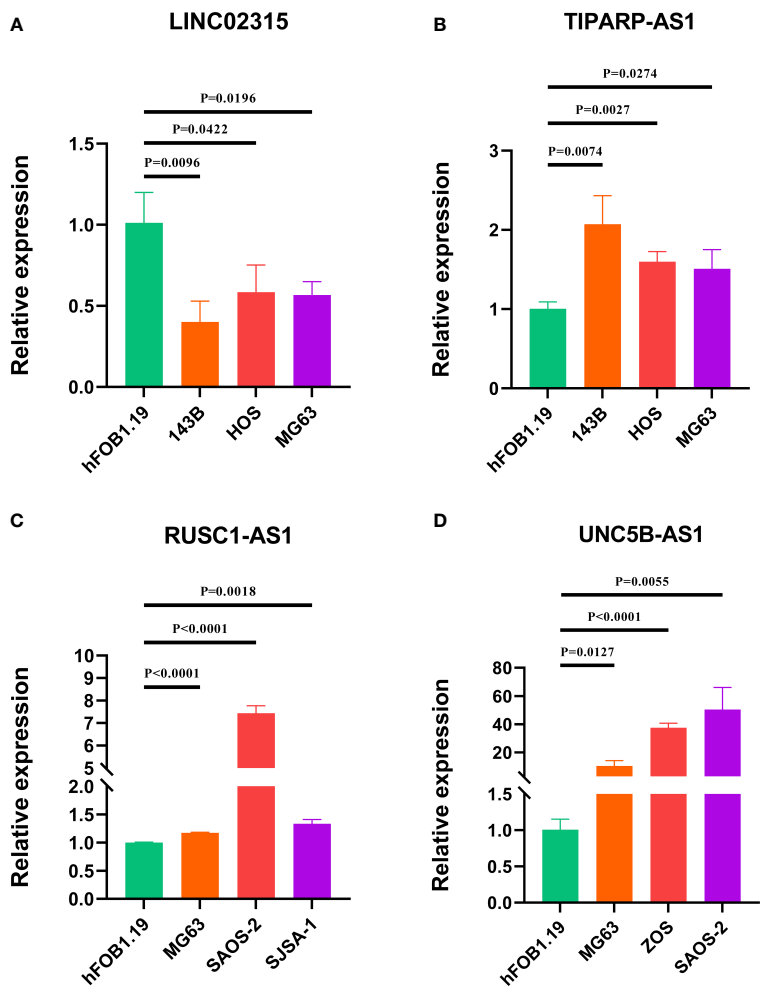

FIGURE 9
Verification of the expression of signature CRLs in OS cell lines by using RT-qPCR. **(A)** LINC02315. **(B)** TIPARP-AS1. **(C)** UNC5B-AS1. **(D)** RUSC1-AS1.

in vivo and *in vitro* experimental validation and further explore the relationship between the novel signature and tumor immunity microenvironment. We will incorporate these efforts into future studies.

Conclusion

In conclusion, we establish a novel signature composed of four CRLs that could robustly predict the prognosis of OS. In addition, the relationships between the CRL signature and tumor immune microenvironment, immunotherapy and chemotherapy response were preliminarily ascertained. It is reasonable to believe that our study may provide valuable insights into clinical decision-making and personalized therapeutic regimens basis for future research.

Data availability statement

The original contributions presented in the study are included in the article/Supplementary Material. Further inquiries can be directed to the corresponding authors.

Author contributions

SSH and CT contributed to the conception and made finalapproval of the version, BFL performed study concept and designand wrote the manuscript. ZYL performed the experiment. ZYL,CYF, CBL, HXZ, and ZHL helped with data analysis. All authorscontributed to the article and approved the submitted version.

Funding

This work was supported by the National Natural Foundation of China (81902745), Hunan Provincial Natural Science Foundation of China (2022JJ30843), the Science and Technology Development Fund Guided by Central Government (2021Szvup169), and Hunan Provincial Administration of Traditional Chinese Medicine Project (No. D2022117).

Conflict of interest

The authors declare that the research was conducted in the absence of any commercial or financial relationships that could be construed as a potential conflict of interest.

Publisher's note

All claims expressed in this article are solely those of the authors and do not necessarily represent those of their affiliated organizations, or those of the publisher, the editors and the reviewers. Any product that may be evaluated in this article, or claim that may be made by its manufacturer, is not guaranteed or endorsed by the publisher.

Supplementary material

The Supplementary Material for this article can be found online at: https://www.frontiersin.org/articles/10.3389/fendo.2022.987942/full#supplementary-material

References

1. Zhang C, He J, Qi L, Wan L, Wang W, Tu C, et al. Diagnostic and prognostic significance of dysregulated expression of circular RNAs in osteosarcoma. *Expert Rev Mol Diagn* (2021) 21(2):235–44. doi: 10.1080/14737159.2021.1874922

2. Gill J, Gorlick R. Advancing therapy for osteosarcoma. *Nat Rev Clin Oncol* (2021) 18(10):609–24. doi: 10.1038/s41571-021-00519-8

3. Sayles LC, Breese MR, Koehne AL, Leung SG, Lee AG, Liu HY, et al. Genome-informed targeted therapy for osteosarcoma. *Cancer Discovery* (2019) 9(1):46–63. doi: 10.1158/2159-8290.Cd-17-1152

4. Chen C, Xie L, Ren T, Huang Y, Xu J, Guo W. Immunotherapy for osteosarcoma: Fundamental mechanism, rationale, and recent breakthroughs. *Cancer Lett* (2021) 500:1–10. doi: 10.1016/j.canlet.2020.12.024

5. Ballatori SE, Hinds PW. Osteosarcoma: prognosis plateau warrants retinoblastoma pathway targeted therapy. *Signal Transduct Target Ther* (2016) 1:16001. doi: 10.1038/sigtrans.2016.1

6. Tu C, He J, Qi L, Ren X, Zhang C, Duan Z, et al. Emerging landscape of circular RNAs as biomarkers and pivotal regulators in osteosarcoma. *J Cell Physiol* (2020) 235(12):9037–58. doi: 10.1002/jcp.29754

7. Li Z, Li X, Xu D, Chen X, Li S, Zhang L, et al. An update on the roles of circular RNAs in osteosarcoma. *Cell Prolif* (2021) 54(1):e12936. doi: 10.1111/cpr.12936

8. Bhan A, Soleimani M, Mandal SS. Long non-coding RNA and cancer: A new paradigm. *Cancer Res* (2017) 77(15):3965–81. doi: 10.1158/0008-5472.Can-16-2634

9. Li J, Meng H, Bai Y, Wang K. Regulation of lncRNA and its role in cancer metastasis. *Oncol Res* (2016) 23(5):205–17. doi: 10.3727/096504016x14549667334007

10. Li Z, Dou P, Liu T, He S. Application of long noncoding RNAs in osteosarcoma: Biomarkers and therapeutic targets. *Cell Physiol Biochem* (2017) 42(4):1407–19. doi: 10.1159/000479205

11. Tu C, Yang K, Wan L, He J, Qi L, Wang W, et al. The crosstalk between lncRNAs and the hippo signalling pathway in cancer progression. *Cell Prolif* (2020) 53(9):e12887. doi: 10.1111/cpr.12887

12. Zhao D, Wang S, Chu X, Han D. LncRNA HIF2PUT inhibited osteosarcoma stem cells proliferation, migration and invasion by regulating HIF2 expression. *Artif Cells Nanomed Biotechnol* (2019) 47(1):1342–8. doi: 10.1080/21691401.2019.1596934

13. Hong-Bin S, Wan-Jun Y, Chen-Hui D, Xiao-Jie Y, Shen-Song L, Peng Z. Identification of an iron metabolism-related lncRNA signature for predicting osteosarcoma survival and immune landscape. *Front Genet* (2022) 13:816460. doi: 10.3389/fgene.2022.816460

14. Xu Z, Peng B, Liang Q, Chen X, Cai Y, Zeng S, et al. Construction of a ferroptosis-related nine-lncRNA signature for predicting prognosis and immune response in hepatocellular carcinoma. *Front Immunol* (2021) 12:719175. doi: 10.3389/fimmu.2021.719175

15. Tsvetkov P, Coy S, Petrova B, Dreishpoon M, Verma A, Abdusamad M, et al. Copper induces cell death by targeting lipoylated TCA cycle proteins. *Science* (2022) 375(6586):1254–61. doi: 10.1126/science.abf0529

16. Fu XZ, Zhang XY, Qiu JY, Zhou X, Yuan M, He YZ, et al. Whole-transcriptome RNA sequencing reveals the global molecular responses and ceRNA regulatory network of mRNAs, lncRNAs, miRNAs and circRNAs in response to copper toxicity in ziyang xiangcheng (Citrus junos sieb. *Ex Tanaka) BMC Plant Biol* (2019) 19(1):509. doi: 10.1186/s12870-019-2087-1

17. Ritchie ME, Phipson B, Wu D, Hu Y, Law CW, Shi W, et al. Limma powers differential expression analyses for RNA-sequencing and microarray studies. *Nucleic Acids Res* (2015) 43(7):e47. doi: 10.1093/nar/gkv007

18. Tang Y, Li C, Zhang YJ, Wu ZH. Ferroptosis-related long non-coding RNA signature predicts the prognosis of head and neck squamous cell carcinoma. *Int J Biol Sci* (2021) 17(3):702–11. doi: 10.7150/ijbs.55552

19. Yu G, Wang LG, Han Y, He QY. clusterProfiler: an r package for comparing biological themes among gene clusters. *Omics* (2012) 16(5):284–7. doi: 10.1089/omi.2011.0118

20. Yu G, Li F, Qin Y, Bo X, Wu Y, Wang S. GOSemSim: an r package for measuring semantic similarity among GO terms and gene products. *Bioinformatics* (2010) 26(7):976–8. doi: 10.1093/bioinformatics/btq064

21. Hänzelmann S, Castelo R, Guinney J. GSVA: gene set variation analysis for microarray and RNA-seq data. *BMC Bioinf* (2013) 14:7. doi: 10.1186/1471-2105-14-7

22. Yoshihara K, Shahmoradgoli M, Martínez E, Vegesna R, Kim H, Torres-Garcia W, et al. Inferring tumour purity and stromal and immune cell admixture from expression data. *Nat Commun* (2013) 4:2612. doi: 10.1038/ncomms3612

23. Yi M, Nissley DV, McCormick F, Stephens RM. ssGSEA score-based ras dependency indexes derived from gene expression data reveal potential ras addiction mechanisms with possible clinical implications. *Sci Rep* (2020) 10(1):10258. doi: 10.1038/s41598-020-66986-8

24. Geeleher P, Cox N, Huang RS. pRRophetic: an r package for prediction of clinical chemotherapeutic response from tumor gene expression levels. *PloS One* (2014) 9(9):e107468. doi: 10.1371/journal.pone.0107468

25. Liu H, Shu W, Liu T, Li Q, Gong M. Analysis of the function and mechanism of DIRAS1 in osteosarcoma. *Tissue Cell* (2022) 76:101794. doi: 10.1016/j.tice.2022.101794

26. Elgaaen BV, Haug KB, Wang J, Olstad OK, Fortunati D, Onsrud M, et al. POLD2 and KSP37 (FGFBP2) correlate strongly with histology, stage and outcome in ovarian carcinomas. *PloS One* (2010) 5(11):e13837. doi: 10.1371/journal.pone.0013837

27. Yadavalli S, Jayaram S, Manda SS, Madugundu AK, Nayakanti DS, Tan TZ, et al. Data-driven discovery of extravasation pathway in circulating tumor cells. *Sci Rep* (2017) 7:43710. doi: 10.1038/srep43710

28. Li H, Weng Y, Wang S, Wang F, Wang Y, Kong P, et al. CDCA7 facilitates tumor progression by directly regulating CCNA2 expression in esophageal squamous cell carcinoma. *Front Oncol* (2021) 11:734655. doi: 10.3389/fonc.2021.734655

29. Liu L, Wang R, Zhang Z, Wang X. Nasopharyngeal carcinoma–associated gene 6 inhibits cell viability, migration, invasion and induces apoptosis in osteosarcoma cells by inactivating the wnt/β–catenin signaling pathway. *Mol Med Rep* (2021) 23(2):93. doi: 10.3892/mmr.2020.11732

30. Pagès F, Mlecnik B, Marliot F, Bindea G, Ou FS, Bifulco C, et al. International validation of the consensus immunoscore for the classification of colon cancer: a prognostic and accuracy study. *Lancet* (2018) 391(10135):2128–39. doi: 10.1016/s0140-6736(18)30789-x

31. Chen Y, Meng Z, Zhang L, Liu F. CD2 is a novel immune-related prognostic biomarker of invasive breast carcinoma that modulates the tumor microenvironment. *Front Immunol* (2021) 12:664845. doi: 10.3389/fimmu.2021.664845

32. Hao X, Sun G, Zhang Y, Kong X, Rong D, Song J, et al. Targeting immune cells in the tumor microenvironment of HCC: New opportunities and challenges. *Front Cell Dev Biol* (2021) 9:775462. doi: 10.3389/fcell.2021.775462

33. Zhu J, Huang Q, Liu S, Peng X, Xue J, Feng T, et al. Construction of a novel LncRNA signature related to genomic instability to predict the prognosis and immune activity of patients with hepatocellular carcinoma. *Front Immunol* (2022) 13:856186. doi: 10.3389/fimmu.2022.856186

34. Wefers C, Duiveman-de Boer T, Zusterzeel PLM, Massuger L, Fuchs D, Torensma R, et al. Different lipid regulation in ovarian cancer: Inhibition of the immune system. *Int J Mol Sci* (2018) 19(1):273. doi: 10.3390/ijms19010273

35. Wang D, DuBois RN. Immunosuppression associated with chronic inflammation in the tumor microenvironment. *Carcinogenesis* (2015) 36 (10):1085–93. doi: 10.1093/carcin/bgv123

36. Wang Y, Bhandari A, Niu J, Yang F, Xia E, Yao Z, et al. The lncRNA UNC5B-AS1 promotes proliferation, migration, and invasion in papillary thyroid cancer cell lines. *Hum Cell* (2019) 32(3):334–42. doi: 10.1007/s13577-019-00242-8

37. Tan JJ, Long SZ, Zhang T. [Effects of LncRNA UNC5B-AS1 on adhesion, invasion and migration of lung cancer cells and its mechanism]. *Zhongguo Ying Yong Sheng Li Xue Za Zhi* (2020) 36(6):622–7. doi: 10.12047/j.cjap.5993.2020.130

38. Tan SF, Ni JX, Xiong H. LncRNA UNC5B-AS1 promotes malignant progression of prostate cancer by competitive binding to caspase-9. *Eur Rev Med Pharmacol Sci* (2020) 24(5):2271–80. doi: 10.26355/eurrev_202003_20493

39. Wang H, Su H, Tan Y. UNC5B-AS1 promoted ovarian cancer progression by regulating the H3K27me on NDRG2 *via* EZH2. *Cell Biol Int* (2020) 44(4):1028–36. doi: 10.1002/cbin.11300

40. Huang X, Pan J, Wang G, Huang T, Li C, Wang Y, et al. UNC5B-AS1 promotes the proliferation, migration and EMT of hepatocellular carcinoma cells *via* regulating miR-4306/KDM2A axis. *Cell Cycle* (2021) 20(20):2114–24. doi: 10.1080/15384101.2021.1962632

41. Jiang R, Zhang Z, Zhong Z, Zhang C. Long-non-coding RNA RUSC1-AS1 accelerates osteosarcoma development by miR-101-3p-mediated Notch1 signalling pathway. J. *Bone Oncol* (2021) 30:100382. doi: 10.1016/j.jbo.2021.100382

42. Tong CJ, Deng QC, Ou DJ, Long X, Liu H, Huang K. LncRNA RUSC1-AS1 promotes osteosarcoma progression through regulating the miR-340-5p and PI3K/AKT pathway. *Aging (Albany NY)* (2021) 13(16):20116–30. doi: 10.18632/aging.203047

43. Liu J, Yao Y, Hu Z, Zhou H, Zhong M. Transcriptional profiling of long-intergenic non-coding RNAs in lung squamous cell carcinoma and its value in diagnosis and prognosis. *Mol Genet Genomic Med* (2019) 7(12):e994. doi: 10.1002/mgg3.994

frontiers | Frontiers in Medicine

TYPE Case Report
PUBLISHED 08 November 2022
DOI 10.3389/fmed.2022.1002324

Check for updates

OPEN ACCESS

EDITED BY
Liam Chen,
University of Minnesota, United States

REVIEWED BY
Hui Li,
Chongqing University, China
Shunyou Gong,
Northwestern University, United States

*CORRESPONDENCE
Hui Tang
chenux@aliyun.com
Chi Xu
chixuzoe@163.com

†These authors have contributed equally to this work

SPECIALTY SECTION
This article was submitted to Hepatology, a section of the journal Frontiers in Medicine

RECEIVED 25 July 2022
ACCEPTED 25 October 2022
PUBLISHED 08 November 2022

CITATION
Ding F, Wang C, Xu C and Tang H (2022) Case report: Hepatic inflammatory pseudotumor-like follicular dendritic cell sarcoma: A rare case and minireview of the literature.
Front. Med. 9:1002324.
doi: 10.3389/fmed.2022.1002324

COPYRIGHT
© 2022 Ding, Wang, Xu and Tang. This is an open-access article distributed under the terms of the Creative Commons Attribution License (CC BY). The use, distribution or reproduction in other forums is permitted, provided the original author(s) and the copyright owner(s) are credited and that the original publication in this journal is cited, in accordance with accepted academic practice. No use, distribution or reproduction is permitted which does not comply with these terms.

Case report: Hepatic inflammatory pseudotumor-like follicular dendritic cell sarcoma: A rare case and minireview of the literature

Fan Ding[1,2†], Chao Wang[3†], Chi Xu[4,5*] and Hui Tang[4,5*]

[1]Center of Gallbladder Disease, East Hospital of Tongji University, Shanghai, China, [2]Institute of Gallstone Disease, Tongji University School of Medicine, Shanghai, China, [3]Department of Radiology, Nanxiang Hospital of Jiading District, Shanghai, China, [4]Department of Hepatic Surgery and Liver Transplantation Center, The Third Affiliated Hospital of Sun Yat-sen University, Guangzhou, China, [5]Organ Transplantation Institute, Sun Yat-sen University, Guangzhou, China

Inflammatory pseudotumor (IPT)-like follicular dendritic cell sarcoma (FDCS) is a rare neoplasm referred to as the FDCS variant. Here we report a 66-year-old female patient suffering from hepatic IPT-like FDCS and summarize IPT-like FDCS reported in the literature. The patient presented with obvious abdominal pain without significant laboratory abnormalities and subsequently underwent surgical resection of a hepatic lesion. Postoperative pathological results demonstrated a vascular tissue-rich neoplasm (7.0-cm maximum diameter). The tumor cells expressed CD21 and CD35, and *in situ* hybridization detected Epstein–Barr virus-encoded RNA (EBER). Metastasis or recurrence was not detected during the 7-year follow-up.

KEYWORDS

inflammatory pseudotumor, follicular dendritic cell, sarcoma, case report, hepatic

Introduction

Follicular dendritic cells (FDCs) develop from perivascular precursors of stromal cell origin that are essential for the organization and maintenance of lymphoid architecture, induction of the germinal center reaction, production of B memory cells, and protection from autoimmune disorders (1). FDC sarcoma (FDCS) is an extremely rare neoplasm with nearly more than half of the cases occurring in lymph nodes (2). Extranodal FDCS, which mainly arises from intraabdominal organs such as liver, spleen, colon, and pancreas, may display systemic clinical symptoms (3). Inflammatory pseudotumor (IPT)-like FDCS is a recently described unique subtype of FDCS with different histological appearances and behavior compared with those of classical FDCS. The most recent World Health Organization (WHO) classification notes that IPT-like FDCS appears to be indolent; however, the data on clinical outcomes are limited (4).

The cause of IPT-like FDCS is unknown, and the diagnostic criteria are not definitive. However, Epstein–Barr virus (EBV) infection is considered one of the most important etiologies of this sarcoma (4). Distinguishing IPT-like FDCS from other tumors is very challenging, and such tumors are commonly misdiagnosed as inflammatory lesions or other malignant neoplasms. Definite diagnosis of IPT-like FDCS should rely on radiology, cellular morphology, histopathology, and immunochemistry. IPT-like FDCS exhibits indolent features, prognosis is favorable, and surgical excision is the best treatment.

Herein, we report the case of a 66-year-old female with an intraabdominal IPT-like FDCS in the hepatic right lobe. By analyzing the distinctive clinicopathologic features of this rare case combined with reviewing the related literature, here we summarize the current clinical features and diagnosis of IPT-like FDCS and discuss the treatment and prognosis of this tumor subtype.

Literature review

We systematically searched the PubMed, EMBASE, and MEDLINE databases using the search terms "inflammatory pseudotumor-like" combined with "follicular dendritic cell sarcoma," or "follicular dendritic cell tumor," or "fibroblastic dendritic cell sarcoma," or "fibroblastic dendritic cell tumor" in research published from 2000 to 2022. We collated demographic, clinicopathological, and follow-up information (**Table 1**).

Case presentation

In 2015, a 66-year-old woman who suffered from right upper abdominal pain was admitted to the Department of Hepatic Surgery and Liver Transplantation Center at the Third Affiliated Hospital of Sun Yat-sen University because of a liver mass detected using abdominal ultrasound at a local hospital. Based on ultrasound examination and medical history, the preliminary diagnosis was liver-occupying lesions and diabetes mellitus type 2. The patient did not complain of vomiting, nausea, fever, or diarrhea. After admission, the values of routine tests including liver and kidney function and routine blood tests were almost within their normal limits. Liver function according to the Child–Pugh classification was class A. Serological analyses to detect hepatitis virus, syphilis, and human immunodeficiency virus were negative. Furthermore, the levels of common female-specific tumor markers, particularly α-fetoprotein (AFP), carcinoembryonic antigen (CEA), carbohydrate antigen (CA)-199, and CA-125 were normal. The patient had a long history of diabetes mellitus type 2 and achieved good fasting plasma-glycemic control with acarbose combined with metformin.

Preoperative enhanced magnetic resonance imaging (MRI) showed a mass approximately 94 × 74 mm with clear borders in hepatic segments VI and VII. On enhanced phase, the images showed progressive enhancement of the lesion, while enhancement was not seen in the necrotic region. Significantly, the lesion demonstrated slightly hypointense speckled signals on in-phase and out-of-phase T_1WI. Therefore, the primary diagnosis highly suggested a hepatic fat-poor angioleiomyolipoma (**Figure 1**).

Although the diagnosis was not definitive, the large liver mass caused significant clinical symptoms (abdominal pain) in the absence of concurrent systematic disease. Our multidisciplinary hepatic surgery team therefore proposed surgical resection as the most appropriate procedure to confirm a diagnosis and further formulate the treatment strategy. Subsequently, the patient underwent resection of hepatic segments VI and VII, and minor complications occurred postoperation. During surgery, lesions were not observed in the gastrointestinal tract, spleen, mesentery, or other abdominal organs. The operation lasted 135 min, and the estimated intraoperative blood loss was approximately 150 mL.

Grossly, the size of the tumor was approximately 7.0 × 5.0 cm, presenting with an indistinct boundary and a patchy gray-red section with intratumor hemorrhage and necrosis. Postoperative pathology showed a sarcoma containing varying sizes of vessel lumens with negative surgical margins. The neoplastic tissue was extensively infiltrated by definite lymphocytes, plasma cells, and spindle cells. The tumor cells were fusiform and ovoid with a translucent cytoplasm and large vacuolated nuclei. According to the infiltration of numerous lymphocytes into the neoplastic tissues and immunohistochemical detection of CD21 and CD35 expression as well as *in situ* hybridization detection of Epstein–Barr virus-encoded RNA (EBER), the morphological and immunophenotypic results were consistent with a diagnosis of IPT-like FDCS (**Figure 2**). Hence, the final diagnosis was revised to IPT-like FDCS.

The patient was discharged without adjuvant chemotherapy or radiotherapy and has been examined at our hepatic surgery follow-up clinic every 6 months. The outcome of the 7-year follow-up was good, and metastasis or recurrence was not detected.

Discussion

Follicular dendritic cell sarcoma (FDCS) is a rare mesenchymal tumor of follicular dendritic cell origin originally identified by Monda et al. in 1986 (2). FDCS is classified into the two histopathological subtypes as follows: conventional and inflammatory pseudotumor-like (5). IPT-like FDCS is

TABLE 1 Clinical characteristics of patients with inflammatory pseudotumor-like follicular dendritic cell sarcoma.

References	Case	Age (y)/ Gender	Location	Main complaints	Maximum diameter (cm)	EBER	Treatment	Follow-up	Recurrence or metastasis
Shi et al. (29)	1	77/F	Colon	Lower abdominal pain with hematochezia	3.0	+	Endoscopic polypectomy	15 months	N
Zhao et al. (30)	2	56/F	Colon	Asymptomatic	3.2	+	Surgery	14 months	N
Xue et al. (31)	3	45/F	Spleen	Waist soreness	2.9	NA	NA	NA	NA
	4	40/F	Spleen	Asymptomatic	7.3	NA	NA	NA	NA
	5	81/M	Spleen	Asymptomatic	8.1	NA	NA	NA	NA
	6	59/F	Spleen	Left upper abdominal pain	15.0	NA	NA	NA	NA
	7	54/F	Spleen	Left upper abdominal pain	3.6	NA	NA	NA	NA
	8	71/F	Spleen	Asymptomatic	4.5	NA	NA	NA	NA
	9	67/M	Spleen	Asymptomatic	6.0	NA	NA	NA	NA
Xu et al. (20)	10	81/M	Liver	Asymptomatic	NA	NA	Resection	12 months	N
	11	53/M	Liver	Abdominal distension	NA	NA	Resection	24 months	N
	12	76/F	Spleen	Asymptomatic	NA	NA	Resection	10 months	N
	13	49/F	Spleen	Asymptomatic	NA	NA	Resection	24 months	N
	14	73/M	Spleen	Asymptomatic	NA	NA	Resection	18 months	N
	15	66/F	Liver and spleen	Epigastric pain	NA	NA	Resection	20 months	N
	16	62/F	Spleen	Asymptomatic	NA	NA	Resection	18 months	N
	17	43/F	Spleen	Abdominal distension	NA	NA	Resection	24 months	N
	18	36/M	Spleen	Fever	NA	NA	Resection	24 months	N
	19	41/F	Spleen	Asymptomatic	NA	NA	Resection	17 months	N
	20	88/M	Spleen	Asymptomatic	NA	NA	Resection	12 months	N
Pascariu et al. (32)	21	34/F	Liver	Epigastric pain	6.0	+	Laparoscopic hepatectomy	2 months after reoperation	72 months after first surgery
Nguyen et al. (33)	22	44/F	Spleen	Left upper quadrant abdominal pain	2.5	+	Laparoscopic splenectomy	NA	12 months after first surgery
Morales-Vargas et al. (34)	23	66/F	Spleen	Left upper quadrant pain	5.0	+	Splenectomy	6 months	N
Lu et al. (35)	24	55/F	Liver	Epigastric pain	14.5	+	Hepatectomy	60 months with PR	Paravertebral metastasis and recurrence
Liu et al. (4)	25	61/M	Liver	Asymptomatic	4.2	–	Laparoscopic hepatectomy	13 months	N
Li et al. (36)	26	47/M	Liver	Right upper quadrant abdominal pain	20.0	+	Hepatectomy	50 months	N
He et al. (37)	27	64/F	Lung	Asymptomatic	2.0	+	Lobectomy	10 months	N
Bruehl et al. (38)	28	70/M	Spleen	Epigastric pain	9.9	+	Splenectomy	24 months	N
Zhuang et al. (8)	29	27/F	Spleen	Desquamative stomatitis	9.0	NA	Splenectomy	12 months	N

(Continued)

10.3389/fmed.2022.1002324

TABLE 1 (Continued)

References	Case	Age (y)/ Gender	Location	Main complaints	Maximum diameter (cm)	EBER	Treatment	Follow-up	Recurrence or metastasis
Jin et al. (39)	30	38/M	Liver	Asymptomatic	12.4	+	Hepatectomy	NA	NA
Mograbi et al. (40)	31	70/F	Pancreas and spleen	Asymptomatic	7.0	+	Pancreatectomy and splenectomy	NA	NA
Li et al. (19)	32	31/F	Liver	Asymptomatic	3.6	+	Hepatectomy	26 months	N
	33	48/M	Liver	Asymptomatic	10.0	+	Hepatectomy	10 months	N
Wu et al. (21)	34	52/M	Spleen	NA	7.0	+	Resection	84 months	N
	35	46/M	Liver	NA	3.5	+	Resection	35 months	N
	36	37/F	Liver	NA	8.5	+	Resection	14 months	N
	37	64/F	Liver	NA	11.0	+	Resection	41 months	N
	38	63/F	Spleen	NA	4.0	+	Resection	17 months	N
	39	54/F	Spleen	NA	8.5	+	Resection	7 months	N
	40	53/M	Spleen	NA	3.0	+	Resection	3 months	N
Li et al. (41)	41	64/F	Spleen	Epigastric pain	7.2	+	Laparoscopic splenectomy	8 months	N
	42	61/M	Spleen	Asymptomatic	6.2	+	Laparoscopic splenectomy	16 months	N
	43	42/F	Spleen	Left-sided flank pain	4.0	+	Laparoscopic splenectomy	9 months	N
	44	57/F	Spleen and lung	Epigastric pain	13.3	+	Laparoscopic splenectomy	4 months	Pulmonary metastasis
	45	52/M	Spleen and vertebra	Back pain	3.7	+	Laparoscopic splenectomy	5 months	Multiple bone metastasis
Kwon et al. (42)	46	58/F	Spleen	Asymptomatic	5.0	+	Splenectomy	24 months	N
Kazemimood et al. (25)	47	53/F	Colon	Abdominal discomfort	3.0	–	Laparoscopic right colectomy	NA	NA
Hang et al. (15)	48	57/M	Spleen	Asymptomatic	2.7	+	laparoscopic splenectomy	9 months	N
Wang et al. (9)	49	60/F	Left axillary region and neck	Myasthenia	6.4	–	Rituximab	2 months after discharge	Dead due to MODS
Kitamura et al. (43)	50	74/F	Spleen	Asymptomatic	2.9	+	Splenectomy	24 months	N
Hu et al. (44)	51	49/F	Left adrenal gland	Asymptomatic	5.0	NA	Left adrenalectomy	58 months	The tail of pancreas recurrence
Gong et al. (45)	52	42/F	Colon	Asymptomatic	4.5	+	Endoscopic excision	16 months	N
Bui et al. (18)	53	50/F	Spleen	Abdominal pain	6.5	+	Splenectomy	NA	NA
You et al. (46)	54	43/M	Liver	Right upper quadrant pain	20.0	+	Unresectable	NA	NA
Vardas et al. (47)	55	61/M	Spleen	Asymptomatic	10.0	+	Splenectomy	12 months	N
Rao et al. (48)	56	39/M	Spleen	Asymptomatic	7.2	+	NA	NA	NA

(Continued)

10.3389/fmed.2022.1002324

TABLE 1 (Continued)

References	Case	Age (y)/ Gender	Location	Main complaints	Maximum diameter (cm)	EBER	Treatment	Follow-up	Recurrence or metastasis
Pan et al. (49)	57	78/F	Colon	Bloody stool	3.9	+	Polypectomy	5 months	N
Li et al. (16)	58	49/F	Spleen	Asymptomatic	4.7	+	Splenectomy	NA	NA
	59	56/F	Spleen	Abdominal pain	8.0	+	Splenectomy	17 months	N
	60	38/M	Liver	Fatigue, anorexia	8.5	+	Left lobectomy of liver	11 months	N
	61	42/F	Liver	Abdominal pain	2.0	+	Wedge resection	36 months	N
	62	50/M	Spleen and liver	Abdominal bloating, fatigue	10.0	+	Splenectomy and left lobectomy of liver	17 months	N
	63	39/F	Liver	Asymptomatic	9.0	+	Hepatic lobectomy	84 months after chemotherapy and mass excision	Recurrence at 12 months
Ge et al. (3)	64	54/F	Spleen	left upper quadrant pain	3.5	+	Splenectomy	10 months	N
	65	79/M	Spleen	Epigastric pain	6.0	+	Splenectomy	18 months	N
Kim et al. (50)	66	76/M	Spleen	Asymptomatic	3.2	+	Splenectomy	7 months	N
Choe et al. (13)	67	64/F	Spleen	Asymptomatic	5.5	+	Splenectomy	78 months	N
	68	72/F	Spleen	Asymptomatic	7.2	+	Splenectomy	18 months	N
	69	53/F	Spleen	Asymptomatic	3.2	+	Splenectomy	13 months	N
	70	76/M	Spleen	Asymptomatic	3.2	+	Splenectomy	8 months	N
	71	72/M	Spleen	Asymptomatic	6.0	+	Splenectomy	18 months	N
	72	75/M	Spleen	Abdominal pain	3.5	+	Splenectomy	30 months	N
Takahashi et al. (27)	73	39/M	Spleen	Asymptomatic	7.0	–	Splenectomy	31 months	N
Kiryu et al. (51)	74	56/F	Spleen	Asymptomatic	4.0	+	Splenectomy	24 months	N
	75	60/M	Spleen	Asymptomatic	2.0	+	Splenectomy	48 months	N
	76	78/F	Spleen	Asymptomatic	2.0	+	Splenectomy	48 months	N
Yoon et al. (52)	77	64/F	Spleen	Asymptomatic	5.1	+	Splenectomy	NA	NA
Agaimy et al. (26)	78	52/M	Ileal mesentery	Acute abdomen	6.0	–	Emergency excision	Lost	Lost
Horiguchi et al. (53)	79	77/F	Spleen	Epigastric pain	8.5	+	Splenectomy	36 months	N
Brittig et al. (54)	80	54/M	Spleen	Asymptomatic	12.0	+	Splenectomy	48 months	N
Wu et al. (55)	81	45/M	Liver	Epigastric pain	6.7	+	Right hepatectomy	9 months	N
Zhang et al. (56)	82	31/F	Liver	Anorexia	3.5	+	Laparoscopic right hepatectomy	10 months	N
	83	48/M	Liver	Asymptomatic	10.0	+	Right hepatectomy	2 months	N
Deng et al. (57)	84	67/F	Liver	Cough	4.0	+	Hepatectomy	NA	NA
Ang et al. (58)	85	63/F	Liver	Fever	13.4	+	Right hemihepatectomy	48 months	N
Zhang et al. (59)	86	19/F	Liver	Abdominal discomfort	6.0	+	Hepatic VII segmental resection	12 months	N

(Continued)

10.3389/fmed.2022.1002324

TABLE 1 (Continued)

References	Case	Age (y)/ Gender	Location	Main complaints	Maximum diameter (cm)	EBER	Treatment	Follow-up	Recurrence or metastasis
Chen et al. (60)	87	28/F	Liver	Abdominal pain	6.0	+	Left lobectomy of liver	NA	Recurrence at 48 months
	88	39/M	Spleen	Asymptomatic	7.4	+	Splenectomy	40 months	N
	89	48/M	Liver	Abdominal pain	23.3	+	Extended right hemihepatectomy	23 months	N
	90	65/M	Spleen and Liver	Epigastric pain	23.3	+	Splenectomy and radical dissection of retroperitoneal lymph nodes	2 months	Dead for cachexia
	91	51/M	Spleen	Malaise, weight loss	8.5	+	Splenectomy	19 months	N
	92	68/M	Spleen	Asymptomatic	2.3	+	Splenectomy	6 months	N
	93	51/F	Spleen	Abdominal discomfort	5.3	+	Splenectomy	5 months	N
	94	67/M	Spleen	Asymptomatic	7.5	+	Splenectomy	5 months	N
	95	60/M	Liver	Asymptomatic	3.0	+	Wedge resection	3 months	N
	96	52/F	Spleen	Asymptomatic	0.9	+	Splenectomy	12 months	N
Nguyen et al. (61)	97	57/F	Liver and Spleen	Weight loss	NA	+	Rejection treatment	NA	NA
Granados et al. (62)	98	57/F	Liver	Abdominal pain	13.0	+	Resection	24 months	N
Cheuk et al. (6)	99	19/F	Liver	Right upper quadrant pain	12.0	+	Resection	40 months	N
	100	56/F	Liver	Abdominal discomfort	15.0	+	Resection of right lobe of liver	56 months	Recurrence at 15, 27, 35 months respectively
	101	40/F	Liver	Epigastric pain	12.5	+	Left hepatectomy	108 months	Recurrence at 108 months
	102	49/F	Liver	Asymptomatic	4.2	+	Resection	9 months	N
	103	37/M	Liver	Weight loss	15.0	+	Right trisegmentectomy	42 months	N
	104	35/F	Liver	Abdominal discomfort	20.0	+	Right hemihepatectomy	95 months	Dead for disseminated tumor
	105	31/F	Liver	Abdominal distension	15.0	+	Right hemihepatectomy	60 months	N
	106	58/F	Spleen	Abdominal discomfort	22.0	+	Splenectomy	4 months	N
	107	39/F	Spleen	Weight loss	7.5	+	Splenectomy	2 months	N
	108	61/F	Spleen	Asymptomatic	3.5	+	Splenectomy	NA	NA
	109	49/F	Peri-pancreas	Abdominal distension	9.5	+	Whipple's operation	NA	NA
Chen et al. (63)	110	57/F	Liver	Epigastric pain	9.5	+	Refusion surgical resection	36 months	N
	111	51/F	Liver	Abdominal distension	12.0	+	Left lobectomy	12 months	N
Lewis et al. (11)	112	81/F	Spleen	Epigastric pain	5.0	+	Splenectomy	18 months	N
Nishiyama et al. (64)	113	73/F	Spleen	Asymptomatic	8.0	+	Splenectomy	144 months	N
Present case	114	66/F	Liver	Abdominal pain	7.0	+	Hepatic segment VI and VII resection	84 months	N

N, none; NA, not available; MODS, multiple organ dysfunction syndrome.

10.3389/fmed.2022.1002324

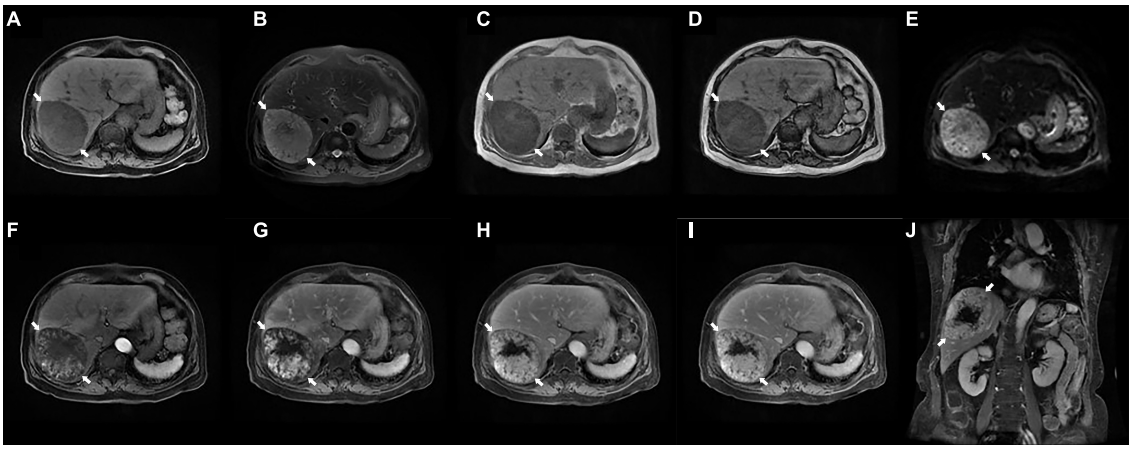

FIGURE 1
Preoperative enhanced magnetic resonance imaging (MRI) examination. **(A)** T1WI shows an ovalshaped hypointense lesion with clear border in the right lobe of the liver (arrows, 94×74 mm). **(B)** Fat-suppressed T2WI shows a slightly hyperintense lesions (arrows). **(C,D)** The in-phase **(C)** and out-of-phase **(D)** of T1WI demonstrates hypointense speckled signals within the mass (arrows). **(E)** DWI shows a hyperintense lesions (arrows). **(F–J)** Enhanced MRI scans showed progressive enhancement of the lesion (arrows) on the early **(F)** and late **(G)** arterial phase, portal venous phase **(H)**, delayed phase **(I)**, and coronal view **(J)**, while no enhancement was seen in the necrotic region. MRI, magnetic resonance imaging; T1WI, T1 weighted image; T2WI, T2 weighted image; DWI, diffusion weighted imaging.

an extremely rare tumor, and only 113 cases are published (**Table 1**).

Inflammatory pseudotumor (IPT)-like FDCS possesses morphological and clinical features intermediate between inflammatory pseudotumors and FDC tumors and was first classified in 2001 as a distinct variant (6). Compared with conventional FDCS, IPT-like FDCS exhibits unique histopathological and clinical features that generally occur in abdominal organs, almost exclusively involving the spleen, liver, or both (104/114); and colonic (5/114), mesenteric (2/114), pancreatic (1/114), pulmonary (2/114), paranephric (1/114), and lymphatic (1/114) involvement occur as well.

Inflammatory pseudotumor (IPT)-like FDCS predominantly occurs in middle-aged adults (median age, 54.5 years; range, 19–88 years), with marked female predominance (female to male ratio = 1.71:1). Patients are mainly asymptomatic or present with abdominal distension or pain, occasionally accompanied by systemic symptoms such as back pain, waist soreness, significant weight loss, fever, and weakness. In rare cases, IPT-like FDCS exhibits paraneoplastic arthritis (7), and paraneoplastic pemphigus (8–10).

The pathogenesis and causes of IPT-like FDCS are unknown, although Epstein–Barr virus (EBV) may play an essential role in etiology. Stimulation by EBV may induce FDCs derived from mesenchymal cells to undergo neoplastic transformation and express CD21 and CD35 (11, 12). Interestingly, Choe et al. (13) found remarkable numbers of IgG4-positive plasma cell in 6 Asian patients with EBV-positive IPT-like FDCS of the spleen, suggesting that the intimate relationship between IgG4 and EBV plays a critical role in IPT-like FDCS, which may be limited to Asians. Moreover, mutations in genes encoding components of the NF-κB pathway, cell cycle regulatory genes (*CDKN2A* and *RB1*), and immune evasion genes (*CD274* and *PDCD1LG2*) may be pathologically associated with IPT-like FDCS (14).

The morphology of IPT-like FDCS is similar to that of the conventional type. Gross examination reveals that most tumors exhibit a well-marginated, thin-walled, yellowish, soft tissue mass (maximum diameter = 7.54 ± 4.93 cm). In particular, localized hemorrhage or necrosis is observed within the tumor. The neoplastic cells, which may exhibit mild atypia, are usually spindle, ovoid, or polygonal and form storiform, fascicles, or trabecular arrays, which exhibit sparsely vesicular chromatin and distinct nucleoli (15). In particular, the inflammatory component of IPT-like FDCS, a more prominent histology, comprises mainly lymphocytes (B and T cells), plasma cells, eosinophils, and rare epithelioid histiocytes, with neoplastic cells often obscured by the inflammatory infiltration (6, 16). Owing to the lack of atypical tumor cells, IPT-like FDCS are often incorrectly identified inflammatory-reactive processes or inflammatory pseudotumor, even other various neoplasms (17). Moreover, the scarcity of cases and lack of specific clinical and imaging features present a formidable challenge to diagnosing IPT-like FDCS. Currently, the diagnosis of IPT-like FDCS requires auxiliary tests, including imaging, detecting distinctive cytological features, immunohistochemical detection of FDC markers, and *in situ* hybridization to detect EBER.

Although limited reports are available on the imaging features of IPT-like FDCS, they aid in making correct diagnoses before treatment when a neoplasm is detected (18). Most unenhanced computed tomography (CT) images display circular or elliptical, slightly hypodense tumors with a clear

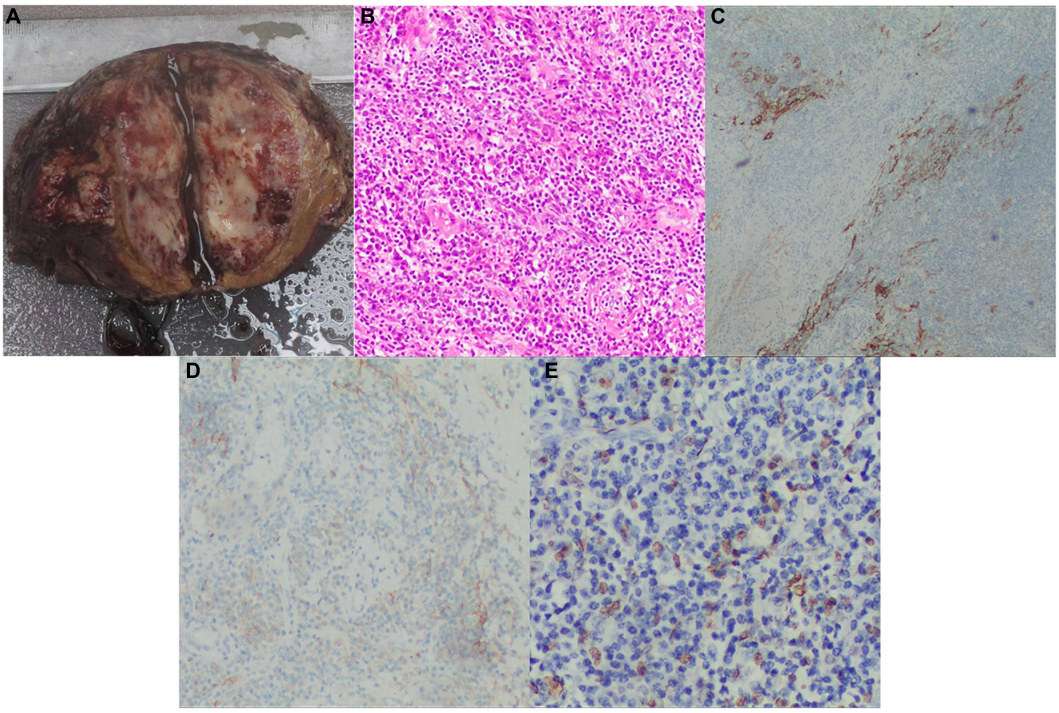

FIGURE 2
Postoperative pathology examinations. **(A)** Grossly, the cut surface of the fleshy neoplasm with necrosis and hemorrhage (tumor size: 7.0×5.0 cm); **(B)** H&E stained image showing that the tumor tissue had a meshwork-like architecture with abundant vascular-like proliferation, magnification: 200X; **(C)** The positive IHC result of CD21, magnification: 100X; **(D)** The positive IHC result of CD35, magnification: 100X; **(E)** The positive result of EBV for *in situ* hybridization, magnification: 200X. H&E, hematoxylin and eosin; IHC, immunohistochemical; EBV, Epstein Barr virus.

boundary. In certain cases, significant necrosis is seen within the tumor, while calcification or hemorrhage is rare. The lesions typically show heterogeneous enhancement in the enhanced phase, although the enhancement state is lower than that of the parenchyma. Therefore, the tumor area is always hypodense compared with the periparenchyma, and annular enhancement is observed in the delayed phase, sparing the central necrotic region (19). MRI and CT images are similar, and most lesions demonstrate enhancement from the center to the periphery in the arterial phase. The enhancement amplitudes of lesions in the portal, venous, and delayed phases tend to be homogeneous and diminished to varying degrees, and annular enhancements are occasionally observed (20).

The diagnosis of IPT-like FDCS is invariably supported by immunohistochemistry, and multiple FDC markers are often necessary, including CD21, CD23, CD35, CXCL-13, D2-40, Clusterin, Fascin, epidermal growth factor receptor, and CNA42 (21, 22). In particular, CD21 and CD35 are the most specific with almost universal positivity (23). Nevertheless, some EBV-related IPT-manifesting lesions do not express FDC markers (16). The immunohistochemical analysis of SSTR2a in FDCS indicates a positive rate significantly higher than CD21 and CD35 in conventional subtypes, while all IPT-like variants are negative (24). Therefore, SSTR2a shows promise as a highly sensitive and differential diagnostic marker to distinguish between FDCS and IPT-like FDCS. As mentioned previously, IPT-like FDCS is closely associated with EBV infection, while conventional types infrequently involve EBV (12). Our literature review identified only five cases of intrabdominal, EBER-negative IPT-like FDCS (4, 9, 25–27). In our present case, immunohistochemical analysis of the pathological specimen detected strongly positive expression of CD21, CD35, Ki67 (> 20%), and EBER (**Figure 2**).

Inflammatory pseudotumor (IPT)-like FDCS is a low-grade malignant tumor with good prognosis. Unlike FDCS, IPT-like FDCS is apparently indolent, with few instances of recurrence and metastasis (3). Disease status at the time of last follow-up is known for 92 patients, with follow-up times ranging from 2 to 144 months. Only 9.65% of patients (n = 11) experienced recurrence or metastasis during follow-up. Yet, PNP-associated IPT-like FDCS predominantly occurs in intraabdominal sites, indicating poor prognosis (8–10). Surgery is the most effective therapy for IPT-like FDCS, and only two cases (Cases 49 and 63) received chemotherapy or targeted therapy. However, chemotherapy, radiotherapy, or targeted therapy do not achieve a significant improvement in overall- or disease-free survival (28). Notably, Cases 49, 90, and 104 died because of multiple organ dysfunction syndrome, cachexia, and disseminated tumor, respectively, during treatment. The

possibility of recurrence and metastasis suggests conducting long surveillance after surgery.

Conclusion

Inflammatory pseudotumor (IPT)-like FDCS is an extremely rare neoplasms that mainly occurs in the intraabdominal region. EBV probably plays an essential role in the etiology of IPT-like FDCS. The diagnosis of IPT-like FDCS is complex and usually relies on fine-needle aspiration biopsy or postoperative pathological diagnosis. Surgical resection is the most effective treatment, although the efficacy and safety of adjuvant chemotherapy, radiotherapy, or targeted therapy for postoperative management are unknown. IPT-like FDCS presents a certain risk of recurrence or metastasis after initial treatment. Thus, regular follow-up visits are strongly recommended.

Data availability statement

The raw data supporting the conclusions of this article will be made available by the authors, without undue reservation.

Ethics statement

The studies involving human participants were reviewed and approved by the Institutional Review Board review ([2021]12-114) at The Third Affiliated Hospital of Sun Yat-sen University in Guangzhou, China. The patients/participants provided their written informed consent to participate in this study.

Author contributions

CX was the patient's physician and responsible for the revision of the manuscript for important intellectual content. FD reviewed the literature and contributed to drafting the manuscript. CW performed the radiographic analysis. FD and HT conceptualized and designed the study, coordinated and supervised data collection, and critically reviewed the manuscript for important intellectual content. All authors issued final approval for the version to be submitted for publication.

Funding

This work was supported by National Natural Science Foundation of China (Grant No. 82100692).

Conflict of interest

The authors declare that the research was conducted in the absence of any commercial or financial relationships that could be construed as a potential conflict of interest.

Publisher's note

All claims expressed in this article are solely those of the authors and do not necessarily represent those of their affiliated organizations, or those of the publisher, the editors and the reviewers. Any product that may be evaluated in this article, or claim that may be made by its manufacturer, is not guaranteed or endorsed by the publisher.

References

1. Abd El-Aleem S, Saber E, Aziz N, El-Sherif H, Abdelraof A, Djouhri L. Follicular dendritic cells. *J Cell Physiol.* (2022) 237:2019–33. doi: 10.1002/jcp.30662

2. Monda L, Warnke R, Rosai J. A primary lymph node malignancy with features suggestive of dendritic reticulum cell differentiation. a report of 4 cases. *Am J Pathol.* (1986) 122:562–72.

3. Ge R, Liu C, Yin X, Chen J, Zhou X, Huang C, et al. Clinicopathologic characteristics of inflammatory pseudotumor-like follicular dendritic cell sarcoma. *Int J Clin Exp Pathol.* (2014) 7:2421–9.

4. Liu X, Cao L, Chin W, Yu J, Liu Y, Zheng S. Epstein-barr virus-negative inflammatory pseudotumor-like variant of follicular dendritic cell sarcoma of the liver: a case report and literature review. *Clin Res Hepatol Gastroenterol.* (2021) 45:101457. doi: 10.1016/j.clinre.2020.05.007

5. Swerdlow SH. In: Swerdlow SH, Campo E, Harris NL, Jaffe ES, Pileri SA, Stein H, et al. editors. *Who Classification of Tumours of Haematopoietic and Lymphoid Tissues*. Geneva: WHO (2017).

6. Cheuk W, Chan JK, Shek TW, Chang JH, Tsou MH, Yuen NW, et al. Inflammatory pseudotumor-like follicular dendritic cell tumor: a distinctive low-grade malignant intra-abdominal neoplasm with consistent epstein-barr virus association. *Am J Surg Pathol.* (2001) 25:721–31. doi: 10.1097/00000478-200106000-00003

7. Levi Sandri GB, Colasanti M, Vennarecci G, Ettorre GM. Paraneoplastic arthritis as first symptom of a liver inflammatory pseudotumor-like follicular dendritic cell sarcoma. *Liver Int.* (2016) 36:1392. doi: 10.1111/liv.13148

8. Zhuang JY, Zhang FF, Li QW, Chen YF. Intra-abdominal inflammatory pseudotumor-like follicular dendritic cell sarcoma associated with paraneoplastic pemphigus: a case report and review of the literature. *World J Clin Cases.* (2020) 8:3097–107. doi: 10.12998/wjcc.v8.i14.3097

9. Zhao CA. Case in which paraneoplastic pemphigus and bronchiolitis obliterans are the main manifestations of inflammatory pseudotumour-like follicular dendritic cell sarcoma. *Aust J Dermatol.* (2020) 61:e376–7. doi: 10.1111/ajd.13287

10. Wang L, Deng H, Mao M. Paraneoplastic pemphigus and myasthenia gravis, associated with inflammatory pseudotumor-like follicular dendritic cell sarcoma: response to rituximab. *Clin Case Rep.* (2016) 4:797–9. doi: 10.1002/ccr3.625

11. Lewis J, Gaffney R, Casey M, Farrell M, Morice W, Macon W. Inflammatory pseudotumor of the spleen associated with a clonal epstein-barr virus genome. Case report and review of the literature. *Am J Clin Pathol.* (2003) 120:56–61. doi: 10.1309/buwn-mg5r-v4d0-9yyh

12. Deyrup AT. Epstein-barr virus-associated epithelial and mesenchymal neoplasms. *Hum Pathol.* (2008) 39:473–83. doi: 10.1016/j.humpath.2007.10.030

13. Choe JY, Go H, Jeon YK, Yun JY, Kim YA, Kim HJ, et al. Inflammatory pseudotumor-like follicular dendritic cell sarcoma of the spleen: a report of six cases with increased igg4-positive plasma cells. *Pathol Int.* (2013) 63:245–51. doi: 10.1111/pin.12057

14. Griffin G, Sholl L, Lindeman N, Fletcher C, Hornick J. Targeted genomic sequencing of follicular dendritic cell sarcoma reveals recurrent alterations in Nf-Kb regulatory genes. *Modern Pathol.* (2016) 29:67–74. doi: 10.1038/modpathol.2015.130

15. Hang JF, Wang LC, Lai CR. Cytological features of inflammatory pseudotumor-like follicular dendritic cell sarcoma of spleen: a case report. *Diagn Cytopathol.* (2017) 45:230–4. doi: 10.1002/dc.23626

16. Li XQ, Cheuk W, Lam PW, Wang Z, Loong F, Yeong ML, et al. Inflammatory pseudotumor-like follicular dendritic cell tumor of liver and spleen: granulomatous and eosinophil-rich variants mimicking inflammatory or infective lesions. *Am J Surg Pathol.* (2014) 38:646–53. doi: 10.1097/pas.0000000000000170

17. Facchetti F, Simbeni M, Lorenzi L. Follicular dendritic cell sarcoma. *Pathologica.* (2021) 113:316–29. doi: 10.32074/1591-951x-331

18. Bui PL, Vicens RA, Westin JR, Jensen CT. Multimodality imaging of epstein-barr virus-associated inflammatory pseudotumor-like follicular dendritic cell tumor of the spleen: case report and literature review. *Clin Imaging.* (2015) 39:525–8. doi: 10.1016/j.clinimag.2014.12.021

19. Li HL, Liu HP, Guo GW, Chen ZH, Zhou FQ, Liu P, et al. Imaging findings of inflammatory pseudotumor-like follicular dendritic cell tumors of the liver: two case reports and literature review. *World J Gastroenterol.* (2019) 25:6693–703. doi: 10.3748/wjg.v25.i45.6693

20. Xu L, Ge R, Gao S. Imaging features and radiologic-pathologic correlations of inflammatory pseudotumor-like follicular dendritic cell sarcoma. *BMC Med Imaging.* (2021) 21:52. doi: 10.1186/s12880-021-00584-6

21. Wu YL, Wu F, Yang L, Sun H, Yan XC, Duan GJ. [Clinicopathologic features and prognosis of inflammatory pseudotumor-like follicular dendritic cell sarcomas in liver and spleen: an analysis of seven cases]. *Zhonghua Bing Li Xue Za Zhi.* (2018) 47:114–8. doi: 10.3760/cma.j.issn.0529-5807.2018.02.007

22. Li Z, Jin K, Yu X, Teng X, Zhou H, Wang Y, et al. Extranodal follicular dendritic cell sarcoma in mesentery: a case report. *Oncol Lett.* (2011) 2:649–52. doi: 10.3892/ol.2011.296

23. Shia J, Chen W, Tang LH, Carlson DL, Qin J, Guillem JG, et al. Extranodal follicular dendritic cell sarcoma: clinical, pathologic, and histogenetic characteristics of an underrecognized disease entity. *Virchows Arch.* (2006) 449:148–58. doi: 10.1007/s00428-006-0231-4

24. Tao LL, Huang YH, Chen YL, Yu GY, Yin WH. Sstr2a is a useful diagnostic marker for follicular dendritic cells and their related tumors. *Am J Surg Pathol.* (2019) 43:374–81. doi: 10.1097/pas.0000000000001205

25. Kazemimood R, Saei Hamedani F, Sharif A, Gaitonde S, Wiley E, Giulianotti PC, et al. A rare case of epstein-barr virus negative inflammatory pseudotumor-like follicular dendritic cell sarcoma presenting as a solitary colonic mass in a 53-year-old woman; case report and review of literature. *Appl Immunohistochem Mol Morphol.* (2017) 25:e30–3. doi: 10.1097/pai.0000000000000405

26. Agaimy A, Wünsch P. Follicular dendritic cell tumor of the gastrointestinal tract: report of a rare neoplasm and literature review. *Pathol Res Pract.* (2006) 202:541–8. doi: 10.1016/j.prp.2006.01.013

27. Takahashi N, Oya T, Matsumoto H, Tago K, Murotani K, Sato T, et al. A case of an inflammatory pseudotumor-like follicular dendritic cell tumor of the spleen unrelated to epstein-barr virus. *Kita Kanto Igaku.* (2011) 61:207–14. doi: 10.2974/kmj.61.207

28. Facchetti F, Lorenzi L. Follicular dendritic cells and related sarcoma. *Semin Diagn Pathol.* (2016) 33:262–76. doi: 10.1053/j.semdp.2016.05.002

29. Shi QY, Zheng Z, Wu HY, Chen JY, Fan XS. [Colonic inflammatory pseudotumor-like follicular dendritic cell sarcoma: report of a case]. *Zhonghua Bing Li Xue Za Zhi.* (2022) 51:138–40. doi: 10.3760/cma.j.cn112151-20210727-00531

30. Zhao M, Du X, OuYang B, Li M, Yang H. Inflammatory pseudotumor-like follicular dendritic cell sarcoma mimicking a colonic polyp. *J Gastrointest Surg.* (2021) 25:2429–30. doi: 10.1007/s11605-021-04961-y

31. Xue N, Xue X, Sheng C, Lu M, Wang Y, Zhang S, et al. Imaging features of inflammatory pseudotumor-like follicular dendritic cell sarcoma of the spleen. *Ann Palliat Med.* (2021) 10:12140–8. doi: 10.21037/apm-21-2776

32. Pascariu AD, Neagu AI, Neagu AV, Bājenaru A, Beţianu CI. Hepatic inflammatory pseudotumor-like follicular dendritic cell tumor: a case report. *J Med Case Rep.* (2021) 15:410. doi: 10.1186/s13256-021-02957-5

33. Nguyen A, Negrete LM, Bulterys PL, Shen L. Inflammatory pseudotumor-like follicular dendritic cell tumor of the spleen: a case report and approach to differential diagnosis. *Radiol Case Rep.* (2021) 16:3213–6. doi: 10.1016/j.radcr.2021.07.078

34. Morales-Vargas B, Deeb K, Peker D. Clinicopathologic and molecular analysis of inflammatory pseudotumor-like follicular/fibroblastic dendritic cell sarcoma: a case report and review of literature. *Turk Patoloji Derg.* (2021) 37:266–72. doi: 10.5146/tjpath.2021.01523

35. Lu SS, Wang Z, Zhao S, Liu WP. [Hepatic inflammatory pseudotumor-like follicular dendritic cell sarcoma with paravertebral metastasis and recurrence: report of a case]. *Zhonghua Bing Li Xue Za Zhi.* (2021) 50:958–60. doi: 10.3760/cma.j.cn112151-20210325-00234

36. Li J, Tao HS, Chen D, Huang ZY, Zhang EL. Hepatic inflammatory pseudotumor-like follicular dendritic cell tumor with hepatic lymphoma history: a case report and literature review. *Medicine.* (2021) 100:e27392. doi: 10.1097/md.0000000000027392

37. He H, Xue Q, Tan F, Yang L, Wang X, Gao Y, et al. A rare case of primary pulmonary inflammatory pseudotumor-like follicular dendritic cell sarcoma successfully treated by lobectomy. *Ann Transl Med.* (2021) 9:77. doi: 10.21037/atm-20-4965

38. Bruehl FK, Azzato E, Durkin L, Farkas DH, Hsi ED, Ondrejka SL. Inflammatory pseudotumor-like follicular/fibroblastic dendritic cell sarcomas of the spleen are EBV-associated and lack other commonly identifiable molecular alterations. *Int J Surg Pathol.* (2021) 29:443–6. doi: 10.1177/1066896920949675

39. Jin K, Li MN, Li S, Li J, Chen N. [Hepatic inflammatory pseudotumor-like follicular dendritic cell sarcoma]. *Zhonghua Gan Zang Bing Za Zhi.* (2020) 28:172–4. doi: 10.3760/cma.j.issn.1007-3418.2020.02.015

40. Mograbi M, Stump MS, Luyimbazi DT, Shakhatreh MH, Grider DJ. Pancreatic inflammatory pseudotumor-like follicular dendritic cell tumor. *Case Rep Pathol.* (2019) 2019:2648123. doi: 10.1155/2019/2648123

41. Li X, Shi Z, You R, Li Y, Cao D, Lin R, et al. Inflammatory pseudotumor-like follicular dendritic cell sarcoma of the spleen: computed tomography imaging characteristics in 5 patients. *J Comput Assist Tomogr.* (2018) 42:399–404. doi: 10.1097/rct.0000000000000700

42. Kwon H. Inflammatory pseudotumor-like follicular dendritic cell tumor of the spleen. *Turk J Gastroenterol.* (2018) 29:128–30. doi: 10.5152/tjg.2018.17220

43. Kitamura Y, Takayama Y, Nishie A, Asayama Y, Ushijima Y, Fujita N, et al. Inflammatory pseudotumor-like follicular dendritic cell tumor of the spleen: case report and review of the literature. *Magn Reson Med Sci.* (2015) 14:347–54. doi: 10.2463/mrms.2014-0052

44. Hu J, Chen LL, Ding BW, Jin DY, Xu XF. Resection is an effective treatment for recurrent follicular dendritic cell sarcoma from retroperitoneum: unusual presentation of a rare tumor. *Int J Clin Exp Med.* (2015) 8:8218–21.

45. Gong S, Auer I, Duggal R, Pittaluga S, Raffeld M, Jaffe ES. Epstein-barr virus-associated inflammatory pseudotumor presenting as a colonic mass. *Hum Pathol.* (2015) 46:1956–61. doi: 10.1016/j.humpath.2015.08.011

46. You Y, Shao H, Bui K, Bui M, Klapman J, Cui Q, et al. Epstein-barr virus positive inflammatory pseudotumor of the liver: report of a challenging case and review of the literature. *Ann Clin Lab Sci.* (2014) 44:489–98.

47. Vardas K, Manganas D, Papadimitriou G, Kalatzis V, Kyriakopoulos G, Chantziara M, et al. Splenic inflammatory pseudotumor-like follicular dendritic cell tumor. *Case Rep Oncol.* (2014) 7:410–6. doi: 10.1159/000365000

48. Rao L, Yang Z, Wang X, Zhang X, Shen B. Imaging findings of inflammatory pseudotumor-like follicular dendritic cell tumor of spleen. *Clin Nucl Med.* (2014) 39:e286–9. doi: 10.1097/RLU.0b013e3182952bfe

49. Pan ST, Cheng CY, Lee NS, Liang PI, Chuang SS. Follicular dendritic cell sarcoma of the inflammatory pseudotumor-like variant presenting as a colonic polyp. *Korean J Pathol.* (2014) 48:140–5. doi: 10.4132/KoreanJPathol.2014.48.2.140

50. Kim HJ, Kim JE, Kang GH, Kim JY, Park K. Inflammatory pseudotumor-like follicular dendritic cell tumor of the spleen with extensive histiocytic granulomas and necrosis: a case report and literature review. *Korean J Pathol.* (2013) 47:599–602. doi: 10.4132/KoreanJPathol.2013.47.6.599

51. Kiryu S, Takeuchi K, Shibahara J, Uozaki H, Fukayama M, Tanaka H, et al. Epstein-barr virus-positive inflammatory pseudotumour and inflammatory pseudotumour-like follicular dendritic cell tumour. *Br J Radiol.* (2009) 82:e67–71. doi: 10.1259/bjr/66918927

52. Yoon S, Ko H, Kim B-H, Kwon G, Jeon Y, Kim C-G. Epstein-barr virus-associated inflammatory pseudotumor-like follicular dendritic cell tumor in the spleen of a patient with diffuse large B cell lymphoma: a case report and review of the literature. *Korean J Pathol.* (2007) 41:198–202.

53. Horiguchi H, Matsui-Horiguchi M, Sakata H, Ichinose M, Yamamoto T, Fujiwara M, et al. Inflammatory pseudotumor-like follicular dendritic cell tumor of the spleen. *Pathol Int.* (2004) 54:124–31. doi: 10.1111/j.1440-1827.2004.01589.x

54. Brittig F, Ajtay E, Jaksó P, Kelényi G. Follicular dendritic reticulum cell tumor mimicking inflammatory pseudotumor of the spleen. *Pathol Oncol Res.* (2004) 10:57–60. doi: 10.1007/bf02893411

55. Wu CY, Wang RC, Chen BJ, Chen WY, Jhuang JY, Chang MC, et al. Granuloma with an underlying lymphoma: a diagnostic challenge and a wider histologic spectrum including adult T-cell leukemia/lymphoma. *Appl Immunohistochem Mol Morphol.* (2020) 28:316–24. doi: 10.1097/pai.0000000000000731

56. Zhang BX, Chen ZH, Liu Y, Zeng YJ, Li YC. Inflammatory pseudotumor-like follicular dendritic cell sarcoma: a brief report of two cases. *World J Gastrointest Oncol.* (2019) 11:1231–9. doi: 10.4251/wjgo.v11.i12.1231

57. Deng S, Gao J. Inflammatory pseudotumor-like follicular dendritic cell sarcoma: a rare presentation of a hepatic mass. *Int J Clin Exp Pathol.* (2019) 12:3149–55.

58. Ang W, Bundele M, Shelat V. Follicular dendritic cell sarcoma: rare presentation of incidental large hepatic mass. *Ann Hepatobiliary Pancreat Surg.* (2019) 23:74–6. doi: 10.14701/ahbps.2019.23.1.74

59. Zhang X, Zhu C, Hu Y, Qin X. Hepatic inflammatory pseudotumour-like follicular dendritic cell tumor: a case report. *Mol Clin Oncol.* (2017) 6:547–9. doi: 10.3892/mco.2017.1188

60. Chen Y, Shi H, Li H, Zhen T, Han A. Clinicopathological features of inflammatory pseudotumour-like follicular dendritic cell tumour of the abdomen. *Histopathology.* (2016) 68:858–65. doi: 10.1111/his.12851

61. Nguyen B, Roarke M, Yang M. Synchronous hepatic and splenic inflammatory pseudotumour-like follicular dendritic cell sarcomas. *Liver Int.* (2015) 35:1917. doi: 10.1111/liv.12738

62. Granados R, Aramburu JA, Rodríguez JM, Nieto MA. Cytopathology of a primary follicular dendritic cell sarcoma of the liver of the inflammatory pseudotumor-like type. *Diagn Cytopathol.* (2008) 36:42–6. doi: 10.1002/dc.20744

63. Chen T, Kuo T, Ng K. Follicular dendritic cell tumor of the liver: a clinicopathologic and epstein-barr virus study of two cases. *Modern Pathol.* (2001) 14:354–60. doi: 10.1038/modpathol.3880315

64. Nishiyama R, Baba S, Watahiki Y, Maruo H. Inflammatory pseudotumour-like follicular dendritic cell tumour of the spleen. *BMJ Case Rep.* (2015) 2015:bcr2014206373. doi: 10.1136/bcr-2014-206373

frontiers | Frontiers in Medicine

TYPE Case Report
PUBLISHED 10 May 2023
DOI 10.3389/fmed.2023.1158334

Check for updates

OPEN ACCESS

EDITED BY
Liam Chen,
University of Minnesota, United States

REVIEWED BY
Mousumi Chaudhury,
Agricultural Research Service (USDA),
United States
Sakinah Mohamad,
Universiti Sains Malaysia Health
Campus, Malaysia

*CORRESPONDENCE
Fei Ye
✉ yefei@csu.edu.cn
Yi Gong
✉ gongyi@126.com;
✉ gongyi5226@csu.edu.cn

†These authors have contributed equally to this work

RECEIVED 07 February 2023
ACCEPTED 29 March 2023
PUBLISHED 10 May 2023

CITATION
Ren C, Li Y, Huang J, Liu S, Cao Z, Jiang Q, Lin X, Ye F and Gong Y (2023) Primary synovial sarcoma of the thyroid gland: a CARE compliant case report and literature review. *Front. Med.* 10:1158334. doi: 10.3389/fmed.2023.1158334

COPYRIGHT
© 2023 Ren, Li, Huang, Liu, Cao, Jiang, Lin, Ye and Gong. This is an open-access article distributed under the terms of the Creative Commons Attribution License (CC BY). The use, distribution or reproduction in other forums is permitted, provided the original author(s) and the copyright owner(s) are credited and that the original publication in this journal is cited, in accordance with accepted academic practice. No use, distribution or reproduction is permitted which does not comply with these terms.

Primary synovial sarcoma of the thyroid gland: a CARE compliant case report and literature review

Chutong Ren[1], Yashan Li[1], Jiangsheng Huang[1], Sushun Liu[1], Zhexu Cao[1], Qin Jiang[1], Xiang Lin[2], Fei Ye[1*†] and Yi Gong[1*†]

[1]Department of General Surgery, The Second Xiangya Hospital, Central South University, Changsha, Hunan, China, [2]Department of General Surgery, Huaihua Second People's Hospital, Huaihua, Hunan, China

Rationale: Synovial sarcoma is a subtype of soft tissue sarcoma. Synovial sarcoma in the head and neck region is relatively unusual. Primary synovial sarcoma of the thyroid gland (PSST) is first reported in 2003 by Inako Kikuchi. PSST is extremely rare with only 15 cases documented globally. PSST shows rapid disease progression and a relatively poor prognosis. However, diagnosis and therapy are challenging for clinical surgeons. In this article, we reported the 16th PSST case and reviewed the PSST cases globally for further clinical application.

Patient concerns: The patient was referred to us because of gradually worsened dyspnea and dysphagia for 20 days. Physical examination showed a 5 × 4 cm mass with a clear boundary and good mobility. Contrast-enhanced ultrasonography (CEUS) and computed tomography (CT) showed a mass in the isthmus of the thyroid gland. The imageology diagnosis tends to be a benign thyroid nodule.

Diagnosis: After surgery, histopathology, immunohistochemistry, and fluorescence, *in situ* hybridization indicated the mass to be primary synovial sarcoma of the thyroid gland with no local and distant metastasis.

Interventions: The patient underwent total thyroidectomy and dissected the lymph nodes in the central compartment. This patient received postoperative chemotherapy (a combination of ifosfamide and epirubicin for five cycles). Patients tolerated chemotherapy well. No recurrence was found during the 9-month follow-up.

Lessons: Although PSST is an extremely rare disease, we should raise our awareness when we encounter a rapidly growing, cystic-solid mixed thyroid mass with neck compression symptoms to avoid misdiagnosis. Intraoperatively, surgeons should refine surgical procedures to avoid capsular rupture and tumor local implantation metastasis. Intraoperative frozen section pathology is necessary sometimes, especially when the diagnosis could not be established before surgery.

KEYWORDS

primary synovial sarcoma of the thyroid gland, SS18 gene, perioperative evaluation, case report, literature review

Introduction

Synovial sarcoma is a kind of histological subtype of soft tissue sarcoma, making up 8–10% of all soft tissue sarcomas. It is a high-grade malignant neoplasm of mesenchymal pluripotent cells, characterized by a specific t(X;18) (p11.2; q11.2) translocation leading to the generation of SYT-SSX fusion gene transcripts (1, 2). According to different ultra structures, synovial sarcoma was divided into monophasic patterns and classic biphasic

patterns (2). Synovial sarcoma in the head and neck region is relatively unusual, and primary synovial sarcoma in the thyroid gland is extremely rare with only 15 cases documented globally (3–13). Due to the rarity of the disease, challenges exist in clinical practice from diagnosis to follow-up. In the study, we report a case of a middle-aged female who was diagnosed with thyroid synovial sarcoma post-surgery. This is the 16th PSST case reported. For deep investigation, the clinical characteristics of 15 previously reported cases were also carefully summarized. Because of a lower survival rate (5-year survival rate of ∼60%) than differentiated thyroid cancer (14), we hope our case report and literature review could arise awareness of thyroid synovial sarcoma and improve the diagnosis and treatment of this disease.

Case presentation

A 59-year-old female patient was admitted to our hospital in June 2022. Her chief complaints were dyspnea and dysphagia for 20 days. She felt dyspnea 20 days before, and the discomfort gradually worsened accompanied by cough and dysphagia. The physical examination showed a palpable hard mass in the center of the neck. The size of the mass was 5 × 4 cm (Figure 1). The boundary of the mass is clear, and no tenderness was found. The mass could move up and down with swallowing. There is no jugular vein distension, and the trachea is centered. No enlarged lymph node was found through palpation. No other signs were found in the physical examination. The patient denied symptoms such as fever, palpitations, shaky hands, and irascibility. There were no abnormalities in defecation and urine. There was no significant change in weight over the past 3 months. The patient underwent a cholecystectomy 10 years ago. She had a history of asthma for a year. Intermittent oral and inhaled drug therapy were used for asthma. The patient has no familial-hereditary disease, and no similar diseases were diagnosed in her family.

Accessory examination before surgery

A Blood test showed no obvious abnormalities. The level of thyroid hormone and calcitonin is in the normal range. No abnormalities were found in the laryngoscopy, chest X-ray, and chest CT. Contrast-enhanced ultrasonography showed a heterogeneous echoic, cystic-solid mixed mass ∼48.8 × 37.2 mm in the isthmus of the thyroid gland. The mass is with clear boundary, regular shape. In total, 0.6 ml perflubutane microspheres were injected through the elbow intravenous for CEUS. The isthmus nodule was mostly equally enhanced and partially no enhancement. The peripheral nodule showed annular enhancement. No obvious enlarged lymph nodes were observed in the cervical region. The mass was classified as TI-RADS 3 (Figure 2). CT scan showed a mass lesion in or below the isthmus of the thyroid gland. The mass was heterogeneous density. There are microcalcifications and liquefaction necrosis areas inside the mass. The average CT value is 28 HU. The edge of the mass is mostly clear. The contrast-enhanced CT demonstrated heterogeneous enhancement. The degree of enhancement is lower than that of the normal thyroid gland. The average CT value is 58 HU. There are multiple small lymph nodes in the I-II area of the cervical region. The CT could not establish a confirmed diagnosis but a low-grade tumor could not be ruled out (Figure 3).

Therapy

The patient was intended for partial thyroidectomy. We made a transverse arc-shaped incision in the suprasternal notch, dissociated the subcutaneous tissue, and opened the interval between the bilateral strap muscles in the neck to expose the thyroid mass. The mass was located in the isthmus of the thyroid gland and extended to the back of the sternum. The mass was cystic-solid mixed. The cyst wall was closely adhered to the trachea. Intraoperatively, the mass was difficult to be mobilized and led to a capsular rupture and an effusion of necrotic, hemorrhagic, and gelatinous liquid. When the mass was cut open, chocolate-like contents could be seen in the capsule. The solid section was fish-like, gray-red, and gray-yellow, and hard calcification was visible in some areas. Frozen section pathology showed soft tissue sarcoma, after which we choose to carry out total thyroidectomy and central cervical lymph nodes dissection.

Histopathology

Histopathology showed that the thyroid isthmus mass was a mesenchymal tissue-derived spindle cell malignant tumor, with epithelioid differentiation in the focal area. The nucleus was atypical. Lots of mitotic figures could be seen. Invasion of surrounding soft tissues was observed. There are no obvious masses in the left and right lobes of the thyroid gland. There was no metastasis in the central cervical lymph nodes (0/6) (Figure 4).

Immunohistochemistry

CK(-), EMA(-), CK7(-), CK19(-), CD99(-), Bcl-2(+), WT-1(-), TLE1(+), Ki-67(50%), P53(30%+), Vim(+), Syn(focally +), S100(-), SMA(-), MyoD1(-), STAT6(-), and SOX-10(-) (Figure 4).

Fluorescence *in situ* hybridization (FISH)

Molecular analysis, performed on the formalin-fixed paraffin-embedded tissue by fluorescent *in situ* hybridization (FISH), showed an SS18 (SYT) gene rearrangement, highly consistent with the diagnosis of a PSST (Figure 4).

Pathology Stage: pT2N0M0. Stage IIA

Abbreviations: PSST, primary synovial sarcoma of the thyroid gland; CEUS, Contrast-enhanced ultrasonography; CT, computed tomography; MTC, medullary thyroid carcinoma; SETTLE, spindle epithelioid tumor with thymus-like differentiation; UTC/ATC, undifferentiated/anaplastic thyroid carcinoma; MRI, magnetic resonance imaging.

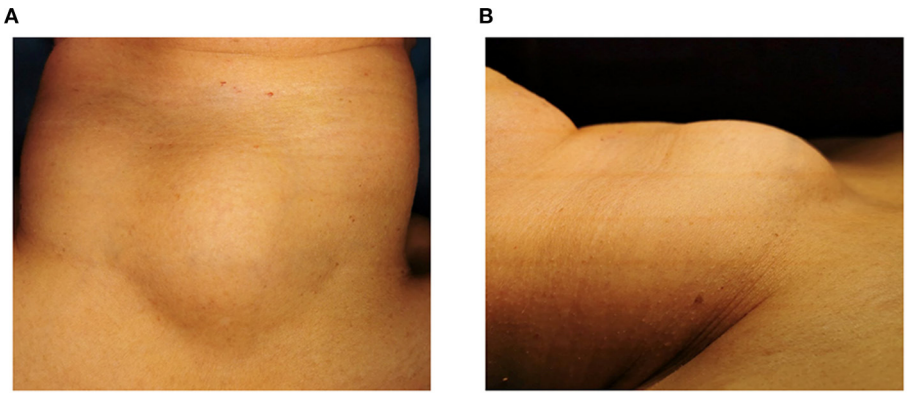

FIGURE 1
Preoperative photo of the tumor anteriorly **(A)** and laterally **(B)**.

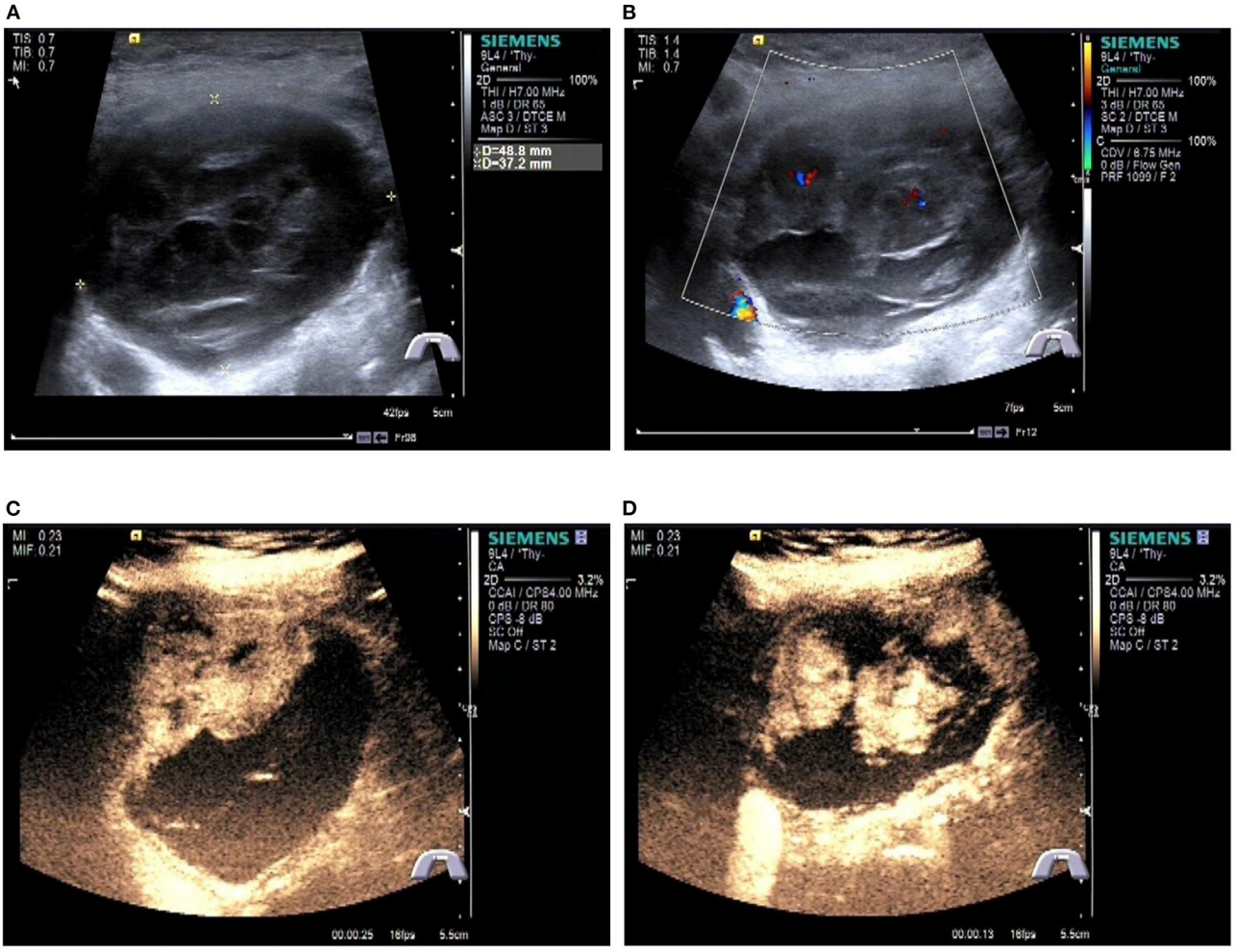

FIGURE 2
Preoperative contrast-enhanced ultrasonography of the patient. **(A)** Gray scale ultrasonography of the mass. **(B)** Color Doppler imaging of the mass. **(C, D)** Contrast-enhanced ultrasonography of the tumor.

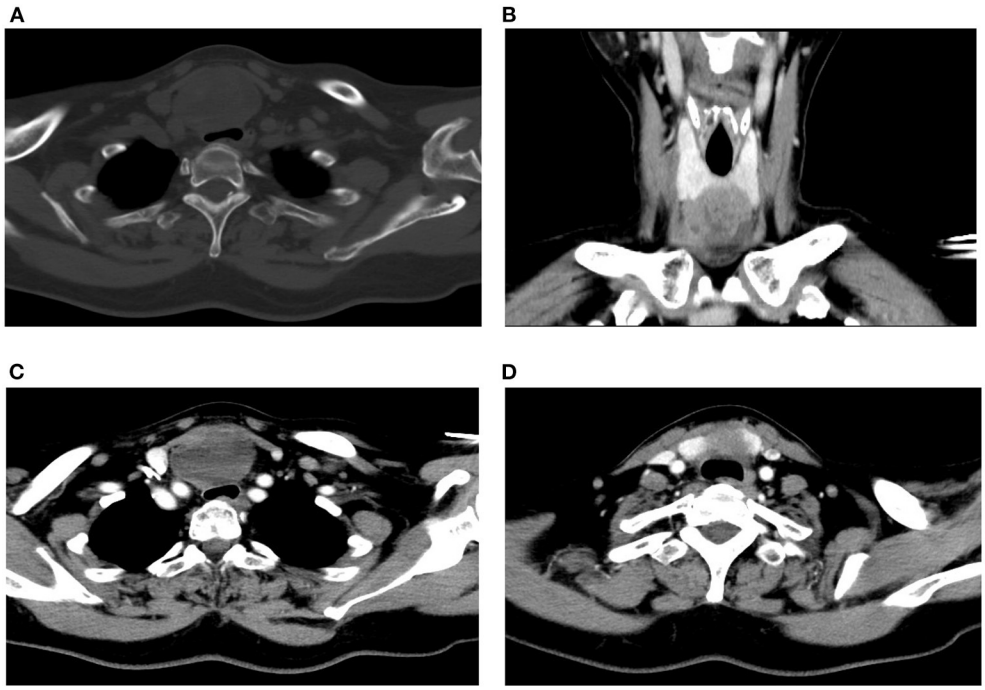

FIGURE 3
Preoperative CT scan of the patient. **(A)** Plain CT of the neck (horizontal plane). **(B)** CT scan of the neck (coronal plane). **(C, D)** Contrast-enhanced CT of the neck (horizontal plane).

Postoperative adjuvant therapy and follow-up

After the initial surgery, chest CT, abdominal CT, MRI of the head, and whole-body bone scan were performed for evaluation. No obvious local and distant recurrence or metastases was found. After evaluation, this patient received chemotherapy (a combination of ifosfamide 3,000 mg and epirubicin 120 mg). The patient tolerated chemotherapy well. The patient received five-cycle chemotherapy. Postoperative adjuvant radiation therapy was recommended by the oncologist, but the patient refused for personal reasons. After 9 months of the surgery, no remarkable recurrence and metastases were detected.

Discussion

In this article, we reported the 16th PSST case globally. Although the mass of this patient was mostly composed of spindle cells, a lack of normal thyroid follicular epithelial cells, the boundary between the mass and the surrounding thyroid tissue was unclear, and a part of the normal thyroid tissue was replaced by the synovial sarcoma. In synovial sarcoma of the head and neck regions originating from other structures, the main tumor foci are usually situated around their local regions instead of the thyroid gland. Therefore, according to a definition in a previous study, this mass was identified to be primary thyroid synovial sarcoma (5). When summarizing the clinical features of this case, we could find that the course of the disease was only 20 days, and the mass has some similarities with the benign thyroid nodule (including clear boundary, regular shape, and annular enhancement on ultrasound). These characteristics may lead to a missed diagnosis of malignancy in preoperative evaluation. However, when trying for total excision, we found that the mass closely adhered to the trachea, which is different from a typical benign thyroid tumor. Therefore, we choose to perform frozen section pathology intraoperatively. The intraoperative frozen section pathology assisted the surgeon to make clinical decisions and helped the patient to avoid reoperation. According to the research by Maduekwe et al. synovial sarcoma was thought to have a predilection for metastases to lymph nodes, necessitating the need for possible sentinel node biopsy (15, 16). Therefore, when we encounter rapidly growing thyroid nodules, we should be careful in perioperative assessment and perform intraoperative frozen section pathology when necessary.

For further investigation, we searched the PSST case in PubMed and Web of Science. A total of 15 cases were reported previously. We summarized the clinical characteristics of the 15 cases in Table 1. In most PSST cases, the course of the disease is <1 year and progressing rapidly. In cases with detailed follow-up, most PSST patients presented recurrence within 2 years. A total of eight cases have detailed survival data. Among them, six patients have fatal events. The longest survival time in these patients is 126 months (in a study by Carina Owen) and four patients died within 3.5 years. The 5-year survival rate is consistent with a previous study (14). Generally, PSST showed rapid disease progression and relatively poor prognosis. Regarding the preoperative evaluation of PSST, the tumor is usually cystic-solid mixed, larger than 5 cm, and presented symptoms of neck compression. In eight cases, fine

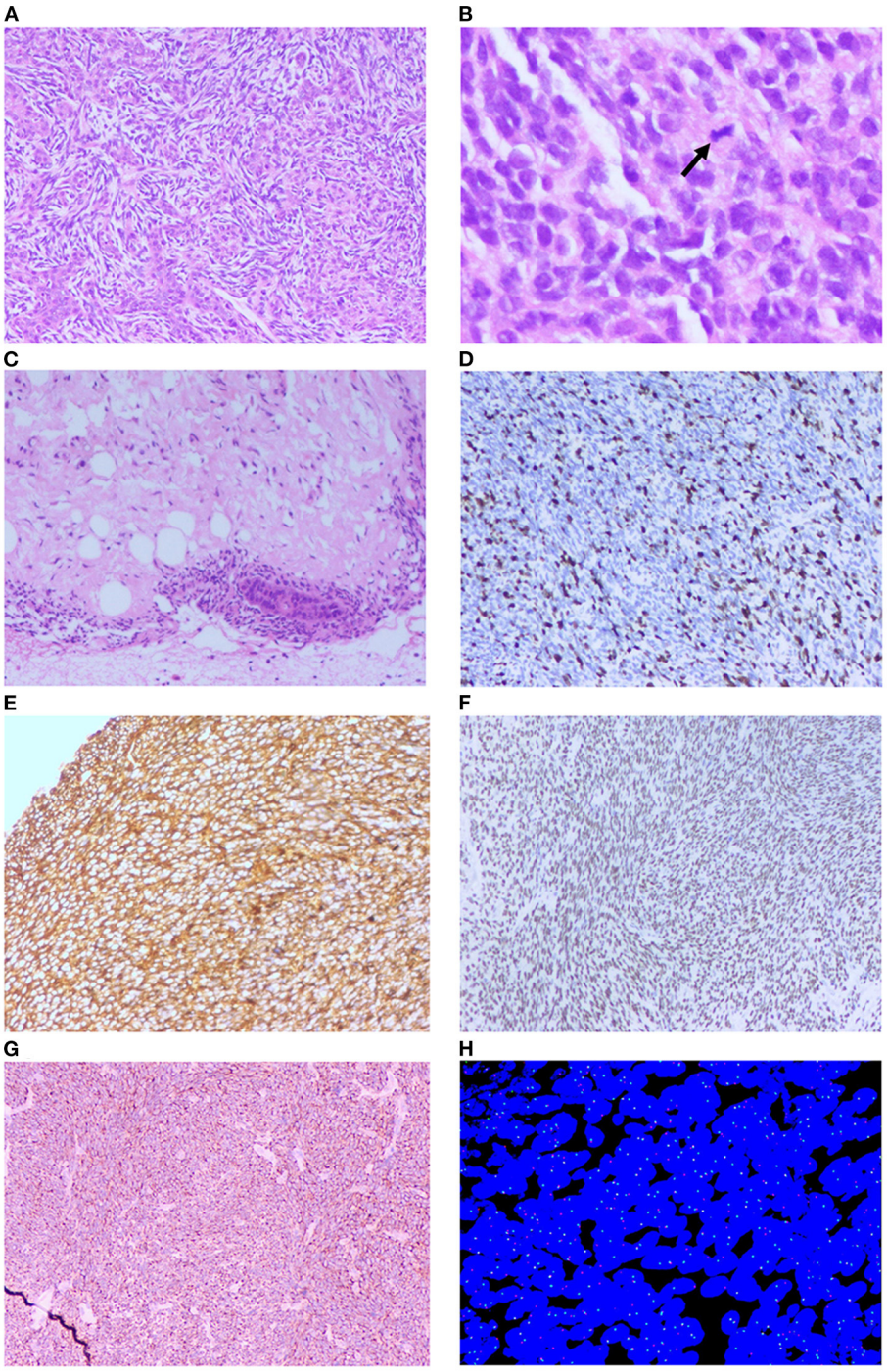

FIGURE 4
Histopathology examination and FISH of the patient. **(A)** Microscopic images showing biphasic tumor (H&E × 100). **(B)** Microscopic images showing pathological mitotic (Black arrow, H&E × 400). **(C)** Microscopic images showing the tumor invasion to adipose tissue (H&E × 100). **(D)** Immunohistochemistry positive to Ki-67 (H&E ×100). **(E)** Immunohistochemistry positive to Vim (H&E ×100). **(F)** Immunohistochemistry positive to TLE1 (H&E × 100). **(G)** Immunohistochemistry positive to Bcl-2 (H&E × 100). **(H)** Fluorescence *in situ* hybridization (FISH) break-apart probe confirmed SS18 gene rearrangement (split red and green signal).

needle aspiration (FNA) was performed for diagnosis. However, only one case has been suspected to be a malignant spindle cell tumor. Most patients were diagnosed with MTC or undifferentiated thyroid carcinoma by FNA, and some patients could not be diagnosed by FNA. These data indicated that the cytopathological diagnosis of PSST is challenging. Although Aisner et al. proposed that FNA is important for diagnosing soft tissue synovial sarcoma, establishing the diagnosis of PSST is difficult due to its rarity (17). We should be careful in clinical practice in order to reduce misdiagnose rate of this rare disease even when FNA indicated a

10.3389/fmed.2023.1158334

TABLE 1 Clinical characteristics of PSST cases reported previously.

No.	Author	Year	Age/gender	Chief complaint	Course	Tumor size	Ultrasound	CT	Initial diagnosis	FNA	Surgery	Histopathology and metastasis	Immunohistochemistry	Gene analysis t (X; 18) (p11; q11) & Tech	Subtype	Postoperative adjuvant therapy	Recurrence	Death	Last follow-up (months after surgery)
1	Inako Kikuchi	2002	60/Male	Hoarseness	1 year	6.8*6.5 cm	Not recorded	Cervical tumor to be accompanied by destruction of the thyroid and cricoid cartilage	Thyroid medullary carcinoma (by FNA)	Thyroid medullary carcinoma	Total thyroidectomy with partial resection of the thyroid and cricoid cartilage, partial resection of the cervical esophagus and dissection of the lymph nodes around the thyroid gland	Mostly long spindle cells	vimentin (+), bcl-2 (+), epithelial membrane antigen (+), cytokeratin (+), Leu-7(+), thyroglobin (-), triiodothyronine (-), thyroxin (-)	Chimera SYT-SSX gene transcripts (by RT-PCR)	Monophasic	Not recorded	Multiple pulmonary metastases and local tumor recurrence (18 months after surgery)	32 months after the surgery	32 months
2	Ki-Seok Jang	2007	15/Male	Palpable neck mass	4 months	6*5*5 cm	Not recorded	A relatively well-demarcated solid mass at the superior and lateral portion of the left thyroid gland	A benign follicular lesion (by FNA)	Moderate cellularity with a predominance of bipolar spindle-shaped cells	Total thyroidectomy and left cervical lymph node dissection	An admixture of spindle and epithelial cell components in almost equal proportions	Cytokeratin (+), vimentin (+), epithelial membrane antigen (+), CD 99 (+), muscle specific actin (-), smooth muscle actin (-), S-100(-), carcinoembryonic antigen (-), synaptophysin (-), chromogranin (-), thyroglobulin (-), and thyroid transcription factor-1(-)	SYT-SSX fusion gene transcript was identified (by RT-PCR)	Biphasic	Not recorded	Not recorded	Not recorded	Not recorded	Not recorded

(Continued)

TABLE 1 (Continued)

No.	Author	Year	Age/gender	Chief complaint	Course	Tumor size	Ultrasound	CT	Initial diagnosis	FNA	Surgery	Histopathology and metastasis	Immunohistochemistry	Gene analysis t (X; 18) (p11; q11) & Tech	Subtype	Postoperative adjuvant therapy	Recurrence	Death	Last follow-up (months after surgery)
3	Chang Hwan Ryu	2011	72/Female	Neck mass, hoarseness and dysphagia	3 months	6∗5∗4.5 cm	A 6∗5cm-sized, heterogeneously hypoechoic nodule with internal calcification in the left lobe of the thyroid gland	A large, low attenuating mass replacing the left thyroid gland extending to the level of the hyoid bone superiorly and superior mediastinum inferiorly with possible invasion to the trachea	Cystic change (by FNA)	Cystic change	Total thyroidectomy with tracheal fenestration	Fascicles and sheets of dense, uniform, relatively small ovoid neoplastic cells	CD 99(+), cytokeratin (-), desmin (-), S-100(-), CD 31(-), CD 34(-), epithelial membrane antigen (EMA) (-)	SYT/SSX fusion gene transcript (+)	Monophasic	Concurrent chemoradiation was planned but not performed	Not recorded	2 months after surgery (due to unknown causes)	2 months
4	Ali Ghafouri	2012	44/Female	Neck mass and dyspnea	4 months	17∗14∗6cm	Not recorded	A large tumor with tracheal deviation	Unknown	Not recorded	Mass biopsy and further surgery (not recorded in detail)	Spindle cell tumor with pleomorphism and necrosis	Thyro (-), TTF1(-), EMA (-), vimentin (+), EGFR(+)	Not recorded	Monophasic	Not recorded	Not recorded	Not recorded	Not recorded
5	Laurys Boudin	2014	55/Male	Palpable neck mass and dysphagia	1 month	Over 12cm in diameter	A 7cm mass of the left thyroid lobe which was heterogeneous, hypervascularized, and mixed (solid and liquid)	Not recorded	Anaplastic thyroid carcinoma	/	Total thyroidectomy	A dense cellular proliferation composed of ovoid-shaped to frankly spindle-shaped cells	EMA (+), pan-cytokeratin (-), desmin (-), H-caldesmon (-), PS100 (-), HMB-45 (-), MDM2(-)	SYT gene rearrangement (by FISH)	Monophasic	Combination of doxorubicin and ifosfamide	A 4cm cervical mass was found (15 days after surgery)	Not recorded	Not recorded after the revision surgery

(Continued)

10.3389/fmed.2023.1158334

TABLE 1 (Continued)

No.	Author	Year	Age/gender	Chief complaint	Course	Tumor size	Ultrasound	CT	Initial diagnosis	FNA	Surgery	Histopathology and metastasis	Immunohistochemistry	Gene analysis t (X; 18) (p11; q11) & Tech	Subtype	Postoperative adjuvant therapy	Recurrence	Death	Last follow-up (months after surgery)
6	RONG-LIANG SHI	2016	31/Male	Neck mass without symptom	1 month	5∗2∗2 cm	A large mass with an area of 5∗2∗2 cm in the right thyroid lobe, which was heterogeneous, hypervascular and solid	Not recorded	Poorly differentiated tumor	/	Total thyroidectomy	The tumor contained two components spindle cells and glandular structures	B-cell lymphoma-2(+), cytokeratin (+)	Not recorded	Biphasic	Adjuvant chemotherapy containing ifosfamide and doxorubicin was administered every 3 weeks for four cycles. A total of 50 Gy of adjuvant radiotherapy was applied.	A patchy LN measuring 2 cm in diameter in the right upper neck (2 years after initial surgery)	Not recorded	34 months
7	Chang-Soo Park	2017	47/Female	Thyroid mass detected on regular health check up	Not recorded	7.8mm in diameter	7.8mm sized anechoic lesion suspected of malignancy was found in the isthmus of right lobe	Not recorded	Unknown	Large quantity of either single or clustered ovoid to spindle cells	Total thyroidectomy	The tumor was composed of ovoid to spindle tumor cells, forming fascicles with an interlacing arrangement	epithelial membrane antigen (+), CK (+), vimentin (+), transduction-like enhancing protein 1(+), neuroendocrine markers (-), CD56(-), synaptophysin (-), chromogranin (-), calcitonin (-), CD34(-), thyroid transcription factor-1(-), S-100(-), c-kit (-)	Translocation (X; 18) (p11;q11) (confirmed by FISH)	Monophasic	Not recorded	No recurrence or metastasis was detected	Alive until 3 years after surgery	36 months

(Continued)

10.3389/fmed.2023.1158334

10.3389/fmed.2023.1158334

TABLE 1 (Continued)

No.	Author	Year	Age/gender	Chief complaint	Course	Tumor size	Ultrasound	CT	Initial diagnosis	FNA	Surgery	Histopathology and metastasis	Immunohistochemistry	Gene analysis t (X; 18) (p11; q11) & Tech	Subtype	Postoperative adjuvant therapy	Recurrence	Death	Last follow-up (months after surgery)
8	Diksha Yadav	2018	12/Male	A gradually progressive neck mass associated with dyspnea, dysphagia and voice change	1.5 years	12∗11∗7cm	Not recorded	A 9.1∗6.9∗6.1cm heterogeneously enhancing lesion involving left lobe of thyroid and adherent to the surrounding structures	Malignant spindle cell tumor or MTC	Malignant spindle cell tumor, with a possibility of non-secretory MTC was rendered	Total thyroidectomy	Spindle cell tumor with small nests of polygonal cells with focal glandular pattern	CK7 (+), CK19 (+), EMA (+), BCL2 (+), CD99 (+)	Translocation (X;18) (p11.2: q11.2) (confirmed by FISH)	Biphasic	Not recorded	Not recorded	7 months after surgery	7 months
9	Carina Owen	2018	37/Male	Initial symptoms were not recorded. Chest pain and haemoptysis were presented when recurrence occurs.	Not recorded	Not recorded	Not recorded	Not recorded	Unclear	Not recorded	Total thyroidectomy and De-bulking surgery	Histopathology of primary site was not recorded. Histopathology of metastatic lesion showed synovial sarcoma, and showed a relatively circumscribed cellular neoplasm, which entrapped lung parenchyma and was composed of elongated slender spindle cells with minimal pleomorphism and mitotic activity.	TLE1(+), focal bcl-2(+), cytokeratins (-), MNF116(-), AE1/AE3(-), epithelial membrane antigen (-), S100 protein (-), CD34(-), TTF-1(-), CD99(-), WT1(-), SMA (-), desmin (-), MUC4(-), CD31(-), CD117(-), DOG1(-), EBER (-), STAT6(-), HHV8(-), calretinin(-)	SS18 gene rearrangement (by FISH)	Suspected Monophasic (not described in detail)	Postoperative radiotherapy; Combination chemotherapy of doxorubicin and ifosfamide; Second-line chemotherapy consisting of an infusional ifosfamide schedule; 4 cycles of trabectedin	8 years after initial surgery	126 months after initial surgery	126 months after initial surgery

(Continued)

TABLE 1 (Continued)

No.	Author	Year	Age/gender	Chief complaint	Course	Tumor size	Ultrasound	CT	Initial diagnosis	FNA	Surgery	Histopathology and metastasis	Immunohistochemistry	Gene analysis t (X; 18) (p11; q11) & Tech	Subtype	Postoperative adjuvant therapy	Recurrence	Death	Last follow-up (months after surgery)
10	Carina Owen	2018	47/Male	An asymptomatic left-sided thyroid nodule	Not recorded	Not recorded	Not recorded	A CT-positron emission tomography (PET) scan showed no distant sites of metastatic disease.	Unknown	A core biopsy was performed, but the diagnosis was not established	Total thyroidectomy and bilateral lymph node dissection. Following chemotherapy, he underwent resection of the two right lung metastases followed by left thoracotomy and resection of a left upper lobe metastasis.	Fascicles of minimally atypical spindle cells with intermixed islands of epithelioid cells. No lymph nodes metastasis was found.	CD56(+), TLE (+), Cytokertins(-), EMA(-)	SS18-SSX2 fusion (by RT-PCR)	Biphasic	Combination therapy with doxorubicin and ifosfamide and post-operative radiation to the left upper lung	Pulmonary metastatic presented two years after initial surgery	55 months after initial surgery	55 months
11	Carina Owen	2018	42/Male	Neck mass	Approximately 5 years	3.5cm	Not recorded	Not recorded	Paraganglioma	Not performed	Tumor excision (Not described detailed)	Fascicles of minimally to mildly spindle cells with elongated or ovoid nuclei, indistinct nucleoli and scanty cytoplasm, and a mitotic index of up to 16/10 hpf.	EMA (+), bcl-2(+), S100(+), MNF116(-), CAM5.2(-), CK903(-), CD99(-), CD34(-), CD117(-), SMA(-), HMB45(-), CD31(-), desmin(-) and neurofilament(-)	SS18 gene rearrangement (confirmed by FISH)	Monophasic	Lung metastases excised and conventional chemotherapy	Multiple lung metastases were found 1years after initial surgery	Not recorded	72 months (no further follow-up was performed)

(Continued)

10.3389/fmed.2023.1158334

TABLE 1 (Continued)

No.	Author	Year	Age/gender	Chief complaint	Course	Tumor size	Ultrasound	CT	Initial diagnosis	FNA	Surgery	Histopathology and metastasis	Immunohistochemistry	Gene analysis t (X; 18) (p11; q11) & Tech	Subtype	Postoperative adjuvant therapy	Recurrence	Death	Last follow-up (months after surgery)
12	Carina Owen	2018	36/Male	A lump on neck (with shortness of breath and difficulty in swallowing)	1 month	5.7*7.5*9cm	Not recorded	A large mass in the right lobe of the thyroid gland (5.7×7.5 cm in the axal plane and craniocaudal, up to 9 cm) as well as numerous lung nodules consistent with metastases	Synovial sarcoma	Not recorded in detail	Not resectable	Not recorded in detail	Not recorded in detail	Translocation involving the SS18 gene at 18 q 11.2.	Not recorded	Combination of doxorubicin and ifosfamide. Radiation and an ATR inhibitor were used in followed therapy.	Not recorded in detail	Not recorded	Not applicable
13	Carina Owen	2018	30/Female	A tumor in the right thyroid lobe which involved adjacent structures in the neck	Not recorded	Not recorded	Not recorded	Not recorded	Poorly differentiated synovial sarcoma	Not recorded	Not recorded	A cellular tumor, composed of sheets of relatively monotonous, mildly atypical rounded to ovoid cells with vesicular nuclei and scanty cytoplasm.	CD56(+), Cytokertins (focally +), EMA (focally +)	Not recorded	Not recorded	Not recorded	Not recorded	Not recorded	Not recorded

(Continued)

10.3389/fmed.2023.1158334

TABLE 1 (Continued)

No.	Author	Year	Age/gender	Chief complaint	Course	Tumor size	Ultrasound	CT	Initial diagnosis	FNA	Surgery	Histopathology and metastasis	Immunohistochemistry	Gene analysis t (X; 18) (p11; q11) & Tech	Subtype	Postoperative adjuvant therapy	Recurrence	Death	Last follow-up (months after surgery)
14	Dilaver Demirel	2020	26/Male	A solid, lobulated mass in the left thyroid lobe	Not recorded	Primary tumor: 4.5cm; Recurrent neck tumor: 5 × 2.5 × 2cm	Not recorded	CT of initial tumor was not scanned. MRI of recurrent tumor shows 6.4 × 4.5 × 3.4cm mass, with necrosis and suspicious invasion of the trachea	Papillary carcinoma (by FNA); Spindle epithelial tumor with thymus-like differentiation (Histopathology of first surgery)	Papillary carcinoma	Total thyroidectomy and lymph node dissection for primary site; Partial laryngectomy for recurrence	Primary tumor: Spindle epithelial tumor with thymus-like differentiation with no evidence of any nodal (0/8) or distant metastasis; Recurrent tumor: diagnosed with synovial sarcoma by	Pan-CK(+), vim(+), TLE-1(+), Bcl-2(+), CD99(+), FLI-1(+), CD56(+), EMA(+), CK-7(+), calponin(+), Ki-67 (50%+); Thyr(-), calc(-), chrom(-), syn(-), CEA(-), CK 8/18(-), HMWCK (34 beta-), P63(-), SMA(-), TTF1(-), CK-20(-), CD34(-), S100(-), des(-)	SYT-SSX1 fusion transcript was verified by FISH and RT-PCR	Biphasic	Radioactive iodine (PT)/ chemotherapy and targeted therapy	Local recurrence: 24 months, lungs, thoracic and lumbar vertebrae, iliac bone: 32 months	41 months after surgery	41 months after surgery
15	Seyed-ahmad Seyed-alagheband	2021	43/Female	Dysphagia and dyspnea	7 months	10∗8∗4 cm	Hypervascularized and mixed (solid and liquid) thyroid mass	A heterogeneous thyroid mass with a 90∗45∗65 mm thyroid nodule with internal necrotic view	Undifferentiated cell carcinoma of thyroid gland	Undifferentiated cell carcinoma of thyroid gland	Total thyroidectomy	Fascicles and sheets of monophasic spindle cell growth pattern with oval nuclei	EMA (+), CK 7(+), CK 19(+), BCL-2(+), TLE1(+), S-100(-), CD99(-), CD31(-), CD34(-), Ki-67(5%+)	SYT-SSX fusion gene transcript was identified (by RT-PCR)	Monophasic	6 cycles of doxorubicin and ifosfamide and radiotherapy	No recurrence or metastasis was detected	Alive	Not recorded

10.3389/fmed.2023.1158334

benign thyroid tumor, especially in a rapidly growing, cystic-solid mixed thyroid mass with neck compression symptoms.

PSST was usually misdiagnosed with MTC, undifferentiated/anaplastic thyroid carcinoma, or SETTLE. In this part, we would discuss the differential diagnosis of PSST. For PSST, the main differential diagnosis is MTC. An elevated calcitonin level is typical in MTC patients. In a microscopic vision, the MTC tissue usually consists of lympho/plasmacytoid cells, atypical cells, or spindle cells. However, a pure spindle cell pattern MTC is uncommon. Giant cells or multinucleated cells could be seen. The MTC tumor cells are generally positive for calcitonin, thyroglobulin, and neuroendocrine markers (18). SETTLE is simple for spindle epithelioid tumors with thymus-like differentiation. SETTLE is common in children and young adults. The mass is slow-growing. The incidence in male is higher than in female. Similar to PSST, the tumor consists of spindle cells with a variable epithelial component. In SETTLE, the mitotic rate is usually low and necrosis is relatively rare. The spindle cells are positive for high-molecular-weight keratin and vimentin (19). Occasionally, PSST would be misdiagnosed as undifferentiated/anaplastic thyroid carcinoma (UTC/ATC). UTC/ATC is usually presented as a rapidly enlarging thyroid mass. It is more common in elderly patients. The tumor is composed of spindle cells with ample cytoplasm, coarse chromatin, frequent mitoses, giant cells, and neutrophils. UTC/ATC is positive for Pax-8 and has p53 mutations (20).

Until now, there is no standard and ideal therapeutic regimen for PSST. Surgical resection remains the mainstay of management for localized synovial sarcoma with or without radiation (11). When the tumor invades important structures and cannot be completely removed, postoperative adjuvant chemoradiotherapy is generally recommended. Some retrospective studies have reported an improvement in local control and disease-free survival conferred by radiotherapy (21–23). A combination of doxorubicin and ifosfamide was considered to be the recommended chemotherapeutic regimen when the primary tumor could not be resected completely in most cases. While PSST did not show an obvious genetic predisposition, the consanguinity of the patient should raise their awareness and perform a regular physical examination.

Limitation

Although we tried our best to document this clinical case report in detail, there are still some limitations. First, because the tumor, in this case, was suspected to be benign in the preoperative examination, we did not perform screening for systemic metastases before surgery, but relevant examinations including chest CT, abdominal CT, and MRI of the head and whole-body bone scan were performed before and during chemotherapy. Second, due to capsular rupture and necrotic effusion during the operation, we are pitiful for failing to take photos of the tumor. The necrotic effusion might lead to tumor local implantation metastasis, making postoperative adjuvant therapy necessary and important. Last but not the least, despite the follow-up of the case being less than 1 year, complete treatment for PSST in this patient has been completed, and no recurrence and metastasis have been detected in 9 months postoperatively. We will continue to focus on the case. We will update this case report and literature review if recurrence or death occurs in the current case.

Established facts

1. Synovial sarcoma is a subtype of soft tissue sarcoma, which is extremely rare in the thyroid gland. PSST showed rapid disease progression and a relatively poor prognosis. However, diagnosis and therapy are challenging.

2. Complete surgical excision and postoperative adjuvant chemotherapy are usually the typical therapeutic regimen for PSST.

Novel insights

1. PSST is difficult to be diagnosed by preoperative evaluation, even FNA. PSST was occasionally misdiagnosed as a benign thyroid tumor. Surgeons should raise their awareness when encountering rapidly growing, cystic-solid mixed thyroid mass with neck compression symptoms.

2. The initial surgery of PSST is of vital importance. Surgeons should avoid capsular rupture and effusion of necrotic during surgery. Intraoperative frozen section pathology should be performed when necessary. Postoperative adjuvant chemotherapy should be scheduled for reduced recurrence and prolonged survival time.

Data availability statement

The original contributions presented in the study are included in the article/supplementary material, further inquiries can be directed to the corresponding authors.

Ethics statement

Ethical review and approval was not required for the study on human participants in accordance with the local legislation and institutional requirements. The patients/participants provided their written informed consent to participate in this study. Written informed consent was obtained from patient for the publication.

Author contributions

JH, YG, FY, and CR performed the surgery. CR, ZC, QJ, and YL collected the data from the patient. CR, XL, and SL drafted the first manuscript. YG and FY revised the manuscript. All authors read and approved the final manuscript.

Funding

This study was supported by the National Key R&D Program of China (Grant No. 2019YFE0190500), the Hunan Provincial Natural Science Foundation of China (No. 2022JJ30806), and the Scientific research project of Hunan Provincial Health Commission (No. 202204014372).

Conflict of interest

The authors declare that the research was conducted in the absence of any commercial or financial relationships that could be construed as a potential conflict of interest.

Publisher's note

All claims expressed in this article are solely those of the authors and do not necessarily represent those of their affiliated organizations, or those of the publisher, the editors and the reviewers. Any product that may be evaluated in this article, or claim that may be made by its manufacturer, is not guaranteed or endorsed by the publisher.

References

1. Fonseca AS, Azevedo AC, Magalhaes FM, Andrade NA. Synovial sarcoma in head and neck: a case report. *Int Arch Otorhinolaryngol.* (2014) 18:87–9. doi: 10.1055/s-0033-1361081

2. Thway K, Fisher C. Synovial sarcoma: defining features and diagnostic evolution. *Ann Diagn Pathol.* (2014) 18:369–80. doi: 10.1016/j.anndiagpath.2014.09.002

3. Kikuchi I, Anbo J, Nakamura S, Sugai T, Sasou S, Yamamoto M, et al. Synovial sarcoma of the thyroid. Report of a case with aspiration cytology findings and gene analysis. *Acta Cytol.* (2003) 47:495–500. doi: 10.1159/000326558

4. Jang KS, Min KW, Jang SH, Paik SS, Tae K, Jang SJ, et al. Primary synovial sarcoma of the thyroid gland. *J Korean Med Sci.* (2007) 22(Suppl):S154–8. doi: 10.3346/jkms.2007.22.S.S154

5. Ryu CH, Cho KJ, Choi SH. Synovial sarcoma of the thyroid gland. *Clin Exp Otorhinolaryngol.* (2011) 4:204–6. doi: 10.3342/ceo.2011.4.4.204

6. Ghafouri A, Anbara T, Mir A, Lashkari M, Nazari M. Thyroid synovial sarcoma: a case report. *Acta Med Iran.* (2013) 51:69–72.

7. Boudin L, Fakhry N, Chetaille B, Perrot D, Nguyen AT, Daidj N, et al. Primary synovial sarcoma of the thyroid gland: case report and review of the literature. *Case Rep Oncol.* (2014) 7:6–13. doi: 10.1159/000357913

8. Shi RL, Qu N, Gao LL, Lu ZW, Sun GH Ji QH. Primary synovial sarcoma of the thyroid with locally repeated relapses in short periods: a case report. *Biomed Rep.* (2016) 5:79–82. doi: 10.3892/br.2016.670

9. Park CS, Kim Y, Jeong EH, Kim NI, Choi YD. Cytologic features of primary monophasic synovial sarcoma of the thyroid gland. *Cytojournal.* (2017) 14:24. doi: 10.4103/cytojournal.cytojournal_14_17

10. Yadav D, Agarwal S, Sharma A, Malik E, Kandasamy D, Thakar A, et al. Synovial sarcoma masquerading as medullary thyroid carcinoma. *Cytopathology.* (2018) 29:468–70. doi: 10.1111/cyt.12582

11. Owen C, Constantinidou A, Miah AB, Thway K, Fisher C, Benson C, et al. Synovial sarcoma of the thyroid gland, diagnostic pitfalls and clinical management. *Anticancer Res.* (2018) 38:5275–82. doi: 10.21873/anticanres.12853

12. Demirel D, Erkul E, Erkilic S, Narli Issin G, Ramzy I. Primary synovial sarcoma of the thyroid: challenges in cytologic diagnosis and review of the literature. *Acta Cytol.* (2020) 64:498–506. doi: 10.1159/000507312

13. Seyed-Alagheband SA, Sharifian M, Adeli OA, Sohooli M, Shekouhi R. Primary synovial sarcoma of thyroid gland: a case report and review of literature. *Int J Surg Case Rep.* (2021) 85:106245. doi: 10.1016/j.ijscr.2021.106245

14. Salcedo-Hernandez RA, Lino-Silva LS, Luna-Ortiz K. Synovial sarcomas of the head and neck: comparative analysis with synovial sarcoma of the extremities. *Auris Nasus Larynx.* (2013) 40:476–80. doi: 10.1016/j.anl.2012.11.015

15. Maduekwe UN, Hornicek FJ, Springfield DS, Raskin KA, Harmon DC, Choy E, et al. Role of sentinel lymph node biopsy in the staging of synovial, epithelioid, and clear cell sarcomas. *Ann Surg Oncol.* (2009) 16:1356–63. doi: 10.1245/s10434-009-0393-9

16. Gazendam AM, Popovic S, Munir S, Parasu N, Wilson D, Ghert M. Synovial sarcoma: a clinical review. *Curr Oncol.* (2021) 28:1909–20. doi: 10.3390/curroncol28030177

17. Aisner SC, Seidman JD, Burke KC, Young JW. Aspiration cytology of biphasic and monophasic synovial sarcoma. *A report of two cases Acta Cytol.* (1993) 37:413–7.

18. Murro D, Slade JM, Syed S, Gattuso P. Fine needle aspiration of secondary synovial sarcoma of the thyroid gland. *Diagn Cytopathol.* (2015) 43:928–32. doi: 10.1002/dc.23327

19. Tong GX, Hamele-Bena D, Wei XJ, O'Toole K. Fine-needle aspiration biopsy of monophasic variant of spindle epithelial tumor with thymus-like differentiation of the thyroid: report of one case and review of the literature. *Diagn Cytopathol.* (2007) 35:113–9. doi: 10.1002/dc.20579

20. Pusztaszeri M, Wang H, Cibas ES, Powers CN, Bongiovanni M, Ali S, et al. Fine-needle aspiration biopsy of secondary neoplasms of the thyroid gland: a multi-institutional study of 62 cases. *Cancer Cytopathol.* (2015) 123:19–29. doi: 10.1002/cncy.21494

21. Guadagnolo BA, Zagars GK, Ballo MT, Patel SR, Lewis VO, Pisters PW, et al. Long-term outcomes for synovial sarcoma treated with conservation surgery and radiotherapy. *Int J Radiat Oncol Biol Phys.* (2007) 69:1173–80. doi: 10.1016/j.ijrobp.2007.04.056

22. Shi W, Indelicato DJ, Morris CG, Scarborough MT, Gibbs CP, Zlotecki RA. Long-term treatment outcomes for patients with synovial sarcoma: a 40-year experience at the University of Florida. *Am J Clin Oncol.* (2013) 36:83–8. doi: 10.1097/COC.0b013e31823fe450

23. Naing KW, Monjazeb AM, Li C-S, Lee L-Y, Yang A, Borys D, et al. Perioperative radiotherapy is associated with improved survival among patients with synovial sarcoma: A SEER analysis. *J Surg Oncol.* (2015) 111:158–64. doi: 10.1002/jso.23780

frontiers | Frontiers in Endocrinology

TYPE Original Research
PUBLISHED 17 July 2023
DOI 10.3389/fendo.2023.1160817

Check for updates

OPEN ACCESS

EDITED BY
Liam Chen,
University of Minnesota, United States

REVIEWED BY
Wengang Li,
Xiamen University, China
Calin Cainap,
University of Medicine and Pharmacy Iuliu Hatieganu, Romania

*CORRESPONDENCE
Fuchu He
hefc@nic.bmi.ac.cn
Weiqi Lu
lu.Weiqi@zs-hospital.sh.cn

†These authors share senior authorship

RECEIVED 07 February 2023
ACCEPTED 12 June 2023
PUBLISHED 17 July 2023

CITATION
Zhuang A, Yue X, Tong H, Zhang Y, He F and Lu W (2023) Nomogram predicting overall survival after surgical resection for retroperitoneal leiomyosarcoma patients. *Front. Endocrinol.* 14:1160817. doi: 10.3389/fendo.2023.1160817

COPYRIGHT
© 2023 Zhuang, Yue, Tong, Zhang, He and Lu. This is an open-access article distributed under the terms of the Creative Commons Attribution License (CC BY). The use, distribution or reproduction in other forums is permitted, provided the original author(s) and the copyright owner(s) are credited and that the original publication in this journal is cited, in accordance with accepted academic practice. No use, distribution or reproduction is permitted which does not comply with these terms.

Nomogram predicting overall survival after surgical resection for retroperitoneal leiomyosarcoma patients

Aojia Zhuang[1†], Xuetong Yue[1†], Hanxing Tong[1], Yong Zhang[1], Fuchu He[1,2*] and Weiqi Lu[1*]

[1]Department of General Surgery, Institutes of Biomedical Sciences, Zhongshan Hospital, Fudan University, Shanghai, China, [2]State Key Laboratory of Proteomics, Beijing Proteome Research Center, National Center for Protein Sciences, Beijing, China

Background: Surgery is the best way to cure the retroperitoneal leiomyosarcoma (RLMS), and there is currently no prediction model on RLMS after surgical resection. The objective of this study was to develop a nomogram to predict the overall survival (OS) of patients with RLMS after surgical resection.

Methods: Patients who underwent surgical resection from September 2010 to December 2020 were included. The nomogram was constructed based on the COX regression model, and the discrimination was assessed using the concordance index. The predicted OS and actual OS were evaluated with the assistance of calibration plots.

Results: 118 patients were included. The median OS for all patients was 47.8 (95% confidence interval (CI), 35.9-59.7) months. Most tumor were completely resected (n=106, 89.8%). The proportions of French National Federation of Comprehensive Cancer Centres (FNCLCC) classification were equal as grade 1, grade 2, and grade 3 (31.4%, 30.5%, and 38.1%, respectively). The tumor diameter of 73.7% (n=85) patients was greater than 5 cm, the lesions of 23.7% (n=28) were multifocal, and 55.1% (n=65) patients had more than one organ resected. The OS nomogram was constructed based on the number of resected organs, tumor diameter, FNCLCC grade, and multifocal lesions. The concordance index of the nomogram was 0.779 (95% CI, 0.659-0.898), the predicted OS and actual OS were in good fitness in calibration curves.

Conclusion: The nomogram prediction model established in this study is helpful for postoperative consultation and the selection of patients for clinical trial enrollment.

KEYWORDS

nomogram, retroperitoneal leiomyosarcoma, survival, prediction of RLMS after surgery, FNCLCC

Abbreviations: RLMS, retroperitoneal leiomyosarcoma; c-index, concordance index; LMS, leiomyosarcoma; STS, soft tissue sarcoma; FNCLCC, Federation Nationale des Centres de Lutte Contre le Cancer; OS, overall survival; RPS, retroperitoneal soft tissue sarcoma.

Introduction

Leiomyosarcoma (LMS) is a mesenchymal malignant tumor with distinct smooth muscle differentiation (1), accounting for about 7-10% of all soft tissue sarcomas (STS). It is the second most common subtype of retroperitoneal sarcoma (RPS) (2). Currently, surgical resection is the best way to cure, but about 70% patients suffer from recurrence within five years after the surgical resection (3). The 5-year overall survival (OS) of the LMS patient is about 50%-60% after surgical resection for primary or recurrent disease (4, 5). The postoperative outcomes after extended resection for RPS have been reported, highlighting differences by specific histologic subtype (4). In addition, a report from the French Sarcoma Group pointed out that LMS represents a heterogeneous group of tumors, and retroperitoneal leiomyosarcoma (RLMS) shows totally different clinical outcomes and molecular features than others (6). Therefore, it is key to find good means to effectively incorporate our understanding of disease biology into clinical decision-making.

Nomogram is a statistical tool to predict the prognosis of an individual patient, and it has been widely applied in RPS (5, 7–9). But the distinct patterns of local and distant recurrence of the various subtypes of RPS suggest that separate nomograms for predicting the OS of RLMS patients will be useful (9). It has been reported that the tumor size, resection margin status, and tumor grade are risk factors for the poor prognosis of RLMS (10–12). However, no nomogram is constructed currently to predict the OS of RLMS patients only.

Therefore, this study aimed to investigate the independent prognostic factors for OS of RLMS patients after surgical resection and to construct a nomogram to predict the 1-, 2-, and 5-year OS of the RLMS patients.

Methods

Patients

118 consecutive patients who underwent surgical resection from September 2010 to December 2020 at General Surgery Department, Shanghai Public Health Clinical Center, Fudan University, Shanghai, China were included. The inclusion criteria were as follows: 1) histologically confirmed LMS, 2) tumors originating in the retroperitoneum, 3) complete clinical pathological information and follow-up information. LMS is diagnosed by pathological features stained by H&E, including oval or cigar-shaped nuclei with blunt ends, variable eosinophilic cytoplasm, and uniform positive staining for α-sma, desmin, and/or h-caldesmon (6). Gastrointestinal stromal tumors were excluded. The study was approved by the Ethics Committee of Shanghai Public Health Clinical Center. All enrolled patients signed informed consent for data collection during hospitalization.

The baseline characteristics including gender, age, metastatic disease, times of surgery, complete resection (complete: R0 and R1, negative gross margins; incomplete: R2, grossly positive margins), number of resected organ, tumor diameter, French National Federation of Comprehensive Cancer Centres (FNCLCC) grade, tumor node metastasis (TNM) stage, multifocality, inferior vena cava invasion, radiation, chemotherapy, and other therapy (focused ultrasound, interventional embolization and intraperitoneal hyperthermia chemotherapy). Treatment plans for all patients were determined by a multidisciplinary team of surgeons, medical oncologists, radiologists, and pathologists. Postoperative follow-up of the patients required physical examination and enhanced CT or MRI of the chest, abdomen and pelvic. The first follow-up was 3 months after surgery, then every 3 months for 2 years; 6 months for 5 years; and every 1 year after 5 years.

Statistical analysis

The primary end-point of the study was OS (defined as the duration from date of the surgery to the date of death or follow-up) which estimated by the Kaplan–Meier method, and the differences between groups were compared with the log-rank test. Because the TNM staging system itself was a predictive tool, which already included relevant variables such as tumor size and tumor grade, it was not included in the risk factor analysis. Risk factors affecting survival were determined by COX regression. Variables with p-values <0.2 in univariate analysis were included in multivariate analysis. A nomogram was then constructed using the variables in the multivariate analysis with p-value < 0.1 to predict OS at 1, 2, and 5 years after surgery. The prediction accuracy of the nomogram was assessed by a calibration curve, and the c-index was judged the discriminative ability. Finally, the cohort was divided into a low-risk group and a high-risk group based on the values of the maximum sum of sensitivity and specificity (Youden index) (13). All the tests were two-tailed and $p < 0.05$ meant the difference was statistically significance.

Statistical analyses were performed with SPSS version 22.0 (Chicago, IL, USA) and R software (The R Foundation for Statistical Computing, Vienna, Austria; version 4.1.1; http://www.r-project.org/).

Results

Baseline characteristics

Characteristics of 118 patients were provided in Table 1. Most patients were female (n=99, 83.9%) without metastasis disease (n=106, 89.8%), and the tumor was completely resected (n=106, 89.8%). Patients with initial surgery, second surgery, and more than twice accounted for 39.8%(n=47), 34.7% (n=41), and 25.4% (n=30), respectively. The proportions of FNCLCC classification were equal as grade 1, grade 2, and grade 3, which were 31.4%, 30.5%, and 38.1%, respectively. The tumor diameter of 73.7% (n=85) patients was greater than 5 cm, the lesions of 23.7% (n=28) were multifocal, and 55.1% (n=65) patients had multiple organs resected. In terms of adjuvant therapy, 22 patients received radiotherapy, 46 received chemotherapy, and 15 received other therapies.

10.3389/fendo.2023.1160817

TABLE 1 Demographics and clinical characteristics of 118 patients with retroperitoneal leiomyosarcoma.

Characteristics	N (N=118)	% of Total
Gender		
Male	19	16.1
Female	99	83.9
Age, years		
<60	76	64.4
≥60	42	35.6
Metastatic disease		
Yes	12	10.2
No	106	89.8
Times of surgery		
Initial	47	39.8
Second	41	34.7
More than twice	30	25.4
Complete resection		
Yes	106	89.8
No	12	10.2
Number of resected organs		
0-1	53	44.9
>1	65	55.1
Tumor burden, cm		
≤5	31	26.3
>5	85	73.7
FNCLCC grade		
I	37	31.4
II	36	30.5
III	45	38.1
TNM stage		
I	35	29.6
II	16	13.5
III	55	46.6
IV	12	10.1
Multifocal disease		
Yes	28	23.7
No	90	76.3
Inferior vena cava invasion		
Yes	17	14.4
No	101	85.6
Radiation		

(Continued)

10.3389/fendo.2023.1160817

TABLE 1 Continued

Characteristics	N (N=118)	% of Total
Yes	22	18.6
No	96	81.4
Chemotherapy		
Yse	46	39.0
No	72	61.0
Other therapy		
Yes	15	12.7
No	103	87.3

Survival analysis

The median OS for all patients was 47.8 (95% CI, 35.9-59.7) months, the median follow-up for all survivors was 31.0 (4 ~ 113 months) months, and the 5 years OS rate was 44.7% (95% CI, 32.6%-56.8%) (Figure 1).

The univariable analysis showed that the number of resected organs (p=0.012), tumor diameter (p=0.005), and FNCLCC grade (p<0.001) were related to OS. The results of multivariate analysis suggested that FNCLCC grade (p<0.001, Grade 2 vs. Grade 1 [HR=3.320, 95% CI 1.088-10.129], Grade 3 vs. Grade 1 [HR=11.693, 95% CI 4.183-32.689]) and multifocal lesions (p=0.025, HR=2.333, 95% CI 1.114-4.887) were independent risk factors of OS of patients (Table 2).

Nomogram development and validation

Variables with p<0.1 in multivariate analysis (the number of resected organs, tumor diameter, FNCLCC grade, and multifocal lesion) were referred to construct the nomogram to predict the OS of patients with RLMS who had the abdominal lesions resected (Figure 2).

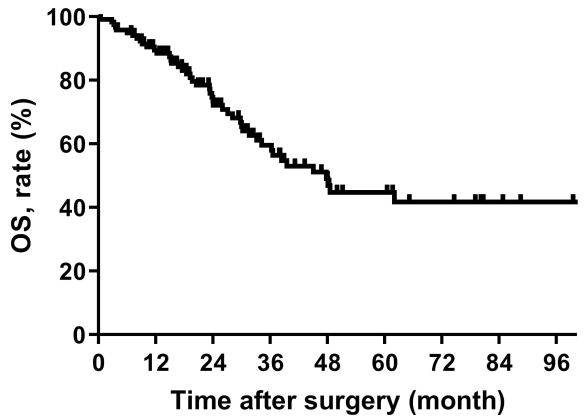

FIGURE 1
Overall survival in patients with retroperitoneal leiomyosarcoma.

The RLMS nomogram had an internal validation c-index of 0.779 (95% CI, 0.659–0.898), which was significantly better than the TNM staging system (c-index=0.697). And the calibration curve showed that the predicted value of OS was in good agreement with the actual value (Figure 3).

The nomogram gave a specific value to quantify each variable. According to the total score, the Youden index was 0.572 with the cut off score of 126. 72 patients were included in the low-risk group (<126) and 46 were enrolled in the high-risk group (≥126), and their median OS was 116.5 (95% CI, NA) and 24.0 (95% CI, 22.9-25.0) months, respectively, showing a statistically significant difference (p<0.001) (Figure 4).

Discussion

RLMS is a very rare mesenchymal malignant that originates in the retroperitoneal space. RLMS is fatal but rare disease, and metastasis, multifocal lesions and resection of multiple organs are usually contraindications to the surgical resection (14). Therefore, it is very important to analyze its long-term survival rate. In addition, the potential beneficial effects of surgical resection are not always obvious, resulting in very complicated decision-making. In other words, it is extremely difficult for clinically determine whether the patients with recurred RLMS could be treated by surgical resection. The nomogram established in this study is conductive for such decision or determination. For example, if the preoperative assessment shows no need for combined organ resection, the tumor diameter is smaller than 5 cm, FNCLCC shows grade 1 and single center disease, and even if it is a multiple recurrence disease, the postoperative 5-year OS rate may exceed 90%, so that patients have a high probability of benefiting from surgical resection. On the contrary, if the combined resection of multiple organs is needed, the tumor diameter is larger than 5cm, the FNCLCC showed grade 3 and multifocal disease, and the nomogram score was greater than 200 points, the postoperative 2-year OS is estimated to be less than 30%, so it has to be carefully considered to take surgical resection.

Since the prediction model can be simplified into a continuous numerical estimate tailored to individual patient conditions, the role of the nomogram prediction model has gradually become

10.3389/fendo.2023.1160817

TABLE 2 Univariable and multivariable analyses to determine independent predictors of overall survival of retroperitoneal leiomyosarcoma.

Variables	Univariate analysis		Multivariate analysis	
	Hazard Ratio(95%CI)	P value	Hazard Ratio (95%CI)	P value
Gender female vs. male	1.006 (0.672-1.507)	0.975		
Age ≥60 vs. <60	1.242 (0.686-2.248)	0.475		
Metastatic disease yes vs. no	1.929 (0.814-4.570)	0.135	1.925 (0.740-5.-12)	0.180
Times of surgery		0.486		
second vs. first	0.664 (0.320-1.379)	0.272		
more than twice vs. first	1.020 (0.510-2.040)	0.955		
Complete resection no vs. yes	1.303 (0.846-2.007)	0.230		
Number of resected organ >1 vs. 0-1	2.173 (1.187-3.981)	0.012	1.797 (0.909-3.552)	0.092
Tumor burden >5 vs. ≤5	5.351 (1.655-17.299)	0.005	2.945 (0.861-10.070)	0.085
FNCLCC grade		<0.001		<0.001
II vs. I	3.352 (1.137-9.880)	0.028	3.320 (1.088-10.129)	0.035
III vs. I	9.355 (3.560-24.589)	<0.001	11.693 (4.183-32.689)	<0.001
Multifocal disease yes vs. no	1.906 (0.995-3.651)	0.052	2.333 (1.114-4.887)	0.025
Inferior vena cava invasion yes vs. no	1.259 (0.753-2.104)	0.380		
Radiation yes vs. no	1.767 (0.786-3.970)	0.168	1.400 (0.580-3.383)	0.454
Chemotherapy yes vs. no	1.005 (0.548-1.842)	0.987		
Other therapys yes vs. no	1.005 (0.395-2.555)	0.992		

prominent with the help of precision medicine. Some nomogram prediction models have been incorporated into the staging system of the American Joint Committee on Cancer (AJCC) to improve the estimation accuracy of the prognosis for patients with subtype pathology. In the eighth edition of the AJCC manual, the nomogram by Trans-Atlantic Retroperitoneal Sarcoma Working Group for RPS (7) was included as a model that met all AJCC quality criteria. In this study, 523 patients were included to provide basis for establishing the nomogram prediction model, and 135 patients were used for foreign language validation. The c-index values for OS in the training set and validation set were 0.74 and 0.68, respectively. However, LMS only accounted for 17.6% in the training set, and its nomogram prediction model could only predict the OS of patients at the seventh year after the surgical resection, while the postoperative 5-year OS was only about 50%, showing limited practicality. In 2010, Anaya et al. established a nomogram model for predicting the postoperative 3-year and 5-year OS of patients by using the clinicopathological characteristics of 343 RPS patients, and its concordance index was 0.73. However, this model defined the pathological type of LMS as "others", which was not listed separately (8). In 2019, Chandrajit et al. established a nomogram model for predicting the 6-year OS in RPS patients with first local recurrence based on the data of 602 patients from 22 sarcoma centers. Likewise, due to the rarity of

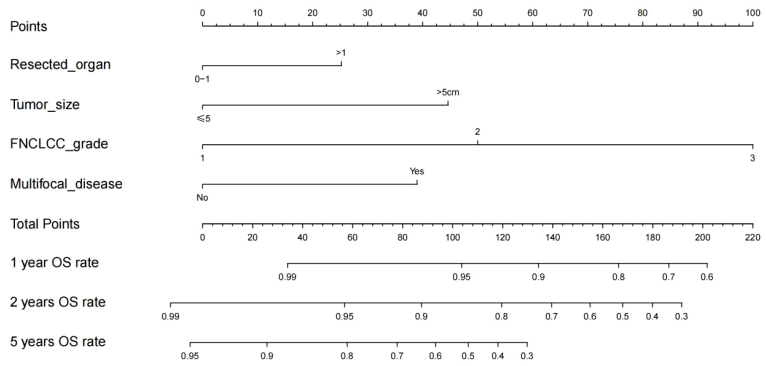

FIGURE 2
Nomogram for 1-year, 2-year and 5-year overall survival in patients with retroperitoneal leiomyosarcoma.

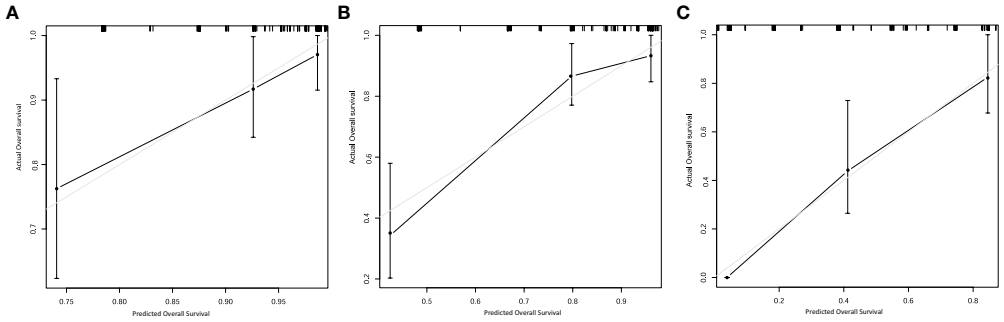

FIGURE 3
Calibration plots for internal validation of **(A)** 1-, **(B)** 2- and **(C)** 5-year overall survival nomogram.

RLMS, only 12.1% of LMS patients were included in the cohort (5).

In addition to nomogram prediction models for retroperitoneal sarcoma, there are also some LMS nomograms for the whole body. MingFeng et al. used the SEER database to establish a nomogram prediction model for predicting extremity LMS OS and cancer specific survival, with c-index of 0.776 and 0.835, respectively (15). And the LMS nomogram prediction model for the 5-year OS of urinary system was established by Oliver et al. with the c-index of 0.67 (16). Although the primary tumor site has a significant impact on the prognosis of LMS, there is currently no nomogram prediction model for LMS originating in the retroperitoneum. Therefore, this study developed and internally validated a novel RLMS-specific nomogram for predicting the 1-, 2-, and 5-year OS of patients with RLMS, and the c-index of the model was 0.779 (95% CI, 0.659-0.898). The calibration plots showed that the predicted OS rate was perfectly match with the actual value. In addition, to enhance the clinical utility, patients were further rolled into high-risk and low-risk groups based on the scores of the nomogram prediction model. The median OS of patients in the high-risk and low-risk groups was 116.5 (95% CI, NA) and 24.0 (95% CI, 22.9-25.0) months, respectively. The TNM staging system of the AJCC is the most commonly used method for staging STS, including RLMS. Staging is based on pathological findings, including tumor size, lymph node status, metastasis, and tumor grade based on the FNCLCC system (17). The RLMS nomogram in this study had a c-index of 0.779 (95% CI, 0.659-0.898) after internal validation, which was superior to the TNM staging system (c-index= 0.697). A more accurate prognosis could lead to a better postoperative counseling for patients, so it is possible to monitor the high-risk patients more appropriately.

In this study, the inclusion of radiation therapy in the multivariate analysis was based on recent reports highlighting its potential therapeutic benefits, despite having a p-value of 0.168 in the univariate analysis. The combination of radiation therapy with radical surgery has been shown to potentially be the standard of care for a subgroup of patients with RPS. Studies have demonstrated that patients treated with RT and surgery have significantly improved median overall survival and 5-year survival rates compared to those treated with surgery alone ($p < 0.00001$, $p < 0.001$). Additionally,

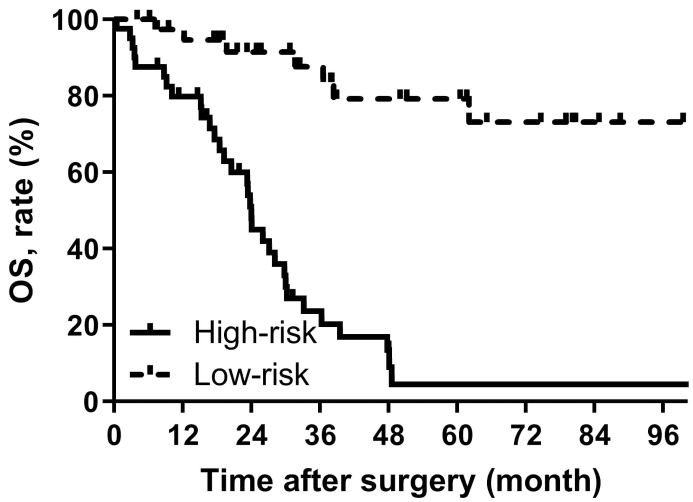

FIGURE 4
OS curves stratified by the score calculated by the nomogram and was stratified according to the risk score as follows: low-risk group (<100) and high-risk group (≥100).

median recurrence-free survival was significantly increased in patients treated with either preoperative or postoperative RT compared to those undergoing surgery alone (18). Another study further supports the use of radiotherapy in RPS, indicating that both preoperative and postoperative radiotherapy are significantly associated with improved overall survival compared to surgery alone (19). However, a recent randomized phase 3 study showed that the addition of preoperative radiotherapy did not improve local control rates or provide survival benefits, particularly in high-grade (G3) liposarcomas and LMS. Nevertheless, for recurrent retroperitoneal sarcomas primarily localized within the abdominal cavity, preoperative radiotherapy may help reduce the risk of local recurrence, especially in well-differentiated liposarcomas and low-grade dedifferentiated liposarcomas (20).Although radiation therapy did not demonstrate a significant association with overall survival in the further multivariate analysis of this study, considering the evidence from the mentioned high-quality studies, we still regard radiation therapy as a potential effective modality for treating leiomyosarcomas sarcoma of the retroperitoneum.

The results of survival analysis suggested that the FNCLCC grade and multifocal lesion were the independent risk factors for postoperative OS. The FNCLCC system is a commonly used histological grading system for STS, and it is one of the best indicators for predicting the metastasis-free survival and OS (21). This study was similar to a previous study reported by Qian Li et al., for RLMS patients with recurrent or metastatic disease who had a higher FNCLCC grade experienced worse prognosis (22). Consistent with previous reports on RPS, patients with multifocal lesions accounted for 23% of all subjects in this study; in addition, the mortality risk of patients with multifocal lesion increased by twice compared with non-multifocal lesion (23). Although there are some reports about the role of multifocal lesions in the prognosis of RPS, this study was the first to report it as an independent prognostic factor in RLMS.

There were some limitations for this study. First, this is a retrospective cohort study, and selection bias is inevitable. Second, the median follow-up time in this study was only 31 months, and further follow-up was needed to improve the reliability of the study. Thirdly, due to the complexity of treatments received by patients in our study cohort, there is a lack of information regarding adjuvant therapies. Finally, although the RLMS nomogram prediction model was internally validated, the cohort of this study was from an Asian tertiary hospital and was not externally validated, so its scope of use may be limited.

Conclusions

We established an RLMS-specific nomogram prediction model that can accurately predict postoperative survival in RLMS patients. Dividing patients into high and low-risk groups by nomogram can assist doctors in clinical decision-making.

Data availability statement

The original contributions presented in the study are included in the article/Supplementary Material. Further inquiries can be directed to the corresponding authors.

Ethics statement

The studies involving human participants were reviewed and approved by the Ethics Committee of Shanghai Public Health Clinical Center (B2020-338). The patients/participants provided their written informed consent to participate in this study.

Author contributions

AZ and HT developed the concept of the article. XY and AZ developed the design and methodology. AZ, XY,YZ, FH and WL contributed to the manuscript revision. AZ, XY and YZ contributed to the collection and analysis of clinical data. AZ, XY and HT contributed to the drafting of the manuscript. All authors contributed to the article and approved the submitted version.

Acknowledgments

We would like to thank our patients, without whom this study would not possible.

Conflict of interest

The authors declare that the research was conducted in the absence of any commercial or financial relationships that could be construed as a potential conflict of interest.

Publisher's note

All claims expressed in this article are solely those of the authors and do not necessarily represent those of their affiliated organizations, or those of the publisher, the editors and the reviewers. Any product that may be evaluated in this article, or claim that may be made by its manufacturer, is not guaranteed or endorsed by the publisher.

Supplementary material

The Supplementary Material for this article can be found online at: https://www.frontiersin.org/articles/10.3389/fendo.2023.1160817/full#supplementary-material

References

1. Anderson WJ, Doyle LA. Updates from the 2020 world health organization classification of soft tissue and bone tumours. *Histopathology* (2021) 78(5):644–57. doi: 10.1111/his.14265

2. Bathan AJ, Constantinidou A, Pollack SM, Jones RL. Diagnosis, prognosis, and management of leiomyosarcoma: recognition of anatomic variants. *Curr Opin Oncol* (2013) 25(4):384–9. doi: 10.1097/CCO.0b013e3283622c77

3. Ikoma N, Torres KE, Lin HY, Ravi V, Roland CL, Mann GN, et al. Recurrence patterns of retroperitoneal leiomyosarcoma and impact of salvage surgery. *J Surg Oncol* (2017) 116(3):313–9. doi: 10.1002/jso.24667

4. Gronchi A, Strauss DC, Miceli R, Bonvalot S, Swallow CJ, Hohenberger P, et al. Variability in patterns of recurrence after resection of primary retroperitoneal sarcoma (RPS): a report on 1007 patients from the multi-institutional collaborative RPS working group. *Ann Surg* (2016) 263(5):1002–9. doi: 10.1097/SLA.0000000000001447

5. Raut CP, Callegaro D, Miceli R, Barretta F, Rutkowski P, Blay JY, et al. Predicting survival in patients undergoing resection for locally recurrent retroperitoneal sarcoma: a study and novel nomogram from TARPSWG. *Clin Cancer Res* (2019) 25(8):2664–71. doi: 10.1158/1078-0432.CCR-18-2700

6. Italiano A, Lagarde P, Brulard C, Terrier P, Lae M, Marques B, et al. Genetic profiling identifies two classes of soft-tissue leiomyosarcomas with distinct clinical characteristics. *Clin Cancer Res* (2013) 19(5):1190–6. doi: 10.1158/1078-0432.CCR-12-2970

7. Gronchi A, Miceli R, Shurell E, Eilber FC, Eilber FR, Anaya DA, et al. Outcome prediction in primary resected retroperitoneal soft tissue sarcoma: histology-specific overall survival and disease-free survival nomograms built on major sarcoma center data sets. *J Clin Oncol* (2013) 31(13):1649–55. doi: 10.1200/JCO.2012.44.3747

8. Anaya DA, Lahat G, Wang X, Xiao L, Pisters PW, Cormier JN, et al. Postoperative nomogram for survival of patients with retroperitoneal sarcoma treated with curative intent. *Ann Oncol* (2010) 21(2):397–402. doi: 10.1093/annonc/mdp298

9. Tan MC, Brennan MF, Kuk D, Agaram NP, Antonescu CR, Qin LX, et al. Histology-based classification predicts pattern of recurrence and improves risk stratification in primary retroperitoneal sarcoma. *Ann Surg* (2016) 263(3):593–600. doi: 10.1097/SLA.0000000000001149

10. Kim HJ, Cho YJ, Kim SH, Rha SY, Ahn JB, Yang WI, et al. Leiomyosarcoma: investigation of prognostic factors for risk-stratification model. *Int J Clin Oncol* (2015) 20(6):1226–32. doi: 10.1007/s10147-015-0847-y

11. Abraham JA, Weaver MJ, Hornick JL, Zurakowski D, Ready JE. Outcomes and prognostic factors for a consecutive case series of 115 patients with somatic leiomyosarcoma. *J Bone Joint Surg Am* (2012) 94(8):736–44. doi: 10.2106/JBJS.K.00460

12. Gronchi A, Miceli R, Allard MA, Callegaro D, Le Pechoux C, Fiore M, et al. Personalizing the approach to retroperitoneal soft tissue sarcoma: histology-specific patterns of failure and postrelapse outcome after primary extended resection. *Ann Surg Oncol* (2015) 22(5):1447–54. doi: 10.1245/s10434-014-4130-7

13. Fluss R, Faraggi D, Reiser B. Estimation of the youden index and its associated cutoff point. *Biom J* (2005) 47(4):458–72. doi: 10.1002/bimj.200410135

14. van Houdt WJ, Fiore M, Barretta F, Rutkowski P, Blay JY, Lahat G, et al. Patterns of recurrence and survival probability after second recurrence of retroperitoneal sarcoma: a study from TARPSWG. *Cancer* (2020) 126(22):4917–25. doi: 10.1002/cncr.33139

15. Xue M, Chen G, Dai J, Hu J. Development and validation of a prognostic nomogram for extremity soft tissue leiomyosarcoma. *Front Oncol* (2019) 9:346. doi: 10.3389/fonc.2019.00346

16. Lu YJ, Wang H, Fang LY, Wang WJ, Song W, Wang Y, et al. A nomogram for predicting overall survival in patients with uterine leiomyosarcoma: a SEER population-based study. *Future Oncol* (2020) 16(10):573–84. doi: 10.2217/fon-2019-0674

17. von Mehren M, Kane JM, Bui MM, Choy E, Connelly M, Dry S, et al. NCCN guidelines insights: soft tissue sarcoma, version 1.2021. *J Natl Compr Canc Netw* (2020) 18(12):1604–12. doi: 10.6004/jnccn.2020.0058

18. Diamantis A, Baloyiannis I, Magouliotis DE, Tolia M, Symeonidis D, Bompou E, et al. Perioperative radiotherapy versus surgery alone for retroperitoneal sarcomas: a systematic review and meta-analysis. *Radiol Oncol* (2020) 54(1):14–21. doi: 10.2478/raon-2020-0012

19. Nussbaum DP, Rushing CN, Lane WO, Cardona DM, Kirsch DG, Peterson BL, et al. Preoperative or postoperative radiotherapy versus surgery alone for retroperitoneal sarcoma: a case-control, propensity score-matched analysis of a nationwide clinical oncology database. *Lancet Oncol* (2016) 17(7):966–75. doi: 10.1016/S1470-2045(16)30050-X

20. Bonvalot S, Gronchi A, Le Pechoux C, Swallow CJ, Strauss D, Meeus P, et al. Preoperative radiotherapy plus surgery versus surgery alone for patients with primary retroperitoneal sarcoma (EORTC-62092: STRASS): a multicentre, open-label, randomised, phase 3 trial. *Lancet Oncol* (2020) 21(10):1366–77. doi: 10.1016/S1470-2045(20)30446-0

21. Coindre JM, Terrier P, Guillou L, Le Doussal V, Collin F, Ranchere D, et al. Predictive value of grade for metastasis development in the main histologic types of adult soft tissue sarcomas: a study of 1240 patients from the French federation of cancer centers sarcoma group. *Cancer* (2001) 91(10):1914–26. doi: 10.1002/1097-0142(20010515)91:10<1914::AID-CNCR1214>3.0.CO;2-3

22. Li Q, Zhuang R, Zhu J, Lu W, Hou Y, Liu J, et al. Prognostic factors in patients with recurrent or metastatic retroperitoneal leiomyosarcoma. *Future Oncol* (2015) 11(12):1759–66. doi: 10.2217/fon.15.54

23. Anaya DA, Lahat G, Liu J, Xing Y, Cormier JN, Pisters PW, et al. Multifocality in retroperitoneal sarcoma: a prognostic factor critical to surgical decision-making. *Ann Surg* (2009) 249(1):137–42. doi: 10.1097/SLA.0b013e3181928f2f

frontiers | Frontiers in Endocrinology

TYPE Original Research
PUBLISHED 29 August 2023
DOI 10.3389/fendo.2023.1166838

Check for updates

OPEN ACCESS

EDITED BY
Liam Chen,
University of Minnesota, United States

REVIEWED BY
Volker Arndt,
German Cancer Research Center (DKFZ), Germany
Nadia Ayub,
Institute of Business Management, Pakistan

*CORRESPONDENCE
Martin Eichler
martin.eichler@ukdd.de

RECEIVED 15 February 2023
ACCEPTED 01 August 2023
PUBLISHED 29 August 2023

CITATION
Eichler M, Hentschel L, Singer S, Hornemann B, Richter S, Hofbauer C, Hohenberger P, Kasper B, Andreou D, Pink D, Jakob J, Grützmann R, Fung S, Wardelmann E, Arndt K, Hermes-Moll K, Schoffer O, Fried M, Jambor HK, Weitz J, Schaser K-D, Bornhäuser M, Schmitt J and Schuler MK (2023) Health related Quality of Life over time in German sarcoma patients. An analysis of associated factors - results of the PROSa study. *Front. Endocrinol.* 14:1166838. doi: 10.3389/fendo.2023.1166838

COPYRIGHT
© 2023 Eichler, Hentschel, Singer, Hornemann, Richter, Hofbauer, Hohenberger, Kasper, Andreou, Pink, Jakob, Grützmann, Fung, Wardelmann, Arndt, Hermes-Moll, Schoffer, Fried, Jambor, Weitz, Schaser, Bornhäuser, Schmitt and Schuler. This is an open-access article distributed under the terms of the Creative Commons Attribution License (CC BY). The use, distribution or reproduction in other forums is permitted, provided the original author(s) and the copyright owner(s) are credited and that the original publication in this journal is cited, in accordance with accepted academic practice. No use, distribution or reproduction is permitted which does not comply with these terms.

Health related Quality of Life over time in German sarcoma patients. An analysis of associated factors - results of the PROSa study

Martin Eichler[1,2,3,4,5]*, Leopold Hentschel[2,3,4,5], Susanne Singer[6], Beate Hornemann[2,3,4,5], Stephan Richter[1], Christine Hofbauer[2,3,4,5,7], Peter Hohenberger[8], Bernd Kasper[9], Dimosthenis Andreou[10,11], Daniel Pink[12,13], Jens Jakob[8,14], Robert Grützmann[15], Stephen Fung[16], Eva Wardelmann[17], Karin Arndt[18], Kerstin Hermes-Moll[19], Olaf Schoffer[2,3,4,5,20], Marius Fried[21], Helena K. Jambor[1,2,3,4,5], Jürgen Weitz[2,3,4,5,22], Klaus-Dieter Schaser[2,3,4,5,7], Martin Bornhäuser[1,2,3,4,5], Jochen Schmitt[2,3,4,5,20] and Markus K. Schuler[1]

[1]Clinic and Polyclinic for Internal Medicine I, University Hospital Carl Gustav Carus, Technical University Dresden, Dresden, Germany, [2]National Center for Tumor Diseases Dresden (NCT/UCC), Dresden, Germany, [3]German Cancer Research Center (DKFZ), Heidelberg, Germany, [4]Faculty of Medicine and University Hospital Carl Gustav Carus, Technical University Dresden, Dresden, Germany, [5]Helmholtz-Center Dresden-Rossendorf (HZDR), Dresden, Germany, [6]Institute of Medical Biostatistics, Epidemiology and Informatics, University Medical Centre of Johannes Gutenberg University Mainz, Mainz, Germany, [7]University Center for Orthopedics and Trauma Surgery, Technical University Dresden, Dresden, Germany, [8]Division of Surgical Oncology & Thoracic Surgery, Mannheim University Medical Center, University of Heidelberg, Mannheim, Germany, [9]Sarcoma Unit, Mannheim Cancer Center, Mannheim University Medical Center, University of Heidelberg, Mannheim, Germany, [10]Department of General Orthopedics and Tumor Orthopedics, Münster University Hospital, Münster, Germany, [11]Department of Orthopedics and Trauma, Medical University of Graz, Graz, Austria, [12]Sarcoma Center Berlin-Brandenburg, Helios Hospital Bad Saarow, Bad Saarow, Germany, [13]Department of Internal Medicine C, University Hospital Greifswald, Greifswald, Germany, [14]Clinic for General, Visceral, and Pediatric Surgery, University Hospital Goettingen, Goettingen, Germany, [15]Clinic for Surgery, University Hospital Erlangen, Erlangen, Germany, [16]Clinic for General, Visceral, and Pediatric Surgery, University Hospital Dusseldorf, Dusseldorfn, Germany, [17]Gerhard-Domagk-Institute of Pathology, University Hospital Münster, Münster, Germany, [18]German Sarcoma Foundation, Woelfersheim, Germany, [19]Scientific Institute of Office-based Hematologists and Oncologists, Cologne, Germany, [20]Center for Evidence-based Healthcare, University Hospital Carl Gustav Carus, Technical University Dresden, Dresden, Germany, [21]Clinic and Polyclinic for Internal Medicine III/University Cancer Center Mainz, University Hospital Mainz, Mainz, Germany, [22]Department of Visceral, Thoracic and Vascular Surgery, University Hospital Carl Gustav Carus, Technical University Dresden, Dresden, Germany

Introduction: Sarcomas are rare cancers and very heterogeneous in their location, histological subtype, and treatment. Health-Related Quality of Life (HRQoL) of sarcoma patients has rarely been investigated in longitudinal studies.

Methods: Here, we assessed adult sarcoma patients and survivors between September 2017 and February 2020, and followed-up for one year in 39 study centers in Germany. Follow-up time points were 6 (t1) and 12 months (t2) after inclusion. We used a standardized, validated questionnaire (the European Organisation for Research and Treatment of Cancer Quality of Life Core

Instrument (EORTC QLQ-C30) and explored predictors of HRQoL in two populations (all patients (Analysis 1), patients in ongoing complete remission (Analysis 2)) using generalized linear mixed models.

Results: In total we included up to 1111 patients at baseline (915 at t1, and 847 at t2), thereof 387 participants were in complete remission at baseline (334 at t1, and 200 at t2). When analyzing all patients, HRQoL differed with regard to tumor locations: patients with sarcoma in lower extremities reported lower HRQoL values than patients with sarcomas in the upper extremities. Treatment which included radiotherapy and/or systemic therapy was associated with lower HRQoL. For patients in complete remission, smoking was associated with worse HRQoL-outcomes. In both analyses, bone sarcomas were associated with the worst HRQoL values. Being female, in the age group 55-<65 years, having lower socioeconomic status, and comorbidities were all associated with a lower HRQoL, in both analyses.

Discussion: HRQoL increased partially over time since treatment and with sporting activities. HRQoL improved with time since treatment, although not in all domains, and was associated with lifestyle and socioeconomic factors. Bone sarcomas were the most affected subgroup. Methods to preserve and improve HRQoL should be developed for sarcoma patients.

KEYWORDS

sarcoma, GIST, health-related quality of life, patient reported outcomes, EORTC QLQ-C30, longitudinal observational cohort

1 Introduction

Sarcomas and gastrointestinal stromal tumors are a group of rare cancers, with about 7000 new cases per year in Germany (1) and an incidence of around 7 per 100,000 in Europe (2). The five-year relative survival in 2010–2016 was 65% for soft tissue sarcomas (STS), 60-79% for bone sarcomas, and 83% for gastrointestinal stromal tumors (GIST) (3). Sarcomas are heterogeneous tumors that include a large variety of over 100 histological subtypes (4), can occur anywhere in the body, and their therapy is based on complex and divergent treatment algorithms (5). Sarcomas are often diagnosed late due to their rarity and the unspecific symptoms they cause (6). Unplanned resections, a result of misdiagnosing the tumors as more common benign or even non-neoplastic lesions, with a negative influence on patient outcome are common (7, 8). Treatment at specialized centers is recommended by international guidelines and is associated with a prolonged survival (9–12).

Cancer patients rate their Health-Related Quality of Life (HRQoL) as an important aspect of their treatment and outcome, and improvement of HRQoL is at times preferred to the mere prolongation of live (13). The multidimensional construct HRQoL itself is a patient-reported outcome, that surveys physical, functional, social, and emotional well-being, as well as disease specific symptoms and restrictions (14).

Literature on HRQoL issues of sarcoma patients has improved over the last few years with two larger studies (15, 16) and a variety of reviews (17–19) published since 2019. Despite these developments, the heterogeneity and rareness of the disease, the variety of treatment pathways experienced by sarcoma patients, as well as the lack of a sarcoma specific measurement tool (20, 21) still leave questions unanswered.

The aim of this analysis was to explore factors associated with longitudinal HRQoL and specifically address lifestyle factors and HRQoL changes over time after the end of treatment. We examined both the predictors of the course of HRQoL in all sarcoma patients regardless of disease stage (Analysis 1) and the predictors of the course of HRQoL in patients in complete remission (Analysis 2).

2 Methods

The prospective PROSa cohort study (Burden and Medical Care of Sarcoma in Germany: Nationwide Cohort Study Focusing on Modifiable Determinants of Patient-Reported Outcome Measures in Sarcoma Patients; www.uniklinikum-dresden.de/prosastudie) was conducted nationwide in 39 study centers in Germany between September 2017 and May 2020 (NCT03521531; ClinicalTrials.gov). Of those, 8 were office-based practices, 22 hospitals of maximum care, and 9 other hospitals. Patients were approached at baseline as well as six (t1) and twelve months (t2) after baseline.

Eligible patients and survivors were asked to participate at the study centers during visits (treatment, diagnosis, aftercare) and

sometimes by phone or letter. Participation required informed consent. The study was approved by the ethics committees of the Technical University of Dresden (IRB00001473, EK1790422017) and the participating centers (22). Baseline and follow-up data (t1, t2) were collected at the study coordination center at University Hospital Dresden. HRQoL data and socio-demographic data were sent by the participants to the study coordination center by mail or online. In case of non-participation in follow-up, a reminder was sent after 4 weeks. Clinical information was submitted to the study coordination center online by the study centers using case report forms. Data collection was performed using REDCap (23).

We included adult patients and survivors with histologically proven sarcoma of any entity (24). We excluded persons who were mentally or linguistically unable to complete questionnaires. For Analysis 1 (all patients) only participants with HRQoL data were included, for Analysis 2 (patients in ongoing complete remission), we excluded all patients not in complete remission, in current treatment, or with unknown disease status.

2.1 Instruments

HRQoL was measured using the European Organisation for Research and Treatment of Cancer Quality of Life Core Questionnaire (EORTC QLQ-C30) (25). This instrument measures global quality of life (global health), 5 functioning, and 9 symptom scales in values from 0 to 100. Higher scores indicate better quality of life for the functioning scales and higher symptom burden for the symptom scales. The relevance of the differences was evaluated using reference values from Cocks et al. (26). With these reference values, each scale difference can be classified as "trivial", "small", "medium" and "large", defined as "Large: one representing unequivocal clinical relevance. Medium: likely to be clinically relevant but to a lesser extent. Small: subtle but nevertheless clinically relevant. Trivial: circumstances unlikely to have any clinical relevance or where there was no difference." (26).

Socioeconomic status (SES) was assessed using the Winkler Index (27). The Winkler Index is a composite score which covers and quantifies three dimensions of SES: income, education and occupational prestige. On a scale of 3 to 21, a lower score means a lower SES.

The extent of sporting activities was measured using the German Exercise and Sport Questionnaire ("Bewegungs- und Sportfragebogen") (28). This questionnaire assesses whether patients regularly exercised over the last 4 weeks and asks about the time spent doing so.

Alcohol consumption was grouped in 4 categories (none, weekly or less, regularly moderate (2-3 times a week of up to 4 drinks or 4 times or more a week up to 2 drinks), and regularly larger amounts (more than 4 drinks 2-3 times a week or more than 2 drinks 4 times or more a week.

For Analysis 1 (all patients), we used the patient reported socio-economic variable SES at baseline, as well as the lifestyle variables sporting activities at baseline, t1, and t2 (none, 1-<15 min per week, 15-<30 min per week, ≥30 min per week, unknown), smoking at baseline, t1, and t2 (never, former, actual, unknown), and alcohol consumption at baseline (never, weekly or less, regularly moderate, regularly larger amounts, unknown). From the medical records we collected age at baseline (18-<40, 40-<55, 55-<65, 65-<75, ≥75 years), gender (male, female)the disease characteristics sarcoma type (liposarcoma, fibroblastic/myofibroblastic/fibrohistiocytic sarcoma, GIST, unclassified sarcoma, leiomyosarcoma, bone sarcoma synovialsarcoma, others) and tumor location (abdomen/retroperitoneum, thorax, pelvis, lower limbs, upper limbs, other), comorbidities (cardiovascular, respiratory, diabetes, second cancer, kidney) at baseline (0, 1, 2, ≥3), disease status at baseline, t1, and t2 (complete remission, partial remission/stable disease, progression, unknown), time since treatment at baseline, t1, and t2 (in treatment, <0.5 year, 0.5-<1 year, 1-<2 years, 2-<5 years, ≥5 years, unknown), performed treatments at baseline, t1 and t2 (surgery alone, surgery + systemic therapy (ST), surgery + radiotherapy (RT), surgery + RT + ST, other). For Analysis 2 (patients in ongoing complete remission), we used the above-mentioned variables, except disease status at baseline.

2.2 Statistics

Continuous variables were evaluated by mean and standard deviation (SD). Categorical variables were presented with absolute and relative frequencies. We compared participants at all timepoints with those who were lost or did not send back the questionnaire during follow-up to estimate possible selection bias. An analysis of non-participants at baseline was reported elsewhere (16).

For both analyses, five pre-specified domains of the EORTC QLQ-C30 in which the most distinct differences were expected were examined for associated factors: global health, physical functioning, role functioning, pain, and fatigue. We used a generalized linear mixed model with patients as level 1 and timepoint of data collection (baseline, 6 months, 12 months) as level 2.

To avoid multicollinearity, correlations, and tolerance between the model variables were calculated before regression analyses. Correlations ≥ 0.7 and tolerance values ≤ 0.1 indicate strong multicollinearity.

For model variables with more than 5 missing cases, a category "unknown" was created. Imputation method for missing values in SES is described elsewhere (16).

Statistical analyses were performed with SPSS V.28 (IBM Corporation, Armonk, New York, USA).

3 Results

3.1 Description of the study population/ analysis of follow-up non-participants and drop-outs

In total, 1309 sarcoma patients agreed to participate at baseline, 1030 were eligible at t1, and 969 at t2. Questions on global health were answered by 1106 (baseline), 909 (t1), and 845 (t2) patients. A number of 144 patients dropped out during the study period, 119 of them died. For the Analysis 2 of patients in ongoing complete remission, the general health data was available for 386 (baseline), 329 (t1), and 198 (t2) patients, respectively. See Figure 1 for a detailed flow-diagram.

10.3389/fendo.2023.1166838

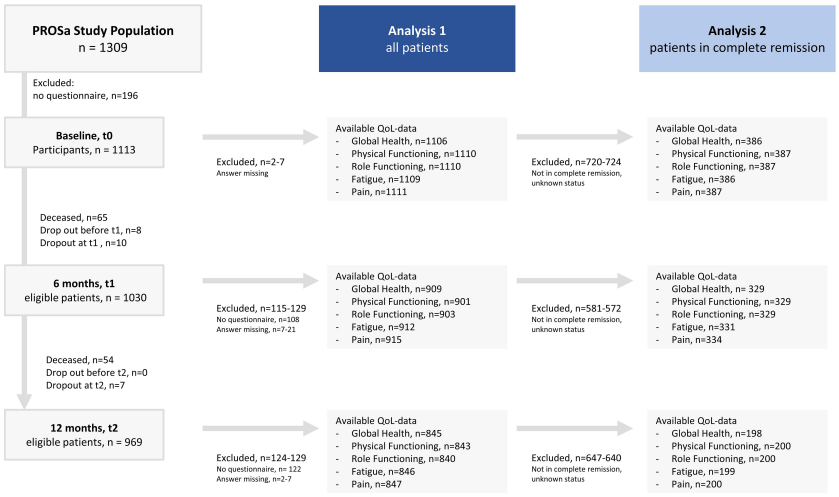

FIGURE 1
Flow-Chart study population.

A full description of the variables used for Analysis 1 and Analysis 2 are presented in Table 1. At baseline, 51% of participants were men, the mean age was 57 years, and around 30% of patients were in treatment. For Analysis 2, 49% of analyzed patients were men, the mean age was 54 years.

The characteristics of patients surveyed, patients who declined responses, and patients who dropped out during follow-up, differed in parts (Table 2). While unadjusted HRQoL values between participants and non-participants were in a range of 2 points, non-participants were on average between 4 and 7 years younger than participants, and more often male than female. Large differences between deceased patients and participants were observed in HRQoL values (ranging from 14 to 20 points) and in gender (overall 50% and 51% of participants were female, among deceased patients this was only 37% and 39%).

3.2 Analysis 1: factors associated with the course of HRQoL in all sarcoma patients

Data for Analysis 1 is summarized in Table 3, and includes non-standardized regression coefficients (B) indicating a B point increase or decrease in the respective scale. The HRQoL was mostly stable over the observed time, with significant, but trivial differences found in physical functioning, fatigue, and pain. In three domains woman were more strongly affected than men: differences were trivial for

TABLE 1 Description of study populations.

Variable	Value	Baseline, all patients, n=1106*		Baseline, patients in complete remission, n= 386*	
		N	%	N	%
Sex **/***	Male	567	51.3	189	49.0
	Female	538	48.7	197	51.0
Age at baseline (18–89)	Mean/Standard Deviation	56.6	15.9	54.4	16.4
Age at baseline **/***	18-<40	185	16.7	82	21.2
	40-<55	262	23.7	90	23.3
	55-<65	297	26.9	99	25.6
	65-<75	230	20.8	85	22.0
	≥75 years	131	11.9	30	7.8
SES at baseline (3–21) **/***	Mean/Standard Deviation	12.8	3.7	12.7	3.6
Sporting activities at baseline **/***	None	711	64.3	205	53.1
	1-<15 min/week	143	12.9	70	18.1

(Continued)

10.3389/fendo.2023.1166838

TABLE 1 Continued

Variable	Value	Baseline, all patients, n=1106*		Baseline, patients in complete remission, n= 386*	
		N	%	N	%
	15-<30 min/week	107	9.7	54	14.0
	≥30 min/week	107	9.7	48	12.4
	Unknown	38	3.4	9	2.3
Smoking at baseline **/***	Never	578	52.3	201	52.1
	Formerly	390	35.3	131	33.9
	Current	128	11.6	48	12.4
	Unknown	10	0.9	6	1.6
Alcohol consumption at baseline **/***	Never	282	25.5	78	20.2
	Weekly or less	541	48.9	202	52.3
	Regularly moderate	242	21.9	87	22.5
	Regularly larger amounts	28	2.5	14	3.6
	Unknown	13	1.2	5	1.3
Sarcoma type **/***	Liposarcoma	210	19.0	72	18.7
	Fibroblastic/myofibroblastic/fibrohistiocytic sarcoma	130	11.8	60	15.5
	GIST	130	11.8	19	4.9
	Unclassified sarcoma	163	14.8	63	16.3
	Leiomyosarcoma	130	11.8	34	8.8
	Bone Sarcoma	205	18.6	90	23.3
	Synovialsarcoma	47	4.3	16	4.1
	Other	88	8.0	32	8.3
Tumor location **/***	Abdomen/retroperitoneum	299	27.0	59	15.3
	Thorax	89	8.0	25	6.5
	Pelvis	160	14.5	44	11.4
	Lower limbs	400	36.2	207	53.6
	Upper limbs	85	7.7	31	8.0
	Other	73	6.6	20	5.2
Time since treatment at baseline **/***	In treatment	365	33.0	–	–
	<0.5 year	79	7.1	27	7.0
	0.5-<1 year	52	4.7	30	7.8
	1-<2 years	84	7.6	59	15.3
	2-<5 years	88	8.0	62	16.1
	≥5 years	80	7.2	59	15.3
	Unknown	358	32.4	149	38.6
Disease status at baseline **	Complete remission	491	44.4	386	100
	Partial remission/stable	328	29.7	-	-
	Progress	160	14.5	-	-
	Unknown	127	11.5	-	-

(Continued)

TABLE 1 Continued

Variable	Value	Baseline, all patients, n=1106*		Baseline, patients in complete remission, n= 386*	
		N	%	N	%
Received treatments until baseline **/***	Surgery only	291	26.3	146	37.8
	Surgery + ST	285	25.8	82	21.2
	Surgery + RT	162	14.6	89	23.1
	Surgery + RT + ST	232	21.0	69	17.9
	Other	136	12.3	–	–
Number of treatment lines **/***	1 line	592	53.6	293	75.9
	2 or more lines	426	38.5	87	22.5
	unknown	88	8.0	6	1.6
Comorbidities at baseline**/***	0	545	49.3	220	57.0
	1	361	32.6	111	28.8
	2	150	13.6	39	10.1
	≥ 3	50	4.5	16	4.1

*Patients with available HRQoL data on Global Health. **Model variables analysis 1 (baseline). ***Model variables analysis 2 (baseline). ST, systemic therapy; RT, radiotherapy; SES, Socioeconomic Status; GIST, gastrointestinal stromal tumors.
"-" not applicable.

TABLE 2 Comparison of Global Health data, sex and age of analyzed (included) patients, unit non responders (no questionnaires) and patients lost to follow up during baseline, 6 months (t1) and 12 months (t2).

	Baseline n	t0 global health mean	Female %	Age at baseline mean	t1 n	t1 global health mean	Female %	Age baseline mean	t2 n	t2 global health mean	Female %	Age at baseline mean
included patients at baseline	1106	59.5	49.7	56.6	-	-	-	-	-	-	-	-
included patients at t1	904	61.1	51.1	57.0	909	61.2	51.2	57.0	-	-	-	-
-deceased until t1	65	39.8	36.9	56.8	–	–	–	–	–	–	–	–
-dropouts before t1	8	46.9	14.3	53.6	–	–	–	–	–	–	–	–
-dropouts at t1	9	47.2	55.6	69.8	–	–	–	–	–	–	–	–
-no questionnaires t1	120	59.7	38.3	52.9	–	–	–	–	–	–	–	–
included patients at t2	840	62.1	50.6	57.1	803	61.8	51.6	57.3	845	62.5	50.7	57.2
-deceased after t1	54	48.0	38.9	59.3	36	49.3	36.1	61.7	–	–	–	–
-dropouts at t2	7	59.5	71.4	61.2	6	62.5	83.3	62.4	–	–	–	–
-no questionnaires t2	123	58.3	46.3	50.5	64	59.9	51.6	50.6	–	–	–	–

Due to changes in item completion, numbers do not always add up to flow-chart numbers. How to read: First column (included patients at baseline): From 1106 patients global health data was available. Second column (included patients t1): From 909 patients with global health data at t1, 904 reported on global health at baseline. Seventh column (included patients at t2): From 845 patients with global health data at t2, 840 reported on global health at baseline and 803 at t1.
"-" not applicable.

TABLE 3 Factors associated with HRQoL domains over time in German sarcoma patients (Analysis 1).

	Global Health	Physical Functioning	Role Functioning	Fatigue	Pain
Value	B (95% CI)	B (95% CI)	B (95% CI)	B (95% CI)	B (95% CI)
Time point (baseline (ref.))					
t1 (6 month)	-0.7 (-2.1; 0.8)	**-2.8 (-4; -1.6)**/T	-0.3 (-2.2; 1.7)	**2.5 (1.0; 4.0)**/T	**2.1 (0.2; 3.9)**/T
t2 (12 month)	-0.2 (-1.9; 1.5)	**-2.8 (-4.2; -1.4)**/T	0.4 (-1.9; 2.6)	**2.8 (1.0; 4.5)**/T	1.7 (-0.4; 3.9)
Sex (male (ref.))					
Female	-1.3 (-3.6; 0.9)	**-3.8 (-6.3; -1.3)**/T	-2.9 (-6.2; 0.5)	**7.1 (4.2; 10.0)**/S	**3.5 (0.1; 6.8)**/T
Age at baseline (18-<40 (ref.))					
40-<55	**-6.1 (-9.6; -2.6)**/S	**-6.6 (-10.6; -2.6)**/S	**-9.5 (-14.8; -4.2)**/S	**7.1 (2.5; 11.8)**/S	**5.7 (0.3; 11.0)**/T
55-<65	**-7.0 (-10.7; -3.3)**/S	**-9.0 (-13.2; -4.9)**/S	**-10.0 (-15.5; -4.5)**/S	**8.0 (3.2; 12.8)**/S	3.3 (-2.3; 8.8)
65-<75	-3.2 (-7.2; 0.9)	**-5.6 (-10.2; -1.1)**/S	-2.6 (-8.6; 3.4)	-0.1 (-5.4; 5.1)	-1.3 (-7.3; 4.8)
≥75 years	**-6.6 (-11.3; -2.0)**/S	**-12.1 (-17.4; -6.9)**/S	-5.7 (-12.7; 1.2)	**7.5 (1.4; 13.6)**/S	-1.3 (-7.3; 4.8)
SES at baseline					
Per point increase¶	**0.7 (0.4; 1.0)**/S	**0.7 (0.4; 1.0)**/S	0.3 (-0.1; 0.8)	**-0.5 (-0.9; -0.1)**/S	**-1.2 (-1.6; -0.7)**/S
Sporting activities (none (ref.))					
1-<15 min per week	**6.2 (4.1; 8.3)**/S	**4.2 (2.4; 6)**/T	**5.4 (2.5; 8.2)**/T	**-4.0 (-6.2; -1.7)**/T	-2.6 (-5.4; 0.1)
15-<30 min per week	**8.8 (6.4; 11.2)**/S	**6.1 (4.0; 8.2)**/S	**7.3 (4.0; 10.6)**/S	**-6.1 (-8.7; -3.5)**/S	**-6.8 (-10.0; -3.7)**/S
≥30 min per week	**9.3 (6.8; 11.9)**/S	**7.0 (4.8; 9.2)**/S	**12.5 (9.1; 15.9)**/S	**-8.5 (-11.2; -5.7)**/S	**-6.3 (-9.6; -3.0)**/S
Unknown	**7.4 (3.9; 11.0)**/S	**3.7 (0.7; 6.7)**/T	**9.1 (4.2; 13.9)**/S	**-6.0 (-9.8; -2.2)**/S	**-5.9 (-10.5; -1.3)**/T
Smoking (never (ref.))					
Formerly	-2.1 (-4.2; 0.1)	**-2.9 (-5.2; -0.7)**/T	**-3.5 (-6.6; -0.3)**/T	2.5 (-0.2; 5.1)	**3.9 (0.9; 7.0)**/T
Current	-1.1 (-4.3; 2.1)	-2.1 (-5.5; 1.2)	-2.0 (-6.8; 2.7)	1.3 (-2.7; 5.3)	1.9 (-2.8; 6.6)
Unknown	-4.5 (-10.7; 1.7)	-0.1 (-5.3; 5.0)	-0.8 (-9.0; 7.4)	-2.0 (-8.5; 4.5)	-0.6 (-8.5; 7.4)
Alcohol consumption at baseline (Never (ref.))					
Weekly or less	**5.1 (2.5; 7.7)**/S	**7.4 (4.5; 10.3)**/S	**7.6 (3.7; 11.6)**/S	**-6.7 (-10.1; -3.2)**/S	**-7.0 (-11.0; -3.1)**/S
Regularly moderate	**9.1 (5.8; 12.3)**/S	**10.4 (6.7; 14.0)**/S	**13.2 (8.3; 18.0)**/S	**-9.9 (-14.2; -5.7)**/S	**-9.9 (-14.8; -5.0)**/S
Regularly larger amounts	-2.0 (-9.0; 5.1)	1.9 (-6.0; 9.8)	3.8 (-6.7; 14.4)	3.9 (-5.3; 13.2)	5.5 (-5.1; 16.1)
Unknown	3.3 (-7.1; 13.7)	7.2 (-4.1; 18.5)	5.1 (-10.1; 20.3)	-7.9 (-21.4; 5.6)	-7.4 (-22.5; 7.8)
Sarcoma Type (liposarcoma (ref.))					
Fibroblastic/myofibro-blastic/fibrohistiocytic s.	-2.5 (-6.5; 1.5)	-1.0 (-5.5; 3.5)	-2.6 (-8.6; 3.4)	2.2 (-3.1; 7.4)	5.4 (-0.7; 11.4)
GIST	1.3 (-3.2; 5.8)	3.2 (-1.9; 8.2)	5.5 (-1.3; 12.2)	0.1 (-5.8; 6.0)	1.5 (-5.3; 8.3)
Unclassified sarcoma	-3.7 (-7.6; 0.2)	**-7.5 (-11.8; -3.2)**/S	**-9.2 (-15.0; -3.5)**/S	**5.9 (0.8; 10.9)**/S	5.6 (-0.2; 11.4)
Leiomyosarcoma.	-0.7 (-4.7; 3.3)	-1.5 (-6.0; 3.0)	-1.6 (-7.5; 4.3)	3.2 (-2.0; 8.4)	-0.7 (-6.7; 5.2)
Bone Sarcoma	**-7.4 (-11.5; -3.2)**/S	**-11.5 (-16.2; -6.9)**/S	**-15.0 (-21.2; -8.7)**/S	**7.7 (2.2; 13.1)**/S	**9.7 (3.4; 16.0)**/S
Synovialsarcoma	**-7.8 (-13.6; -1.9)**/S	-5.6 (-12.1; 1.0)	-8.6 (-17.4; 0.2)	6.5 (-1.1; 14.2)	4.1 (-4.7; 12.9)
Other	-0.3 (-4.6; 4.0)	-3.6 (-8.4; 1.3)	-4.4 (-10.8; 2.1)	4.4 (-1.3; 10.0)	5.2 (-1.3; 11.7)

(Continued)

10.3389/fendo.2023.1166838

TABLE 3 Continued

	Global Health	Physical Functioning	Role Functioning	Fatigue	Pain
Value	B (95% CI)	B (95% CI)	B (95% CI)	B (95% CI)	B (95% CI)
Tumor location (abdomen/retroperitoneum (ref.))					
Thorax	0.0 (-4.8; 4.8)	3.0 (-2.4; 8.4)	0.1 (-7.1; 7.3)	0.9 (-5.5; 7.2)	-2.6 (-9.9; 4.6)
Pelvis	-3.4 (-7.4; 0.5)	-3.4 (-7.8; 1.0)	-1.2 (-7.1; 4.6)	1.3 (-3.8; 6.5)	5.8 (-0.1; 11.7)
Lower limbs	-2.5 (-6.0; 0.9)	**-5.5 (-9.4; -1.6)/^{S}**	**-6.7 (-11.9; -1.5)/^{S}**	0.1 (-4.5; 4.6)	**6.6 (1.4; 11.8)/^{S}**
Upper limbs	4.5 (-0.5; 9.4)	4.5 (-1.1; 10.0)	-0.8 (-8.1; 6.6)	**-7.0 (-13.5; -0.5)/^{S}**	-4.0 (-11.4; 3.5)
Other	-1.5 (-6.7; 3.8)	0.4 (-5.4; 6.3)	-0.2 (-8.0; 7.6)	0.2 (-6.6; 7.1)	0.8 (-7.1; 8.7)
Time since treatment (currently under treatment (ref.))					
<0.5 year	1.5 (-1.0; 4.0)	-1.8 (-4.0; 0.3)	2.0 (-1.5; 5.5)	-2.3 (-5.0; 0.4)	1.5 (-1.8; 4.8)
0.5-<1 year	**4.0 (0.6; 7.4)/^{S}**	0.3 (-2.6; 3.2)	**5.4 (0.7; 10.0)/^{T}**	-4.5 (-8.1; -0.8)	-0.6 (-5.0; 3.9)
1-<2 years	**5.1 (1.7; 8.4)/^{S}**	1.8 (-1.1; 4.8)	**5.5 (0.9; 10.1)/^{T}**	**-3.7 (-7.4; -0.05)/^{T}**	-1.8 (-6.2; 2.7)
2-<5 years	**7.8 (4.1; 11.5)/^{S}**	**3.7 (0.4; 7.1)/^{T}**	**9.3 (4.1; 14.5)/^{S}**	**-4.5 (-8.6; -0.3)/^{T}**	-1.6 (-6.6; 3.4)
≥5 years	**5.9 (1.9; 9.9)/^{S}**	**4.6 (0.9; 8.4)/^{T}**	**11.3 (5.6; 17.0)/^{S}**	**-6.2 (-10.7; -1.6)/^{S}**	-2.8 (-8.2; 2.7)
Unknown	**6.0 (3.7; 8.3)/^{S}**	**3.1 (1.0; 5.1)/^{T}**	**11.3 (8.0; 14.5)/^{S}**	**-7.4 (-9.9; -4.8)/^{S}**	**-3.3 (-6.4; -0.3)/^{T}**
Disease status (complete remission (ref.))					
Partial remission/stable	**-2.6 (-4.9; -0.3)/^{T}**	-1.8 (-4.0; 0.3)	**-3.7 (-7.0; -0.5)/^{T}**	**3.6 (0.9; 6.2)/^{T}**	2.2 (-1.0; 5.4)
Progress	**-6.0 (-8.7; -3.2)/^{S}**	**-3.7 (-6.2; -1.2)/^{T}**	**-5.7 (-9.5; -1.9)/^{T}**	**3.7 (0.6; 6.7)/^{T}**	**5.4 (1.7; 9.1)/^{T}**
Unknown	-1.6 (-3.8; 0.6)	-1.4 (-3.2; 0.5)	**-4.0 (-7.0; -1.1)/^{T}**	1.2 (-1.2; 3.6)	1.2 (-1.7; 4.1)
Received treatments (surgery alone (ref.))					
Surgery + ST	0.7 (-2.3; 3.8)	**-4.8 (-8.1; -1.5)/^{T}**	-1.8 (-6.3; 2.7)	3.2 (-0.7; 7.0)	-1.3 (-5.8; 3.2)
Surgery + RT	-0.4 (-3.4; 2.6)	**-4.6 (-7.8; -1.4)/^{T}**	-2.3 (-6.8; 2.2)	**7.9 (4.1; 11.6)/^{S}**	**6.1 (1.7; 10.5)/^{S}**
Surgery + ST + RT	0.3 (-2.8; 3.4)	**-6.0 (-9.3; -2.8)/^{S}**	-3.9 (-8.4; 0.6)	**6.9 (3.1; 10.8)/^{S}**	2.1 (-2.4; 6.6)
Other	-2.2 (-6.0; 1.7)	**-4.1 (-8.0; -0.3)/^{T}**	2.1 (-3.6; 7.7)	**7.0 (2.3; 11.6)/^{S}**	4.1 (-1.4; 9.6)
Number of treatment lines (1 (ref.))					
2 or more	**-3.4 (-6.1; -0.7)/^{T}**	**-4.0 (-6.9; -1.1)/^{T}**	**-7.4 (-11.4; -3.5)/^{S}**	**5.6 (2.2; 9.0)/^{S}**	**4.3 (0.4; 8.3)/^{T}**
unknown	-0.5 (-4.9; 4)	1.6 (-3.3; 6.5)	-4.1 (-10.7; 2.5)	-0.9 (-6.6; 4.8)	4.0 (-2.6; 10.6)
Comorbidities at baseline (none (ref.))					
1	**-2.8 (-5.3; -0.3)/^{T}**	**-3.5 (-6.3; -0.7)/^{T}**	**-4.6 (-8.4; -0.9)/^{T}**	2.9 (-0.4; 6.2)	**4.6 (0.9; 8.4)/^{T}**
2	**-4.0 (-7.5; -0.5)/^{S}**	**-5.3 (-9.2; -1.3)/^{S}**	-4.3 (-9.5; 1.0)	**5.2 (0.6; 9.8)/^{S}**	2.5 (-2.8; 7.8)
≥ 3	**-9.2 (-14.7; -3.8)/^{S}**	**-13.5 (-19.6; -7.4)/^{S}**	**-14.7 (-22.8; -6.5)/^{S}**	**14.2 (7.1; 21.3)/^{M}**	**9.3 (1.1; 17.5)/^{S}**

Results of Generalized Linear Regression Models. B, non-standardized regression coefficient (indicating a B point increase or decrease in the respective scale); GIST, gastrointestinal stromal tumor; ST, systemic therapy, RT, radiotherapy; SES, Socioeconomic Status. 95% CI: 95% confidence interval. T, trivial. S, small. M, medium. L, large differences. ¶ Relevance of differences calculated with 10 points.
Bold: significant differences.

physical functioning and pain; small clinically relevant differences were found for fatigue. With younger patients (age: 18-<40 years) as reference value, we observed small but significant differences in all analyzed domains: the most affected groups were patients aged 55-<65 (global health, physical functioning, role functioning and fatigue) and those ≥75 (global health, physical functioning, fatigue, and pain). A 10-point increase in the socioeconomic status was associated with small and significant beneficial changes in global health, physical functioning, fatigue, and pain. Sporting activities were significantly associated with higher HRQoL in all HRQoL domains. Former smokers (comparison: those who never smoked) experienced lower HRQoL in three domains, but those differences were trivial. Compared to patients who consumed no alcohol at all, those with weekly or less consumption or those with a regular, but moderate

consumption reported small clinically relevant better outcomes in all domains.

Using liposarcoma patients as reference group, bone sarcoma patients were the worst performing group. They showed small clinically relevant and significant differences in all analyzed domains. Patients with unclassified sarcomas experienced worse HRQoL in three (physical functioning, role functioning, fatigue), those with synovialsarcoma in one domain (global health). Patients with tumors located at the lower limbs (reference: abdominal/retroperitoneal sarcomas) reported lower physical and role functioning as well as higher pain. In contrast, patients with tumors located at the upper limbs reported better global health and less fatigue.

With respect to treatment status and time since treatment (reference: patients in treatment), an relevant improvement over time was observed in all domains except pain and physical functioning. Clinically relevant improvements over time were not uniform across domains. For global healtha small clinically relevant improvement was observed 6 months, for role functioning 2 years and for fatigue 5 years after treatment. Differences between patients in complete remission and partial remission/stable disease remained trivial. Patients with progressive disease showed small clinically relevant differences in global health. In comparison to patients treated with surgery alone, those treated additionally with systemic therapy (ST) + radiotherapy (RT) experienced worse physical functioning and more fatigue, and those treated additionally with RT worse fatigue and pain. Patients who received (at least) second line treatment were more affected than those in first line treatment. Small significant differences were observed in role functioning and fatigue. The number of comorbidities was also associated with lower HRQoL for patients with 3 or more comorbidities as the worst performing group over all 5 domains.

3.3 Analysis 2: factors associated with the course of HRQoL in patients in ongoing complete remission

Data for Analysis 2 is summarized in Table 4. HRQoL stayed largely stable over the observed period, with a significant, but trivial difference found in role functioning. Woman were in three domains more affected than men; significant small clinically relevant differences were found in global health, physical functioning, and fatigue. With younger patients (age: 18-<40 years) as reference, small to medium significant differences were found in all analyzed domains: the most affected groups were patients aged 55-<65 (all domains) and ≥75 (physical and role functioning, fatigue and pain). A 10-point increase in socioeconomic status showed small significant improvements in global health, physical functioning, and pain. Sporting activities were significantly associated with better HRQoL in all HRQoL domains. Current smokers (comparison: never smoked) experienced worse HRQoL in two domains (role functioning and fatigue), those differences were small. Compared to patients who consumed no alcohol at all, those with weekly or less consumption or those with a regular, but moderate consumption reported small clinically relevant better outcomes in all domains.

Compared to liposarcoma patients as reference, patients with bone sarcoma were the worst performing group. They showed small clinically relevant and significant differences in general health, physical and role functioning. Other differences did not reach significance. No significant differences were observed with regard to tumor location.

With respect to time since treatment (reference: up to 6 months after treatment) an improvement over time was observed in all domains except pain and fatigue. Improvement over time was not uniform across domains and took longest in role functioning, reaching clinical relevance in this domain 5 years after treatment. In global health, a small clinically relevant improvement was observed 12 months after treatment and a medium improvement after 5 years. In physical functioning a small clinically relevant improvement was observed 2 years after treatment.

No significant differences were observed for the received treatment or the number of treatment lines. The number of comorbidities was associated with lower HRQoL experiences in general health and physical functioning.

4 Discussion

4.1 Results in context

Our study extends previous quality of life research in oncology through the analysis of a large national sample of sarcoma patients with standardized follow-up over a 1-year period. As expected, in our heterogeneous population of sarcoma patients, differences were found between factors studied in both longitudinal analyses.

The observed differences between gender and age-groups in Analyses 1 and 2 are reported in almost all HRQoL studies in cancer populations (29). It is noteworthy that patients between 55-<65 years (in addition to those ≥75) represented the most restricted age group. This implies that reaching retirement age is accompanied by a temporary improvement in various quality-of-life domains, possibly associated with retirement itself, an aspect we previously reported in more detail for a cross sectional analysis of the data (16). Differences between women and men seemed to be larger in patients in complete remission compared to all patients. The association between HRQoL and SES was already observed in the aforementioned study, indicating that a holistic approach to health always should include the social-economic situation of patients.

To our knowledge, there is little sarcoma specific literature on the relation of HRQoL and the analyzed lifestyle factors sporting activities (30, 31), smoking, and alcohol consumption, even if the importance of maintaining physical activity is discussed (32–34). Sporting activities were in both analyses and across all domains associated with improved HRQoL. In the literature about cancers in general, this observation is well established (35, 36). However, our study design – even if longitudinal – does not allow causal conclusions, as it remains possible that a better HRQoL enables sporting activities and is not the result of it. This may be particularly obvious in the case of role functioning (fulfilling everyday tasks), which can conceptually include sporting activities. In the analysis of all patients, former smoking, but not current smoking, was

10.3389/fendo.2023.1166838

TABLE 4 Factors associated with HRQoL domains over time in German sarcoma patients in complete remission (analysis 2).

	Global Health	Physical Functioning	Role Functioning	Fatigue	Pain
Variable/ Value	B (95% CI)	B (95% CI)	B (95% CI)	B (95% CI)	B (95% CI)
Time point (baseline (ref.))					
t1 (6 month)	0.1 (-1.9; 2.1)	-0.8 (-2.5; 0.8)	1.8 (-1.0; 4.5)	0.5 (-1.6; 2.5)	1.5 (-1.1; 4.2)
t2 (12 month)	1.3 (-1.2; 3.7)	-0.9 (-2.8; 0.9)	**3.5 (0.3; 6.8)**/T	0.3 (-2.3; 2.9)	-0.8 (-4.2; 2.6)
Sex (male (ref.))					
Female	**-4.4 (-8.2; -0.6)**/S	**-7.3 (-11.4; -3.1)**/S	-4.7 (-10.6; 1.1)	**10.1 (5.2; 15.1)**/S	5.5 (-0.1; 11.1)
Age at baseline (18-<40 (ref.))					
40-<55	**-5.7 (-11.3; -0.01)**/S	**-8.7 (-14.8; -2.6)**/S	**-12.4 (-21.1; -3.7)**/S	**10.7 (3.3; 18.0)**/S	**10.4 (2.1; 18.7)**/S
55-<65	**-8.7 (-14.6; -2.7)**/S	**-12.4 (-18.8; -5.9)**/S	**-17.8 (-27.0; -8.6)**/S	**14.7 (6.9; 22.5)**/M	**11.2 (2.5; 20.0)**/S
65-<75	-1.9 (-8.7; 4.9)	-6.8 (-14.1; 0.5)	-9.9 (-20.3; 0.5)	5.0 (-3.8; 13.9)	8.3 (-1.7; 18.2)
≥75 years	-8.8 (-18.1; 0.6)	**-20.0 (-30.0; -9.9)**/M	**-17.2 (-31.4; -2.9)**/S	**15.7 (3.6; 27.9)**/M	**14.7 (1.1; 28.3)**/M
SES at baseline					
Per point increase¶	**0.5 (0.02; 1.1)**/S	**0.8 (0.2; 1.3)**/S	0.6 (-0.2; 1.4)	-0.6 (-1.3; 0.1)	**-1.1 (-1.9; -0.3)**/S
Sporting activities (none (ref.))					
1-<15 min per week	**6.1 (2.9; 9.4)**/S	2.3 (-0.3; 4.9)	1.0 (-3.4; 5.3)	-2.0 (-5.4; 1.4)	1.7 (-2.6; 6.0)
15-<30 min per week	**7.3 (3.8; 10.8)**/S	**4.5 (1.7; 7.3)**/T	4.1 (-0.6; 8.8)	**-4.5 (-8.2; -0.8)**/S	-3.6 (-8.2; 1.1)
≥30 min per week	**7.1 (3.4; 10.8)**/S	**6.4 (3.4; 9.3)**/S	**8.9 (4.0; 13.9)**/S	**-6.6 (-10.5; -2.7)**/S	**-6.1 (-11; -1.2)**/S
Unknown	2.7 (-3.2; 8.6)	1.5 (-2.9; 6.0)	5.1 (-2.5; 12.8)	-2.9 (-8.9; 3.0)	-3.9 (-11.5; 3.7)
Smoking (never (ref.))					
Formerly	0.4 (-3.3; 4.0)	-1.9 (-5.5; 1.7)	-2.0 (-7.4; 3.4)	3.7 (-0.8; 8.1)	-0.8 (-6.0; 4.4)
Current	-2.5 (-7.9; 3.0)	-5.3 (-10.7; 0.1)	**-10.0 (-18.2; -1.9)**/S	**9.3 (2.5; 16.0)**/S	-2.9 (-10.8; 4.9)
Unknown	-3.8 (-13.2; 5.5)	3.5 (-3.2; 10.2)	4.5 (-7.1; 16.2)	-3.7 (-12.9; 5.6)	-3.6 (-14.9; 7.8)
Alcohol consumption at baseline (Never (ref.))					
Weekly or less	**6.1 (1.3; 10.8)**/S	4.3 (-0.9; 9.5)	**7.5 (0.1; 14.8)**/S	**-7.8 (-14.0; -1.6)**/S	**-7.3 (-14.3; -0.3)**/S
Regularly moderate	**8.7 (2.8; 14.7)**/S	**7.3 (0.9; 13.7)**/S	**14.5 (5.5; 23.6)**/S	**-11.9 (-19.6; -4.2)**/S	**-10.5 (-19.2; -1.8)**/S
Regularly larger amounts	-5.6 (-16.1; 4.9)	-1.7 (-13.2; 9.7)	3.5 (-12.7; 19.7)	2.9 (-10.9; 16.6)	1.1 (-14.4; 16.6)
Unknown	-0.1 (-18.8; 18.5)	2.4 (-16.0; 20.7)	14.5 (-11.8; 40.8)	-15.7 (-39.9; 8.5)	-17.8 (-42.7; 7.1)
Sarcoma Type (liposarcoma (ref.))					
Fibroblastic/myofibro-blastic/fibrohistiocytic s.	-1.6 (-7.9; 4.7)	0.1 (-6.7; 7.0)	1.5 (-8.2; 11.3)	1.7 (-6.5; 9.9)	-0.2 (-9.5; 9.1)
GIST	-1.1 (-11.6; 9.4)	5.7 (-5.8; 17.1)	7.1 (-9.0; 23.2)	-2.0 (-15.7; 11.8)	-6.7 (-22.1; 8.7)
Unclassified sarcoma	-3.1 (-9.5; 3.3)	-6.2 (-13.1; 0.7)	-4.8 (-14.5; 4.9)	5.3 (-3.0; 13.6)	7.3 (-2.0; 16.6)
Leiomyosarcoma.	1.3 (-6.2; 8.7)	6.8 (-1.4; 14.9)	4.4 (-7.1; 15.8)	-3.0 (-12.7; 6.8)	-7.6 (-18.6; 3.3)
Bone Sarcoma	**-7.6 (-14.4; -0.9)**/S	**-9.4 (-16.8; -2.0)**/S	**-12.1 (-22.5; -1.7)**/S	7.4 (-1.4; 16.3)	7.1 (-2.9; 17.0)
Synovialsarcoma	-2.2 (-12.3; 8.0)	-3.6 (-14.6; 7.4)	1.1 (-14.5; 16.7)	1.1 (-12.1; 14.3)	2.2 (-12.7; 17.0)

(Continued)

TABLE 4 Continued

	Global Health	Physical Functioning	Role Functioning	Fatigue	Pain
Variable/ Value	B (95% CI)	B (95% CI)	B (95% CI)	B (95% CI)	B (95% CI)
Other	1.0 (-6.9; 8.9)	-1.3 (-9.8; 7.2)	1.5 (-10.6; 13.6)	1.9 (-8.3; 12.1)	-1.4 (-13.0; 10.1)
Tumor location (abdomen/retroperitoneum (ref.))					
Thorax	2.8 (-6.5; 12)	2.6 (-7.4; 12.7)	1.8 (-12.5; 16.0)	-0.3 (-12.3; 11.8)	-12.0 (-25.6; 1.6)
Pelvis	-0.1 (-8.2; 7.9)	-4.6 (-13.3; 4.1)	-0.8 (-13.1; 11.5)	1.3 (-9.2; 11.7)	3.9 (-7.9; 15.6)
Lower limbs	-0.1 (-6.7; 6.6)	-6.5 (-13.7; 0.7)	-4.5 (-14.7; 5.8)	1.3 (-7.4; 9.9)	0.6 (-9.2; 10.3)
Upper limbs	4.3 (-4.7; 13.3)	-1.2 (-10.9; 8.6)	-2.9 (-16.8; 11.0)	-0.9 (-12.7; 10.8)	-10.3 (-23.6; 3.0)
Other	0.2 (-9.9; 10.4)	-5.8 (-16.8; 5.2)	-0.6 (-16.2; 15.0)	7.0 (-6.3; 20.3)	3.7 (-11.2; 18.6)
Time since treatment (<0.5 year (ref.))					
0.5-<1 year	5.7 (-0.9; 12.3)	4.8 (-0.4; 10.1)	7.5 (-1.7; 16.6)	-3.7 (-10.6; 3.3)	-5.8 (-14.5; 2.9)
1-<2 years	**7.9 (1.3; 14.5)/^{S}**	5.4 (-0.04; 10.8)	8.4 (-1.0; 17.8)	-0.5 (-7.8; 6.8)	-2.6 (-11.7; 6.5)
2-<5 years	**8.6 (1.4; 15.9)/^{S}**	**6.7 (0.6; 12.8)/^{S}**	6.6 (-3.8; 17.0)	-0.6 (-8.7; 7.4)	1.7 (-8.2; 11.6)
≥5 years	**10.7 (2.9; 18.6)/^{M}**	**8.9 (2.0; 15.8)/^{S}**	**12.4 (1.1; 23.8)/^{S}**	-4.5 (-13.4; 4.4)	-2.7 (-13.4; 8.0)
Unknown	**8.5 (0.9; 16.1)/^{S}**	**4.9 (-1.8; 11.6)/^{T}**	**11.7 (0.7; 22.7)/^{S}**	-2.6 (-11.2; 6.0)	-2.6 (-13.0; 7.8)
Received treatments (surgery alone (ref.))					
Surgery + ST	-1.4 (-6.7; 3.9)	-4.6 (-10.3; 1.1)	-4.7 (-12.9; 3.4)	4.2 (-2.7; 11.1)	1.0 (-6.8; 8.7)
Surgery + RT	-1.6 (-6.9; 3.8)	2.3 (-3.5; 8.0)	2.9 (-5.2; 11.1)	2.5 (-4.4; 9.4)	0.7 (-7.0; 8.5)
Surgery + ST + RT	2.4 (-3.3; 8.1)	2.2 (-4.0; 8.4)	-0.7 (-9.5; 8.0)	3.6 (-3.9; 11.0)	-4.4 (-12.8; 3.9)
Number of treatment lines (1 (ref.))					
2 or more	0.5 (-5.0; 6.0)	-1.1 (-6.8; 4.6)	-5.2 (-13.5; 3.2)	1.0 (-6.0; 7.9)	5.4 (-2.6; 13.4)
unknown	6.2 (-9.4; 21.7)	-1.3 (-17.9; 15.3)	-8.6 (-32.4; 15.2)	-0.1 (-20.1; 19.9)	-8.5 (-31.0; 14.1)
Comorbidities at baseline (none (ref.))					
1	-2.9 (-7.3; 1.5)	-4.3 (-9.1; 0.5)	-5.8 (-12.5; 1.0)	4.4 (-1.3; 10.1)	4.2 (-2.3; 10.6)
2	**-6.6 (-13.3; 0.2)/^{S}**	**-8.0 (-15.3; -0.6)/^{S}**	-0.8 (-11.2; 9.6)	6.3 (-2.6; 15.1)	-5.8 (-15.8; 4.1)
≥ 3	-7.5 (-17; 2.0)	**-11.7 (-22.0; -1.3)/^{S}**	-10.3 (-24.9; 4.2)	12.1 (-0.3; 24.5)	5.3 (-8.6; 19.2)

Results of Generalized Linear Regression Models. B, non-standardized regression coefficient (indicating a B point increase or decrease in the respective scale); GIST, gastrointestinal stromal tumor. ST, systemic therapy, RT, radiotherapy; SES, Socioeconomic Status. 95% CI: 95% confidence interval. T, trivial. S, small. M, medium. L, large differences. ¶ Relevance of differences calculated with 10 points.
Bold: significant differences.

associated with deteriorated HRQoL. It might be the case, that decreased HRQoL lead to smoking cessation. In the analysis of patients in complete remission, however, current smoking was associated with poorer HRQoL. This association is well established in the literature (37–39).

Moderate alcohol consumption was associated with an improvement in HRQoL compared to no consumption in both analyzed groups. This at first glance counterintuitive result is observed in other studies (40–42) and likely reflects the fact, when alcohol consumption is widespread and socially acceptable as is the case for Germany (43), many of those who do not consume alcohol (anymore) may be doing so because they are too ill or weak to drink alcohol. So here we might observe reverse causality, too.

Exploring the relation between time since treatment and analyzed HRQoL domains, a heterogenous picture was revealed. While in Analysis 1 (all patients), a rapid improvement over time was observed for general health, for role functioning, and fatigue clinically relevant improvements were observed only 2 resp. 5 years post treatment, while pain did not improve at all significantly and physical functioning not in a clinically relevant manner. In Analysis 2 (complete remission), HRQoL did not improve regarding pain and fatigue and improved at different times in general health, physical, and role functioning. This ambiguous picture is somewhat reflected in the literature, where for different populations some studies reported improvements 1 year after treatment (44, 45), while others reported more stable trajectories (46, 47). As the study population in the complete remission analysis is more homogenous than in the all-patients analysis, conclusions are probably easier to draw from the former one. Here, the stable trajectory in pain and fatigue raises the question, whether there is room for improvement especially in follow-up care (48, 49).

In Analysis 1, the heterogeneity of sarcoma patients was reflected in the analysis of subgroups and tumor location (15, 16). In Analysis 2, those differences did not remain statistically significant, which might be, at least partly a result of the smaller sample size. The exception are bone sarcoma patients, which were in both analyses stronger affected by functional impairments and lower general health than liposarcoma patients. Van Eck et al. reported that patients with sarcomas of the axial skeleton were the most affected group, a location that we did not document separately (15).

Patients treated with surgery alone had the lowest restrictions in terms of functional impairment and symptom burden in the all-patients analysis. Patients treated with surgery + ST + RT were most affected in all other domains, with the exception of pain, where patients with surgery + RT reported strongest symptoms. Interestingly, no differences were observed in the complete remission cohort. Winnette et al. reported increased burden after CT and RT, as well (50). Further, van Eck et al. compiled a comprehensive list of problems associated with specific treatments (15). Van Tine et al. observed a relatively rapid decline in HRQoL during doxorubicin-based treatment (51). An ongoing observational cohort study is investigating effects of CT on HRQoL (52).

As expected, progressive disease and the number of comorbidities were significantly and relevantly associated with most domains (53).

Overall, our research extends the existing knowledge on the HRQoL in sarcoma patients by providing a comprehensive and longitudinal analysis of a diverse national sample. Moreover, the inclusion of lifestyle factors, socio-economic status, the examination of time since treatment and disease-related factors add valuable insights to the current understanding of HRQoL in this patient population. We were thus able to capture a more holistic picture of the disease.

4.2 Strength and limitations

The PROSa study is one of the largest studies on HRQoL in sarcoma patients and survivors worldwide. Patients from 39 German hospitals and practices were included, representing a broad spectrum of sarcoma treating facilities and disciplines. We were able to follow patients for one year and thus to collect and analyze longitudinal data. The analysis has a limitation in the heterogenous patients collective. Despite being able to collect information about a relatively large number of patients, heterogeneity of the disease makes a subgroup analysis difficult. We were not able to compute interaction-analyses, especially on potential different HRQoL-trajectories in sarcoma subgroups (type, location, or treatment).

Although the present study has a longitudinal design, causal conclusions should be drawn cautiously. As discussed with respect to sporting activities, changes in HRQoL outcomes may have occurred before changes in independent variables. Unobserved or spurious confounding is also possible and the study is subject to selection bias. The majority of our patients were recruited in university hospitals and/or specialized centers and thus might not be representative for all sarcoma patients. In addition, we suspect a sick survivor bias, as healthy survivors have less frequent contact with our recruiting study centers. For Analysis 1, it should additionally be considered, that, as patients were in most cases recruited during hospital visits, the probability that the course of HRQoL over time is influenced by a subsequent treatment or worsening of disease is higher than in a sarcoma population recruited at a random timepoint. Our study population changed over the course of one-year, with younger patients and men being overrepresented in non-participants during follow-up, and there is the possibility that this influenced our results.

5 Conclusion

The heterogeneity of sarcomas regarding type, location, and treatment is reflected in the HRQoL outcomes in the analysis of all sarcoma patients, but only to a certain extent in the complete remission cohort. Bone sarcoma patients were in both analyses the most affected sarcoma type, while significant differences regarding location (patients with tumors located at the lower extremities performed worst and those with sarcomas at the upper extremities best) and treatment (having received radiotherapy and/or systemic therapy was associated with lower HRQoL in some domains) were only found in the analysis of all patients.

In both cohorts, sociodemographic factors like age, sex, and socioeconomic status were associated with HRQoL as well. Patients between 55-<65 years of age were the most affected group, indicating that certain life circumstances, like work, may increase the disease burden.

Lifestyle factors, especially sporting activities were strongly associated with HRQoL outcomes. Additionally, smokers had a higher probability of experiencing deteriorated HRQoL scores. It is thus important that clinicians are aware of these factors and take them into account and address them during treatment and follow-up. They should be considered in the development of supportive care programs.

Outcomes improved in both analyses over time since treatment, albeit in different patterns. Patients in ongoing complete remission improved over time in global health, physical, and role functioning. Such improvements were not observed for fatigue and pain. These findings can inform healthcare professionals and policymakers in developing targeted interventions and support services to enhance the well-being and overall quality of life for sarcoma patients.

Data availability statement

The raw data supporting the conclusions of this article will be made available by the authors, without undue reservation.

Ethics statement

The studies involving humans were approved by Ethics committees of the Technical University of Dresden. The studies were conducted in accordance with the local legislation and

institutional requirements. The participants provided their written informed consent to participate in this study.

Author contributions

ME wrote the article and analyzed the data. ME, MS, and LH developed questionnaires and study design. JS and MS developed the conception of the study and supervised with MB the work throughout the whole study. EW supervised development of inclusion criteria. KA supervised the study from a patient's perspective. ME and SS developed the statistical analysis plan for this paper. OS supervised statistical analysis. HJ did scientific editing and developed visualizations. SR, CH, PH, BK, DA, DP, JJ, RG, SF, KH-M, MF, JW, K-DS, and MS were responsible for the recruitment of patients or recruited patients directly. All authors have revised the manuscript critically and approved the published version.

Funding

The PROSa study was funded by the German Cancer Aid (No. 111713). ME, HJ, and MB received support by the German Cancer Aid, Mildred Scheel Early Career Center P^2. The Article Processing Charges (APC) were funded by the joint publication funds of the TU Dresden, including Carl Gustav Carus Faculty of Medicine, and the SLUB Dresden as well as the Open Access Publication Funding of the DFG.

Conflict of interest

LH received fees from SERVIER, outside of this work. SS received lecture fees from Lilly, Pfizer and fees for consulting services from Content Ed Net, all outside of this work. SR - received fees for consulting services from Bayer, PharmaMar, Boehringer Ingelheim and fees for lectures PharmaMar, all outside of this work. DA received lecture fees from PharmaMar, outside of this work. DP received fees for consulting services from Lilly, PharmaMar, Roche and fees for lectures from Lilly, PharmaMar, all outside of this work. JJ received fees from Lilly and Boehringer Ingelheim, all outside of this work. SF received reimbursements for congress attendance fees from PharmaMar, all outside of this work. OS received consulting fees from Novartis outside of this work. JS received consulting fees from Novartis, Sanofi, ALK, and Lilly, all outside of this work. MS received research funding from PharmaMar and Novartis, all outside of this work.

The remaining authors declare that the research was conducted in the absence of any commercial or financial relationships that could be construed as a potential conflict of interest.

Publisher's note

All claims expressed in this article are solely those of the authors and do not necessarily represent those of their affiliated organizations, or those of the publisher, the editors and the reviewers. Any product that may be evaluated in this article, or claim that may be made by its manufacturer, is not guaranteed or endorsed by the publisher.

References

1. Ressing M, Wardelmann E, Hohenberger P, Jakob J, Kasper B, Emrich K, et al. Strengthening health data on a rare and heterogeneous disease: sarcoma incidence and histological subtypes in Germany. *BMC Public Health* (2018) 18(1):235. doi: 10.1186/s12889-018-5131-4

2. Stiller CA, Trama A, Serraino D, Rossi S, Navarro C, Chirlaque MD, et al. Descriptive epidemiology of sarcomas in Europe: Report from the RARECARE project. *Eur J Cancer* (2013) 49(3):684–95. doi: 10.1016/j.ejca.2012.09.011

3. *Survival Rates for Soft Tissue Sarcoma*. Available at: https://www.cancer.org/cancer/soft-tissue-sarcoma/detection-diagnosis-staging/survival-rates.html.

4. Organisation mondiale de la santé, Centre international de recherche sur le cancer. *Soft tissue and bone tumours. 5th ed*. Geneva: OMS: World health organization classification of tumours (2020).

5. Gronchi A, Miah AB, Tos APD, Abecassis N, Bajpai J, Bauer S, et al. Soft tissue and visceral sarcomas: ESMO-EURACAN-GENTURIS Clinical Practice Guidelines for diagnosis, treatment and follow-up†. *Ann Oncol* (2021) 32(11):1348–65. doi: 10.1016/j.annonc.2021.07.006

6. Soomers V, Husson O, Young R, Desar I, van der Graaf W. The sarcoma diagnostic interval: a systematic review on length, contributing factors and patient outcomes. *ESMO Open* (2020) 5(1):e000592. doi: 10.1136/esmoopen-2019-000592

7. Traub F, Griffin AM, Wunder JS, Ferguson PC. Influence of unplanned excisions on the outcomes of patients with stage III extremity soft-tissue sarcoma: Outcome of Unplanned Excisions in STS. *Cancer* (2018) 124(19):3868–75. doi: 10.1002/cncr.31648

8. Kang S, Kim HS, Han I. Unplanned excision of extremity soft tissue sarcoma in korea: A nationwide study based on a claims registry. *PloS One* (2015) 10(8):e0134354. doi: 10.1371/journal.pone.0134354

9. Keung EZ, Chiang YJ, Cormier JN, Torres KE, Hunt KK, Feig BW, et al. Treatment at low-volume hospitals is associated with reduced short-term and long-term outcomes for patients with retroperitoneal sarcoma. *Cancer* (2018) 124(23):4495–503. doi: 10.1002/cncr.31699

10. Gutierrez JC, Perez EA, Moffat FL, Livingstone AS, Franceschi D, Koniaris LG. Should soft tissue sarcomas be treated at high-volume centers? An analysis of 4205 patients. *Ann Surg* (2007) 245(6):952–8. doi: 10.1097/01.sla.0000250438.04393.a8

11. Dangoor A, Seddon B, Gerrand C, Grimer R, Whelan J, Judson I. UK guidelines for the management of soft tissue sarcomas. *Clin Sarcoma Res* (2016) 6(1):20. doi: 10.1186/s13569-016-0060-4

12. *Leitlinienprogramm Onkologie (Deutsche Krebsgesellschaft, Deutsche Krebshilfe, AWMF. S3-Leitlinie Adulte Weichgewebesarkome, Langversion Version 1.0, 2021, AWMF-Registernummer: 032/044OL*. Available at: https://www.leitlinienprogramm-onkologie.de/leitlinien/adulte-weichgewebesarkome.

13. Shrestha A, Martin C, Burton M, Walters S, Collins K, Wyld L. Quality of life versus length of life considerations in cancer patients: A systematic literature review. *Psychooncology* (2019) 28(7):1367–80. doi: 10.1002/pon.5054

14. Webster KA, Peipert JD, Lent LF, Bredle J, Cella D. The functional assessment of chronic illness therapy (FACIT) measurement system: guidance for use in research and clinical practice. In: Kassianos AP, editor. *Handbook of Quality of Life in Cancer*. Cham: Springer International Publishing (2022). p. 79–104. doi: 10.1007/978-3-030-84702-9_6

15. van Eck I, den Hollander D, Desar IME, Soomers VLMN, van de Sande MAJ, de Haan JJ, et al. Unraveling the heterogeneity of sarcoma survivors' Health-related quality of life regarding primary sarcoma location: results from the SURVSARC study. *Cancers* (2020) 12(11):3083. doi: 10.3390/cancers12113083

16. Eichler M, Hentschel L, Richter S, Hohenberger P, Kasper B, Andreou D, et al. The health-related quality of life of sarcoma patients and survivors in Germany—Cross-sectional results of a nationwide observational study (PROSa). *Cancers* (2020) 12(12):3590. doi: 10.3390/cancers12123590

17. McDonough J, Eliott J, Neuhaus S, Reid J, Butow P. Health-related quality of life, psychosocial functioning, and unmet health needs in patients with sarcoma: A systematic review. *Psycho-Oncology* (2019) 28(4):653–64. doi: 10.1002/pon.5007

18. Almeida A, Martins T, Lima L. Patient-Reported Outcomes in Sarcoma: A scoping review. *Eur J Oncol Nursing* (2021) 50:101897. doi: 10.1016/j.ejon.2021.101897

19. den Hollander D, der Graaf WTAV, Fiore M, Kasper B, Singer S, Desar IME, et al. Unravelling the heterogeneity of soft tissue and bone sarcoma patients' health-related quality of life: a systematic literature review with focus on tumour location. *ESMO Open* (2020) 5(5):1–39. doi: 10.1136/esmoopen-2020-000914

20. den Hollander D, Fiore M, Martin-Broto J, Kasper B, Casado Herraez A, Kulis D, et al. Incorporating the patient voice in sarcoma research: how can we assess health-related quality of life in this heterogeneous group of patients? A study protocol. *Cancers* (2020) 13(1):1. doi: 10.3390/cancers13010001

21. Husson O, den Hollander D, van der Graaf WTA. The complexity of assessing health-related quality of life among sarcoma patients. *Qual Life Res* (2020) 29 (10):2613–4. doi: 10.1007/s11136-020-02561-y

22. Eichler M, Schmitt J, Schuler MK. Die Dauer von Ethikvoten in Deutschland am Beispiel einer nicht-interventionellen Beobachtungsstudie mit 44 teilnehmenden Zentren (PROSa). *Z für Evidenz Fortbildung und Qualität im Gesundheitswesen* (2019) 146:15–20. doi: 10.1016/j.zefq.2019.07.006

23. Harris PA, Taylor R, Thielke R, Payne J, Gonzalez N, Conde JG. Research electronic data capture (REDCap)—A metadata-driven methodology and workflow process for providing translational research informatics support. *J Biomed Informatics* (2009) 42(2):377–81. doi: 10.1016/j.jbi.2008.08.010

24. Eichler M, Andreou D, Golcher H, Hentschel L, Richter S, Hohenberger P, et al. Utilization of interdisciplinary tumor boards for sarcoma care in Germany: results from the PROSa study. *ORT* (2021) 44(6):301–12. doi: 10.1159/000516262

25. Aaronson NK, Ahmedzai S, Bergman B, Bullinger M, Cull A, Duez NJ, et al. The European Organization for Research and Treatment of Cancer QLQ-C30: a quality-of-life instrument for use in international clinical trials in oncology. *J Natl Cancer Inst* (1993) 85(5):365–76. doi: 10.1093/jnci/85.5.365

26. Cocks K, King MT, Velikova G, Martyn St-James M, Fayers PM, Brown JM. Evidence-based guidelines for determination of sample size and interpretation of the european organisation for the research and treatment of cancer quality of life questionnaire core 30. *JCO* (2011) 29(1):89–96. doi: 10.1200/JCO.2010.28.0107

27. Lampert T, Kroll LE, Müters S, Stolzenberg H. Messung des sozioökonomischen Status in der Studie "Gesundheit in Deutschland aktuell" (GEDA). *Bundesgesundheitsblatt - Gesundheitsforschung - Gesundheitsschutz* (2013) 56(1):131–43. doi: 10.1007/s00103-012-1583-3

28. Fuchs R, Klaperski S, Gerber M, Seelig H. Messung der Bewegungs- und Sportaktivität mit dem BSA-Fragebogen: Eine methodische Zwischenbilanz. *Z für Gesundheitspsychol* (2015) 23:60–76. doi: 10.1026/0943-8149/a000137

29. Schwarz R, Hinz A. Reference data for the quality of life questionnaire EORTC QLQ-C30 in the general German population. *Eur J Cancer* (2001) 37(11):1345–51. doi: 10.1016/S0959-8049(00)00447-0

30. Mason G, Aung L, Gall S, Meyers P, Butler R, Krug S, et al. Quality of life following amputation or limb preservation in patients with lower extremity bone sarcoma. *Front Oncol* (2013) 3:210. doi: 10.3389/fonc.2013.00210

31. Refaat Y, Gunnoe J, Hornicek FJ, Mankin HJ. Comparison of quality of life after amputation or limb salvage. *Clin Orthopaedics Related Research®* (2002) 397:298. doi: 10.1097/00003086-200204000-00034

32. Dewhurst S, Tigue R, Sandsund C, Mein G, Shaw C. Factors influencing people's ability to maintain their activity levels during treatment for soft tissue sarcoma - A qualitative study. *Physiother Theory Pract* (2020) 36(8):923–32. doi: 10.1080/09593985.2018.1519622

33. Garcia MB, Ness KK, SChadler KL. Exercise and physical activity in patients with osteosarcoma and survivors. *Adv Exp Med Biol* (2020) 1257:193–207. doi: 10.1007/978-3-030-43032-0_16

34. Ranft A, Seidel C, Hoffmann C, Paulussen M, Warby AC, van den Berg H, et al. Quality of survivorship in a rare disease: clinicofunctional outcome and physical activity in an observational cohort study of 618 long-term survivors of ewing sarcoma. *J Clin Oncol* (2017) 35(15):1704–12. doi: 10.1200/JCO.2016.70.6226

35. Stout NL, Baima J, Swisher AK, Winters-Stone KM, Welsh J. A systematic review of exercise systematic reviews in the cancer literature (2005-2017). *PM R* (2017) 9(9S2):S347–84. doi: 10.1016/j.pmrj.2017.07.074

36. Posadzki P, Pieper D, Bajpai R, Makaruk H, Könsgen N, Neuhaus AL, et al. Exercise/physical activity and health outcomes: an overview of Cochrane systematic reviews. *BMC Public Health* (2020) 20(1):1724. doi: 10.1186/s12889-020-09855-3

37. Goldenberg M, Danovitch I, IsHak WW. Quality of life and smoking. *Am J Addict* (2014) 23(6):540–62. doi: 10.1111/j.1521-0391.2014.12148.x

38. Piper ME, Kenford S, Fiore MC, Baker TB. Smoking cessation and quality of life: changes in life satisfaction over 3 years following a quit attempt. *Ann Behav Med* (2012) 43(2):262–70. doi: 10.1007/s12160-011-9329-2

39. Underner M, Perriot J, Merson F, Peiffer G, Meurice JC. [Influence of tobacco smoking on quality of life in patients with lung cancer]. *Rev Mal Respir* (2015) 32 (6):586–98. doi: 10.1016/j.rmr.2014.08.011

40. Eichler M, Keszte J, Meyer A, Danker H, Guntinas-Lichius O, Oeken J, et al. Tobacco and alcohol consumption after total laryngectomy and survival: A German multicenter prospective cohort study: Tobacco and alcohol consumption after laryngectomy. *Head Neck* (2016) 38(9):1324–9. doi: 10.1002/hed.24436

41. Révész D, Bours MJL, Wegdam JA, Keulen ETP, Breukink SO, Slooter GD, et al. Associations between alcohol consumption and anxiety, depression, and health-related quality of life in colorectal cancer survivors. *J Cancer Surviv* (2022) 16(5):988–97. doi: 10.1007/s11764-021-01090-y

42. Zhang FF, Hudson MM, Huang IC, Bhakta N, Ness KK, Brinkman TM, et al. Lifestyle factors and health-related quality of life in adult survivors of childhood cancer: A report from the St. *Jude Lifetime Cohort Study Cancer* (2018) 124(19):3918–23. doi: 10.1002/cncr.31647

43. Our World in Data. *Alcohol consumption across the world today*. Available at: https://ourworldindata.org/alcohol-consumption.

44. Sun YJ, Hu YJ, Jin D, Li JW, Yu B. Health-related quality of life after treatment for Malignant bone tumors: a follow-up study in China. *Asian Pac J Cancer Prev* (2012) 13(7):3099–102. doi: 10.7314/APJCP.2012.13.7.3099

45. Rivard JD, Puloski SS, Temple WJ, Fyfe A, Kwan M, Schachar N, et al. Quality of life, functional outcomes, and wound complications in patients with soft tissue sarcomas treated with preoperative chemoradiation: a prospective study. *Ann Surg Oncol* (2015) 22(9):2869–75. doi: 10.1245/s10434-015-4490-7

46. Paredes T, Pereira M, Moreira H, Simões MR, Canavarro MC. Quality of life of sarcoma patients from diagnosis to treatments: Predictors and longitudinal trajectories. *Eur J Oncol Nursing* (2011) 15(5):492–9. doi: 10.1016/j.ejon.2011.01.001

47. Davidson D, Barr RD, Riad S, Griffin AM, Chung PW, Catton CN, et al. Health-related quality of life following treatment for extremity soft tissue sarcoma: HRQL in Extremity Soft Tissue Sarcoma. *J Surg Oncol* (2016) 114(7):821–7. doi: 10.1002/jso.24424

48. Smith SR. Rehabilitation strategies and outcomes of the sarcoma patient. *Phys Med Rehabil Clin N Am* (2017) 28(1):171–80. doi: 10.1016/j.pmr.2016.08.008

49. Andrews CC, Siegel G, Smith S. Rehabilitation to improve the function and quality of life of soft tissue and bony sarcoma patients. *Patient Relat Outcome Meas.* (2019) 10:417–25. doi: 10.2147/PROM.S130183

50. Winnette R, Hess LM, Nicol SJ, Tai DF, Copley-Merriman C. The patient experience with soft tissue sarcoma: A systematic review of the literature. *Patient* (2017) 10(2):153–62. doi: 10.1007/s40271-016-0200-1

51. Van Tine BA, Krarup-Hansen A, Hess LM, Abdul Razak AR, Soldatenkova V, Wright J, et al. Quality of life of patients with soft tissue sarcoma treated with doxorubicin in the ANNOUNCE phase III clinical trial. *Rare Tumors* (2022) 14:20363613221100030. doi: 10.1177/20363613221100033

52. Younger E, Jones RL, Desar IME, Peckitt C, van der Graaf WTA, Husson O. Health-related quality Of Life In patients with advanced Soft TIssue sarcomas treated with Chemotherapy (The HOLISTIC study): protocol for an international observational cohort study. *BMJ Open* (2020) 10(6):e035171. doi: 10.1136/bmjopen-2019-035171

53. Shingler SL, Swinburn P, Lloyd A, Diaz J, Isbell R, Manson S, et al. Elicitation of health state utilities in soft tissue sarcoma. *Qual Life Res* (2013) 22(7):1697–706. doi: 10.1007/s11136-012-0301-9

frontiers | Frontiers in Oncology

TYPE Case Report
PUBLISHED 12 January 2024
DOI 10.3389/fonc.2023.1290603

Check for updates

OPEN ACCESS

EDITED BY
Liam Chen,
University of Minnesota, United States

REVIEWED BY
Yolandi Marais,
National Health Laboratory Service (NHLS), South Africa
Katerina Kopeckova,
University Hospital in Motol, Czechia

*CORRESPONDENCE
Junjie Zhang
zjjnjmu@sina.com

RECEIVED 07 September 2023
ACCEPTED 26 December 2023
PUBLISHED 12 January 2024

CITATION
Su C, Zhu X and Zhang J (2024) Primary mediastinal Ewing's sarcoma presenting with sudden and severe chest pain: a case report. *Front. Oncol.* 13:1290603. doi: 10.3389/fonc.2023.1290603

COPYRIGHT
© 2024 Su, Zhu and Zhang. This is an open-access article distributed under the terms of the Creative Commons Attribution License (CC BY). The use, distribution or reproduction in other forums is permitted, provided the original author(s) and the copyright owner(s) are credited and that the original publication in this journal is cited, in accordance with accepted academic practice. No use, distribution or reproduction is permitted which does not comply with these terms.

Primary mediastinal Ewing's sarcoma presenting with sudden and severe chest pain: a case report

Chen Su[1,2], Xiaobo Zhu[1,2] and Junjie Zhang[1,2]*

[1]Department of Cardiothoracic Surgery, Wujin Hospital Affiliated with Jiangsu University, Changzhou, China, [2]Department of Cardiothoracic Surgery, Wujin Clinical College of Xuzhou Medical University, Changzhou, China

Ewing's sarcoma, characterized by small round cell morphology, is a rare malignancy, with mediastinal Ewing's sarcoma being even less common. This case describes a distinctive presentation of primary mediastinal Ewing's sarcoma in a 32-year-old male presenting with sudden and severe chest pain. Initial evaluation excluded cardiac and pulmonary emergencies, revealing a posterior mediastinal mass through advanced imaging. The patient's clinical symptoms significantly improved following the complete resection of the tumor via thoracoscopy. Subsequent analysis incorporating imaging, histological, immunohistochemical and genetic findings led to the conclusive diagnosis of primary mediastinal Ewing's sarcoma.

KEYWORDS

Ewing's sarcoma, mediastinum, case report, thoracic cancer, chest pain

Introduction

Ewing's sarcoma (EwS) is a rare and aggressive malignant neoplasm primarily affecting the bones and soft tissues, with a predilection for the long bones of extremities (1, 2). However, in exceedingly rare instances, this aggressive tumor can manifest in the mediastinum. Due to the restricted mediastinal space and the marked malignancy of the tumor, patients frequently exhibit a rapid onset of clinical symptoms. In this case report, we delineate a particularly rare and perplexing presentation of EwS originating in the posterior mediastinum and manifesting with acute chest pain. The patient underwent thoracoscopic surgical exploration and tumor resection. The postoperative pathological diagnosis confirmed the presence of primary EwS in the mediastinum.

Case report

A 32-year-old young male patient presented to the emergency department with a 1-day history of severe right chest and back pain. He had no significant medical history and denied

any tobacco or alcohol use. Initial vital signs at the emergency department showed a blood pressure of 150/90 mmHg, a heart rate of 100 beats/min, and an oxygen saturation of 98%. Cardiac markers and inflammatory markers were within normal limits, and the electrocardiogram (ECG) showed sinus rhythm without ST-segment elevation. Given the patient's increasing discomfort, admission for further evaluation was arranged. Enhanced chest computed tomography (CT) revealed a 4cm x 4cm x 3cm mass in the right posterior lateral spine at the thoracic inlet, closely adjacent to the esophagus, trachea, right subclavian artery, right lung apex and posterior ribs. The tumor exhibited well-defined margins, heterogeneous internal density and partial internal enhancement after contrast enhancement (Figures 1A, B). In addition, laboratory testing showed normal tumor markers and lactate levels. Contrast-enhanced magnetic resonance imaging (MRI) revealed high signal intensity at the periphery and moderate signal within the interior on T2-weighted images (Figures 1C, D). Subsequent 18F-flurodeoxyglucose positron emission tomography/computed tomography scan showed no evidence of distant malignancy. The preliminary diagnosis was a primary mediastinal neurogenic tumor. After the failure of common analgesics to relieve the symptoms, the patient consent to surgery. Thoracoscopic exploration of the chest and tumor resection were performed on the fourth day after admission. Intraoperatively, the pleural cavity was free of adhesions and pleural effusion. The tumor, located in the right pleural apex, exhibited a smooth cystic wall with a rich vascular supply on its surface, and no evidence of invasion. The tumor was successfully excised *en bloc* via thoracoscopy, and subsequent histopathological analysis revealed a small round cell malignant tumor (Figures 2A, B). Immunohistochemical testing demonstrated strong positivity for CD99, CyclinD1, and negativity for CK, EMA, S-100, MyoD1, CD20, WT-1, Bcl-2, Vimentin and Desmin. The proliferation marker Ki-67 was found to be approximately 35% (Figures 2C–F). All indicators strongly suggest the presence of a sarcoma in this patient. To refine the classification of the specific sarcoma subtype, we engaged expert pathologists from Shanghai Zhongshan Hospital to reassess the histologic and immunohistochemical findings. Ultimately, genetic testing confirmed the existence of EWSR1::FLI1 fusion within the sarcoma tissue. Based on the combined findings of histopathological analysis, immunohistochemical and genetic testing, the conclusive diagnosis was recognized as primary mediastinal EwS. Postoperatively, the patient had no complications and was discharged. Continued chemotherapy was recommended, but due to financial constraints, he declined radiotherapy or chemotherapy during follow-up. Remarkably, he has survived nearly one year since the operation, attributing his longevity to his mindset. Despite recommendations for postoperative CT and chemotherapy, he remains resilient in his decision.

Abbreviations: CD99, Cluster of differentiation 99; CK, Cytokines; EMA, Epithelial membrane antigen; MyoD1, Myogenic Differentiation 1; CD20, Cluster of differentiation 20; WT-1, Wilms' tumor protein; Bcl-2, B-cell lymphoma 2; Ki-67, Antigen Kiel 67; EWSR1, Ewing sarcoma breakpoint region 1 gene; FLI1, Friend leukemia integration 1 transcription factor; MIC2, MHC class I chain-related Gene 2; NKX2.2, NK2 Homeobox 2; ETS, E twenty-six; CIC, Capicua; BCOR, BCL6 corepressor; LSD1, Lysine-specific histone demethylase 1A.

Discussion

EwS is a highly aggressive and poorly prognostic malignant tumor that usually originates in the metaphysis of the long bones and the pelvis (3). It primarily affects children and young adults, with a slight male predominance (4). The EwS family includes extra-skeletal EwS, accounting for around 12% of EwS cases, and mainly occurs in the thigh, upper arm, and shoulder (5). However, EwS originating in the mediastinum is extremely rare, with no more than 20 cases of mediastinal EwS reported in the literature. Given its low incidence and atypical clinical manifestation, accurate diagnosis, differential diagnosis, and subsequent treatment options pose numerous challenges.

EwS displays a rapid growth pattern, and when growing in the mediastinum, it may compress the trachea, resulting in symptoms such as chest tightness, wheezing and coughing (6, 7). Furthermore, compression of the heart or major blood vessels can lead to mediastinal shift or superior vena cava obstruction syndrome, while intercostal nerve compression may cause chest pain (8, 9). These clinical manifestations of mediastinal EwS are atypical and may easily be mistaken for other mediastinal tumors or diseases. In this particular case, the patient was urgently admitted to the hospital due to severe chest pain accompanied by back pain. Given the patient's age, potential conditions such as aortic dissection, pulmonary embolism, and tension pneumothorax could not be eliminated as possibilities. However, enhanced chest CT and ECG were able to rule out these acute and debilitating illnesses. Although the posterior mediastinal mass visible in preoperative imaging was initially deemed to be a neurogenic tumor, its location in the cervical pleura made it unsafe to perform a puncture biopsy for pathology. From these perspectives, the differential diagnosis of a mass found in the mediastinum is extensive and encompasses lymphomas, germ cell tumors, thymic tumors, and neurogenic tumors, necessitating a comprehensive approach to rule out various possibilities. CT and MRI play a crucial role in localizing and characterizing mediastinal tumors.

Histopathological evaluation, immunohistochemistry and genetic testing are all indispensable for confirming the diagnosis of primary mediastinal EwS. A prominent characteristic of EwS is the abundance of solid sheets of small round blue cells with high ratio of nuclear to cytoplasmic volume and scant eosinophilic cytoplasm, as observed in Hematoxylin and eosin (H&E) staining (7, 10, 11). It is crucial to acknowledge that other tumors might display comparable H&E staining characteristics, such as embryonal rhabdomyosarcoma, neuroblastoma and lymphoma (11). Therefore, the precise diagnosis of primary mediastinal EwS necessitates a range of techniques, including immunohistochemistry, genetic testing and other procedures. CD99, a protein product encoded by MIC2, serves as a crucial molecular marker for the diagnosis of EwS (1, 11). Although there are limited reports on primary mediastinal EwS cases, CD99 has been found to exhibit robust positive expression. However, the diagnostic specificity of CD99 for EwS is not 100%, and

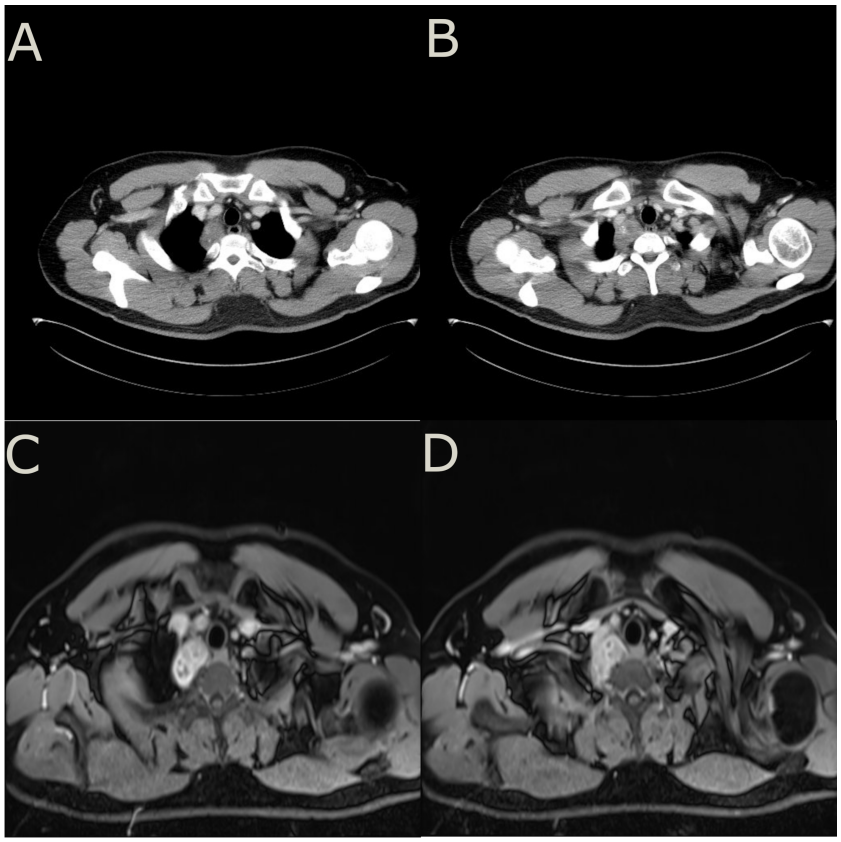

FIGURE 1
(A, B), enhanced chest CT showed a mass adjacent to spine at the thoracic inlet with uneven density and the tumor is adjacent to 2nd and 3rd posterior ribs. **(C, D)**, enhanced MRI showed a higher signal intensity at the periphery of the tumor on T2-weighted images. The internal signal distribution was found to be heterogeneous, while the tumor margins were clearly demarcated with no apparent signs of adjacent tissue or structure infiltration.

strong positive expression of CD99 can also be manifested in ependymoma (12). At the same time, the diagnostic sensitivity of CD99 for EwS is not 100%, and a small number of EwS cases can be weakly positive or negative for CD99 (13). NKX2.2 is considered to be another highly specific molecular marker in the diagnosis of EwS (14). Its combination with CD99 may improve the accuracy of diagnosis of EwS. Notably, histology and immunohistochemistry cannot definitively diagnose EwS, and further accurate diagnosis depends on genetic testing. Genetic testing can help rule out other types of sarcomas, including round cell sarcomas with EWSR1::non-ETS fusions, CIC-rearranged sarcomas, and sarcomas with BCOR gene alteration (15). Typically, FET::ETS gene family fusion can be used for the diagnosis of EwS (16). The EWSR1::FLI1 fusion formed by t(11,22)(q24;12) chromosomal translocation can be found in about 80% of EwS cases (13).

Due to its rarity, the optimal management of mediastinal EwS remains a subject of debate and a corresponding guideline reference is lacking. Current therapeutic strategies are predominantly adapted from the treatment regimens utilized for osseous EwS, encompassing a multimodal approach that includes surgery, chemotherapy, and radiotherapy. Surgical resection is considered a crucial intervention when viable, as complete tumor removal can alleviate symptoms and facilitate subsequent adjuvant therapies. ESMO Clinical Practice Guidelines suggest initiating combination chemotherapy for 3 to 6 cycles post-tumor diagnosis, followed by local treatment, and then up to another 6 to 10 cycles of chemotherapy. The duration of treatment is estimated at 10 to 12 months. The combination chemotherapy drugs encompass doxorubicin, cyclophosphamide, ifosfamide, vincristine, actinomycin, and etoposide (18). The EURO EWING 2012 phase 3 trial compared European and US chemotherapy regimens for newly diagnosed EwS. The study found that dose-intensive chemotherapy with vincristine, doxorubicin, cyclophosphamide, ifosfamide, and etoposide was more effective, less toxic, and shorter in duration, establishing it as the recommended standard of care for EwS (19). Radiotherapy is indicated in cases with incomplete excision, positive surgical margins, or inoperable tumors (20). The post-operative radiation treatment dose ranges from 45 to 60 Gy, contingent on tumor resection margin, reaction, and location (18). While multimodal therapy is the conventional method, tailored treatment plans should be taken into account to accommodate the distinct circumstances of each patient. When there is no evidence of local

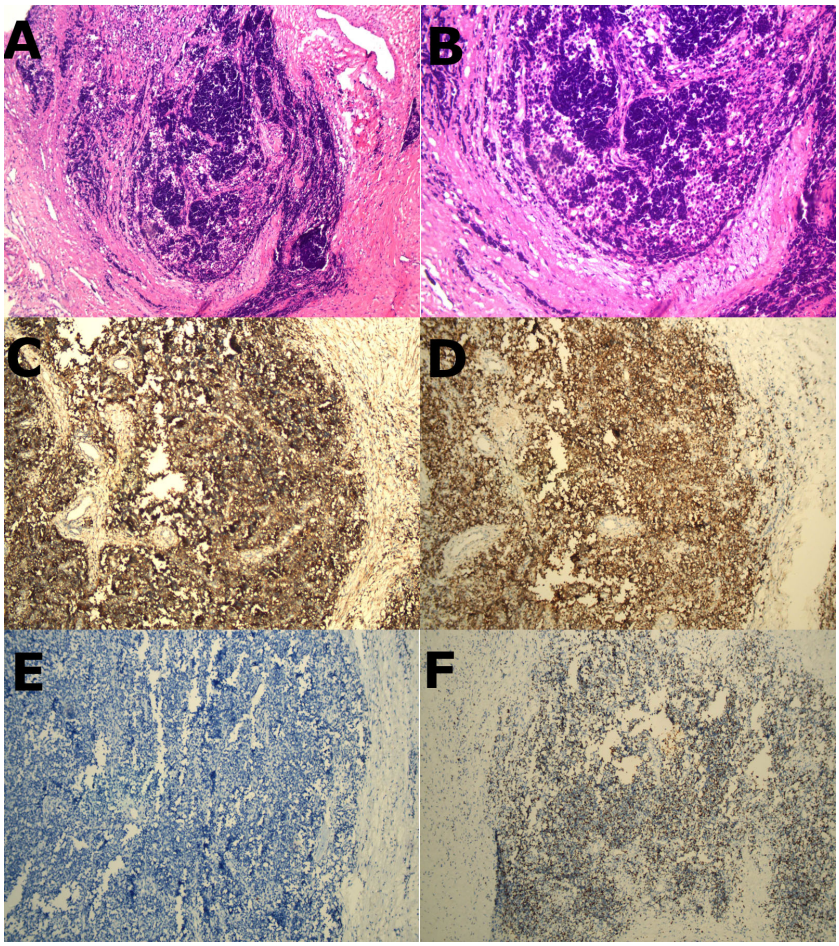

FIGURE 2
(A, B), H&E staining revealed a homogeneous population of spherical cells with basophilic cytoplasm, and hyperchromatic nuclei (x100 and x200 respectively). **(C–F)** (immunohistochemistry), **(C)** showed strong positive expression of CD99 membrane staining. **(D)** showed strong positive expression of CyclinD1 membrane staining. **(E)** showed CK marking is negative in tumor cells. **(F)** showed the proportion of tumor cells exhibiting Ki-67 positivity was approximately 35%.

or distant metastases and complete removal is possible, surgery should be chosen without delay. We summarize most of the case studies on primary mediastinal EwS in Table 1. Tumor biopsy should be site-specific in the mediastinum, CT-guided transthoracic biopsy is preferred. In case of need, endobronchial ultrasound guided transbronchial needle aspiration or mediastinoscopic biopsy can be utilized. Occasionally, the tumor is extensive or infiltrates adjacent organs and tissues, and neoadjuvant therapy may provide patients

TABLE 1 Management and prognosis of primary mediastinal Ewing's sarcoma in previous studies.

Study	Age and Sex	Site	Biopsy	Treatment	Prognosis
Reali A, et al (9)	66-F	Anterior mediastinum	Mediastinoscopy	Unresectable, chemotherapy and radiotherapy	Post-treatment, multiple pulmonary metastases appeared two months later
Koc U, et al (21)	63-M	Anterior mediastinum	NA	Unresectable, chemotherapy	NA
Cui M, et al (22)	66-M	Anterior mediastinum	None	Thoracotomy	Post-surgery, pericardial metastasis appeared two months later
Silver JM, et al (23)	17-M	Posterior mediastinum	None	Thoracotomy, postoperative chemotherapy and radiotherapy	NA

(Continued)

TABLE 1 Continued

Study	Age and Sex	Site	Biopsy	Treatment	Prognosis
Caltavituro A, et al (24)	30-F	Anterior mediastinum	None	Thoracotomy, postoperative chemotherapy and stem cell transplantation	Post-surgery, local recurrence appeared a few months later. But the patient is still alive after adjuvant therapy
Halliday J, et al (7)	16-F	Anterior mediastinum	An open biopsy of the neck was performed but failed	Thoracotomy	NA
Halefoglu AM, et al (25)	19-F	Posterior mediastinum	CT-guided biopsy	Thoracotomy	NA
Ata F, et al (8)	16-M	Anterior and posterior mediastinum	CT-guided biopsy	None	NA
Li X, et al (6)	15-F	Anterior mediastinum	CT-guided biopsy	Chemotherapy	Remission

M, male; F, female; NA, not applicable.

with access to surgery. Multidisciplinary management emerges as the primary strategy to augment the survival rate of patients afflicted with mediastinal EwS. Beyond traditional surgical, radiotherapeutic, and chemotherapeutic interventions, molecular therapeutic strategies may be integrated clinically in potential future scenarios. Inhibitors of the histone demethylase LSD1 selectively induce programmed cell death in EwS cell lines and are presently under evaluation in a clinical trial (26). The recommended follow-up strategy is to undertake MRI examinations every 2 to 3 months post-treatment, to scrutinize the condition of the soft tissue within the mediastinum. If survival surpasses 5 years, a follow-up may be conducted biannually (18). Our patient's one-year survival after surgery, despite the unavailability of comprehensive adjuvant therapies, suggests that surgery can play a crucial role in managing early mediastinal EwS. Early studies indicate that patients with EWSR1::FLI1 fusions have higher disease-free survival rates than patients with other types of fusions (17, 27). Nonetheless, it is important to acknowledge that our study is limited to a single case, and given the aggressive nature of EwS, it is imperative that eligible patients receive standard postoperative chemoradiotherapy to enhance their long-term survival. Further research and larger case series with more comprehensive follow-up data are warranted to establish the most effective treatment paradigm for this rare entity.

Conclusion

Our case illuminates the intricate diagnosis and management of primary mediastinal EwS, an uncommon and highly aggressive malignancy with an atypical presentation. We aim to expand the existing knowledge on this unusual entity and promote further research to enhance therapeutic strategies for primary mediastinal EwS. Furthermore, it underscores the indispensable significance of an interdisciplinary approach in handling rare and intricate cases in thoracic surgery and oncology.

Data availability statement

The original contributions presented in the study are included in the article/supplementary material. Further inquiries can be directed to the corresponding author.

Ethics statement

Ethical approval was not required for this case report as it involved standard clinical practice, maintained patient confidentiality, and obtained informed consent for data usage, aligning with established ethical principles. The studies were conducted in accordance with the local legislation and institutional requirements. Written informed consent was obtained from the patients/participants for the publication of this case report.

Author contributions

CS: Writing – original draft. XZ: Writing – review & editing. JZ: Conceptualization, Funding acquisition, Supervision, Validation, Writing – review & editing.

Funding

The author(s) declare financial support was received for the research, authorship, and/or publication of this article. This work

was supported by the Changzhou Sci & Tech Program (CJ20220165), Young Talent Development Plan of Changzhou Health Commission (CZQM2022027), and Changzhou Longcheng Medical Star Health Youth Sci & Tech Talent Support Project.

Acknowledgments

We acknowledge the patient in the study who was able to provide his own medical information, and to everyone in our research team.

Conflict of interest

The authors declare that the research was conducted in the absence of any commercial or financial relationships that could be construed as a potential conflict of interest.

Publisher's note

All claims expressed in this article are solely those of the authors and do not necessarily represent those of their affiliated organizations, or those of the publisher, the editors and the reviewers. Any product that may be evaluated in this article, or claim that may be made by its manufacturer, is not guaranteed or endorsed by the publisher.

References

1. El Weshi A, Allam A, Ajarim D, Al Dayel F, Pant R, Bazarbashi S, et al. Extraskeletal Ewing's sarcoma family of tumours in adults: analysis of 57 patients from a single institution. *Clin Oncol (R Coll Radiol).* (2010) 22(5):374–81. doi: 10.1016/j.clon.2010.02.010

2. Andrei M, Cramer SF, Kramer ZB, Zeidan A, Faltas B. Adult primary pulmonary primitive neuroectodermal tumor: molecular features and translational opportunities. *Cancer Biol Ther* (2013) 14(2):75–80. doi: 10.4161/cbt.22635

3. Sparreboom BD, Trautman J, Yaxley J. Ewing sarcoma: A pictorial review of typical and atypical locations with reference to the updated 2020 WHO classification system. *J Med Imaging Radiat Oncol* (2022) 66(6):812–8. doi: 10.1111/1754-9485.13456

4. Haveman LM, van Ewijk R, van Dalen EC, Breunis WB, Kremer LC, van den Berg H, et al. High-dose chemotherapy followed by autologous haematopoietic cell transplantation for children, adolescents, and young adults with primary metastatic Ewing sarcoma. *Cochrane Database Syst Rev* (2021) 9(9):CD011405. doi: 10.1002/14651858.CD011405.pub2

5. Choi JH, Ro JY. The 2020 WHO classification of tumors of soft tissue: selected changes and new entities. *Adv Anat Pathol* (2021) 28(1):44–58. doi: 10.1097/PAP.0000000000000284

6. Li X, Qi S, Zhu T, Jiang Y, Wang W. Primary mediastinum Ewing's sarcoma with pleural effusion: A case report and literature review. *Open Life Sci* (2023) 18 (1):20220669. doi: 10.1515/biol-2022-0669

7. Halliday J, Soon SY, Monaghan H, Walker WS, Zamvar V. Extraskeletal Ewing's sarcoma presenting as a mediastinal mass. *Ann Thorac Surg* (2010) 90(3):1016–7. doi: 10.1016/j.athoracsur.2010.01.083

8. Ata F, Safwan Aljafar M, Mohammed AM, Mirza S, Zafar AA. Primary Mediastinal Ewing sarcoma presenting as a massive lung lesion with a mediastinal shift. *Clin Case Rep* (2021) 9(10):e04857. doi: 10.1002/ccr3.4857

9. Reali A, Mortellaro G, Allis S, Trevisiol E, Anglesio SM, Bartoncini S, et al. A case of primary mediastinal Ewing's sarcoma / primitive neuroectodermal tumor presenting with initial compression of superior vena cava. *Ann Thorac Med* (2013) 8(2):121–3. doi: 10.4103/1817-1737.109834

10. Folpe AL, Goldblum JR, Rubin BP, Shehata BM, Liu W, Dei Tos AP, et al. Morphologic and immunophenotypic diversity in Ewing family tumors: a study of 66 genetically confirmed cases. *Am J Surg Pathol* (2005) 29(8):1025–33. doi: 10.1097/01.pas.0000167056.13614.62

11. Zhang WD, Zhao LL, Huang XB, Cai PQ, Xu GX. Computed tomography imaging of anterior and middle mediastinal Ewing sarcoma/primitive neuroectodermal tumors. *J Thorac Imaging.* (2010) 25(2):168–72. doi: 10.1097/RTI.0b013e3181a99117

12. Kurdi M, Eberhart C. Immunohistochemical expression of Olig2, CD99, and EMA to differentiate oligodendroglial-like neoplasms. *Folia Neuropathol.* (2021) 59 (3):284–90. doi: 10.5114/fn.2021.108526

13. Tsuda Y, Zhang L, Meyers P, Tap WD, Healey JH, Antonescu CR. The clinical heterogeneity of round cell sarcomas with EWSR1/FUS gene fusions: Impact of gene fusion type on clinical features and outcome. *Genes Chromosomes Cancer.* (2020) 59 (9):525–34. doi: 10.1002/gcc.22857

14. MaChado I, Yoshida A, Lopez-Guerrero JA, Nieto MG, Navarro S, Picci P, et al. Immunohistochemical analysis of NKX2.2, ETV4, and BCOR in a large series of genetically confirmed Ewing sarcoma family of tumors. *Pathol Res Pract* (2017) 213 (9):1048–53. doi: 10.1016/j.prp.2017.08.002

15. Bridge JA. *Soft tissue and bone tumours, WHO classification of tumours. 5th ed.* IARC (2020) France.

16. Kinnaman MD, Zhu C, Weiser DA, Mohiuddin S, Hingorani P, Roth M, et al. Survey of paediatric oncologists and pathologists regarding their views and experiences with variant translocations in ewing and ewing-like sarcoma: A report of the children's oncology group. *Sarcoma.* (2020) 2020:3498549. doi: 10.1155/2020/3498549

17. de Alava E, Kawai A, Healey JH, Fligman I, Meyers PA, Huvos AG, et al. EWS-FLI1 fusion transcript structure is an independent determinant of prognosis in Ewing's sarcoma. *J Clin Oncol* (1998) 16(4):1248–55. doi: 10.1200/JCO.1998.16.4.1248

18. ESMO/European Sarcoma Network Working Group. Bone sarcomas: ESMO Clinical Practice Guidelines for diagnosis, treatment and follow-up. *Ann Oncol* (2015) 26 Suppl 5:v174–7. doi: 10.1093/annonc/mdu256

19. Brennan B, Kirton L, Marec-Berard P, Gaspar N, Laurence V, Martin-Broto J, et al. Comparison of two chemotherapy regimens in patients with newly diagnosed Ewing sarcoma (EE2012): an open-label, randomised, phase 3 trial. *Lancet.* (2022) 400 (10362):1513–21. doi: 10.1016/S0140-6736(22)01790-1

20. Denbo JW, Shannon Orr W, Wu Y, Wu J, Billups CA, Navid F, et al. Timing of surgery and the role of adjuvant radiotherapy in ewing sarcoma of the chest wall: a single-institution experience. *Ann Surg Oncol* (2012) 19(12):3809–15. doi: 10.1245/s10434-012-2449-5

21. Koc U, Duman E. A case of primary mediastinal Ewing's sarcoma/ primitive neuroectodermal tumor presenting with chest pain. *Turk J Emerg Med* (2017) 17(2):77–8. doi: 10.1016/j.tjem.2016.11.002

22. Cui M, Zhai D, Liu Y, Zhou X, Wang T, Wang L, et al. Case report: Primary mediastinal Ewing's sarcoma presenting with chest tightness. *Front Oncol* (2022) 12:1020339. doi: 10.3389/fonc.2022.1020339

23. Silver JM, Losken A, Young AN, Mansour KA. Ewing's sarcoma presenting as a posterior mediastinal mass: a lesson learned. *Ann Thorac Surg* (1999) 67(3):845–7. doi: 10.1016/S0003-4975(99)00045-4

24. Caltavituro A, Buonaiuto R, Salomone F, Morra R, Pietroluongo E, De Placido P, et al. Extraskeletal Ewing's sarcoma of the mediastinum: Case report. *Front Oncol* (2023) 13:1074378. doi: 10.3389/fonc.2023.1074378

25. Halefoglu AM. Extraskeletal Ewing's sarcoma presenting as a posterior mediastinal mass. *Arch Bronconeumol.* (2013) 49(2):82–4. doi: 10.1016/j.arbr.2012.11.010

26. Pishas KI, Drenberg CD, Taslim C, Theisen ER, Johnson KM, Saund RS, et al. Therapeutic targeting of KDM1A/LSD1 in ewing sarcoma with SP-2509 engages the endoplasmic reticulum stress response. *Mol Cancer Ther* (2018) 17(9):1902–16. doi: 10.1158/1535-7163.MCT-18-0373

27. Zoubek A, Dockhorn-Dworniczak B, Delattre O, Christiansen H, Niggli F, Gatterer-Menz I, et al. Does expression of different EWS chimeric transcripts define clinically distinct risk groups of Ewing tumor patients? *J Clin Oncol* (1996) 14 (4):1245–51. doi: 10.1200/JCO.1996.14.4.1245

frontiers | Frontiers in Medicine

TYPE Case Report
PUBLISHED 01 February 2024
DOI 10.3389/fmed.2024.1172746

Check for updates

OPEN ACCESS

EDITED BY
Liam Chen,
University of Minnesota, United States

REVIEWED BY
Shorabh Sharma,
SBH Health System, United States
Luit Penninga,
Rigshospitalet, Denmark

*CORRESPONDENCE
Lei Kang
✉ kanglei@bjmu.edu.cn

†These authors have contributed equally to this work

RECEIVED 23 May 2023
ACCEPTED 22 January 2024
PUBLISHED 01 February 2024

CITATION
Zhang X, Qiu Y, Zhang J, Chen Z, Yang Q, Huang W, Song L and Kang L (2024) An elderly low-grade fibromyxoid sarcoma patient with early postoperative recurrences and metastases: a case report and literature review.
Front. Med. 11:1172746.
doi: 10.3389/fmed.2024.1172746

COPYRIGHT
© 2024 Zhang, Qiu, Zhang, Chen, Yang, Huang, Song and Kang. This is an open-access article distributed under the terms of the Creative Commons Attribution License (CC BY). The use, distribution or reproduction in other forums is permitted, provided the original author(s) and the copyright owner(s) are credited and that the original publication in this journal is cited, in accordance with accepted academic practice. No use, distribution or reproduction is permitted which does not comply with these terms.

An elderly low-grade fibromyxoid sarcoma patient with early postoperative recurrences and metastases: a case report and literature review

Xiaoyue Zhang[1†], Yongkang Qiu[1†], Jixin Zhang[2], Zhao Chen[1], Qi Yang[1], Wenpeng Huang[1], Lele Song[1] and Lei Kang[1*]

[1]Department of Nuclear Medicine, Peking University First Hospital, Beijing, China, [2]Department of Pathology, Peking University First Hospital, Beijing, China

Background: Low-grade fibromyxoid sarcoma (LGFMS) is a rare type of soft tissue sarcoma that often involves the deep soft tissue of the extremities and trunk in young and middle-aged adults. It is uncommon in the elderly. Here we discuss a case of LGFMS in an elderly patient who had recurrence and metastasis within 2 years of resection of the primary tumor.

Case report: A 71-year-old LGFMS patient was presented with a mass in the left forearm accompanied by pain and numbness from the left upper arm to fingers. The patient subsequently underwent 3 surgical resections, although she had 3 recurrences within 6 months after the initial diagnosis. Considering the malignant biological behavior of the tumor, an amputation at 5 cm above the elbow was eventually performed. However, recurrence in the extremity of the stump and chest wall metastasis were observed 2 years after amputation. Then resection of the metastases, radiotherapy and particle implantation therapy were performed. The patient is currently undergoing follow-up and has no evidence of recurrence.

Conclusion: In our case, multiple early postoperative recurrences may be associated with a positive margin at initial operation. The patient underwent a total of 5 operations including local resection of the primary tumor, twice wide resections, amputation and metastatic surgery with 4 early postoperative recurrences and metastases within 4 years, suggesting that LGFMS may have highly invasive biological behavior. Our case demonstrated that early aggressive surgical treatment is recommended for LGFMS patients with a positive margin at initial operation and patients who had recurrence even after wide resection rather than local resection. Further research is needed to develop more effective treatment options for rapidly progress and highly aggressive LGFMS.

KEYWORDS

low-grade fibromyxoid sarcoma, postoperative recurrences, metastasis, magnetic resonance imaging, PET/CT

Introduction

Low-grade fibromyxoid sarcoma (LGFMS) is a rare type of soft tissue sarcoma that is classified as a "fibroblastic/myofibroblastic tumor" according to the 2020 edition of the World Health Organization (WHO) Classification of Bone and Soft Tissue Tumors. LGFMS often involves the deep soft tissue of the extremities and trunk in young and middle-aged adults with a deceptively benign histologic appearance (1). Its biological behavior is both indolent and malignant. About 9% of patients have recurrence and 6% have metastasis within 2 years after resection of primary tumor (2). However, the long-term local recurrence rate and the eventual metastasis rate can reach 64 and 46%, and the clinical course is often prolonged (3). Here, we described a rare case of a 71-year-old LGFMS patient who underwent a total of 5 operations with 4 early postoperative recurrences and metastases within 4 years. In addition, we summarized characteristics of LGFMS cases with twice or more local recurrences by reviewing previous relevant literature in order to assist the clinician in decision making and treatment planning for achieving a good prognosis for this rare tumor.

Case presentation

A 71-year-old female patient presented with a mass in the left forearm for 3 years. When the patient sought medical attention 1 year ago, the doctor considered a diagnosis of fibroma and did not proceed with surgical treatment. The mass began to enlarge and harden significantly more than 5 months ago, accompanied by pain and numbness from the left upper arm to fingers. The patient had no family history of a similar condition. Physical examination revealed an 8 cm × 6 cm tender fixed mass on the patient's left forearm with an unclear boundary. Laboratory tests showed no obvious abnormalities. Magnetic resonance imaging (MRI) was performed to further assess the lesion. The pronator teres, flexor carpi radialis, flexor digitorum superficialis, flexor carpi ulnaris and intermuscular space showed patchy and irregular isointense signals on T1-weighted image (Figure 1A) and high signal intensity on T2-weighted image (Figures 1B–E). The boundary of the lesion is not clear, with intermuscular edema (Figures 1A–E).

The patient subsequently underwent a resection of the left forearm mass with a size of 8 cm × 6 cm × 6 cm. Intraoperative findings showed the mass borders were indistinct from surrounding muscle fibers and tendon. The trunk and branches of the dorsal interosseous nerve were also tightly adhered to the tumor and the nerve branches surrounded by tumor tissue were removed. Postoperative histopathology showed alternating myxoid and fibrous areas and that the tumor cells were predominantly spindle-shaped cells arranged in bundles with uneven proliferation. Moderate cytologic atypia and up to 11 mitoses per 10 hpf in the most active part of the tumor were observed (Figures 1L,M). By immunohistochemistry (IHC), the tumor cells were diffusely positive for vimentin, focally for SMA, KP1, MSA, and negative for S^{-100}, CD34, EMA, HMB-45, desmin, LCA, AE1/AE3, ALK (1A4), SOX10, TLE1 and ß-catenin. Ki-67 staining showed the proportion of the positive tumor cells was about 20%. Upon pathologic examination with immunohistochemistry, low-grade soft tissue sarcoma was diagnosed. Using the French Federation of Cancer Centers Sarcoma Group (FNCLCC) guidelines for the histopathologic grading, the final scores were 4 and the tumor was graded as 2. The tumor cells infiltrated surrounding skeletal muscle tissue. Presence of tumor cells at the surgical resection margin can also be observed. Genetic test was performed to differentiate between low-grade fibromyxoid sarcoma and low-grade/well-differentiated myxofibrosarcoma. *In situ* hybridization (ISH) and fluorescence *in situ* hybridization (FISH) detected *FUS* gene rearrangement, which was consistent with the diagnosis of LGFMS (Figure 1N).

Two months after the primary surgery, MRI revealed multiple subcutaneous and intermuscular soft tissue nodules in the left forearm (Figures 1F–K). The patient subsequently had a wide resection of the local recurrent tumor with a 2 cm margin in all directions to the mass or the scar from the previous surgery. The postoperative histopathological findings reveal a proliferation of spindle-shaped tumor cells, with some arranged in a fascicular pattern. These cells exhibit moderate to severe cytologic atypia, and up to 31 mitoses per 10 hpf in the most active regions were observed. A mucinous background is evident in certain areas of the stroma. Three months after the second surgery, the patient found a mass in the left forearm again. MRI also showed multiple intermuscular and subcutaneous soft tissue nodules and abnormal signals at the left ulna and proximal radius. Then, the patient underwent another larger-scale resection. The postoperative histopathological features exhibit resemblances to those observed in the preceding recurrence. After the wide resections, the follow-up MRI showed multiple masses in the left forearm muscle (Figures 2A–E) and abnormal signals in the T8, T11 vertebral body (Figure 2F) and accessory of T11 (Figure 2G). To assess the patient's whole-body situation, ^{18}F-flurodeoxyglucose (^{18}F-FDG) positron emission tomography/computed tomography (PET/CT) examination was further performed. It revealed increased metabolic uptake with a maximum standardized uptake value (SUVmax) of 11.2 within the left forearm mass (Figures 3A–C) and increased FDG uptake in the T8 and T11 vertebral body (SUVmax 3.3, 4.1) where slightly lower bone mineral density was observed (Figures 3A,D). Then, her left arm was amputated 5 cm above the elbow and the mass was about 10 cm from the incision, protruding from the skin with a necrosis surface. The histopathological characteristics of the tumor manifest similarities to those observed in prior recurrences. IHC assessment demonstrated diffusely positive for vimentin, focally for CD34, CD31, and negative for S^{-100}, SMA, desmin, AE1/AE3. Ki-67 staining showed the proportion of the positive tumor cells was 90%.

Two years after amputation, the patient was found to have a mass on the back. MRI showed a mass in the right back muscle (Figure 2H) and the adjacent right 7th rib (Figure 2I). PET/CT revealed increased FDG uptake at the extremity of the left stump (SUVmax 5.4; Figures 3E–G), irregular thickening of the right chest wall and bone destruction of the adjacent right 8th rib (Figure 3H). Resection of the metastases in the right chest wall and the 8th rib was performed on the patient. She was also treated with radiotherapy and particle therapy. The patient is currently undergoing follow-up and has no PET/CT evidence of recurrence.

Discussion

LGFMS was first reported by Evans (1) in 1987, which has a deceptively benign histologic appearance and relatively frequent recurrence and metastasis. In Evans' early reports, 7 out of 12

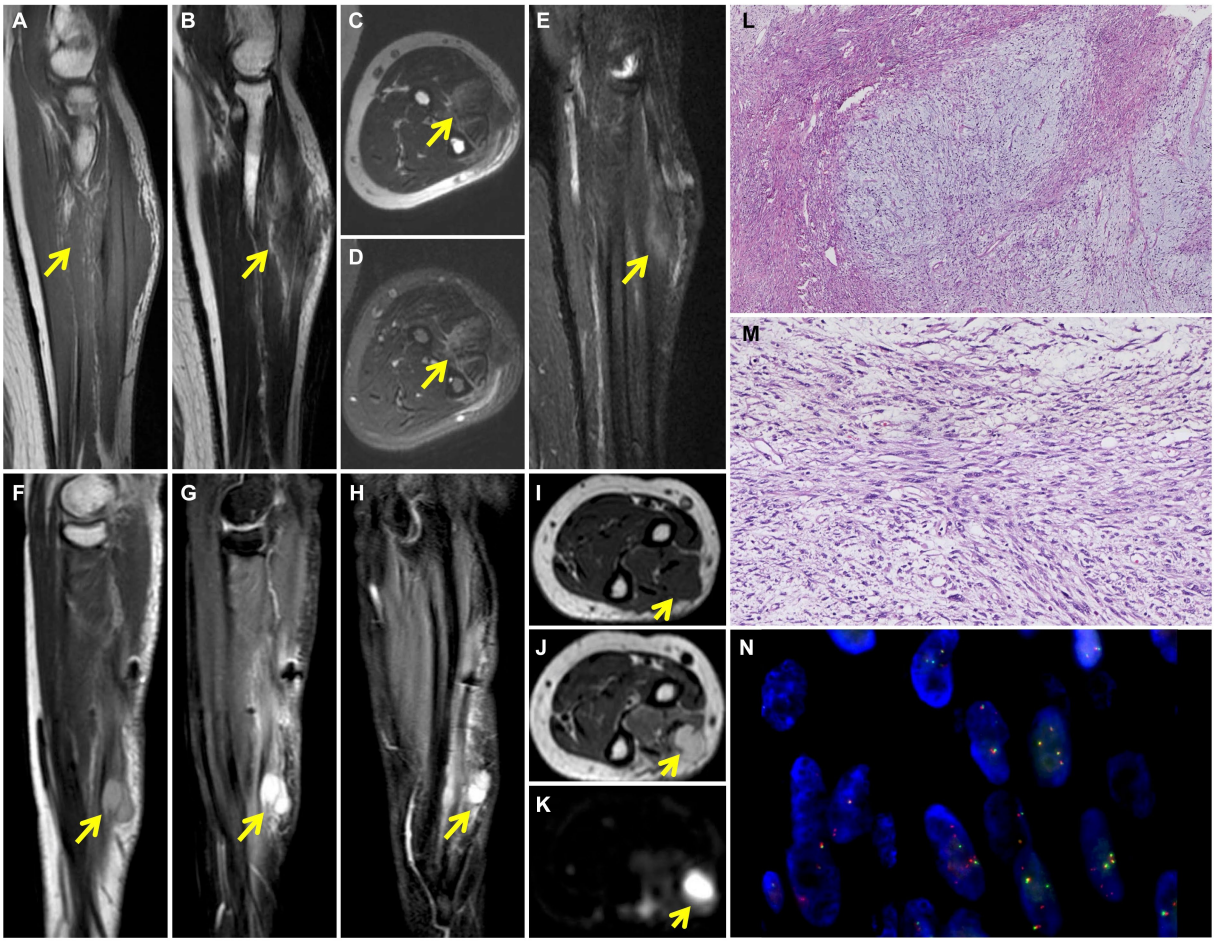

FIGURE 1
Preoperative MRI shows the soft tissue mass in the left arm. T1-weighted coronal image **(A)** shows patchy and irregular isointense signal lesion (yellow arrow). The soft tissue mass (yellow arrow) shows slightly high signal intensity on T2-weighted coronal **(B)** and axial **(C)** images and high signal intensity on T2 fat-suppressed axial **(D)** and coronal **(E)** images. 6-months postoperative MRI shows recurrence of left arm LGFMS after initial resection. Multiple nodules (yellow arrow) were detected in the extensor digitorium at the medial of the ulna, which exhibited high signal intensity on T2-weighted sagittal **(F)**, T2 fat-suppressed sagittal **(G)** and coronal **(H)** images. The nodules (yellow arrow) demonstrate low signal intensity on T1-weighted axial image **(I)**, high signal intensity on T2-weighted **(J)** and diffused **(K)** weighted axial images. Photomicrograph shows the alternating myxoid and fibrous area in the lesion **(L)** (HE, original magnification × 40). Higher magnification shows the spindle-shaped tumor cells arranged in bundles with uneven proliferation **(M)** (HE, original magnification × 200). FISH analysis of *FUS* detected both fused-and split-signals **(N)**.

LGFMS patients developed distant metastasis, with a follow-up ranging from 5.5 to 50 years (4). However, among the 54 LGFMS patients reported by Folpe et al. (2), only 5 (9%) had local recurrence and 3 (6%) had distant metastasis, possibly due to the fact that most of the patients had been treated with aggressive surgery or the relatively short follow-up time, with a median of 24 months. In 33 cases of LGFMS later reported by Evans, the interval to local recurrence was up to 15 years with a median of 3.5 years, while the interval to metastasis was up to 45 years with a median of 5 years. (3) These reports suggest that LGFMS is characterized by late recurrence and metastasis with a prolonged clinical course, therefore a short-term follow-up may not be sufficient to assess the biological behavior of this tumor. In our case, pathology indicated a positive surgery margin upon the resection of primary mass. Local recurrence occurred 2 months later and a wide resection was performed. However, local recurrence and bone metastasis were found 1 month later. The patient underwent radiotherapy, particle therapy and amputation. She was regularly followed up for 2 years without recurrence. Two years after the amputation, PET/CT scans revealed increased FDG uptake at the extremity of the stump and metastatic lesions in the back that invaded adjacent ribs. The patient had to undergo another resection of the metastatic lesion in the chest wall. This patient had 3 recurrences within 6 months of the initial diagnosis, underwent a total of 5 surgeries within 4 years, which is probably the most detailed report of the fastest recurrence with the shortest interval of LGFMS so far.

We identified 19 LGFMS cases with twice or more local recurrences based on the literature search on PubMed from 1987 to 2022. The keywords were "low grade fibromyxoid sarcoma." The characteristics of all cases are summarized in Table 1. The median age of the patients was 26 years (range, 6–53 years). Tumor size (maximum diameter) was known in 10 cases, in which it ranged from 3.5 to 15 cm with a median of 10 cm. Among the 19 patients, 13 were men, with a male-to-female ratio of 2.17:1. All patients received surgery as initial treatment, only 3 had data on surgical margin status, all of which were positive. The median time of first recurrence was 3 years while the

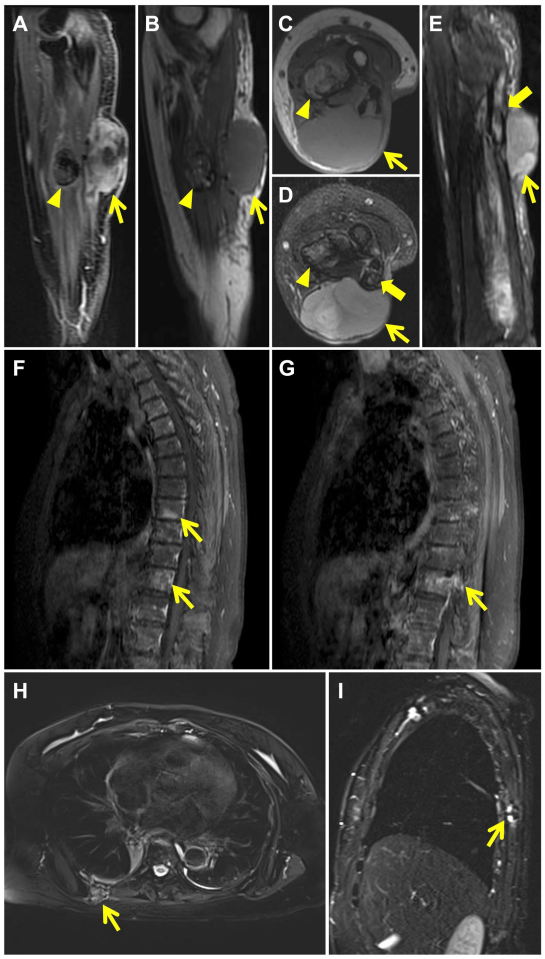

FIGURE 2
MRI after wide resections shows recurrence of left arm LGFMS. The mass in the extensor carpi ulnaris (thin yellow arrow) demonstrates high signal intensity on contrast enhanced T1 weighted sagittal image **(A)** and isointense signal intensity on T1-weighted sagittal **(B)** and axial **(C)** images. T2 fat-suppressed axial **(D)** and sagittal **(E)** images reveal high signal intensity in the mass (thin yellow arrow) and in the cavity of the left ulna with discontinuous cortical bone (thick yellow arrow). The nodule in the flexor digitorum profundus (yellow arrow head) demonstrates rim enhancement on contrast enhanced T1 weighted sagittal image **(A)** and mixed signal intensity on T1-weighted sagittal **(B)** and axial **(C)** images. T2 fat-suppressed axial image **(D)** reveals mixed high signal in the nodule (yellow arrow head). Images of contrast-enhanced MRI of the thoracic spine after wide resections show patchy high signal intensity in the T8, T11 vertebral body **(F)** (thin yellow arrows) and abnormal enhancement in T11 vertebral body and accessory **(G)** (thin yellow arrow). MRI after amputation shows chest wall metastases. T2 fat-suppressed axial **(H)** and sagittal **(I)** images reveal a mass with mixed signal intensity in the right back muscle (thin yellow arrow) and show discontinuous bone cortex of the adjacent right 7th rib with high signal intensity (thin yellow arrow).

median time from illness onset to death was 28 years. Five patients had metastases, including lung ($n = 5$), bone ($n = 1$) and chest wall ($n = 1$). Characteristics of dedifferentiated sarcoma were observed in 2 recurrent tumors and features of sclerosing epithelioid fibrosarcoma (SEF) was observed in one case.

LGFMS tends to occur in young and middle-aged people. It often involves the deep soft tissues of lower limbs, followed by the chest wall, shoulder, groin and other areas. The most common site of metastasis is the lung. It is histologically characterized by alternating myxoid and fibrous areas, bland fusiform cells, a whorled growth pattern (6). Other histological variations include giant rosettes (8), areas of hypercellularity, foci with rounded epithelioid cells, less commonly observed are focal osseous metaplasia and significant nuclear pleomorphism. In addition, characteristics of focal sclerosing epithelioid fibrosarcoma has been reported in LGFMS (9). However, the relationship between these histological variations and tumor biological behavior has not been reported. In our case, focal dense cells with less stroma and higher atypia were found in the resected recurrent tumor, which may be related to its rapidly proliferation and aggressive behavior.

Most LGFMS appear to be well-circumscribed but have no capsule. Local infiltration may occur, and resection is usually incomplete (10). Therefore, the preferred treatment for LGFMS is wide resection and radical surgery (11, 12). Prognosis of LGFMS is based on tumor size at diagnosis, invasion to adjacent tissues, and surgical margin (3, 4). Patients with negative margins after active surgical resection have a lower recurrence probability and a longer recurrence interval (13). Our case had a positive surgical margin, which may account for the multiple early postoperative recurrences. If possible, wide resection should be the preferred treatment for all local recurrences (14). There is currently little guidance on how to treat LGFMS patients with metastatic disease. Due to the very low mitotic rate in LGFMS, chemotherapy and radiotherapy usually have no significant effect on the long-term prognosis (12). When bone metastases occur, especially vertebral metastases, local radiotherapy and particle therapy may be alternative treatments to reduce skeletal related events, while radical surgery for distant metastases (usually to the lungs) may still be the best option for patients. The efficacy of conventional systemic therapy for advanced LGFMS is also limited (15). A recent study suggested that Trabectedin could be effective on metastatic patients (16), which may be related to the *FUS::CREB3L2* fusion gene in LGFMS.

In our case, the tumor progressed rapidly with early postoperative recurrences and metastases. These clinical manifestations along with histopathological findings of focal dense cells and less stroma are similar to SEF. It is necessary to distinguish LGFMS from SEF. SEF, originally reported by Meis-Kindblom et al. (17), is characterized by a large number of sclerotic stroma and rounded or polygonal epithelioid cells growing in cords or nests. In a study of LGFMS, Guillou et al. (18) included 4 cases of SEF as a comparison, one of which was similar to LGFMS. Despite the short follow-up of these SEF patients, 3 had metastases at presentation and 4 had local recurrence at 6 months. SEF often occurs in older people, metastasizes more frequently, and has a higher mortality rate and shorter overall survival than LGFMS. Antonescu et al. (19) mentioned that a few SEF tumors had fibroma-like areas and myxoid components similar to LGFMS. When the typical morphological features of SEF and LGFMS appear simultaneously or sequentially, it is called hybrid SEF/LGFMS (17, 20, 21). Compared with LGFMS, hybrid SEF/LGFMS exhibit more aggressive tumor behavior, and the recurrence, metastasis and death caused by tumors occur earlier and at shorter intervals. The histological morphology and clinical features of LGFMS and SEF partially overlap but also differ to some extent, which may be related to their common and unique genetic characteristics (16, 22–25). Based on these findings, we speculate that SEF may be a variant of

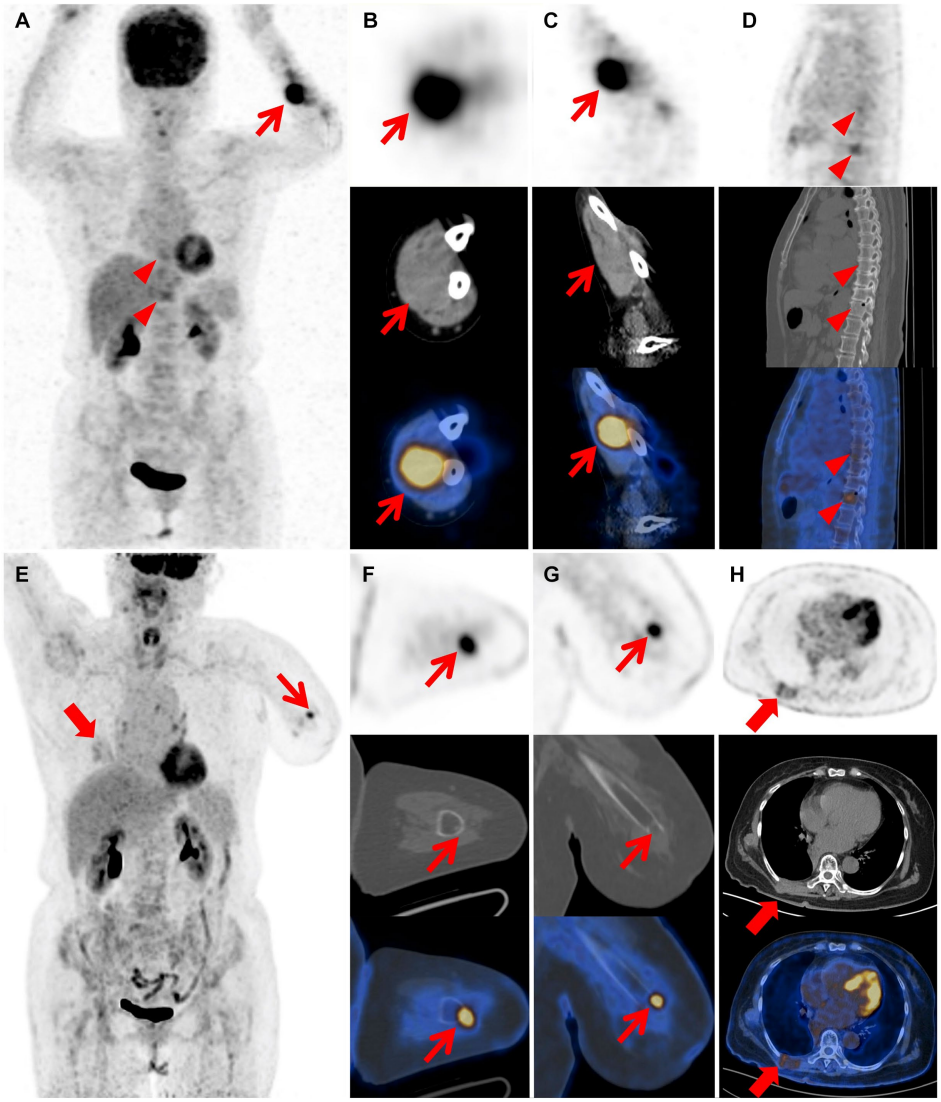

FIGURE 3
Images of ^{18}F-FDG PET/CT after wide resections and PET/CT after amputation. The MIP image **(A)** shows left forearm (red arrow) and T8, T11 vertebral body lesions (red arrow heads) with varying degrees of FDG uptake. The coronal **(B)** and axial **(C)** views of mass in the left forearm demonstrate increased metabolic uptake (red arrow; SUVmax 11.2). The sagittal image **(D)** demonstrates increased metabolic uptake in the T8 and T11 vertebral body (red arrow heads; SUVmax 3.3, 4.1), suggesting the presence of bone metastasis. The MIP image **(E)** reveals absence of the left forearm and lesions of the left stump (thin red arrow) and chest wall (thick red arrow) with varying degrees of FDG uptake. The axial **(F)** and coronal **(G)** views of the left stump demonstrate increased metabolic uptake at the extremity (thin red arrow; SUVmax 5.4). The axial image **(H)** reveals irregular thickening of the right chest wall with mildly increased metabolic uptake (thick red arrow; SUVmax 2.9).

LGFMS rather than a distinct fibrosarcoma under certain circumstances.

Pure SEF and hybrid SEF/LGFMS SEF are extremely rare, and therefore very limited data about the clinical behavior and the effectiveness of different treatments are known. Surgery remains the mainstay of treatment, especially wide resection with histologically negative margins. Perioperative or postoperative radiotherapy can be used due to the rapid growth and relatively more aggressive clinical features of pure SEF or mixed SEF/LGFMS, which may help to control tumor recurrence and metastasis, although its efficacy has not been proven by previous studies (26). A recent study suggests that chemotherapy has very limited efficacy in SEF (27).

^{18}F-FDG PET/CT is a wildly used imaging modality in oncology. Metabolically active, high-grade soft tissue sarcomas tend to have high uptake of ^{18}F-FDG on PET/CT. In our case, increased metabolic uptake was observed within the recurrent tumor (SUVmax 11.2), which could be related to aggressive tumor biology and frequent postoperative recurrences. Yoshimura et al. (28) reported a case of primary pulmonary LGFMS with ^{18}F-FDG PET/CT findings suggestive of malignancy. Preoperative ^{18}F-FDG PET/CT showed focal FDG uptake, with a maximum standardized uptake value of 5.59 in the mass. In addition, ^{18}F-FDG PET/CT could also provide a whole-body assessment of the patient as part of tumor monitoring and follow up.

The recurrent tumors in the elderly patient we reported had histopathological findings of focal dense cells, less stroma, and high atypia. Thus, the possibility of mixed SEF/LGFMS being the diagnosis cannot be excluded. Our patient suffered multiple early postoperative

TABLE 1 Characteristics of LGFMS cases with twice or more local recurrences.

Author	Case no.	Age/Sex	Site	Maximum primary tumor site(cm)	Initial treatment	Follow up
Goodlad et al. (5)	1	53/M	Trunk (anterior chest wall)	NA	Excision (margin unknown)	LR at 4, 6, 7, 9 and 10 years
	2	50/M	Groin	5	Excision (margin unknown)	LR at 2, 9 and 10 years
	3	18/M	Lower limb (thigh)	NA	Excision (margin unknown)	LR at 7, 11 and 15 years
	4	53/M	Trunk (anterior chest wall)	13	Excision (margin unknown)	LR at 2 and 5 years
Oda et al. (6)	1	13/M	Buttock	NA	Excision (margin unknown)	LR at 2, 3, 5 years; wide excision; NED at 63 months
Evans et al. (3)	1	28/F	Axilla-chest wall area	11	Excision (margin unknown)	Lung metastases at presentation. LR at 3, 26, 30 years, showed features of SEF. Alive at 31 years.
	2	6/F	Inguinal area	3.5	Excision (margin probably +)	LR at 13, 19, 25, 30 and 39 years. Lung metastases at 45 years. Alive at 70 years.
	3	30/M	Perineum	>6	Excision (margin unknown)	Recurrences excised 17 times over a 29-year period. Died of recurrent at 31 years.
	4	51/M	Inguinal area	13.5	Excision (margin unknown)	LR at 5, 9 years. Lung and bone metastases. Died postoperatively at 9 years.
	5	26/M	Small bowel mesentery	15	Excision (margin +)	LR at 3 and at 10 years. Died of recurrence at 28 years.
	6	26/M	Neck	NA	Excision (margin unknown)	LR at 3, 10, 14, 22, 24, 27, 31, 36 and 43 years. Alive and NED at 44 years.
	7	38/M	Buttock	NA	Excision (margin unknown)	LR at 4, 6, 12, 14, 21, 23 and 28 years. Biopsy showed dedifferentiated sarcoma. Died at 31 years.
	8	22/F	Abdominal wall (lower)	NA	Excision (margin unknown)	LR at 3, 6 and 11 years. Lung metastases. Alive at 12 years.
	9	9/M	Neck	NA	Excision (margin unknown)	LR at 5, 9, 12, 17, 20, 22 and 23 years. Died of lung and chest wall metastases at 42 years
	10	24/F	Inguinal area	NA	Excision (margin unknown)	LR at 4 and at 14 years. Alive and NED at 19 years.
	11	39/M	Mesentery	10	Excision (margin unknown)	LR at 2 and at 18 years. Alive at 18 years.
	12	41/F	Chest wall	10	Excision (margin probably +)	LR at 1, 2 and 4 years. Died at 6 years.
	13	26/M	Retroperitoneum	10	Excision (margin unknown)	Recurrent dedifferentiated tumor excised at 2 years and more recurrent tumor shortly after. Died at 6 years.
Indap et al. (7)	1	20/F	Shoulder	NA	Excision (margin unknown)	LR at 3 and 20 years. Alive at 22 years.

10.3389/fmed.2024.1172746

recurrences and bone invasion, reflecting the biological behavior characteristics of rapid growth and strong invasion potential. Long-term follow-up should be performed for LGFMS patients with a positive margin at initial operation and patients who had recurrence even after wide resection to closely monitor recurrence or metastasis. The preferred treatment is early wide resection to reduce local recurrence. For metastatic lesions, radical excision should be performed if possible. Our case expands our understanding of the biological behavior of LGFMS and provides clinical experience in diagnosis and treatment.

Conclusion

In our case, multiple early postoperative recurrences may be associated with a positive margin at initial operation. The patient underwent a total of 5 operations including local resection of the primary tumor, two wide resections, amputation and metastatic surgery with 4 early postoperative recurrences and metastases within 4 years, suggesting that LGFMS may have highly invasive biological behavior. Our case expands our understanding of the biological behavior of LGFMS and provides clinical experience in diagnosis and treatment. Further research is needed to develop more effective treatment options for rapidly progressing and highly aggressive LGFMS.

Data availability statement

The original contributions presented in the study are included in the article/Supplementary material, further inquiries can be directed to the corresponding author.

Ethics statement

Written informed consent was obtained from the individual(s) for the publication of any potentially identifiable images or data included in this article.

Author contributions

XZ and YQ: acquisition and analysis of the work, draft the manuscript, imaging data collection, and analysis. ZC: manuscript editing. QY, WH, and LS: formal analysis and resources. LK and JZ: supervision and writing—review and editing. All authors contributed to the article and approved the submitted version.

Funding

This study was funded by the Beijing Science Foundation for Distinguished Young Scholars (JQ21025) and the Peking University Medicine Fund of Fostering Young Scholars' Scientific & Technological Innovation (BMU2022PY006).

Conflict of interest

The authors declare that the research was conducted in the absence of any commercial or financial relationships that could be construed as a potential conflict of interest.

Publisher's note

All claims expressed in this article are solely those of the authors and do not necessarily represent those of their affiliated organizations, or those of the publisher, the editors and the reviewers. Any product that may be evaluated in this article, or claim that may be made by its manufacturer, is not guaranteed or endorsed by the publisher.

Supplementary material

The Supplementary material for this article can be found online at: https://www.frontiersin.org/articles/10.3389/fmed.2024.1172746/full#supplementary-material

References

1. Evans HL. Low-grade Fibromyxoid sarcoma: a report of two metastasizing neoplasms having a deceptively benign appearance. *Am J Clin Pathol*. (1987) 88:615–9. doi: 10.1093/ajcp/88.5.615

2. Folpe AL, Lane KL, Paull G, Weiss SW. Low-grade Fibromyxoid sarcoma and Hyalinizing spindle cell tumor with Giant rosettes: a Clinicopathologic study of 73 cases supporting their identity and assessing the impact of high-grade areas. *Am J Surg Pathol*. (2000) 24:1353–60. doi: 10.1097/00000478-200010000-00004

3. Evans HL. Low-grade Fibromyxoid sarcoma: a Clinicopathologic study of 33 cases with long-term follow-up. *Am J Surg Pathol*. (2011) 35:1450–62. doi: 10.1097/PAS.0b013e31822b3687

4. Evans HL. Low-grade Fibromyxoid sarcoma. A report of 12 cases. *Am J Surg Pathol*. (1993) 17:595–600. doi: 10.1097/00000478-199306000-00007

5. Goodlad JR, Mentzel T, Fletcher CD. Low grade Fibromyxoid sarcoma: Clinicopathological analysis of eleven new cases in support of a distinct entity. *Histopathology*. (1995) 26:229–37. doi: 10.1111/j.1365-2559.1995.tb01436.x

6. Oda Y, Takahira T, Kawaguchi K, Yamamoto H, Tamiya S, Matsuda S, et al. Low-grade Fibromyxoid sarcoma versus low-grade myxofibrosarcoma in the extremities and trunk. A comparison of Clinicopathological and Immunohistochemical features. *Histopathology*. (2004) 45:29–38. doi: 10.1111/j.1365-2559.2004.01886.x

7. Indap S, Dasgupta M, Chakrabarti N, Agarwal A. Low grade Fibromyxoid sarcoma (Evans tumour) of the arm. *Indian J Plast Surg*. (2014) 47:259–62. doi: 10.4103/0970-0358.138973

8. Lane KL, Shannon RJ, Weiss SW. Hyalinizing spindle cell tumor with Giant rosettes: a distinctive tumor closely resembling low-grade Fibromyxoid sarcoma. *Am J Surg Pathol*. (1997) 21:1481–8. doi: 10.1097/00000478-199712000-00011

9. Périgny M, Dion N, Couture C, Lagacé R. Low grade Fibromyxoid sarcoma: a Clinico-pathologic analysis of 7 cases. *Ann Pathol*. (2006) 26:419–25. doi: 10.1016/s0242-6498(06)70750-7

10. Kim SY, Kim M-Y, Hwang YJ, Han YH, Seo JW, Kim YH, et al. Low-grade Fibromyxoid sarcoma: Ct, sonography, and Mr findings in 3 cases. *J Thorac Imaging*. (2005) 20:294–7. doi: 10.1097/01.rti.0000171420.81428.16

11. Abe Y, Hashimoto I, Nakanishi H. Recurring facial low-grade Fibromyxoid sarcoma in an elderly patient: a case report. *J Med Invest*. (2012) 59:266–9. doi: 10.2152/jmi.59.266

12. Maretty-Nielsen K, Baerentzen S, Keller J, Dyrop HB, Safwat A. Low-grade Fibromyxoid sarcoma: incidence, treatment strategy of metastases, and clinical significance of the Fus gene. *Sarcoma*. (2013) 2013:256280. doi: 10.1155/2013/256280

13. Scheer M, Vokuhl C, Veit-Friedrich I, Münter M, von Kalle T, Greulich M, et al. Low-grade Fibromyxoid sarcoma: a report of the cooperative Weichteilsarkom Studiengruppe (Cws). *Pediatr Blood Cancer*. (2020) 67:e28009. doi: 10.1002/pbc.28009

14. Mastoraki A, Strigkos T, Tatakis FP, Christophi A, Smyrniotis V. Recurrent low-grade Fibromyxoid sarcoma of the neck: report of a case and review of the literature. *Indian J Surg Oncol*. (2015) 6:296–9. doi: 10.1007/s13193-015-0429-5

15. Chamberlain F, Engelmann B, Al-Muderis O, Messiou C, Thway K, Miah A, et al. Low-grade Fibromyxoid sarcoma: treatment outcomes and efficacy of chemotherapy. *In Vivo*. (2020) 34:239–45. doi: 10.21873/invivo.11766

16. Matsuyama A, Hisaoka M, Shimajiri S, Hayashi T, Imamura T, Ishida T, et al. Molecular detection of Fus-Creb3l2 fusion transcripts in low-grade Fibromyxoid sarcoma using formalin-fixed, paraffin-embedded tissue specimens. *Am J Surg Pathol*. (2006) 30:1077–84. doi: 10.1097/01.pas.0000209830.24230.1f

17. Meis-Kindblom JM, Kindblom LG, Enzinger FM. Sclerosing epithelioid Fibrosarcoma. A variant of Fibrosarcoma simulating carcinoma. *Am J Surg Pathol*. (1995) 19:979–93. doi: 10.1097/00000478-199509000-00001

18. Guillou L, Benhattar J, Gengler C, Gallagher G, Ranchère-Vince D, Collin F, et al. Translocation-positive low-grade Fibromyxoid sarcoma: Clinicopathologic and molecular analysis of a series expanding the morphologic Spectrum and suggesting potential relationship to Sclerosing epithelioid Fibrosarcoma: a study from the French sarcoma group. *Am J Surg Pathol*. (2007) 31:1387–402. doi: 10.1097/PAS.0b013e3180321959

19. Antonescu CR, Rosenblum MK, Pereira P, Nascimento AG, Woodruff JM. Sclerosing epithelioid Fibrosarcoma: a study of 16 cases and confirmation of a Clinicopathologically distinct tumor. *Am J Surg Pathol*. (2001) 25:699–709. doi: 10.1097/00000478-200106000-00001

20. Eyden BP, Manson C, Banerjee SS, Roberts IS, Harris M. Sclerosing epithelioid Fibrosarcoma: a study of five cases emphasizing diagnostic criteria. *Histopathology*. (1998) 33:354–60. doi: 10.1046/j.1365-2559.1998.00530.x

21. Rekhi B, Folpe AL, Deshmukh M, Jambhekar NA. Sclerosing epithelioid Fibrosarcoma - a report of two cases with cytogenetic analysis of Fus gene rearrangement by Fish technique. *Pathol Oncol Res*. (2011) 17:145–8. doi: 10.1007/s12253-010-9277-3

22. Panagopoulos I, Tiziana Storlazzi C, Fletcher CDM, Fletcher JA, Nascimento A, Domanski HA, et al. The chimeric Fus/Creb3l2 gene is specific for low-grade Fibromyxoid sarcoma. *Genes Chromosomes Cancer*. (2004) 40:218–28. doi: 10.1002/gcc.20037

23. Mertens F, Fletcher CDM, Antonescu CR, Coindre J-M, Colecchia M, Domanski HA, et al. Clinicopathologic and molecular genetic characterization of low-grade Fibromyxoid sarcoma, and cloning of a novel Fus/Creb3l1 fusion gene. *Lab Invest*. (2005) 85:408–15. doi: 10.1038/labinvest.3700230

24. Lau PPL, Lui PCW, Lau GTC, Yau DTW, Cheung ETY, Chan JKC. Ewsr1-Creb3l1 gene fusion: a novel alternative molecular aberration of low-grade Fibromyxoid sarcoma. *Am J Surg Pathol*. (2013) 37:734–8. doi: 10.1097/PAS.0b013e31827560f8

25. Prieto-Granada C, Zhang L, Chen HW, Sung YS, Agaram NP, Jungbluth AA, et al. A genetic dichotomy between pure Sclerosing epithelioid Fibrosarcoma (Sef) and hybrid Sef/low-grade Fibromyxoid sarcoma: a pathologic and molecular study of 18 cases. *Genes Chromosomes Cancer*. (2015) 54:28–38. doi: 10.1002/gcc.22215

26. Bilsky MH, Schefler AC, Sandberg DI, Dunkel IJ, Rosenblum MK. Sclerosing epithelioid Fibrosarcomas involving the Neuraxis: report of three cases. *Neurosurgery*. (2000) 47:956–60. doi: 10.1097/00006123-200010000-00031

27. Chew W, Benson C, Thway K, Hayes A, Miah A, Zaidi S, et al. Clinical characteristics and efficacy of chemotherapy in Sclerosing epithelioid Fibrosarcoma. *Med Oncol*. (2018) 35:138. doi: 10.1007/s12032-018-1192-6

28. Yoshimura R, Nishiya M, Yanagawa N, Deguchi H, Tomoyasu M, Kudo S, et al. Low-grade Fibromyxoid sarcoma arising from the lung: a case report. *Thorac Cancer*. (2021) 12:2517–20. doi: 10.1111/1759-7714.14107

frontiers | Frontiers in Oncology

TYPE Case Report
PUBLISHED 01 March 2024
DOI 10.3389/fonc.2024.1329264

Check for updates

OPEN ACCESS

EDITED BY
Liam Chen,
University of Minnesota, United States

REVIEWED BY
Vijay Anand Reddy Palkonda,
Apollo Cancer Centre, Hyderabad, India
Hongying Zhang,
Sichuan University, China

*CORRESPONDENCE
Qixing Gong
gongqixing@hotmail.com;
Qinhe Fan
fanqinhe@aliyun.com

†These authors have contributed equally to this work and share first authorship

RECEIVED 28 October 2023
ACCEPTED 14 February 2024
PUBLISHED 01 March 2024

CITATION
Zhang J, Fang H, Zhu X, Yao C, Fan Q and Gong Q (2024) Case report: Primary pulmonary low grade fibromyxoid sarcoma progressing to dedifferentiation: probably due to *TP53* driver mutation.
Front. Oncol. 14:1329264.
doi: 10.3389/fonc.2024.1329264

COPYRIGHT
© 2024 Zhang, Fang, Zhu, Yao, Fan and Gong. This is an open-access article distributed under the terms of the Creative Commons Attribution License (CC BY). The use, distribution or reproduction in other forums is permitted, provided the original author(s) and the copyright owner(s) are credited and that the original publication in this journal is cited, in accordance with accepted academic practice. No use, distribution or reproduction is permitted which does not comply with these terms.

Case report: Primary pulmonary low grade fibromyxoid sarcoma progressing to dedifferentiation: probably due to *TP53* driver mutation

Jiawen Zhang[1†], Haisheng Fang[1†], Xiaomei Zhu[2], Chenchen Yao[3], Qinhe Fan[1*] and Qixing Gong[1*]

[1]Department of Pathology, The First Affiliated Hospital with Nanjing Medical University, Nanjing, China, [2]Department of Radiology, The First Affiliated Hospital with Nanjing Medical University, Nanjing, China, [3]Department of Pathology, Women's and Children's Hospital Affiliated to Xiamen University (Xiamen Maternal and Child Health Care Hospital), Xiamen, China

Low Grade Fibromyxoid Sarcoma (LGFMS), a rare entity characterized by bland histologic features, typically affects deep soft tissues of the trunk and lower extremities. Rare cases have been reported arising from the viscera and few demonstrating morphology of high-grade dedifferentiation. Here we report a 39-year-old Chinese woman presenting with primary lung LGFMS, which metastasized to the pancreas five years after diagnosis and then relapsed ten years later as a mediastinum mass. Microscopically, the lung and pancreatic lumps shared similar classical features of LGFMS, composed of bland spindle-shaped cells with low mitotic activity. However, the mediastinal mass had dedifferentiated morphology of dense sheets of round and epithelioid cells with high degree of nuclear pleomorphism and brisk mitosis. Molecular studies showed both classical and dedifferentiated areas had FUS::CREB3L2 rearrangement. However, the mediastinal dedifferentiated area presented with extra H193Y mutation of the *TP53*. Moreover, the mediastinal tumor displayed a strong and diffuse pattern of p53 expression immunohistochemically, but the primary lung and secondary pancreatic masses did not. Thus, we diagnosed the mediastinal mass as dedifferentiated LGFMS and proposed that *TP53* mutation was probably the driver gene alteration in the process, which, to the best of our knowledge, has not been reported in the existing literature.

KEYWORDS

LGFMS, lung, dedifferentiated, *TP53*, next-generation sequencing

Introduction

Low Grade Fibromyxoid Sarcoma (LGFMS) is a low-grade malignant fibroblastic neoplasm predominantly arising from the deep soft tissues of the trunk and lower extremities among young to middle-aged adults. It's characterized by bland spindle-shaped cells with mild nuclear pleomorphism in a fibrous and myxoid background. MUC4 is often expressed in LGFMS (1). Furthermore, LGFMS mostly harbors FUS::CREB3L1/2 gene fusions, and EWSR1::CREB3L1 gene fusion has also been reported (2). However, LGFMS can be diagnostically challenging in unusual locations with advanced morphological features. We here report a 39-year-old woman with LGFMS originating from the lungs, metastasized to the pancreas and then relapsed as a mediastinum mass, showing dedifferentiated morphology with over ten years of follow-up, and carrying FUS::CREB3L2 gene fusion and *TP53* mutation. To the best of our knowledge, this is the first published case of LGFMS harboring the mutation of *TP53*.

Case report

A 39-year-old woman was referred to our hospital due to a diagnostic dilemma concerning the left mediastinal occupancy. Her medical history revealed an admission to another hospital in 2012 for non-inducible hemoptysis. A computed tomography (CT) scan at the time revealed a mass in the left upper lobe (Figure 1A), initially diagnosed as a solitary fibrous tumor (SFT). No pancreatic lesion was observed then (Figure 1B). One year after the pneumonectomy, a follow-up CT (Figure 1C) scan showed a small shadow near the main pulmonary artery, considered to be a postoperative change, without further treatment. In 2017, an abdominal CT scan (Figure 1D) uncovered a well-demarcated pancreatic tumor (60mm×50mm×30mm), leading to middle segment pancreatectomy and LGFMS diagnosis. In 2020, a CT (Figure 1E) scan showed a mass (70mm×56mm×53mm) in the left upper lobe and middle mediastinum, pressing on the left pulmonary artery. As surgical treatment was no longer an option, the patient was treated with anlotinib for 1.5 months, discontinued because of recurring infections. In 2022, she was admitted to another hospital for shortness of breath. A chest CT scan (Figure 1F) revealed a larger mass occupying the left thoracic cavity, with pleural and pericardial effusions. Bronchoscopic examination reported broccoli-like neoplasms completely blocking the left main bronchus. A small biopsy was made and concurrent bronchial stent placement was performed. There was no recurrence of pancreatic mass then. After the diagnosis, the patient started combined chemotherapy and immunotherapy in early September 2022. The specific plan was doxorubicin (60mg d1), ifosphosate (2g d1-d3) and sintilimab (200mg d1). After the first cycle of treatment, the patient developed myelosuppression (Grade 3). After another cycle of treatment with this regimen, the patient developed nauseating pericardial effusion. As a result, the treatment was adjusted to Liposu (210mg d1), carboplatin (500mg d1) and sintilimab (200mg d1) for the third to sixth cycles of treatment, during which the patient's condition was evaluated as stable disease (SD). In February 2023, the plan was changed to immunotherapy and anti-vascular targeted therapy with sugalimab (1200mg d1) and bevacizumab (400mg d1), the 7th to 10th cycles of treatment were performed, progressive disease (PD) was assessed during this period. In May 2023, the patient experienced a sudden epileptic episode. CT showed multiple abnormal signals in both cerebral hemispheres and the right cerebellar hemisphere. Multiple brain metastases were considered, and the patient underwent whole-brain radiotherapy (CTV-haima 30 Gy/12f). Subsequently, treatment with sugalimab (1200mg d1), bevacizumab (400mg d1) and etoposide (200mg d1-d5) were continued for 11th-13th cycles. Current assessment of disease progression. The timeline of the patient's clinical history is presented (Figure 1G).

Histologically, the left lung mass was composed of bland spindle-shaped cells with a fibrous stroma and thin-walled blood vessels in the background (Figure 2A). In some areas, the spindle cells were densely composed and arranged in fascicular, whorled or random manner. While in other areas, cells with a spindle to stellate configuration were randomly distributed within a fibrous to myxoid background. Although the tumor cells appeared mild and amicable, the surrounding bronchial and alveolar epithelia were observed entrapped in the tumor (Figure 2B). Upon careful observation, a network of curvilinear and branching capillary-sized blood vessels was observed in both cellular and the myxoid areas. Some vessels were slender, while others were dilatated as staghorn vessels (Figure 2C). At high magnification, the tumor cells displayed mild nuclear pleomorphism, finely clumped chromatin, pale eosinophilic cytoplasm, and few mitotic figures. Focally, epithelioid cells were present, and a giant collagen rosette was witnessed (Figure 2D). There was no necrosis, and the average number of mitotic figures was approximately 1-2/10 high power fields (HPFs).

The pancreatic tumor shared similar microscopic features to the lung tumor, displaying low aggressiveness as involvement of the surrounding pancreatic tissues was limited (Figure 2E), but the spindle tumor cells were more sparsely distributed within a myxoid background, alongside thin-walled branching vessels (Figure 2F).

The biopsy of recurrent left upper lobe and mediastinal mass revealed notably aggressive morphological features. Sheets of anaplastic cells were observed beneath the squamous metaplasia bronchial surface epithelium (Figure 2G). Tumor cells displayed a round, polygonal to epithelioid shape with significant nuclear pleomorphism and some vacuolated cytoplasmic changes in a disordered arrangement (Figure 2H). Mitosis was active, with visible pathological mitotic figures (Figure 2I). Extensive necrosis was observed. The classical LGFMS with mild spindle tumor cells was hardly identifiable.

Immunohistochemistry of the lung and pancreatic masses showed strong MUC4 expression (Figure 2J), but were negative for S-100, CD117, CK, EMA, Desmin, CD34, SMA, and β-Catenin. The Ki-67 index was about 5%+ (Figure 2K). The mediastinal mass biopsy showed positive staining for vimentin, CD99, INI-1, MDM2, and MUC4 (Figure 2M), but was negative for CKp, Desmin, SMA, S-100, CD31, CD34, TTF-1, P40, STAT6, and SOX10. The Ki-67 index averaged 50% (Figure 2N). Additionally, the mediastinal tumor cells strongly and diffusely expressed p53 (Figure 2O), while the pancreatic tumor cells did not (Figure 2L).

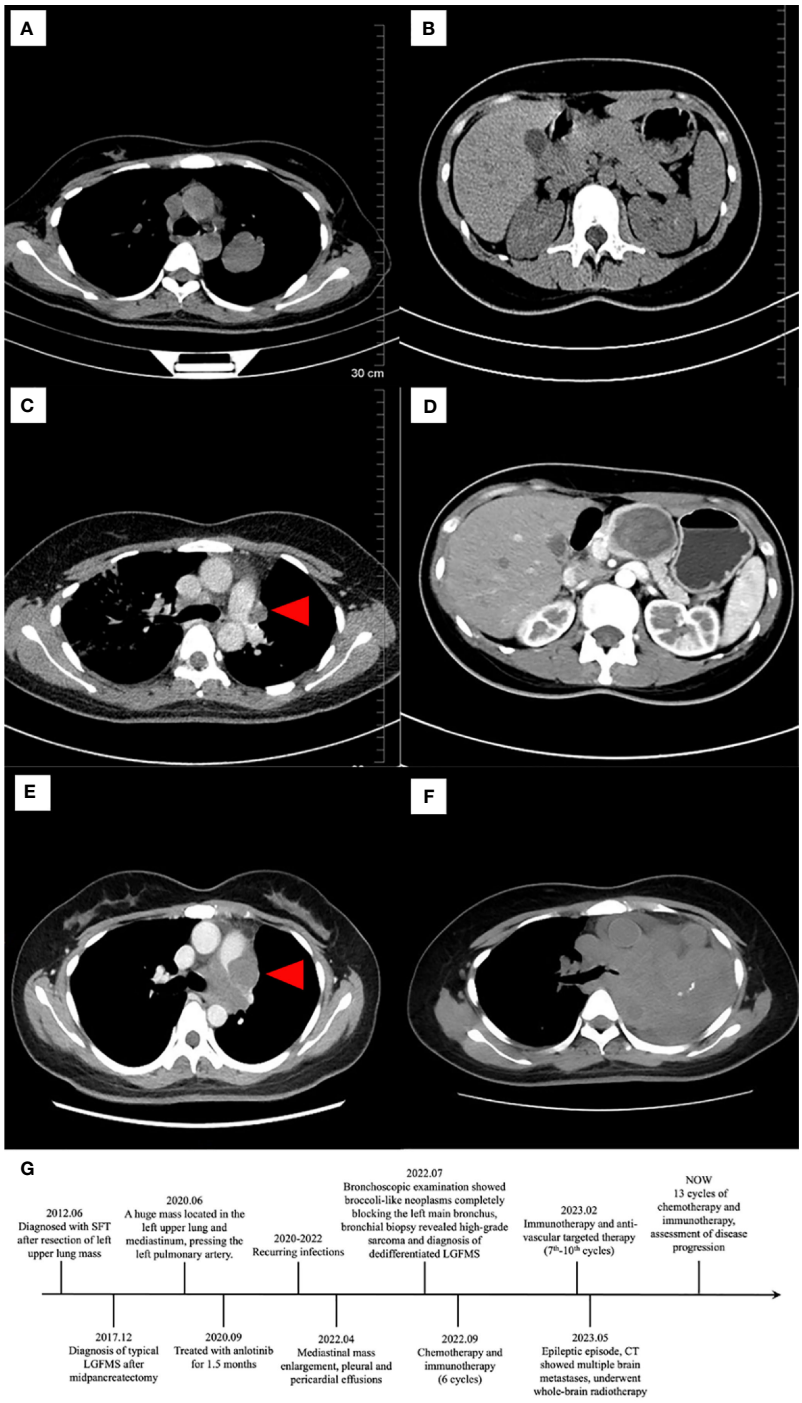

FIGURE 1
Computed tomography (CT) of lung (left) and pancreas (right). In 2012, CT showed a mass in left upper lobe **(A)**. No lesion was seen in the pancreas **(B)**. In 2016, CT found a small rise at the left edge of the main pulmonary artery (**(C)**, red arrowhead). Then in 2017, CT revealed a low-density mass measuring 60mm×50mm×30 mm in the body of pancreas, the mass being mildly enhanced and homogeneous, the pancreatic duct dilatated, and the splenic artery slightly compressed **(D)**. In 2020, there was a tumor in the left middle and upper mediastinal mass measuring 70mm×56mm×53mm, pressing the left pulmonary artery (**(E)**, red arrowhead). In 2022, on the left side of the mediastinum, a mass-like soft tissue mass was seen, with a larger size than the lesion in 2020 **(F)**. The timeline of the patient's clinical history is presented **(G)**.

Dual-color break-apart commercial probes of FUS (Anbiping, Guangzhou, China) were used for fluorescence *in situ* hybridization (FISH) assays, showing separate signals in over 30% of pancreatic and mediastinal tumor cells (Figures 3A, B), indicating FUS rearrangement. Next-generation sequencing (NGS) was performed on the mediastinal mass, revealing a FUS exon 6::CREB3L2 exon 5 fusion (Figure 3C) and H193Y mutation of *TP53* (Figure 3D). Otherwise, reverse transcription polymerase chain reaction (RT-PCR) on the pancreatic tumor confirmed the presence of the same FUS exon 6::CREB3L2 exon 5 fusion as the mediastinal mass

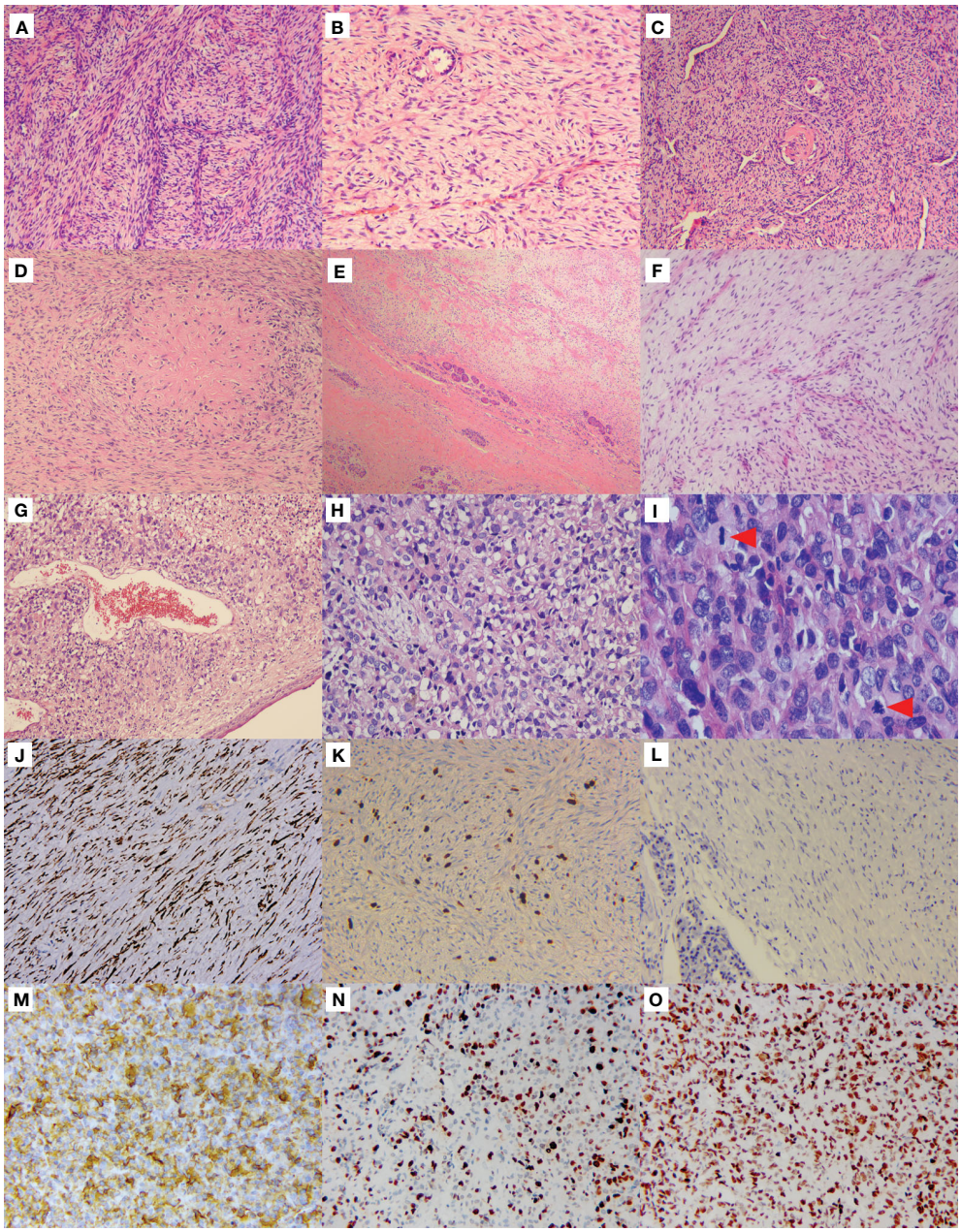

FIGURE 2
Morphological features and immunophenotype of LGFMS, a primary, metastasized, and dedifferentiated tumor. Primary lung tumor **(A–D)**. Hematoxylin & eosin (HE) staining in the low-power view showed spindle cells were densely composed and arranged in a fascicular manner **(A)**. Spindle to stellate cells were sparsely distributed in the fibrous to myxoid background, with the surrounding alveolar epithelial cells entrapped in the tumor **(B)**. Curvilinear and branching capillary-sized blood vessels were observed, some of which were dilatated as staghorn vessels **(C)**. Giant collagen rosettes characterized by a central zone of eosinophilic collagen surrounded by spindle to oval tumor cells **(D)**. Metastatic pancreatic tumor **(E, F)**. Pancreatic tissues were limitedly involved in the tumor cells **(E)**. Bland spindle cells sparsely distributed in a mucus background with thin-walled branching vessels **(F)**. Dedifferentiated mediastinal tumor **(G–I)**. Anaplastic cells were present beneath the squamous metaplasia bronchial surface epithelium **(G)**. The tumor cells were round, polygonal to epithelioid with high degree of nuclear pleomorphism and abu4ndant eosinophilic cytoplasm, and some cells showed vacuolated changes in cytoplasm **(H)**. Mitosis was active (I, red arrowheads), and pathological mitosis could be seen (**(I)**, the red arrowhead below). Immunohistochemistry **(J–O)**. The pancreatic tumor cells strongly expressed MUC4 **(J)**. The Ki-67 proliferation index was about 5%+ **(K)**, but negative for p53 **(L)**. The mediastinal tumor cells were strongly positive for MUC4 **(M)** as well. The Ki-67 proliferation index was averagely 50% **(N)**. The p53 staining was strongly and diffusely expressed **(O)**.

(Figure 3E), but *TP53* mutation was absent (Figure 3F). Considering these morphological and molecular findings along with the clinical history, the relapsed mediastinal tumor was diagnosed as dedifferentiated LGFMS.

Discussion

Some low-grade soft-tissue sarcomas may undergo high-grade transformation, including dedifferentiation, namely losing

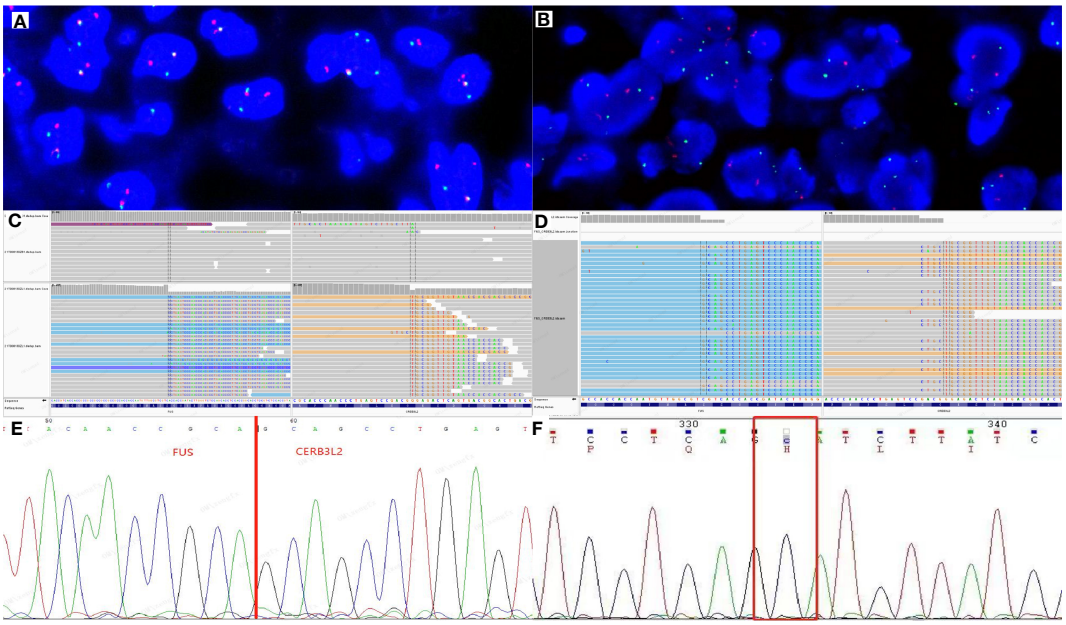

FIGURE 3
Molecular characterization of pancreatic and mediastinal tumors. Two fusions and one extra green signal were detected in more than 30% of tumor cells by FUS break-apart fluorescence *in situ* hybridization (FISH) test in pancreatic **(A)** and mediastinal **(B)** masses. Genetically, next-generation sequencing (NGS) test of the mediastinal mass revealed that FUS exon 6 was fused to CREB3L2 exon 5 **(C)** and the *TP53* had an H193Y mutation **(D)**. By direct sequencing of RT-PCR product in pancreatic tumor, chimeric transcripts were detected between FUS exon 6 and CREB3L2 exon 5 **(E)**, but *TP53* mutation was not detected **(F)**.

their original characteristics. Dedifferentiated components can coexistxwith the original components either synchronously or heterochronously. This phenomenon has been reported in many tumors, including liposarcoma (3), chondrosarcoma, chordoma, SFT (4), gastrointestinal stromal tumor (GIST) (5), and LGFMS (6). Dedifferentiated LGFMS was first described by Evans in 1993 (7). In contrast to the classical morphology, dedifferentiated LGFMS is characterized by densely distributed epithelioid or round cells with obvious atypia. In 2006, Périgny (8) reported a case of LGFMS that dedifferentiated into a high-grade sarcoma upon recurrence, with regions resembling pleomorphic undifferentiated sarcoma and sclerosing epithelioid fibrosarcoma (SEF). In 2011, Evans reported three cases of LGFMS with high-grade transformation during relapse (6), with one case showing SEF-like changes and survived after treatment, while the other two showed high-grade round cell components and survived for only one year after dedifferentiation. More recently, Dobin (9) and Tay (10) reported molecularly confirmed cases of dedifferentiated LGFMS with FUS rearrangement validated by FISH, RT-PCR or NGS, respectively. To date, the mechanism of dedifferentiation has not been further explored. We summarize clinicopathological characteristics in Supplementary Table 1. The patients in this cohort exhibit a broad age range, spanning from 3 to 85 years old, with the majority of middle-aged individuals. Predominantly, the affected areas involve deep tissues of the limbs and trunk, with one case located in the retroperitoneum. Histological morphology and molecular characteristics have been described above. Surgical resection was performed in all 6 cases, with additional treatments including chemotherapy, radiotherapy, and immunotherapy in some instances. Overall survival (OS) varied from 17 months to 31.5 years, with 5 cases experiencing relapse post-surgery. Remarkably, one case remained disease-free for 17 months following surgery.

In our case, the dedifferentiated morphological features of the mediastinum tumor and misdiagnosis of the primary pulmonary LGFMS as SFT in her medical history posed diagnostic dilemmas. Initially, the mediastinal mass did not express any particular diagnostic antibodies except for MUC4, which was once considered a marker for LGFMS and SEF. However, MUC4 can also be positively expressed in synovial sarcomas, ossifying fibromyxoid tumors, and EWSR1::CREB family rearranged tumors as recently reported (11). Considering the high-grade morphology of the mediastinal tumor, the diagnosis needed more backups, although there was a history of pancreatic LGFMS. Therefore, we borrowed and reviewed the slides of the lung mass. We witnessed closed or dilated thin-walled vessels, spindle cells in fibromyxoid background, and giant collagen rosettes, which indicating the diagnosis of pulmonary LGFMS. Meanwhile, the NGS test identified FUS::CREB3L2 fusion in the mediastinal tumor. Hence, we considered the diagnosis of primary pulmonary LGFMS with pancreatic metastasis and recurrence at the original site with dedifferentiated changes. To date, there are only 4 cases of LGFMS originating from the lungs in the available English literature (12–15). The initial misdiagnosis of SFT likely stemmed from the rarity of pulmonary LGFMS and the presence of dilated staghorn vessels, which are often considered a diagnostic hallmark of SFT. However, as Papp (1) has pointed out, LGFMS can also exhibit staghorn vessels. Moreover, it's essential to highlight that the pancreas can be

a target organ for tumor metastasis (16). Hence, as in our case, when LGFMS occurs in atypical locations such as the lungs or pancreas, it warrants a careful distinction from other spindle cell tumors such as SFT, desmoid fibromatosis, fibrosarcoma, leiomyosarcoma, synovial sarcoma, etc. Immunohistochemical and molecular testing do help the differentiation. Moreover, when LGFMS undergoes dedifferentiation, it needs to be differentiated from various high-grade sarcomas such as round cell liposarcoma, small round cell sarcomas, undifferentiated sarcoma, etc. Accurate diagnosis relies on auxiliary detection and the relationship with the primary low-grade tumor or with reference to the clinical history.

Interestingly, recurred dedifferentiated LGFMS showed a driver mutation in *TP53* gene and p53 protein overexpression, but the pancreatic tumor did not. *TP53* plays a crucial role in cell cycle regulation (17). Previous studies have identified the positive expression of p53 in classical LGFMS (18), but there was no molecular test to confirm the presence of *TP53* mutation in either LGFMS or EFS. However, the presence of *TP53* mutations or *TP53* pathway-related gene alterations have been demonstrated in the progression and dedifferentiation of a variety of soft-tissue sarcomas, such as dedifferentiated liposarcoma, dedifferentiated SFT (4), and dedifferentiated GIST (5) for instance. Thus, we hypothesized that *TP53* mutations might similarly play a significant role in the dedifferentiation process in this case.

Clearly, LGFMS with dedifferentiated morphology has poor prognosis according to Evans' study (6). For LGFMS, either classic or dedifferentiated, surgical resection is the main treatment thus far. When the tumor is removed incompletely, it is more prone to relapse. On the other hand, conventional chemoradiotherapy has limited efficacy for LGFMS. Our patient was still assessed as having progressive disease after 13 courses of chemotherapy and immunotherapy, and developed multiple brain metastases, indicating a poor prognosis.

Overall, we here describe the first case of primary pulmonary LGFMS undergoing dedifferentiation changes and associated with a diver mutation in the *TP53* gene. This case underscores the critical role of precise diagnosis in treatment. To ensure accurate diagnosis and comprehensive understanding of the disease, enough attention can never be overpaid to the application of molecular testing such as NGS, as well as careful inquiry or examine the clinical history.

Data availability statement

The original contributions presented in the study are included in the article/Supplementary Material. Further inquiries can be directed to the corresponding authors.

Ethics statement

The studies involving humans were approved by Ethics Committee of the First Affiliated Hospital of Nanjing Medical University (No.2022-SR-338). The studies were conducted in accordance with the local legislation and institutional requirements. Written informed consent was obtained from the participant/patient(s) for the publication of this case report.

Author contributions

JZ: Conceptualization, Investigation, Resources, Writing – original draft, Writing – review & editing. HF: Conceptualization, Investigation, Resources, Writing – original draft, Writing – review & editing. XZ: Investigation, Resources, Writing – original draft. CY: Investigation, Resources, Writing – review & editing. QF: Project administration, Supervision, Validation, Visualization, Writing – review & editing. QG: Funding acquisition, Project administration, Supervision, Validation, Visualization, Writing – review & editing.

Funding

The author(s) declare financial support was received for the research, authorship, and/or publication of this article. The study was supported by the Jiangsu Province Capability Improvement Project through Science, Technology and Education (ZDXYS202210) and by the Open Project of Jiangsu Health Development Research Center (JSHD2022040), and the Fund of the priority Academic Program Development of Jiangsu Higher Education Institution (JX1023-1801).

Acknowledgments

We thank the patient's family for their help in the preparation of this case report.

Conflict of interest

The authors declare that the research was conducted in the absence of any commercial or financial relationships that could be construed as a potential conflict of interest.

Publisher's note

All claims expressed in this article are solely those of the authors and do not necessarily represent those of their affiliated organizations, or those of the publisher, the editors and the reviewers. Any product that may be evaluated in this article, or claim that may be made by its manufacturer, is not guaranteed or endorsed by the publisher.

Supplementary material

The Supplementary Material for this article can be found online at: https://www.frontiersin.org/articles/10.3389/fonc.2024.1329264/full#supplementary-material

References

1. Papp S, Dickson BC, Chetty R. Low-grade fibromyxoid sarcoma mimicking solitary fibrous tumor: A report of two cases. *Virchows Arch*. (2015) 466:223–8. doi: 10.1007/s00428-014-1684-5

2. Lau PP, Lui PC, Lau GT, Yau DT, Cheung ET, Chan JK. Ewsr1-creb3l1 gene fusion: A novel alternative molecular aberration of low-grade fibromyxoid sarcoma. *Am J Surg Pathol*. (2013) 37:734–8. doi: 10.1097/PAS.0b013e31827560f8

3. Dei Tos AP, Doglioni C, Piccinin S, Maestro R, Mentzel T, Barbareschi M, et al. Molecular abnormalities of the P53 pathway in dedifferentiated liposarcoma. *J Pathol*. (1997) 181:8–13. doi: 10.1002/(SICI)1096-9896(199701)181:1<8::AID-PATH700>3.0.CO;2-#

4. Akaike K, Kurisaki-Arakawa A, Hara K, Suehara Y, Takagi T, Mitani K, et al. Distinct clinicopathological features of nab2-stat6 fusion gene variants in solitary fibrous tumor with emphasis on the acquisition of highly Malignant potential. *Hum Pathol*. (2015) 46:347–56. doi: 10.1016/j.humpath.2014.11.018

5. Antonescu CR, Romeo S, Zhang L, Nafa K, Hornick JL, Nielsen GP, et al. Dedifferentiation in gastrointestinal stromal tumor to an anaplastic kit-negative phenotype: A diagnostic pitfall: morphologic and molecular characterization of 8 cases occurring either *de novo* or after imatinib therapy. *Am J Surg Pathol*. (2013) 37:385–92. doi: 10.1097/PAS.0b013e31826c1761

6. Evans HL. Low-grade fibromyxoid sarcoma: A clinicopathologic study of 33 cases with long-term follow-up. *Am J Surg Pathol*. (2011) 35:1450–62. doi: 10.1097/PAS.0b013e31822b3687

7. Evans HL. Low-grade fibromyxoid sarcoma. A Report of 12 Cases. *Am J Surg Pathol*. (1993) 17:595–600. doi: 10.1097/00000478-199306000-00007

8. Perigny M, Dion N, Couture C, Lagace R. [Low grade fibromyxoid sarcoma: A clinico-pathologic analysis of 7 cases]. *Ann Pathol*. (2006) 26:419–25. doi: 10.1016/s0242-6498(06)70750-7

9. Dobin SM, Malone VS, Lopez L, Donner LR. Unusual histologic variant of a low-grade fibromyxoid sarcoma in a 3-year-old boy with complex chromosomal translocations involving 7q34, 10q11.2, and 16p11.2 and rearrangement of the fus gene. *Pediatr Dev Pathol*. (2013) 16:86–90. doi: 10.2350/12-07-1225-CR.1

10. Tay TKY, Kuick CH, Lim TH, Chang KTE, Sittampalam KS. A case of low grade fibromyxoid sarcoma with dedifferentiation. *Pathology*. (2018) 50:348–51. doi: 10.1016/j.pathol.2017.09.022

11. Agaimy A, Stoehr R, Otto M, Brasen JH, Pfarr N, Konukiewitz B, et al. Intra-abdominal ewsr1/fus-crem-rearranged Malignant epithelioid neoplasms: two cases of an emerging aggressive entity with emphasis on misleading immunophenotype. *Virchows Arch*. (2022) 480:481–6. doi: 10.1007/s00428-021-03140-3

12. Kim L, Yoon YH, Choi SJ, Han JY, Park IS, Kim JM, et al. Hyalinizing spindle cell tumor with giant rosettes arising in the lung: report of a case with fus-creb3l2 fusion transcripts. *Pathol Int*. (2007) 57:153–7. doi: 10.1111/j.1440-1827.2006.02073.x

13. Magro G, Fraggetta F, Manusia M, Mingrino A. Hyalinizing spindle cell tumor with giant rosettes: A previously undescribed lesion of the lung. *Am J Surg Pathol*. (1998) 22:1431–3. doi: 10.1097/00000478-199811000-00018

14. Sargar K, Kao SC, Spunt SL, Hawkins DS, Parham DM, Coffin C, et al. Mri and ct of low-grade fibromyxoid sarcoma in children: A report from children's oncology group study arst0332. *AJR Am J Roentgenol*. (2015) 205:414–20. doi: 10.2214/AJR.14.13972

15. Yoshimura R, Nishiya M, Yanagawa N, Deguchi H, Tomoyasu M, Kudo S, et al. Low-grade fibromyxoid sarcoma arising from the lung: A case report. *Thorac Cancer*. (2021) 12:2517–20. doi: 10.1111/1759-7714.14107

16. Adsay NV, Andea A, Basturk O, Kilinc N, Nassar H, Cheng JD. Secondary tumors of the pancreas: an analysis of a surgical and autopsy database and review of the literature. *Virchows Arch*. (2004) 444:527–35. doi: 10.1007/s00428-004-0987-3

17. Seligson ND, Stets CW, Demoret BW, Awasthi A, Grosenbacher N, Shakya R, et al. Inhibition of histone deacetylase 2 reduces mdm2 expression and reduces tumor growth in dedifferentiated liposarcoma. *Oncotarget*. (2019) 10:5671–9. doi: 10.18632/oncotarget.27144

18. Oda Y, Takahira T, Kawaguchi K, Yamamoto H, Tamiya S, Matsuda S, et al. Low-grade fibromyxoid sarcoma versus low-grade myxofibrosarcoma in the extremities and trunk. A comparison of clinicopathological and immunohistochemical features. *Histopathology*. (2004) 45:29–38. doi: 10.1111/j.1365-2559.2004.01886.x

frontiers | Frontiers in Medicine

TYPE Case Report
PUBLISHED 21 March 2024
DOI 10.3389/fmed.2024.1364937

Check for updates

OPEN ACCESS

EDITED BY
Liam Chen,
University of Minnesota, United States

REVIEWED BY
Apurva Patel,
Gujarat Cancer & Research Institute, India
Carmelo Caldarella,
Fondazione Policlinico Universitario A. Gemelli IRCCS, Italy

*CORRESPONDENCE
Meng Li
✉ lmcams@163.com
Li Zhang
✉ Zhangli_cicams@163.com

RECEIVED 03 January 2024
ACCEPTED 11 March 2024
PUBLISHED 21 March 2024

CITATION
Wen X, Xue L, Jiang X, Jiang J, Li M and Zhang L (2024) Case report: A 17-year-old male with primary pulmonary osteosarcoma. *Front. Med.* 11:1364937. doi: 10.3389/fmed.2024.1364937

COPYRIGHT
© 2024 Wen, Xue, Jiang, Jiang, Li and Zhang. This is an open-access article distributed under the terms of the Creative Commons Attribution License (CC BY). The use, distribution or reproduction in other forums is permitted, provided the original author(s) and the copyright owner(s) are credited and that the original publication in this journal is cited, in accordance with accepted academic practice. No use, distribution or reproduction is permitted which does not comply with these terms.

Case report: A 17-year-old male with primary pulmonary osteosarcoma

Xin Wen[1], Liyan Xue[2], Xu Jiang[1], Jiuming Jiang[1], Meng Li[1]*and Li Zhang[1]*

[1]Department of Diagnostic Radiology, Center for National Cancer, Cancer Hospital, Chinese Academy of Medical Sciences and Peking Union Medical College, Beijing, China, [2]Department of Pathology, Center for National Cancer, Cancer Hospital, Chinese Academy of Medical Sciences and Peking Union Medical College, Beijing, China

Primary pulmonary osteosarcoma is one of the extraskeletal osteosarcomas originating from the lung with an extremely low incidence and highly invasive potential. Here we report a case of primary pulmonary osteosarcoma treated in our hospital with a literature review. The patient, a 17-year-old male, had a cough and hemoptysis for 20 days. Computed tomography (CT) and positron emission tomography (PET)/CT were performed in our hospital. According to pathological examination after surgery, the tumor was diagnosed as a high-grade sarcoma with remarkable osteogenesis and necrosis. Based on radiological and histological examinations, a diagnosis of primary pulmonary osteosarcoma originating was considered. The patient underwent surgery and adjuvant chemotherapy. This patient has been under consecutive follow-up for nearly 8 years, showing no signs of recurrence or distant metastasis. Primary pulmonary osteosarcoma is a rare lung malignancy that shows rapid progression, nonspecific symptoms and inapparent signs at an early stage. The diagnosis of primary pulmonary osteosarcoma highly relies on imaging and histological examinations, among which chest CT is the predominant method to check this disease.

KEYWORDS

primary pulmonary osteosarcoma, computed tomography, positron emission tomography, imaging, diagnosis

1 Introduction

Primary pulmonary sarcoma is extremely uncommon with an incidence of one sarcoma for every 500 carcinomas, and primary pulmonary osteosarcoma, a highly malignant soft tissue tumor, is the rarest histological type of primary pulmonary sarcoma (1, 2), therefore it is often misdiagnosed. Consequently, more knowledge is beneficial to the early detection and treatment of this disease, which is also vital to the improvement of prognosis (3, 4). A case of primary pulmonary sarcoma treated in our hospital is reported in this paper with a literature review.

2 Case description

A 17-year-old male patient had a cough and hemoptysis for 20 days, a mass in the lower lobe of the left lung was observed during the examination of an external hospital, therefore he came to visit our hospital. His medical history and family history were negative. Laboratory examination demonstrated no abnormalities in the examination of lung cancer tumor markers CA125, cyfra21-1, NSE, SCC, or CEA. In CT images, the lesion appeared as a soft tissue density mass at the lateral bronchus of the dorsal segment of the left inferior lobe, which also grew towards the lumen of the left interlobular pulmonary artery. It was a spherical-like mass with a maximum diameter of 4.2 cm and uneven density. In addition, there were small striations and areas of bone density to the right of the center, and its postero-lateral side appeared hypodense. The mass was ill-defined, with no abnormal density in the surrounding lung tissue, no clear enlarged lymph nodes in the mediastinum, and no abnormal density changes at the rib scan level. The enhancement scan revealed mild to moderate heterogeneous enhancement with poorly defined boundaries and no enhancement in the cystic region. ^{18}F FDG PET/CT images demonstrated a tumor in the left lower lobe of the lung with an unevenly increased metabolic rate and increased mediastinal lymph node metabolism with no other systemic PET/CT abnormalities observed, which indicates the high potential of lymph node metastasis and no distant metastasis. This lesion exhibits the obvious absence of elevated metabolism in its postero-lateral side, where the density was relatively low in contrast-enhanced CT. Combining CT and PET/CT assessments, the initial preoperative TNM staging was determined to be T2N1M0.

After a comprehensive evaluation, the surgical resection was performed. The dimension of the postoperative lobectomy specimen was 14 × 10 × 3.8 cm. As the lung was dissected along the bronchus, a mass measuring 4.2 × 4 × 3.8 cm with a firm, off-white surface and locally discernible ossification was discovered at the root of the lung. The mass involved the lobar and segmental bronchi and did not involve the visceral pleura. At a maximum diameter of 0.4–1.0 cm, peripheral lungs were grey-red and mushy, with localized lamellar thickening apparent under the surrounding pleura. Pathological diagnosis: the mass in the lower lobe of the left lung was a high-grade sarcoma with significant osteogenesis and necrosis, indicating that it was an extraosseous osteosarcoma based on the morphology and immunophenotype. The tumor had a maximal diameter of 4.2 cm and involved the segmental and lobar bronchi, but not the visceral pleura and lymph nodes. The immunohistochemistry results showed AE1/AE3 (−), EMA (−), Vimentin (3+), Bcl2 (1+), CD99 (2+), Ki67 (40%+), SMA (−), Desmin (−), TTF1 (a few scattered cells+), CD34 (−), S100 (−), Calponin (−). The patient underwent surgery for osteosarcoma resection, along with lymph node clearance. Subsequently, he received six cycles of systemic chemotherapy with doxorubicin at a dose of 25 mg/m^2 (day 1–day 3) and cisplatin at a dose of 100 mg/m^2 (day 4), with one cycle consist of 21 days. After treatment, the patient's vital physical signs and health conditions remained stable. This patient has been under consecutive follow-up for nearly 8 years, showing no signs of recurrence or distant metastasis which are assessed by CT or MRI. The timeline of patient's diagnosis, treatment and follow-up has been displayed in Figure 1.

3 Discussion

Primary pulmonary osteosarcoma is a relatively rare tumor that originates in the lung and accounts for only 0.01% of malignant tumors (3). There have only been 31 cases of primary pulmonary osteosarcoma reported (Table 1). So far, no confirmed etiology for the disease has been found, and radiation therapy administered near the lesion's location and trauma may contribute to primary intrapulmonary osteosarcoma's development (1). Takamura et al. (23) reported a case of extraosseous osteosarcoma secondary to chemoradiotherapy in the lung. But in this case, there was no history of such treatment in this patient.

In contrast to osteosarcoma originating from the bone which tends to affect younger patients, primary pulmonary osteosarcoma mostly affects patients over the age of 50, with a male-to-female ratio of 1.9:1 according to previous case reports. But in this case, we reported a 17-year-old case of primary pulmonary osteosarcoma, and as we know, this is the youngest patient reported to date.

The clinical manifestations have always been unremarkable, with the primary symptoms being chest pain, cough, and hemoptysis (3, 24–26). Among the published reported cases (including the current one), the left lung was affected in 21 cases, the right lung in 11 cases, and the upper lobe of the left lung in 12 cases (Table 1).

Imaging and pathological examinations are the key methods used to determine the diagnosis of primary pulmonary osteosarcoma. Extraskeletal osteosarcoma frequently presents on radiographs as soft tissue opacity with various degrees of mineralization. The primary examination method for this disease is a chest CT scan, which typically reveals a large, lobulated soft tissue mass in the lung with irregular stripes and nodular dense calcifications inside and around the lung, as well as intact neighboring bone structures and no signs of destruction. When necrosis and hemorrhage occur within the tumor, the enhanced scan is typically unevenly enhanced. Calcification or osteoid matrix formation occurs in approximately 50% of primary lesions and can appear during the course of the disease or worsen over time, which also appeared in the images of this case. Calcification on CT scan was clearly indicated in 26% (8/31) of the reported cases (Table 1). PET/CT showed increased metabolic rate of this mass (21). Under the microscope, malignant, primitive spindle cells and osteoid matrix are the hallmarks of primary pulmonary osteosarcoma's pathology (26). A lung mass must meet the following diagnostic criteria to be considered primary lung osteosarcoma: (1) the tumor must consist of a uniform pattern of osteosarcomatous tissue; (2) the tumor must produce osteoid or bone matrix; and (3) the tumor must be originated from the lung and exclude the possibility of a primary osteogenic tumor (26).

Several differential diagnoses should be considered when a primary pulmonary osteosarcoma is suspected. Clinically, primary pulmonary osteosarcoma first needs to be separated from pulmonary metastases of osteosarcoma that originated from bone. The lung is the principal location of metastasis of osteosarcoma, which typically occurs in adolescents, and primary pulmonary osteosarcoma mainly predominates in middle-aged people and elders. One of the key methods for distinguishing between the two is a whole-body bone scintigraphy, which can identify high uptake changes in the primary bone lesion while also ruling out primary osteosarcoma elsewhere in the body, particularly in the chest wall and nearby ribs. Additional

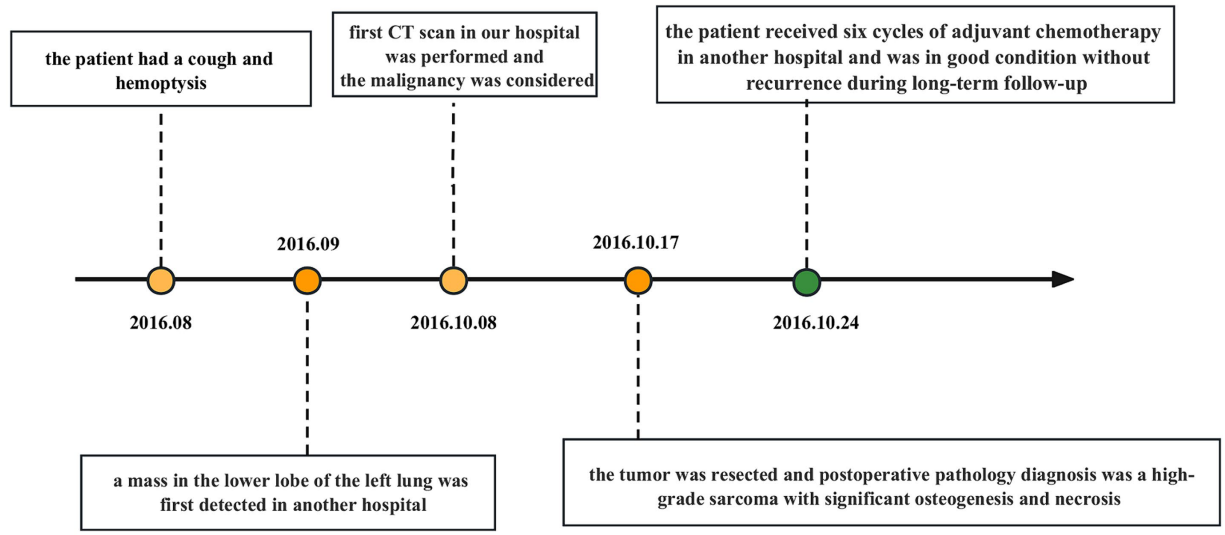

FIGURE 1
Timeline with relevant data about the onset, diagnosis, and therapy of the patient with primary pulmonary osteosarcoma.

disorders that require differentiation include primary lung cancer with substantial intrapulmonary calcifications, intrapulmonary hamartoma and benign pulmonary calcifications (2, 27). The key points of differentiation in terms of imaging are as follows. Multiple round variable-sized nodules and diffuse interstitial thickening are typical radiologic findings of pulmonary metastasis (28). Stratified or annular calcification is usually harmless which occurs more frequently in granulomas or tuberculous lesions. Hamartomas are characterized by popcorn calcifications (29). None of the above features were present in this patient (see Figures 2, 3).

The preferred method of treatment, which has been applied in 12 of the cases that have been recently described, is surgical removal of the primary tumor, and there are relevant studies suggesting that compared with En bloc resection or extensive surgery, inadequate resection was referred to as poor survival (14). While the effectiveness of chemotherapy and radiotherapy is still debatable. In terms of prognosis, it is difficult to predict the prognosis of primary pulmonary osteosarcoma because of its rarity, but the prognosis appears to be poor. Of the reported cases, 15 patients died of their own disease within 1 year and 4 died of unrelated causes, with the longest survival being 42 months after total pneumonectomy, but this patient developed extensive metastases. All the above cases indicated that this disease typically has a relatively poor prognosis, however, in this case, there has been no evidence of metastasis or recurrence during an 8 years follow-up period. This may perhaps be related to his relatively younger age and timely treatment. The prognosis may also be impacted by the greatest tumor diameter, the presence of calcification, insufficient surgical resection, and local recurrence. Nascimento et al. considered that the prognosis is bad when the maximum tumor diameter is more than 5 cm. Benign indicators are thought to be the presence of osteoid in microscopic results and calcification in imaging (2, 3, 14).

Additionally, we should point out that although the final diagnosis was primary pulmonary osteosarcoma, we highly suspected that it was originating from the left interlobular pulmonary artery for the reason that it was located at the lateral bronchus within the dorsal segment of the left inferior lobe and extended towards the lumen of the left interlobular pulmonary artery, and Zhai et al. (26) once reported a case of osteosarcoma originating from the pulmonary artery. But in this case, the possibility that the tumor originated in the lung and later invaded the pulmonary arteries cannot be excluded completely, which is difficult to differentiate by the imaging examination.

In summary, primary pulmonary osteosarcoma is an extremely scarce malignancy that is associated with a high incident rate of lymphatic and hematogenous metastasis, and early diagnosis and treatment are crucial to the patient's prognosis. We can identify original intrapulmonary osteosarcoma using imaging and histopathological findings. To be more specific, imaging helps to diagnose the lesion and make a differential diagnosis by giving a clear visual of the lesion. A CT scan of the lung typically displays a large, lobulated soft tissue mass with irregular stripes and nodular dense calcifications inside and around the lung, as well as intact neighboring bone structures and no signs of destruction. The enhanced scan is often unevenly increased when necrosis and bleeding occur within the tumor. PET/CT is commonly performed in oncology patients to exclude distant and lymph node metastasis, perform neoplasms staging and evaluate treatment response. Tumor cells typically exhibit heightened metabolic activity, and increased uptake of radiopharmaceuticals in PET/CT suggests the potential for metastasis (30). The histopathological identification of this tumor is based on the microscopically observed tumor cells and osteoid matrix (4, 26).

4 Patients' perspective

Our patient states that upon identifying the mass in the lower lobe of my left lung, the medical team promptly conducted a surgical

TABLE 1 Reported cases of primary pulmonary osteosarcoma.

Author	Age	Gender	Chief complaints	Size and location	Procedure to make definite diagnosis	Calcification on CT scan	Bone scintigraphy uptake	Treatment	Prognosis
Greenspan (5)	35	F	Pain, hemoptysis	Left main bronchus, 7 cm	Autopsy	ND	ND	No radical treatment	DOD 11 M after symptoms onset
Yamashita et al. (6)	74	F	Progressive asthmatic symptoms	Large mass replacing left lung	Autopsy	ND	ND	No radical treatment	DOD 6 M after symptoms onset
Reingold and Amromin (7)	62	M	Pneumonia	Right middle lobe, 6 × 6 × 4 cm	Necropsy	ND	ND	Chemotherapy	DOD 7 M after symptoms onset
	56	F	Chills, fever, chest pain	Left upper lobe, 7 × 5 × 4 cm	Surgery	ND	ND	Surgery	Alive 14 M after surgery
Nosanchuk and Weatherbee (8)	66	M	Weakness dyspnea, chest pain, and hemoptysis	Entire left upper lobe and most of lower lobe	Autopsy	ND	ND	No radical treatment	DOD 4 M after symptoms onset
Nascimento (9)	77	F	Asymptomatic	Right middle lobe, 4 cm	Surgery	ND	ND	Surgery	DUC 6 M after surgery
	72	M	Asymptomatic	Right middle lobe, 5.5 cm	Surgery	ND	ND	Surgery	DUC 10 M after surgery
Bagaric and Belicza (10)	49	F	ND	Right lower lobe	ND	ND	ND	ND	DOD
Saito et al. (11)	83	M	Chest pain	Right middle lobe 10 cm	ND	ND	ND	ND	DOD 4 M after symptoms onset
Colby et al. (12)	61	M	Respiratory symptoms	Right lung, 16 × 10	ND	ND	ND	ND	Died several months later of unknown causes
	51	M	Cough	Left lower lobe, 11 × 7 cm	ND	ND	ND	ND	Alive 6 M after surgery
	77	F	Pneumonia	Right middle lobe, 4 × 3 cm	ND	ND	ND	ND	DUC 6 M after surgery
Loose et al. (13)	54	M	Chest pain, left upper extremity paresthesia	Left upper lobe, 10 cm	Surgery	(+)	Performed after surgery	Surgery, chemotherapy, radiation	Alive 7 M after surgery
	45	F	Chest pain	Left lower lobe, 5.5 cm	Surgery	(−)	ND	Surgery	Alive 2 M after surgery
Petersen (14)	70	M	Asymptomatic	Left lower lobe, 5 × 3.5 × 6 cm	Surgery	(+)	(+)	Surgery, radiation	Alive 6 M after surgery
Stark et al. (15)	59	M	Asymptomatic	Left lower lobe, 6.5 × 7 × 11 cm	Surgery	(+)	ND	Surgery	ND
Bhalla et al. (16)	58	M	Fever and cough	Left upper lobe, 18 × 9 × 8 cm	Autopsy	(+)	ND	No radical treatment	DOD about 1 M after first admission
Miller and Allen (17)	72	M	ND	ND	TBLB, splenectomy	ND	ND	Chemotherapy, radiation	DOD 12 M after symptoms onset
Sievert et al. (18)	56	M	Tingling in left fingertips	Left upper lobe, 4 × 2 × 2 cm	Surgery	(−)	Performed after surgery	Surgery	Alive 12 M after surgery

(Continued)

10.3389/fmed.2024.1364937

TABLE 1 (Continued)

Author	Age	Gender	Chief complaints	Size and location	Procedure to make definite diagnosis	Calcification on CT scan	Bone scintigraphy uptake	Treatment	Prognosis
Chapman et al. (4)	33	F	Cough, left-sided chest pain	Left lung, 5.5 × 5 × 4 cm	Surgery	ND	(+)	Surgery, chemotherapy	Alive 42 Mafter surgery
Magishi et al. (19)	74	F	Asymptomatic	Left upper lobe, 5.7 × 5 × 3.3 cm	Surgery	(−)	Performed after surgery	Surgery	DOD 11 Mafter surgery
Kadowaki et al. (2)	72	M	Chest pain, dyspnea	Left lower lobe, 9 × 9 cm	Needle biopsy	(+)	(+)	ND	DOD 3 M after symptoms onset
	77	M	Hemoptysis	Left lower lobe, 11 × 8 cm	Needle biopsy	(+)	(+)	ND	DOD 3 M after symptoms onset
Yamazaki et al. (20)	73	M	Cough, hemoptysis	Left upper lobe, 7 × 6.5 cm	ND	ND	ND	ND	DOD 7 M after operation
	77	M	Hemoptysis	Left lower lobe, 11 × 8 cm	ND	ND	ND	ND	DOD 3 M after symptoms onset
Gu et al. (21)	58	M	Chest pain	Right lung, 5.7 × 8.0 × 5.3 cm	Surgery	(+)	(+)	Surgery, chemotherapy	ND
Shenjere et al. (22)	66	M	Found on assessment for trapped nerve	Left upper lobe, 6 × 5 cm	Biopsy	ND	ND	Surgery	Alive 12 M after initial symptoms
	79	M	Shortness of breath	Left upper lobe, 11 × 9 cm	Biopsy	(−)	(+)	Radiation	DOD 5 M after initial symptoms
	56	F	Cough	Right lower lobe, 3.2 × 2.2 × 2 cm	ND	ND	ND	ND	ND
	58	F	Chest pain, cough	Left lower lobe, 25 × 24 × 6 cm	ND	ND	ND	ND	ND
Takamura et al. (23)	80	M	ND	Right middle lower lobe, 14 cm	Autopsy	ND	ND	Radiotherapy, chemotherapy	DOD
Current case	17	M	Cough and hemoptysis	Left lower lobe, 4.2 × 4 × 3.8 cm	Surgery	(+)	(+)	ND	ND

DOD, died of disease; DUC, died of unrelated cause; M, month; ND, not documented; TBLB, transbronchial lung biopsy.

10.3389/fmed.2024.1364937

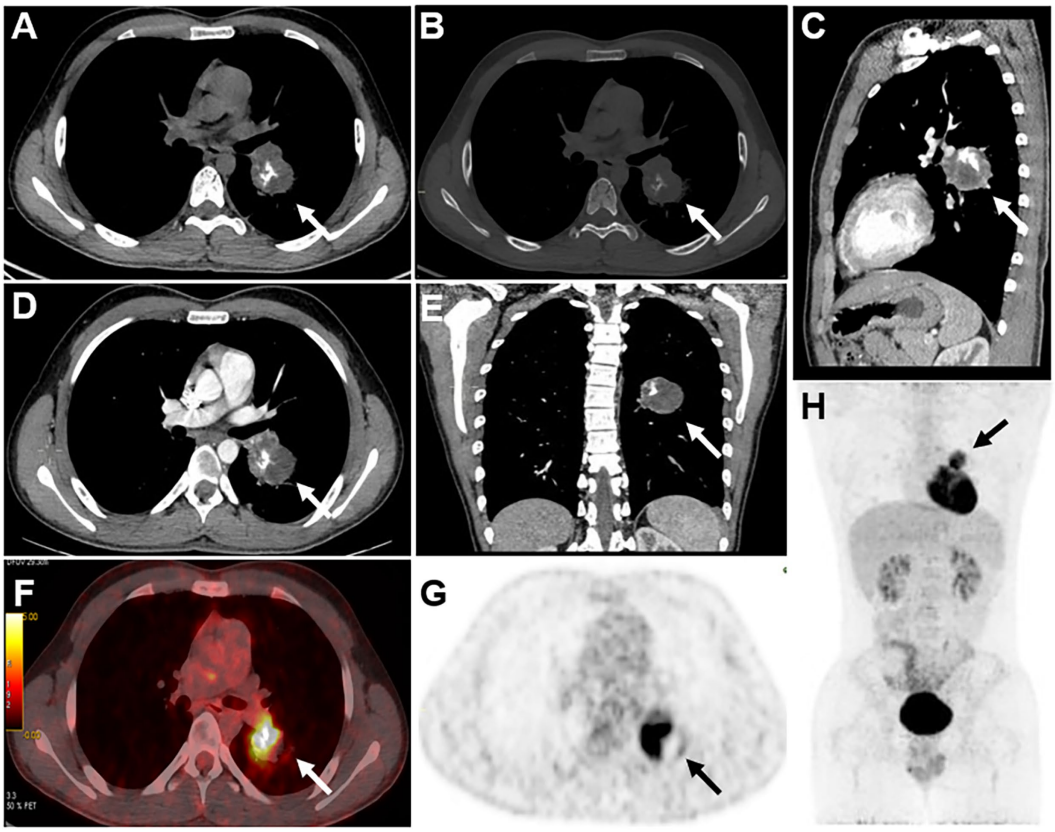

FIGURE 2
CT scans of the mediastinal window **(A)**, bone window **(B)**, and sagittal mediastinal window **(C)** revealed a mass-like soft tissue density shadow in the dorsal segment of the lower lobe of the left lung. The mass had an irregular sphere-like margin, uneven density within the mass, and irregular eccentric ossification or calcification. In addition, axial **(D)** and coronal **(E)** enhanced CT images also revealed a heterogeneous mass with no enhancement in the cystic portion. ^{18}F-FDG PET/CT revealed uneven increased metabolism of the mass in the lower lobe of the left lung, with barely absent uptake in its postero-lateral side **(F,G)**, and the area in the postero-lateral side with increased metabolic activity in lymph nodes was also observed, which also appears hypodense on contrast-enhanced CT. No elevated metabolic activity was observed in other areas on the PET/CT scan **(H)**. Based on a comprehensive evaluation of CT and PET/CT findings, the initial staging before surgery was T2N1M0.

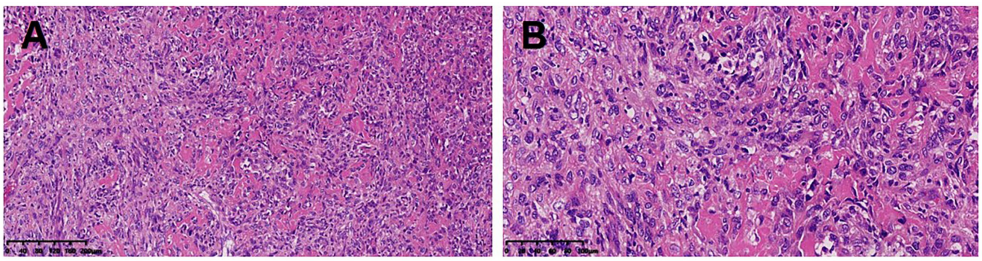

FIGURE 3
Malignant, primitive spindle cells and osteoid matrix were observed **(A,B)**.

procedure, providing me with a corresponding postoperative plan. As of now, my condition has been favorable.

Data availability statement

The original contributions presented in the study are included in the article/supplementary material, further inquiries can be directed to the corresponding authors.

Ethics statement

The studies involving humans were approved by Ethics Committee of Cancer Hospital, Chinese Academy of Medical Sciences. The studies were conducted in accordance with the local legislation and institutional requirements. The participants provided their written informed consent to participate in this study. Written informed consent was obtained from the individual(s) for the publication of any potentially identifiable images or data included in this article.

Author contributions

XW: Formal analysis, Writing – original draft. LX: Formal analysis, Writing – review & editing. XJ: Writing – original draft. JJ: Formal analysis, Writing – review & editing. ML: Formal analysis, Funding acquisition, Supervision, Writing – review & editing. LZ: Formal analysis, Funding acquisition, Supervision, Writing – review & editing.

Funding

The author(s) declare that no financial support was received for the research, authorship, and/or publication of this article.

Conflict of interest

The authors declare that the research was conducted in the absence of any commercial or financial relationships that could be construed as a potential conflict of interest.

Publisher's note

All claims expressed in this article are solely those of the authors and do not necessarily represent those of their affiliated organizations, or those of the publisher, the editors and the reviewers. Any product that may be evaluated in this article, or claim that may be made by its manufacturer, is not guaranteed or endorsed by the publisher.

References

1. Lee JS, Fetsch JF, Wasdhal DA, Lee BP, Pritchard DJ, Nascimento AG. A review of 40 patients with extraskeletal osteosarcoma. *Cancer*. (1995) 76:2253–9. doi: 10.1002/1097-0142(19951201)76:11<2253::AID-CNCR2820761112>3.0.CO;2-8

2. Kadowaki T, Hamada H, Yokoyama A, Katayama H, Abe M, Nishimura K, et al. Two cases of primary pulmonary osteosarcoma. *Intern Med*. (2005) 44:632–7. doi: 10.2169/internalmedicine.44.632

3. Huang W, Deng HY, Li D, Li P, Xu K, Zhang YX, et al. Characteristics and prognosis of primary pulmonary osteosarcoma: a pooled analysis. *J Cardiothorac Surg*. (2022) 17:240. doi: 10.1186/s13019-022-02010-6

4. Chapman AD, Pritchard SC, Yap WW, Rooney PH, Cockburn JS, Hutcheon AW, et al. Primary pulmonary osteosarcoma: case report and molecular analysis. *Cancer*. (2001) 91:779–84. doi: 10.1002/1097-0142(20010215)91:4<779::AID-CNCR1064>3.0.CO;2-J

5. Greenspan EB. Primary osteoid chondrosarcoma of the lung report of a case. *Am J Cancer*. (1933) 18:603–9.

6. Yamashita T, Kiyota T, Ukishima G, Hayama T, Yabuki E. Autopsy case of chondro-osteoidsarcoma originating in the lung. *Showa Igakkai Zasshi*. (1964) 23:472–3.

7. Reingold IM, Amromin GD. Extraosseous osteosarcoma of the lung. *Cancer*. (1971) 28:491–8. doi: 10.1002/1097-0142(197108)28:2<491::AID-CNCR2820280231>3.0.CO;2-7

8. Nosanchuk JS, Weatherbee L. Primary osteogenic sarcoma in lung: report of a case. *J Thorac Cardiovasc Surg*. (1969) 58:242–7. doi: 10.1016/S0022-5223(19)42608-1

9. Nascimento AG, Unni KK, Bernatz PE. Sarcomas of the lung. *Mayo Clin Proc*. (1982) 57:355–9.

10. Bagaric I, Belicza M. Extraskeletal osteogenic sarcoma of the lungs. *Lijec Vjesn*. (1982) 104:467–70.

11. Saito H, Sakai S, Kobayashi T, Ishioroshi Y, Uno Y. Primary osteosarcoma of the lung—a case report. *Nihon Kyobu Shikkan Gakkai Zasshi*. (1983) 21:153–6.

12. Colby TV, Bilbao JE, Battifora H, Unni KK. Primary osteosarcoma of the lung. A reappraisal following immunohistologic study. *Arch Pathol Lab Med*. (1989) 113:1147–50.

13. Loose JH, El-Naggar AK, Ro JY, Huang WL, MJ MM, Ayala AG. Primary osteosarcoma of the lung. Report of two cases and review of the literature. *J Thorac Cardiovasc Surg*. (1990) 100:867–73. doi: 10.1016/S0022-5223(19)36829-1

14. Petersen M. Radionuclide detection of primary pulmonary osteogenic sarcoma: a case report and review of the literature. *J Nucl Med*. (1990) 31:1110–4.

15. Stark P, Smith DC, Watkins GE, Chun KE. Primary intrathoracic extraosseous osteogenic sarcoma: report of three cases. *Radiology*. (1990) 174:725–6. doi: 10.1148/radiology.174.3.2305056

16. Bhalla M, Thompson BG, Harley RA, McLoud TC. Primary extraosseous pulmonary osteogenic sarcoma: CT findings. *J Comput Assist Tomogr*. (1992) 16:974–6. doi: 10.1097/00004728-199211000-00027

17. Miller DL, Allen MS. Rare pulmonary neoplasms. *Mayo Clin Proc*. (1993) 68:492–8. doi: 10.1016/S0025-6196(12)60199-2

18. Sievert LJ, Elwing TJ, Evans ML. Primary pulmonary osteogenic sarcoma. *Skeletal Radiol*. (2000) 29:283–5. doi: 10.1007/s002560050609

19. Magishi K, Yoshida H, Izumi Y, Ishikawa N, Kubota H. Primary osteosarcoma of the lung: report of a case. *Surg Today*. (2004) 34:150–2. doi: 10.1007/s00595-003-2651-y

20. Yamazaki K, Okabayashi K, Hamatake D, Maekawa S, Yoshida Y, Yoshino I, et al. Primary osteosarcoma of the lung: a case report. *Ann Thorac Cardiovasc Surg*. (2006) 12:126–8.

21. Gu T, Shi H, Xiu Y, Gu Y. Primary pulmonary osteosarcoma: PET/CT and SPECT/CT findings. *Clin Nucl Med*. (2011) 36:e209–12. doi: 10.1097/RLU.0b013e3182291ec3

22. Shenjere P, Travis WD, Franks TJ, Doran HM, Hasleton PS. Primary pulmonary osteosarcoma: a report of 4 cases and a review of the literature. *Int J Surg Pathol*. (2011) 19:225–9. doi: 10.1177/1066896909332382

23. Takamura K, Ogi T, Yamamoto M, Kikuchi K. Extraskeletal osteosarcoma of the lung following treatment of primary small-cell lung carcinoma with chemoradiotherapy: a case report. *Mol Clin Oncol*. (2018) 8:99–102. doi: 10.3892/mco.2017.1500

24. Karfis EA, Karaiskos T, Cheva A, Drossos GE. Primary extraosseous osteosarcoma of the lung. *Acta Oncol*. (2010) 49:114–6. doi: 10.3109/02841860902953864

25. Niimi R, Matsumine A, Kusuzaki K, Inada Y, Kato Y, Maeda M, et al. Primary osteosarcoma of the lung: a case report and review of the literature. *Med Oncol*. (2008) 25:251–5. doi: 10.1007/s12032-007-9022-2

26. Zhai D, Cai W, Fan G, Yang J, Liu C. Case report: primary extraskeletal osteosarcoma in the lung and pulmonary artery. *Front Oncol*. (2021) 11:673494. doi: 10.3389/fonc.2021.673494

27. Mc Auley G, Jagannathan J, O'Regan K, Krajewski KM, Hornick JL, Butrynski J, et al. Extraskeletal osteosarcoma: spectrum of imaging findings. *AJR Am J Roentgenol*. (2012) 198:W31–7. doi: 10.2214/AJR.11.6927

28. Seo JB, Im JG, Goo JM, Chung MJ, Kim MY. Atypical pulmonary metastases: spectrum of radiologic findings. *Radiographics*. (2001) 21:403–17. doi: 10.1148/radiographics.21.2.g01mr17403

29. Hong P, Lee JS, Lee KS. Pulmonary heterotopic ossification simulating a pulmonary hamartoma: imaging and pathologic findings and differential diagnosis. *Korean J Radiol*. (2022) 23:688–90. doi: 10.3348/kjr.2022.0156

30. Rahman WT, Wale DJ, Viglianti BL, Townsend DM, Manganaro MS, Gross MD, et al. The impact of infection and inflammation in oncologic ^{18}F-FDG PET/CT imaging. *Biomed Pharmacother*. (2019) 117:109168. doi: 10.1016/j.biopha.2019.109168

Frontiers in Endocrinology

Explores the endocrine system to find new therapies for key health issues

The second most-cited endocrinology and metabolism journal, which advances our understanding of the endocrine system. It uncovers new therapies for prevalent health issues such as obesity, diabetes, reproduction, and aging.

Discover the latest Research Topics

See more →

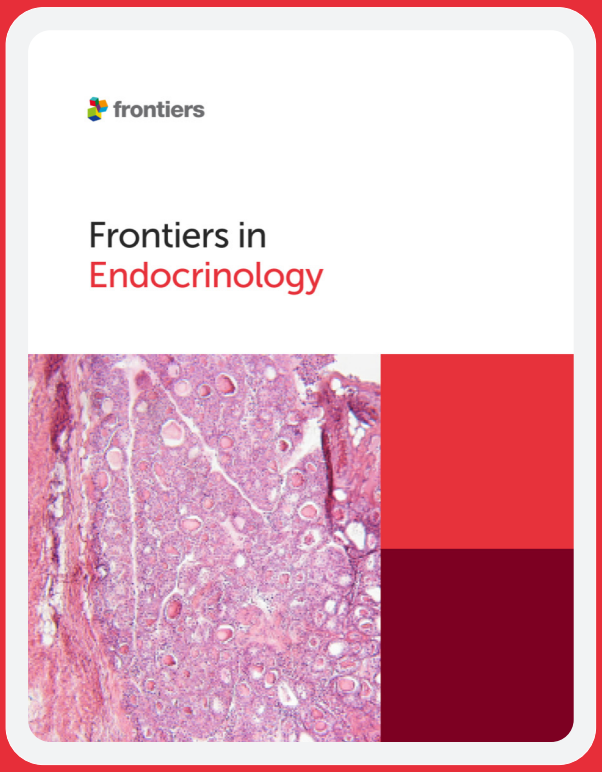

Frontiers

Avenue du Tribunal-Fédéral 34
1005 Lausanne, Switzerland
frontiersin.org

Contact us

+41 (0)21 510 17 00
frontiersin.org/about/contact